

**Designing an optimal cryopreservation  
protocol for human embryonic stem cells: A  
systematic approach**

*Oluseun Olushola Olarewaju*

Bachelor of Science, Biochemistry

A thesis submitted for the degree Master of Philosophy

University of York

Department of Biology

August 2010

---

## **Abstract**

Human embryonic stem cells (hESCs) are derived from the inner cell mass of the human blastocyst. They are pluripotent cells which can differentiate into a wide range of cell types, making them potentially useful for the treatment of diseases such as diabetes, Alzheimer's disease and heart disease. The growing numbers of hESC lines being derived demands that suitable storage conditions are identified in order to maximise their potential for future therapies. Current methods employed for cryopreserving hESCs were adopted from embryo storage (vitrification) and conventionally-frozen mouse embryonic stem cells (mESCs) with post-thaw cell survival ranging from 1-90%. Thus, generating large numbers of cells is often time consuming and potentially prone to clonal selection from the limited post-thaw population. In this work, the approach used was to determine the fundamental physical properties important for cryopreservation including the hydraulic conductivity ( $L_p$ ), solute permeability ( $P_s$ ) and the non-osmotic volume ( $V_b$ ). The hESC lines, RH1 and SHEF3, were compared with the embryonal carcinoma (EC) cell line 2102Ep, which was used as a reference cell line. RH1 and SHEF3 had values for  $V_b$  of 0.22 and 0.19, respectively, which was comparable to that of human oocytes and human haematopoietic progenitor cells from bone marrow. The  $L_p$  and  $P_s$  values for RH1 and SHEF3 were determined in the presence of each of two cryoprotectants, dimethyl sulphoxide ( $\text{Me}_2\text{SO}$ ) and propylene glycol (PG), at RT and at  $+2^\circ\text{C}$ . Cell growth and membrane integrity assays indicated that the RH1 and SHEF3 cells tolerated volume excursions between 40-130% and 40-170% of isotonic volume, respectively. These data were used to model protocols for the addition and elution of cryoprotectant that minimise osmotic stress during the storage of hESCs. The final protocols were tested and shown to support the hESC morphology and expression of TRA-1-60/81 and SSEA4.

Table of Contents

Chapter 1	INTRODUCTION .....	1
1.1	Water and freezing .....	1
1.2	Cells .....	1
1.2.1	Mode of water and solute permeation .....	3
1.2.2	Aquaporins .....	4
1.2.3	Boyle van't Hoff .....	6
1.3	Cryobiology .....	6
1.3.1	Cryo-induced injuries .....	6
1.3.2	Chilling injury .....	7
1.3.3	Intracellular ice formation (IIF) .....	7
1.3.4	Other forms of cryoinjury .....	10
1.3.5	Cell-cell contact .....	10
1.3.6	Cryoprotectants (CPAs) .....	11
1.4	Vitrification .....	16
1.5	Stem cells .....	17
1.5.1	Hematopoietic stem cells .....	17
1.5.2	Embryonal carcinoma cells .....	18
1.5.3	Embryonic stem cells (mouse and human) .....	19
1.5.4	Induced pluripotent stem cells (iPSCs) .....	26
1.6	Current cryopreservation protocols for SCs .....	27
1.6.1	Cryopreservation of HSCs .....	28
1.6.2	Cryopreservation of mESCs .....	29
1.6.3	Cryopreservation of iPSCs .....	30

---

1.6.4	Cryopreservation of hESCs .....	30
1.7	Summary of cryopreservation protocols.....	32
1.8	Project objectives .....	34
1.9	Optimal cryopreservation protocol for hESCs .....	35
Chapter 2	MATERIALS AND METHODS.....	37
2.1	Cell culture .....	38
2.2	Mycoplasma testing.....	38
2.3	Human embryonic stem cell lines used in project .....	38
2.4	Transportation of hESC lines and MEFs between UKSCB and University of York	38
2.5	2102Ep cell culture .....	38
2.6	Mouse embryonic fibroblast (MEF) culture.....	39
2.6.1	Inactivation of mouse embryonic fibroblasts .....	39
2.7	Human embryonic stem cell (hESC) culture .....	39
2.7.1	Derivation of human embryonic stem cells and acquisition of cell lines..	39
2.7.2	hESC in vitro culture.....	39
2.8	MTT Assay .....	40
2.9	RNA Extraction .....	41
2.10	DNase treatment of RNA.....	41
2.11	cDNA synthesis .....	42
2.12	Reverse Transcription-polymerase chain reaction (RT- PCR).....	42
2.13	Characterisation by surface marker expression using flow cytometry .....	42
2.14	Coulter counter .....	43
2.15	Preparation of anisotonic conditions .....	44

---

2.16	Cell Volume Analysis .....	44
2.17	Membrane integrity assay.....	44
2.18	Assessment of cell growth .....	44
2.19	Adhesion assay .....	45
2.20	Membrane Integrity assessment.....	45
2.21	Statistical analysis .....	45
Chapter 3	BIOPHYSICAL PROPERTIES OF HUMAN EMBRYONIC STEM CELLS	
	46	
3.1	INTRODUCTION .....	47
3.1.1	Nonosmotic volume ( $V_b$ ) .....	47
3.1.2	Membrane permeability properties ( $L_p$ and $P_s$ ).....	50
3.1.3	PG and $Me_2SO$ .....	51
3.2	Chapter aims .....	52
3.3	Materials and Methods .....	53
3.3.1	Volume calibration .....	53
3.3.2	Non-osmotic cell volume ( $V_b$ ).....	53
3.3.3	Adhesion assay .....	53
3.3.4	Timecourse experiments .....	54
3.3.5	$L_p$ and $P_s$ determination .....	54
3.3.6	Growth and propidium iodide exclusion assays .....	55
3.4	Results .....	55
3.4.1	Determination of offset voltage .....	55
3.4.2	Determination of non-osmotic volume ( $V_b$ ).....	57
3.4.3	Basic cell properties .....	61

---

3.4.4	Adhesion assay .....	61
3.4.5	Determination of tolerance limits.....	64
3.4.6	Effect of anisotonic medium on hESC colony morphology .....	68
3.4.7	Timecourse responses of cells to CPAs .....	70
3.4.8	Summary of data from curve-fitting .....	77
3.4.9	Permeability variables determined.....	77
3.5	Discussion .....	79
Chapter 4	84	
PROTOCOL MODELLING AND DESIGN.....		84
4.1	Introduction.....	84
4.1.1	Cryoinjury .....	85
4.1.2	Cryopreservation protocol design .....	86
4.2	Chapter aims .....	87
4.3	Materials and Methods .....	88
4.3.1	Toxicity after exposure to cryoprotectant .....	89
4.3.2	Stepwise addition of PG .....	89
4.3.3	Stepwise elution of PG .....	89
4.3.4	Stepwise addition of Me <sub>2</sub> SO .....	89
4.3.5	Stepwise elution of Me <sub>2</sub> SO .....	89
4.3.6	Addition and elution modelling.....	89
4.3.7	Cooling .....	90
4.3.8	Thawing.....	90
4.4	Results .....	90
4.4.1	Addition modelling data .....	91

---

4.4.2	Summary of modelling for CPA addition .....	99
4.4.3	Elution modelling data .....	100
4.4.4	Summary of modelled protocols for elution of PG and Me <sub>2</sub> SO .....	107
4.4.5	Effect of cryoprotectant on membrane integrity and functionality of the cells 116	
4.4.6	Effect of cooling rate .....	121
4.5	Discussion .....	128
4.6	Designed cryopreservation protocols .....	132
4.7	132	
Chapter 5	PROTOCOL ASSESSMENT .....	133
5.1	Introduction .....	134
5.1.1	Post-thaw assessment of cell survival .....	137
5.1.2	Functionality of Human Embryonic Stem Cells .....	137
5.1.3	Criteria for testing optimal cryopreservation protocol .....	140
5.2	Chapter aims .....	140
5.3	Materials and Methods .....	141
5.3.1	Embryoid body formation .....	141
5.3.2	Surface Marker Expression profiles .....	141
5.3.3	Differentiation potential of hESCs .....	141
5.3.4	Cell viability assay using conventional Annexin-V/PI .....	144
5.4	Results .....	146
5.4.1	Surface marker expression prior to freeze-thaw process .....	146
5.4.2	Formation of embryoid bodies (EBs) and spontaneous differentiation .	146
5.4.3	Osteogenic differentiation .....	146

---

5.4.4	Analysis of colony morphology .....	152
5.4.5	Post-thaw marker expression .....	152
5.4.6	Comparative analysis of cell survival using Annexin V/PI .....	152
5.5	Discussion .....	157
Chapter 6	GENERAL DISCUSSION .....	162
6.1	Challenges .....	163
6.2	Achievements .....	164
6.3	Future Work.....	166
6.3.1	Warming rate experiments.....	166
6.3.2	Addition of caspase inhibitors to optimised CPA media .....	167
6.3.3	Improvement of differentiation protocols .....	167
6.3.4	Expression of aquaporins on hESC membranes.....	168
6.4	Study conclusion .....	168

**Table of Figures**

Figure 1.1 Freezing in a binary system .....	2
Figure 1.2 Schematic of cell volume response in hypertonic and isotonic solutions .....	5
Figure 1.3 Two-factor hypothesis of freezing injury .....	9
Figure 1.4 Effect of cryoprotectant concentration on ice formation .....	13
Figure 1.5 Graph demonstrating cryoprotective action on salt concentration in red blood cells during cooling .....	15
Figure 1.6 Derivation of embryonic stem cells .....	21
Figure 1.7 Effect of LIF on pluripotency of hESCs .....	23
Figure 3.1 Standard curve for latex bead volume .....	56
Figure 3.2 Boyle van't Hoff plot for 2102Ep .....	58
Figure 3.3 Boyle van't Hoff plot for RH1 .....	59
Figure 3.4 Boyle van't Hoff plot for SHEF3 .....	60
Figure 3.5 2102Ep cell adhesion following exposure to anisotonic media .....	63
Figure 3.6 Cell volume excursion limits for 2102Ep .....	65
Figure 3.7 Cell volume excursion limits for RH1 .....	66
Figure 3.8 Cell volume excursion limits for SHEF3 .....	67
Figure 3.9 Best-fit curves for 2102Ep in Me <sub>2</sub> SO .....	71
Figure 3.10 Best-fit curves for 2102Ep in PG .....	72
Figure 3.11 Best-fit curves for RH1 in Me <sub>2</sub> SO .....	73
Figure 3.12 Best-fit curves for RH1 in PG .....	74
Figure 3.13 Best-fit curves for SHEF3 in Me <sub>2</sub> SO .....	75
Figure 3.14 Best-fit curves for SHEF3 in 5%PG .....	76
Figure 4.1 Schematic diagram of designing a cryopreservation protocol .....	87

---

Figure 4.2 Modelled protocols for addition of Me <sub>2</sub> SO to 2102Ep cells .....	92
Figure 4.3 Modelled protocols for addition of PG to 2102Ep cells .....	93
Figure 4.4 Modelled protocols for addition of PG to RH1 cells .....	94
Figure 4.5 Modelled protocols for addition of Me <sub>2</sub> SO to RH1 cells .....	95
Figure 4.6 Modelled protocols for addition of PG to SHEF3 cells .....	96
Figure 4.7 Modelled protocols for addition of Me <sub>2</sub> SO to SHEF3 cells.....	97
Figure 4.8 Modelled protocols for elution of Me <sub>2</sub> SO from 2102Ep cells.....	101
Figure 4.9 Modelled protocols for elution of PG from 2102Ep cells .....	102
Figure 4.10 Modelled protocols for elution of Me <sub>2</sub> SO from RH1 cells .....	103
Figure 4.11 Modelled protocols for elution of PG from RH1 cells .....	104
Figure 4.12 Modelled protocols for elution of Me <sub>2</sub> SO from SHEF3 cells.....	105
Figure 4.13 Modelled protocols for elution of PG from SHEF3 cells .....	106
Figure 4.14 Effect of exposure to 10% Me <sub>2</sub> SO on RH1 cells.....	117
Figure 4.15 Effect of exposure to 5%PG on RH1 cells.....	119
Figure 4.16 Effect of exposure to 10% Me <sub>2</sub> SO on SHEF3 cells .....	118
Figure 4.17 Effect of exposure to 5%PG on SHEF3 cells.....	120
Figure 4.18 Membrane integrity of RH1 cells in 10%PG at +20°C.....	122
Figure 4.19 Post-thaw results RH1 frozen in 10%PG.....	123
Figure 4.20 Membrane integrity of SHEF3 cells in 10%PG at +20°C. ....	124
Figure 4.21 Graphical representation of post-thaw results SHEF3 frozen in 10%PG.	125
Figure 4.22 Membrane integrity of RH1 cells in 10%Me <sub>2</sub> SO at +20°C. ....	126
Figure 4.23 Post-thaw results RH1 frozen in 10%Me <sub>2</sub> SO.....	127
Figure 5.1 hESC Colonies .....	139
Figure 5.2 Schematic diagram of viability assessment by Annexin V .....	145

---

Figure 5.3 Surface marker expression of 2102Ep cells .....	147
Figure 5.4 Surface marker expression of RH1 cells. ....	148
Figure 5.5 Surface marker expression of SHEF3 cells. ....	149
Figure 5.6. Embryoid bodies .....	150
Figure 5.7 RT-PCR analysis of hESC gene expression .....	151
Figure 5.8 Post-thaw analysis of hESC colony in Me <sub>2</sub> SO and PG.....	153
Figure 5.9 Surface marker expression of hESCs after undergoing freezing in Me <sub>2</sub> SO and PG. ....	154
Figure 5.10 Flow cytometry analysis of apoptosis following freeze-thaw using designed and unoptimised protocols. ....	155
Figure 5.11 Post-thaw analysis of apoptotic events in hESCs.....	156

## Acknowledgement

It has been a challenging journey and I would like to thank certain individuals who have helped me along the way. I am a sum of all the input from these individuals to whom I am very grateful.

First I would like to thank each of my three supervisors, David Pegg, Paul Genever and Charles Hunt for their insight, guidance and support. They were approachable and made it easy for me to ask questions of which there were many.

Thanks to the scientists at the UK Stem Cell Bank who were there to trouble-shoot especially when I encountered problems with culturing the human embryonic stem cell lines. They always provided helpful support and I am grateful.

The members of the Genever laboratory have been great with their help whenever I needed it. It was great to work with people who made the journey a bit easier and were always empathetic. I will miss all the cake eating, laughter and debates about world issues. I would like to thank Fatima Saleh who has been a colleague and, more importantly, a friend inside and outside the laboratory. I miss your Lebanese jokes.

Huge thanks goes to my super husband who has always been there for me. His was the shoulder I cried on through different frustrations and disappointments. He made me feel smarter than I felt I was. I was certain that he was praying for me. Gbenga, you are the best. To Tofunmi, my greatest achievement in life, I love you very much. Thank you for bringing smiles to my face.

I have been blessed with the greatest family anyone could have. Although none of them live in York, their support was very much felt. They were always ready to listen to me when I needed support and never made me feel I could not achieve what I had set out to do. I also thank my fantastic group of friends who have helped with babysitting my daughter so I could get work done. I love you guys very much.

“Trust in the LORD with all your heart and lean not on your own understanding; in all your ways acknowledge him, and he will make your paths straight.” I am not sure what I would do without my faith in God who I have had to trust these past few years to carry me through. Thank you.

## **Declaration**

All the work presented in this thesis is of my own. Human ES, SHEF3 and RH1 were kindly provided by the UK Stem Cell Bank. This thesis has not been submitted for any other degrees. Some of the data has been presented at scientific conferences.

# **Chapter 1**

## **INTRODUCTION**

## 1.1 Water and freezing

Pure water would normally freeze at temperatures below 0°C, but the presence of solutes (for example, salt) depresses the temperature at which the system freezes. As temperature decreases, water molecules spontaneously arrange (through hydrogen bonding) into a high energy crystalline structure that forms a 'nucleus' in a process known as nucleation. Due to the thermodynamically unstable nature of this 3-dimensional structure, the small high energy ice crystals coalesce to form larger, more stable ice crystals. However, the behaviour of the ice crystals is dependent on the rate of cooling and warming. When cooling is slow, it allows more time for small ice crystals to aggregate to form larger crystals while rapid cooling maintains the presence of many small ice crystals. This process, where water molecules initiate ice formation, is specifically known as homogeneous or primary nucleation, while a heterogeneous or secondary nucleation refers to ice formation initiated by the presence of an appropriate particle on which water molecules can bind. In a binary system of sodium chloride (NaCl) and water, the presence of the solute (ie NaCl) initiates freezing by bringing about a reduction in temperature below the freezing point of the system (Fig. 1.1). The water in the system form ice crystals, leading to an increase in the concentration of NaCl.

## 1.2 Cells

Cells are known to be largely composed of water which is important in the function and structure of organelles, protein and the plasma membrane. However, the volume of water reduces when cells are exposed to very low temperatures, thereby influencing the structure and function of proteins and the cell membrane. At such temperatures, it has been found that water bound to cell components does not freeze. This was done through measurements of the amount of electric energy required to melt a known sample of protein solutions and determining the latent heat of fusion released (Privalov, 1968). The latent heat of fusion released was less than expected, leading to the categorising of such bound water as nonsolvent water. Other work have determined that about 10% of the water in fully hydrated cells is not involved in the crystallisation of water into ice or melting (Koga et al., 1966;Schreuders et al., 1996;Sun, 1999).

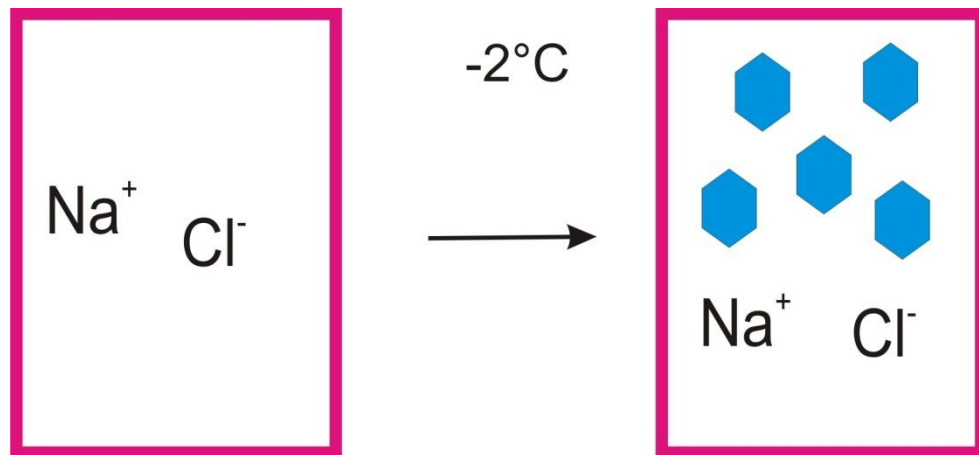


**Figure 1.1 Freezing in a binary system**

An illustration of the process of freezing in a binary system comprising of sodium chloride and water. As temperature depresses, secondary nucleation occurs where sodium chloride particles serve as nuclei onto which water molecules bind to initiate ice formation. The blue hexagonal structures represent ice crystals.

### 1.2.1 Mode of water and solute permeation

It is important to know the method by which 'freezable' water permeates the plasma membrane as this would impact upon the rate of water movement and therefore the location of ice. Based on the structure of the plasma membrane proposed by Davson and Danielli, the membrane is made up of a lipid bilayer. The polar head groups of the lipids are orientated into the cytoplasm while the nonpolar chains of each layer are faced inward towards each other (Fig.1.2). The mode of water permeation might then be proposed to occur through passive diffusion. A modified version of this bilayer model which is known as the fluid mosaic model, where the lipid bilayer is interspersed with proteins, is now the accepted structure of the plasma membrane (Singer and Nicolson, 1972). It has since been discovered that there are proteins which act as water channels known as aquaporins.

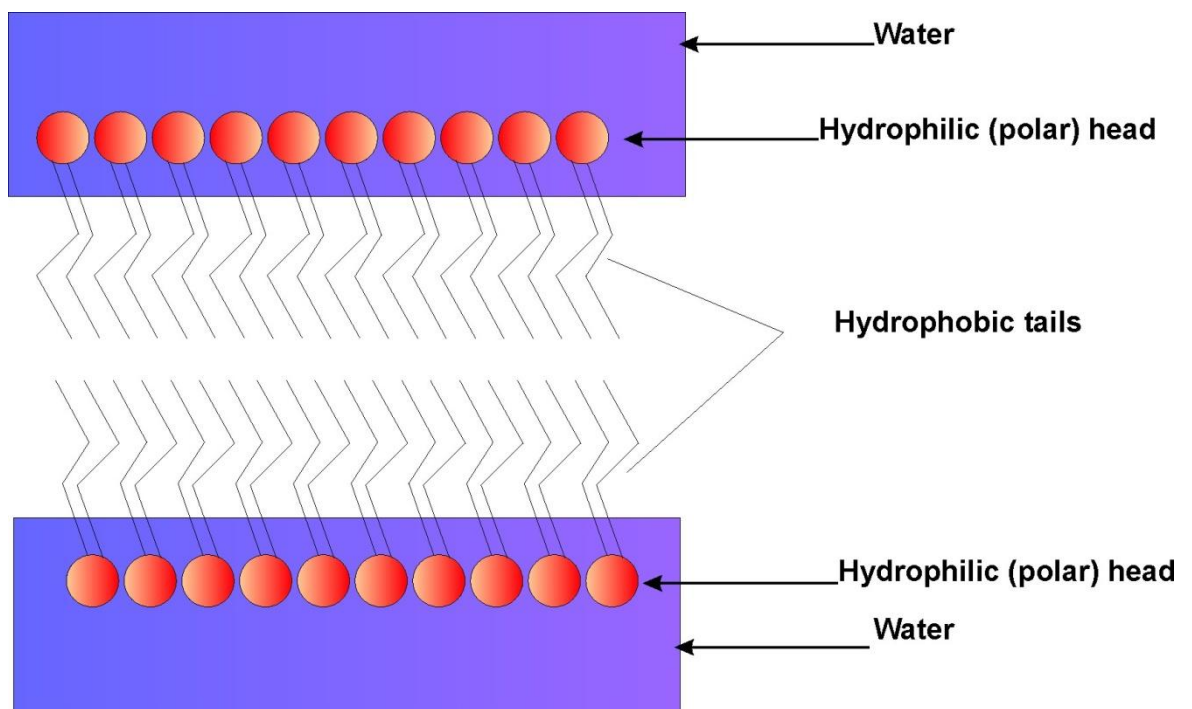


**Figure 1.2 Plasma membrane (Lipid Bilayer model)**

Structure of the plasma membrane with hydrophilic polar head groups facing the cytoplasm and aqueous extracellular space, while nonpolar tails form a hydrophobic core.

### 1.2.2 Aquaporins

The first aquaporin was found in red blood cell membranes and was initially termed CHIP28 (Benga et al., 1986; Moon et al., 1993; Agre et al., 1993a). Since then, aquaporins have been found in other mammalian cells and tissues such as rat testis (Ishibashi et al., 1997a), xenopus oocytes (Ishibashi et al., 1994a) and mouse oocytes and embryos (Edashige et al., 2000b; Sui et al., 2001). To date, nine aquaporins have been discovered, and shown to be responsible in transporting water and also small nonelectrolytes such as glycerol and urea (Ishibashi et al., 1994b; Ishibashi et al., 1997b).

The mode of transport of solutes and water through the lipid bilayer has been debated. Kedem and Katchalsky proposed the co-transport of water and solutes and developed a mathematical formula to describe this transport; this formula is known as the Kedem-Katchalsky (KK) formalism (Kedem and Katchalsky, 1958e). The variable referred to as reflection coefficient,  $\sigma$ , describes the degree of interaction between water and solutes; a value of 1 means that all of the solute is being reflected from the cell membrane and therefore there is no interaction between solute and water during transport while a value of 0 denotes that the membrane cannot distinguish between water and solute, hence resulting in their transport through a common channel.

The need for a reflection coefficient to determine the mechanism of water and solute transport has been opposed by the two-parameter (2P) formula, which assumes independent transport across the bilayer and characterises the cell membrane using the water permeability variable known as hydraulic conductivity ( $\mu\text{m}/\text{atm}/\text{min}$ ),  $L_p$ , and solute permeability ( $\text{cm}/\text{min}$ ),  $P_s$  (Jacobs, 1933c). Using a hypothetical cell with a known volume, the cell response when placed in a hypertonic solution with a subsequent return into isotonic medium was modelled. This produced a typical shrink-swell curve (Fig. 1.3) due to the initial efflux of water from the cell and the re-entry of both water and solute to maintain osmotic and solute concentration equilibrium. Using the KK and 2P formalisms to produce a curve that matched the cell volume response resulted in similar curves; the use of  $\sigma$  in the KK formalism did not produce a more accurate curve (Kleinhans, 1998d). More recently, the use of the 2P and KK formalisms to determine the permeability parameters of human blood platelets concluded that the 2P formalism produced more accurate results (Woods et al., 1999c). As a result, the 2P formalism provides a simpler means of determining permeability parameters of a cell and is widely used in cryopreservation experiments.

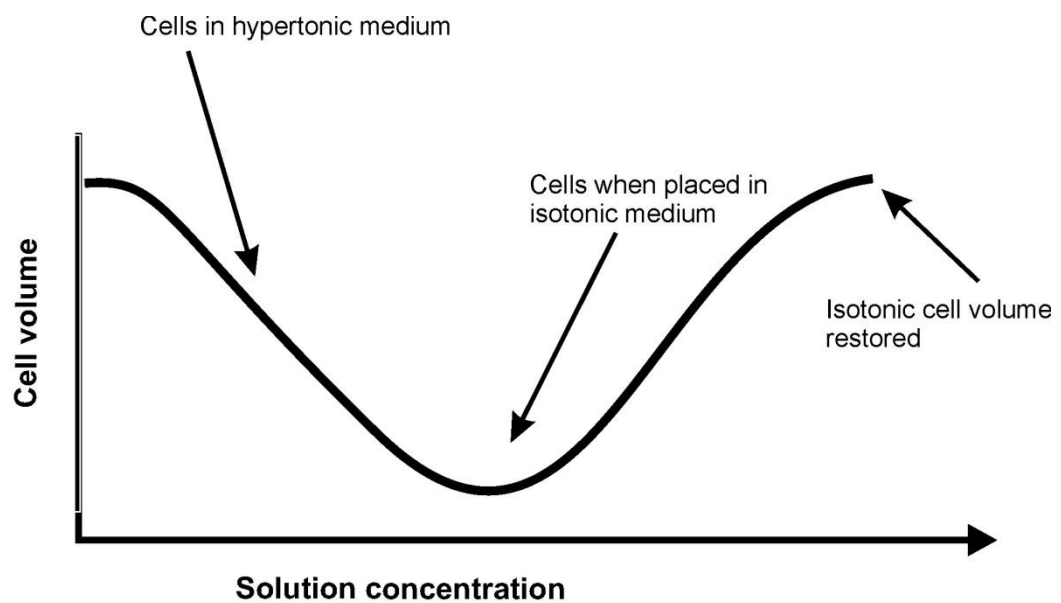


**Figure 1.3 Schematic of cell volume response in hypertonic and isotonic solutions**

Cells, when placed in hypertonic solutions respond by shrinking in cell volume due to water efflux and regain cell volume when placed in isotonic solution. The curve produced when plotting solution concentration and cell response is typically known as a shrink-swell curve.

### 1.2.3 Boyle van't Hoff

As mentioned above, a shrink-swell curve is produced when a cell is placed into hypertonic medium. However, the volume of water that is moving between the intra- and extracellular spaces is unknown but can be determined if cells are placed in hypo- and hypertonic media. The hypertonic solutions can be composed of variable amounts of impermeable solutes such as sucrose or sodium chloride (NaCl), while varying amounts of water can be used to dilute isotonic media in order to produce hypotonic solutions. In hypotonic solutions, cell volume increases from the influx of water while the opposite is true in hypertonic media due to the efflux of cell water. Consequently, any cell which responds accordingly is referred to as an 'ideal osmometer' as is the case with red blood cells (Lovelock, 1953c; Jacobs, 1962c; Pegg, 1984). Other cells such as mouse and bovine embryos have also been found to behave as ideal osmometers in anisotonic solutions (Mazur and Schneider, 1986). The resulting curve is known as the Boyle van't Hoff (BvH) plot which relates cell volume with osmotic pressure (or solute concentration). Extrapolation of the plot to determine cell volume at infinite osmolality reveals the nonosmotic volume,  $V_b$ , or the volume that does not get involved in a cell's osmotic response (Cook, 1967b); it can also be referred to as nonsolvent water (Bobo, 1967). More importantly, the BvH plot also identifies a cell's volume excursion limit, which is the extent of swelling or shrinkage that can be tolerated by a cell before any damage is experienced. Identifying a cell's value for  $V_b$  also helps determine the volume of osmotic or moveable water, which is important during the cryopreservation process because the volume of water diminishes as water becomes ice. Subsequently, the concentration of solutes in the system also changes. Both ice and high concentrations of salts have been found to be detrimental to cell survival (Lovelock, 1953b; Diller, 1979b).

## 1.3 Cryobiology

The science of cryobiology explores the effect of low temperature on living organisms. The subset field of cryopreservation aims to preserve the structure and function of cells and tissues by preventing or minimising damage experienced during the process of preservation.

### 1.3.1 Cryo-induced injuries

As already mentioned, ice formation and high solute concentration can cause damage to cells during the process of preservation, but there is also chilling injury which is a result of exposure to low temperatures. The various forms of damage are discussed below.

### 1.3.2 Chilling injury

Although organisms such as insects, frogs and snakes have developed methods of surviving whilst exposed to sub-physiological temperatures, many mammalian tissues and cells are unable to withstand low temperature exposure such as insect embryos belonging to *Drosophila* (Mazur et al., 1992), boar spermatozoa (Drobnis et al., 1993a) and *Caenorhabditis elegans* (Moss et al., 1997). Chilling injury has been associated with lipid-phase transition (LPT) in phospholipids of the cell membrane (Watson and Morris, 1987). Using Fourier transform infrared spectroscopy (FTIR), Drobnis and colleagues measured LPT in boar spermatozoa, shrimp (*Sicyonia ingentis*) and human sperm (Drobnis et al., 1993b). In addition, concentration of potassium ions was measured because potassium leakage has been shown to accompany lipid phase transitions from liquid crystalline to the gel phase (Quinn, 1985; Morris and Clarke, 1987). Each sperm sample was maintained at a range of low temperatures before the concentration of potassium in the extracellular medium was measured from each sample. For pig sperm, significant loss of potassium ions occurred between 18 and 20°C; for shrimp, LPT occurred between 13 and -2°C at the completion of which potassium leakage was maximum; human sperm, on the contrary, resisted chilling injury and no leakage was detected by FTIR possibly due to the high cholesterol content of the membrane (Watson and Morris, 1987; Drobnis et al., 1993c). LPT has also been detected in immature bovine oocytes between 13 and 20°C, while it was observed around 10°C in *in vitro* matured oocytes (Arav et al., 1996). In order to reduce chilling injury, therefore, membrane phospholipids should be stabilised using stabilisers such as sugars or lipids which bind to the polar groups of phospholipids (Strauss et al., 1986; Zeron et al., 2002).

Sugars are natural cryoprotective agents (CPAs) that have also been found to have an effect on the location of ice formed during freezing (Lee Jr et al., 1992) by ensuring that sufficient dehydration occurs in order to maintain equilibrium between the volume of water inside the cell and in its suspending medium in order to ensure that all ice formation occurs in the extracellular space. The effect of exposure to cold temperatures without sufficient dehydration of intracellular water creates susceptibility for intracellular ice formation (IIF) to occur when cells reach temperatures at which ice forms.

### 1.3.3 Intracellular ice formation (IIF)

To understand the damaging effects of ice, the process of freezing must be explored. Freezing occurs when the water in a system converts to ice through the spontaneous binding of water molecules to form a crystalline structure (Pegg, 2006). At 0°C, water and ice crystals coexist in equilibrium which is why the process can also be referred to

as 'equilibrium freezing'. When heat is added, the ice crystals melt while removing heat increases the amount of ice, therefore 0°C can be referred to as the freezing point or melting point ( $T_m$ ) depending on whether heat is being added or removed. As a result, freezing requires temperatures below the freezing point, a process known as supercooling, which can occur as low as -39°C where the presence of a nucleus initiates ice formation (Mazur, 1963a; Mazur, 1984c; Muldrew and McGann, 1990b). Once freezing is initiated, the latent heat of fusion is released (334kJ/kg), leading to a rise in temperature up to the freezing point. The temperature then remains at 0°C until all water in the system becomes ice.

The location of ice formation is influenced by the rate of cooling and the extent of supercooling (Mazur et al., 1969a; Diller, 1979a; Pegg et al., 1984a; Toner et al., 1991). Cells need to be in osmotic equilibrium before undergoing cooling in order to achieve high percentage of survival which has been found to follow the pattern of an inverted U when plotted against cooling rate (Fig. 1.4). It has been shown that survival is lowest at very low and very high cooling rates. Mazur and colleagues used Chinese hamster culture cells frozen at different cooling rates to illustrate this phenomenon (Mazur et al., 1972). Greatest loss of cell survival at very low cooling rate was attributed to the extended exposure of cells to high solute concentration; this is known as solution effect. At very high cooling rates, intracellular water is supercooled with tiny ice crystals which do not coalesce to form ice. However, the aggregation of these ice crystals to form larger ice can occur during warming in a process known as recrystallisation, and may explain the loss of cell survival. Consequently, rapid warming has been adopted as the preferred method of warming as it minimises the growth of intracellular ice by causing cells to bypass the nucleation temperature where ice crystals could grow (Mazur et al., 1972). These explanations of the causes of damage are referred to as Mazur's 'two factor hypothesis' (Mazur et al., 1972). An intermediate cooling rate where cells are able to lose water in order to maintain equilibrium with the suspending solution ensures highest survival.

Moreover, the formation of ice inside the cytoplasm has been found to be one of the main causes in the loss of survival of frozen cells (Pegg, 1987). Extracellular ice has also been found to have deleterious effects especially in tissues and organs because it disrupts the structure of the tissue (Pegg, 1987; Rubinsky and Pegg, 1988; Toner et al., 1990b).

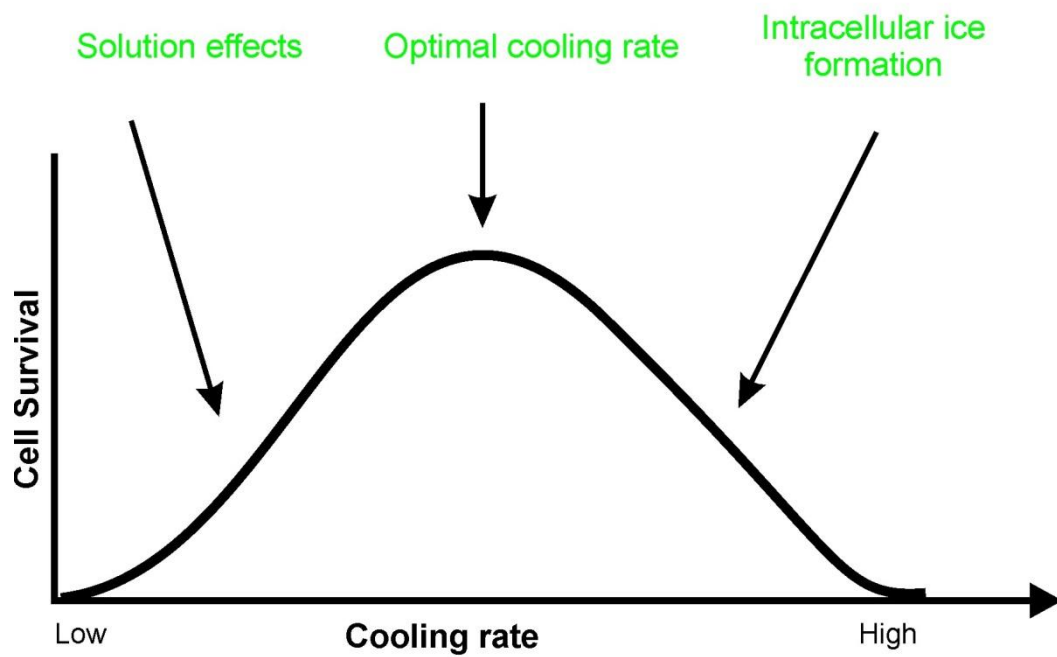


**Figure 1.4 Two-factor hypothesis of freezing injury**

A schematic diagram depicting the effect of cooling rate on cell survival; cell survival is compromised at very low cooling rates by solution effects and at very high cooling rates by intracellular freezing.

### 1.3.4 Other forms of cryoinjury

It has also been argued that it is not the formation of ice in the system which causes damage but the resulting high salt concentration that the cells are exposed to (Mazur, 1984b). Published literature by Lovelock demonstrated the effect of solute concentration by using red blood cells suspended in isotonic saline. Subsequent freezing of the red cells showed damage between -3 and -10°C, which corresponds to the freezing point of isotonic saline, showing that haemolysis occurred where salt concentration was high (Lovelock, 1953a).

Using erythrocytes suspended in 1300mOsm/kg of non-penetrating solutes, it was hypothesised that the solutes in the suspending medium exerted osmotic pressure on the cell membrane through the excessive shrinkage in cell volume causing haemolysis (Meryman, 1971). This led to the '*minimum volume*' theory (Meryman, 1968; Meryman, 1974), which states that cells can only tolerate a certain level of volume reduction. If this volume is exceeded due to the loss of osmotically active water, it can lead to the disorganisation of the cell contents and undue pressure on the plasma membrane, resulting in injury. Each cell type has its unique volume excursion limit. Generally, cell volume excursion for mammalian cells should be restricted to  $\pm 40\%$  (Pegg, 1994).

### 1.3.5 Cell-cell contact

Other mechanisms for freezing injury have been attributed to cell density, which theorises that densely packed cells are more susceptible to damage as a result of mechanical stress due to the propagation of ice crystals during recrystallisation (Pegg, 2006). Ice crystals disrupt the organisation of the cells, which is particularly crucial in tissues and organs which have a complex of cells to maintain their structure and functionality (Acker and McGann, 2000c).

Evidence shows that the cell membrane plays an integral role in the propagation of ice crystals. In a study which investigated the mechanism of how this occurs, hamster fibroblast cells were cultured in 3 different ways: as a confluent monolayer, in suspension and as single cells attached to tissue culture plastic (Acker and McGann, 2000b). The fluorescent stain, SYTO, which attaches to nucleic acids, was used to detect the presence of intracellular ice through the lack of fluorescence when IIF occurs. Ethidium bromide (EB) was used to detect damaged cell membranes through the presence of red fluorescence. It was found that the cells in a monolayer which had cell-cell contact had the highest occurrence of intracellular ice of all the culture models, indicating that the occurrence of IIF in one cell can initiate nucleation in other cells when they are in contact. Furthermore, cells which were in suspension or individually

attached to the tissue culture vessel showed no significant difference in the number of cells with intracellular ice and those with damaged cell membranes. However, cells in a confluent monolayer showed a significant difference in the occurrence of IIF and cells that had lost membrane integrity; at  $-9^{\circ}\text{C}$ , 100% of the cells showed an incidence of IIF while only 20% of the cells showed damaged membranes, which suggests that intracellular ice does not have mechanical effect on cell membranes (Acker and McGann, 2000a). From the evidence in this particular study, it may be concluded that damaged cell membranes may lead to IIF by allowing ice formed in the extracellular medium pass through the membrane to induce nucleation in the cytoplasm. Mazur has also shown that the cell membrane is a site of injury when frozen yeast cells were found to leak their cell contents showing that cells with IIF possess damaged cell membranes (Mazur, 1965c). It has been suggested that extracellular ice changes the chemical, electrical and physical properties of the cell membrane leading to the loss of membrane integrity (Mazur, 1965b; Toner et al., 1990a; Harris et al., 1991).

In addition, it could be argued that cells in the confluent layer are contact inhibited and in the quiescent (G0) phase of the cell cycle. While sub-confluent cells, individually attached to tissue culture are likely to be actively cycling and continue to proliferate. Freezing should, therefore, occur while cells are still dividing in order to maximise recovery.

Gap junctions, protein channels which connect one cell to another and allow passage of solutes, been recorded to facilitate ice formation. Madin-Darby canine kidney (MDCK) cells which do not form gap junctions when in monolayer culture, were frozen at cooling rates ranging from  $0.2$  to  $10^{\circ}\text{C}$  with no difference in survival at slow or rapid cooling. This suggests that the cells were not susceptible to intracellular freezing (Armitage and Juss, 2003b). In contrast, tissues and organs which have a complex system of cellular interactions pose challenges as shown in various studies (Berger and Uhrig, 1996; Acker et al., 1999).

### *1.3.6 Cryoprotectants (CPAs)*

In order to minimise damage in cells and tissues during the process of preservation, compounds referred to as cryoprotectants (CPAs) have been shown to provide protection. The protective nature of one such compound was realised with glycerol in 1969 by Smith, Polge and Parkes. It was discovered that the compound preserved the motility of fowl spermatozoa upon thawing from  $80^{\circ}\text{C}$  (Polge et al., 1949b). CPAs can be categorised into permeating and non-permeating groups. Permeating CPAs can traverse the lipid membrane, and are therefore able to maintain osmotic equilibrium by balancing the solute concentration gradient that occurs when cell water effluxes. These

compounds include glycerol, dimethyl sulphoxide ( $\text{Me}_2\text{SO}$ ), ethanediol (also known as ethylene glycol, EG), and propylene glycol (PG). Nonpermeating CPAs are unable to address the concentration gradient which makes them a less preferable choice for cryoprotection. Impermeable or non-penetrating CPAs include compounds such as trehalose, D-mannitol and sucrose.

### **1.3.6.1 Mechanisms of CPA protection**

The mechanism by which CPAs protect cells is unknown but several theories exist. Generally, CPAs act by reducing the nucleation temperature of cells which means that ice formation occurs at a much lower temperature due to increased concentration of solutes in the system (Pegg, 1994). To illustrate this action, cold-acclimated and non-cold acclimated rye protoplasts were suspended in a hyperosmotic solution. Cold-acclimated protoplasts accumulate more solutes, and it was found that their nucleation temperature was much lower than that of non-cold acclimated rye protoplasts ( $-42^\circ\text{C}$  and  $-14^\circ\text{C}$ , respectively) despite equal cell volumes (Dowgert and Steponkus, 1983).

Moreover, media containing glycerol, sodium chloride and water were subjected to varying sub-zero temperatures with concentration of salts measured at different temperatures (Mazur et al., 1981a). The results of the experiment are displayed in figure 1.5, which shows a higher proportion of unfrozen water with increasing concentrations of glycerol. This means that ice forms at a lower temperature with increasing CPA concentration, resulting in the presence of a larger volume of unfrozen water at lower temperatures. Although a comparative study using  $\text{Me}_2\text{SO}$  was not carried out, the experiment illustrates the cryoprotective action of permeable CPAs. However, since  $\text{Me}_2\text{SO}$  is more permeable to the cell membrane, it is more likely to cause a larger proportion of unfrozen water at similar subzero temperatures than glycerol which means ice would form at even lower temperatures.

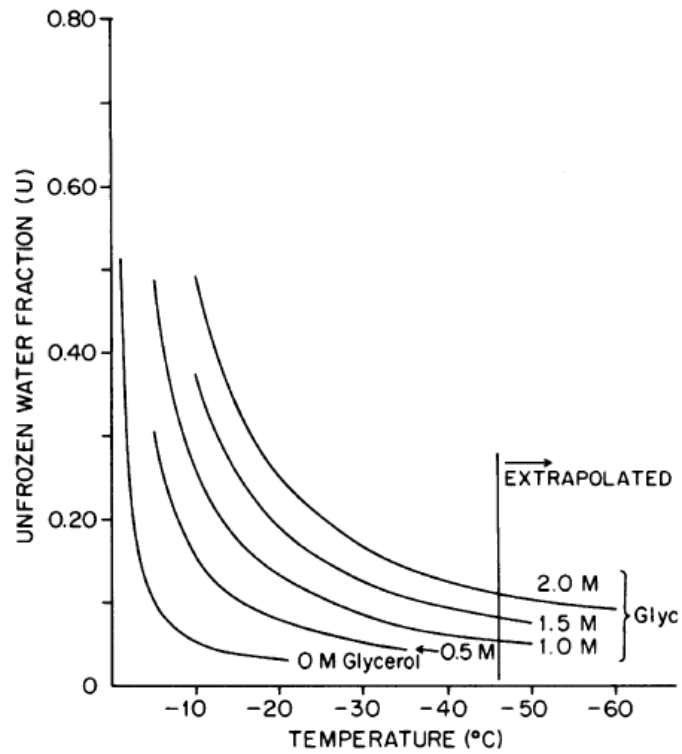


**Figure 1.5 Effect of cryoprotectant concentration on ice formation**

The diagram from Mazur 1981 shows the proportion of water that remains unfrozen at any given subzero temperature in a NaCl-glycerol-water solution with varying concentrations of glycerol. The unfrozen water fraction increases with increasing concentrations of glycerol, meaning that ice formation decreases with increased concentrations of cryoprotectant.

Furthermore, CPAs have been shown to protect cells by decreasing the concentration of damaging salts that the cells are exposed to, which is referred to as colligative action (Lovelock, 1953d). Solutions containing glycerol, salts and water were also used to demonstrate the protective action of CPAs. Measuring the concentration of salts in the solution at various temperatures showed that the concentration of salts at any temperature was lower with increasing concentrations of glycerol (Figure 1.6) (Lovelock, 1953e). This same protective action has been found with  $\text{Me}_2\text{SO}$  (Lovelock and BISHOP, 1959). Simulations carried out by Sum and Pablo of dipalmitoylphosphatidylcholine (DPPC) lipid bilayer/water systems in the presence of  $\text{Me}_2\text{SO}$  found that  $\text{Me}_2\text{SO}$  caused dehydration of the lipid bilayer through hydrogen-bonding with water molecules (Sum and de Pablo, 2003). Its hydrophobic groups (two methyl groups) and small molecular size gives  $\text{Me}_2\text{SO}$  ability to permeate the lipid bilayer with its hydrophobic and hydrophilic regions (Anchordoguy et al., 1992). However, it is important to note that glycerol has been found to make cells such as red blood cells and MDCK cells more susceptible to intracellular freezing and therefore lower survival (Diller, 1979c; Armitage and Juss, 2003a). In a comparison of the cryoprotective action of glycerol and PG, it was found that PG was better at protecting red blood cells than glycerol (Boutron and Arnaud, 1984). PG was also found to be most effective for mature bovine oocytes (Lim et al., 1999). However, PG has been shown to adversely affect the physiology of mouse oocytes by increasing the concentration of calcium, thereby hardening the zona pellucida (Larman et al., 2007c). Moreover, disaccharides have been found to stabilise the cell membrane during freezing through interactions with the phosphate groups of the lipid bilayer more than other compounds such as  $\text{Me}_2\text{SO}$  and glycerol, which are more toxic to the membrane (Anchordoguy et al., 1987c). As a result, the choice of CPA must therefore be determined for each cell type to find which is most suitable. The requirements for CPAs to confer protective action are that they are penetrable to the cell membrane, of low toxicity and molecular weight, and possess high solubility in aqueous solutions (Pegg, 1994).

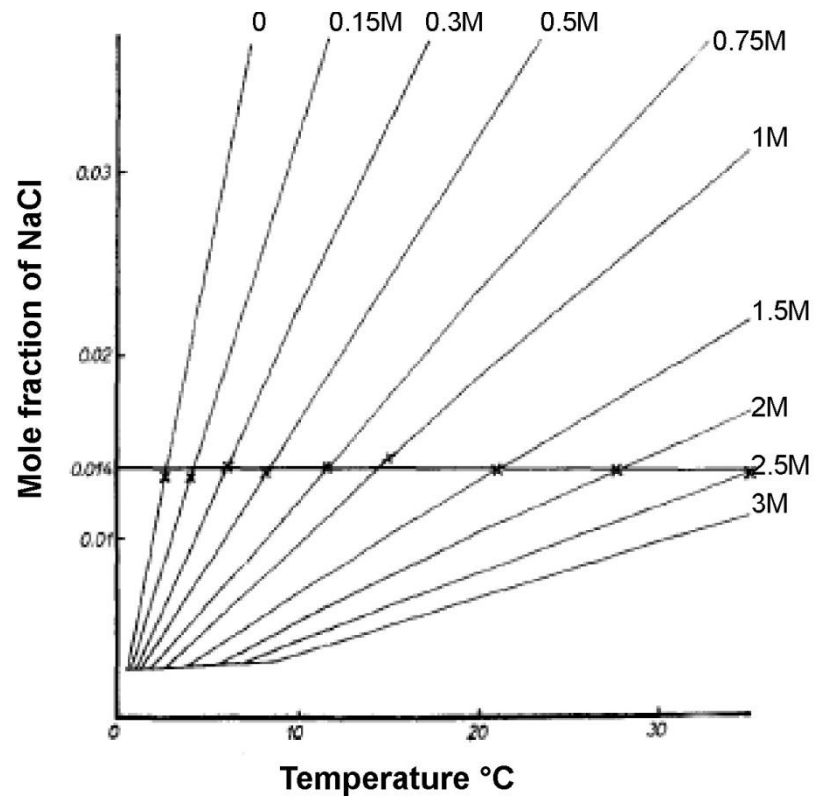


**Figure 1.6 Graph demonstrating cryoprotective action on salt concentration in red blood cells during cooling**

The lines represent solutions with increasing concentrations of glycerol. It can be seen that the concentration of sodium chloride at a given temperature reduces as the glycerol concentrations increase. The horizontal line at 0.014 represents the salt concentration at which haemolysis of red blood cells first occurred. Diagram was adapted from Lovelock, 1953.

## 1.4 Vitrification

A cocktail of CPAs is generally used in vitrification where, unlike freezing, cell material solidifies into a highly viscous state without the formation of ice occurring (Mazur, 1984a). A combination of different CPAs have been utilised in cryopreservation in order to avoid using damaging concentrations of one CPA and to achieve the necessary cell volume that would avoid damage (Ishimori et al., 1992; Ishimori et al., 1993; Paynter et al., 2005c). Viscosity is measured using the unit Poise (Pascal.second, Pa.s) and describes a fluid's resistivity to flow. The viscosity of pure water is  $9 \times 10^{-3}$  Poise or Pa.s (Yannas, 1968) while that of a vitrified solution is about  $10^{13}$  Poises. This state of viscosity can be described as 'glassy.'

During freezing, the decrease in temperature causes an increase in solute concentration due to ice formation until the temperature reaches the glass transition temperature ( $T_g$ ) where any remaining liquid, which has not been converted to ice, vitrifies. The  $T_g$  of pure water is about  $-140^\circ\text{C}$  but the presence of CPAs causes vitrification to occur at a higher temperature. This means that frozen materials contain both vitrified liquid and ice crystals. In addition, due to the fact that there is no phase change in vitrification as in freezing, no latent heat is released. However, there is a change in specific heat, the amount of heat required to raise the temperature of a material by one degree Celsius.

Although cells can tolerate conventional freezing, the high concentrations of CPA required for vitrification pose a toxic effect. Generally, a 60% (w/w) concentration of CPA to cell material is required in order for vitrification to occur. Glass-forming CPAs such as butanediol, PG and EG, differ in their glass-forming capacities. Butanediol is the best glass former of the CPAs mentioned, vitrifying at a concentration of about 35% (w/w). Moreover, there is a higher probability of vitrification occurring when cooling is rapid because the nucleation temperature is passed too rapidly to permit formation of ice. However, vitrification can occur with slow cooling if the concentration of CPA is extremely high, but again this is disadvantageous due to the toxic effects of the chemicals. Progress in developing vitrification solutions that will produce better vitrification more easily has been reported (Fahy et al., 1984; Fahy et al., 2004). Solutions combining sugars and polyalcohols are currently utilised. It has also been discovered that vitrification is most easily realised with minimum sample volume because of a lesser volume of water which has to be cooled. The small sample size decreases the probability of ice formation and ensures rapid cooling can occur (Arav et al., 2002).

While ice formation does not occur during vitrification compared to freezing, there is a probability of ice crystals forming during rewarming of vitrified material. This process is called devitrification where the nucleation temperature is encountered, leading to an increase in the number of nuclei which then support crystal growth as temperature increases. The occurrence of freezing or vitrification is dependent on two main factors: the type of CPA present and the cooling rate (Mazur, 1963b; Sutton, 1991; Yavin and Arav, 2007).

Vitrification has proven a useful cryopreservation procedure as it has been successfully employed in the storage of human oocytes and embryos (Kuwayama, 2007), mouse embryos (Kasai et al., 1990) and human embryonic stem cells (hESCs) (Reubinoff et al., 2001b; Richards et al., 2004a; Li et al., 2010c).

## 1.5 Stem cells

At the root of every cell type are a group of cells known as stem cells which have not acquired a defined identity and therefore can generate any cell type. It is this developmental potential of stem cells that make them attractive for research investigations and possible use in cell therapy.

There are different categories of stem cells; totipotent stem cells refer to germ cells (spermatozoa and oocytes) which can generate fertilised ova and continue in embryonic development to differentiate into every cell in the body. Pluripotent stem cells, however, have a more restricted differentiation capability but are still able to generate cells from the three germ layers: endoderm, mesoderm and ectoderm. Pluripotent stem cells can be isolated *in vitro* at the blastocyst stage of embryonic development. Moreover, there are multipotent stem cells which are only able to differentiate into cells of specific lineages such as mesenchymal stem cells (MSCs), neural and haematopoietic stem cells (HSC). The most characterised of these cells is the HSC.

### 1.5.1 Hematopoietic stem cells

The repopulation of blood cells (also known as haematopoiesis) is dependent on the self renewal capability of a small population of HSCs, which are found in 0.05 to 0.5% of the cells in the bone marrow (Gunsilius et al., 2001c) and have a turnover rate of about 2 weeks (Wilson et al., 2008). Although HSCs have also been found in peripheral blood, evidence shows that the population in the bone marrow of mice is 50-150 times that found in peripheral blood, while up to 10 times the population is found in human bone marrow than the peripheral blood counterpart (Lewis et al., 1968; Richman et al.,

1976). HSCs have also been found isolated from umbilical cord blood (Broxmeyer et al., 2003).

Phenotypically, murine HSCs have high level expression of the multidrug resistant (MDR) proteins, aldehyde hydrogenase (ALDH) and surface marker, sca-1 (Jones et al., 1996). Human HSCs, however, can be identified by their high level expression of the surface glycoprotein CD34 and very low expression or absence of CD33, CD38, thy-1 and CD71 (Gunsilius et al., 2001b).

HSCs can be categorised into short-term and long-term repopulating cells. Short-term HSCs are the more committed cells and do not self-renew while the rare long-term HSCs possess self-renewing capabilities (Gunsilius et al., 2001a; Yoder, 2005). It is important to note that long-term human HSCs express high levels of CD34 which is down-regulated in long-term murine HSCs (Okuno et al., 2002). The combination of HSCs and more differentiated cells called progenitors accounts for the reconstitution of the haematopoietic system. There are two groups of progenitors, common lymphoid progenitors and common myeloid progenitors, which are responsible for the generation of B and T cells, natural killer cells, platelets, granulocytes and monocytes (Akashi et al., 2000).

Numerous cytokines are responsible for maintaining the activity of HSCs and haematopoietic progenitor cells (HPCs) in the body through the binding of specific receptors and the activation of various signalling pathways (Smith, 2003b). Granulocyte colony stimulating factor (G-CSF) promotes proliferation while tumour necrosis factor-alpha (TNF- $\alpha$ ) can either inhibit or activate HSCs depending on their concentration (Smith, 2003a). Wnt3a protein has also been found to act as a growth factor for HSCs (Ema and Nakauchi, 2003).

### 1.5.2 Embryonal carcinoma cells

Although adult stem cells like HPCs have been useful in the regeneration of blood and its derivatives- platelets, leukocytes and erythrocytes, - more primitive cells which possess greater differentiation capabilities would advance the field of cell therapy. Cells which have been useful in cell therapy research were discovered by Finch and Ephrussi in mice (Finch and Ephrussi, 1967a). These cells were referred to as teratocarcinomas because they were derived from a tumour, or teratoma, in mouse testis. These tumours occur more frequently in ovaries and are also known as ovarian cysts (Stevens and Varnum, 1974). The isolation of the tumours and sub-culturing of these cells *in vitro* revealed pluripotent cells that could differentiate into cells of the germ layers- endoderm, mesoderm and ectoderm- which led to the term embryonal

carcinoma (EC) cells (Martin, 1981b;Evans and Kaufman, 1981f;Evans and Kaufman, 1981g). EC cells maintained their undifferentiated status while in culture (Finch and Ephrussi, 1967b;Evans and Kaufman, 1981e) which was confirmed by subsequent teratoma formation when the cells were injected back into a mouse host. This was a major discovery which enhanced the understanding of early embryonic development.

Following the successful derivation of murine EC cells, human EC cell lines have since been established. Many of the early cell lines, such as TERA1 and TERA2 (Fogh and Trempe, 1975), possessed limited differentiation capacity. Successive cell lines such as the subclonal line of TERA2 and NTERA2 possessed wider differentiation capabilities (Andrews et al., 1984b). Although mouse and human EC cells are similar in morphology, expression of alkaline phosphatase (Bernstine et al., 1973;Benham et al., 1981) and growth characteristics, they differ in their expression of the stage-specific embryonic antigen SSEA1 (Kannagi et al., 1982). In mouse EC cells, the expression of SSEA-1 is an indication of their undifferentiated state, while the opposite is the case in human EC cells. In addition, human EC cells express SSEA3 and SSEA-4 antigens which are not expressed in murine EC cells (Kannagi et al., 1983). A further discovery was made when pluripotent cells were directly derived from the mouse blastocyst. These cells were termed mouse embryonic stem (mESC) cells (Martin, 1981a). It was important that mESCs were harvested at the right stage of embryonic development, which was determined to be 5 days post-coitum (Evans and Kaufman, 1981d). Earlier attempts to obtain ESCs from 3.5-day inner cell mass (ICM) and 6.5-day ectoderm failed (Solter and Knowles, 1975;Atienza-Samols and Sherman, 1978). It was also discovered that greater success in acquiring mESCs was influenced by the occurrence of diapause, a naturally occurring delay in blastocyst development which leads to an increase in the number of epiblast cells and therefore ESCs (Evans and Kaufman, 1981c). Diapause occurs in female mice that have produced one litter and become pregnant while still nursing (Evans and Kaufman, 1981b).

### 1.5.3 Embryonic stem cells (mouse and human)

Following the discovery about mouse blastocysts, ESCs have also been derived from human blastocysts. The first human embryonic stem cells (hESCs) were derived from the ICM of pre-implantation embryos (Thomson et al., 1998g) (Fig. 1.7). One study found that there were more ICM cells in day 8 blastocysts than in earlier blastocysts (Stojkovic et al., 2004a), resulting in greater probability of forming a hESC line. The embryos are cultured *in vitro* for 5-8 days before the ICM is isolated from the blastocysts and transferred onto a feeder layer comprising mouse embryonic fibroblasts (MEFs) (Bongso et al., 1994;Reubinoff et al., 2000f;Stojkovic et al., 2004b).

Feeder-free culture of hESCs have been developed (Xu et al., 2001a;Rosler et al., 2004d;Mallon et al., 2006;Van Hoof et al., 2008b) but requires an initial culture on MEFs for a few passages before transferring to a matrigel-coated tissue culture vessel which is then maintained in culture with MEF-conditioned media. Advances have been made to develop defined media that support feeder-free cultures of hESCs such as mTeSR by Stemcell Technologies and NutriStem by Stemgent. However, the cost of creating large banks of MEF cells is eliminated, and hESCs cultured without feeders may be utilised for clinical purposes. In order to bypass the use of MEFs at any stage of hESC culture, human-derived feeder cells have been developed from human foreskin fibroblasts (Inzunza et al., 2005a;Amit and Itskovitz-Eldor, 2006;Stacey et al., 2006). hESC colonies grown on mitotically-inactivated human feeders have been found to be comparable to those cultured on MEFs, which makes the use of hESCs more clinically acceptable because of the lack of animal components in the growing of the cells. Moreover, serum-free media have also been developed in aid of creating hESCs which have not been in contact with animal-derived reagents before being used for therapeutic purposes (Richards et al., 2004a;Inzunza et al., 2005b;Passier et al., 2005b).

Mouse ESCs (mESCs) also require a feeder layer or the presence of leukaemia inhibitory factor (LIF) in growth medium to sustain an undifferentiated status (Nichols et al., 1990c;Fagundez et al., 2009). The absence of a feeder layer or LIF results in the development of three-dimensional cell aggregates known as embryoid bodies (EBs), which have been found to possess cells from all three germ layers (Evans and Kaufman, 1981a;Itskovitz-Eldor et al., 2000d;Reubinoff et al., 2000e;Fagundez et al., 2009).

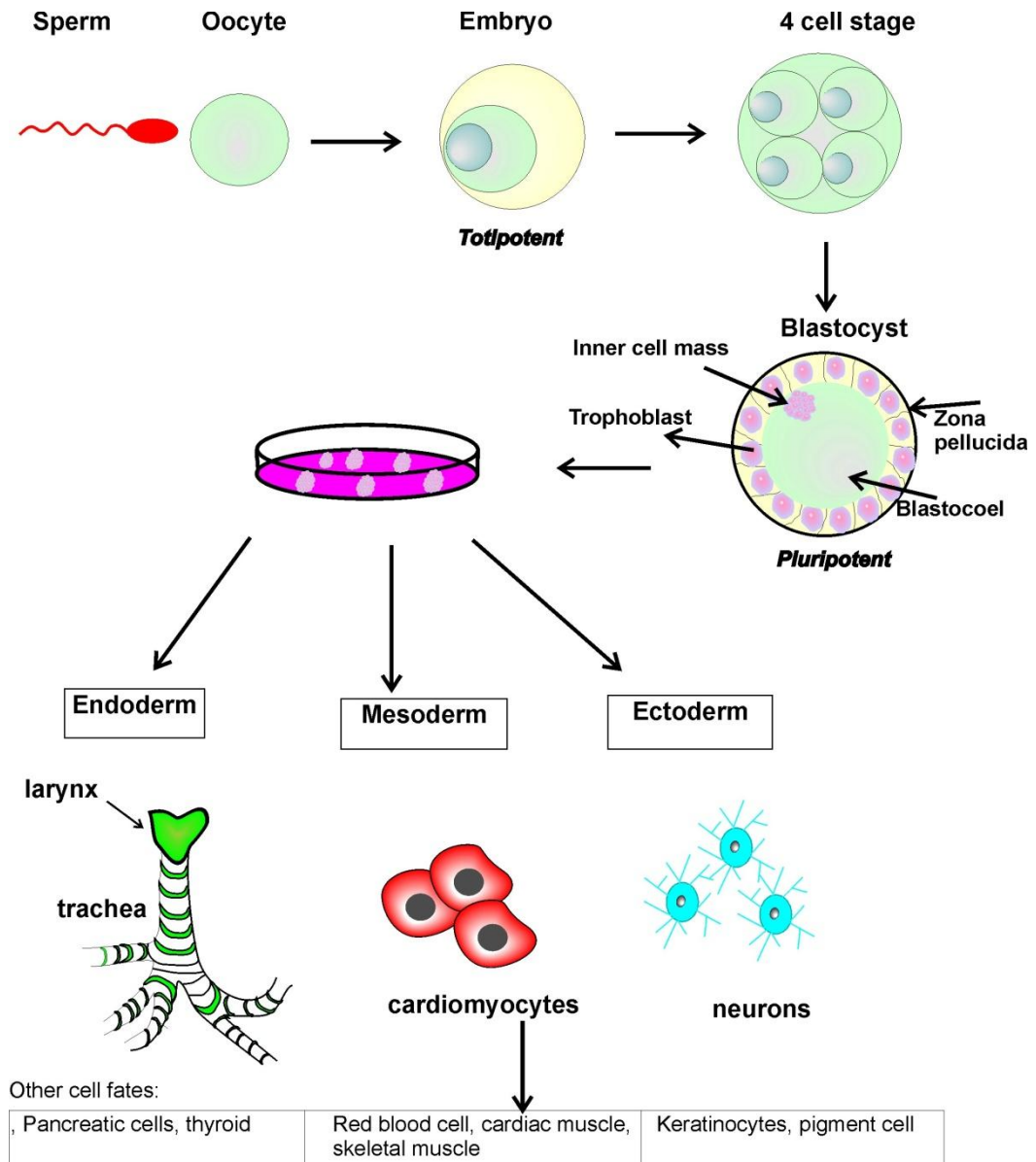


**Figure 1.7 Derivation of embryonic stem cells**

The inner cell mass from pre-implantation embryos is separated from the blastocyst and cultured *in vitro*. The resulting colonies formed have been found to contain cells which are pluripotent and differentiate into cells from the three germ layers. Examples of the types of cells they can potentially differentiate into are displayed.

It is not entirely clear how MEFs maintain the undifferentiated state of hESCs, but one study found that factors such as differentiation inhibiting activity (DIA) and leukaemia inhibitory factor (LIF), which are expressed in MEFs, seemed to regulate the pluripotentiality of hESCs (Nichols et al., 1990b). LIF binds to its receptor complex comprising a LIF receptor and a transmembrane protein known as gp130, activating the JAK/STAT3 pathway (Fig. 1.8). The janus family tyrosine kinases (JAK) phosphorylate STAT3 protein resulting in its translocation from the cytoplasm to the nucleus. STAT3 then binds to DNA, inducing the transcription of self-renewal genes (Kristensen et al., 2005). Although hESCs have remained undifferentiated in the absence of feeders, the hESC medium was supplemented with DIA and LIF (Nichols et al., 1990a). In addition to providing an extracellular matrix (ECM) to maintain the undifferentiated state of hESCs, MEFs are known to also detoxify the culture medium and secrete proteins required to promote cell growth (Lim and Bodnar, 2002). As a result, feeder-free systems which have been developed incorporate the use of MEF-conditioned medium for hESCs in *in vitro* culture (Xu et al., 2001b; Rosler et al., 2004c; Amit and Itskovitz-Eldor, 2006). Although LIF is integral to the maintenance of mESCs in culture, it is not adequate for the self-renewal process of hESCs.

Other factors such as basic fibroblast growth factor (bFGF) (also known as FGF-2) and activin/nodal have been deemed essential for the self-renewal of hESCs (Brons et al., 2007). bFGF promotes self-renewal of hESCs by inhibiting differentiation through the activation of phosphatidylinositol 3-kinase (PI3K)/Akt/PKB pathway (Kim et al., 2005). The PI3K/Akt/PKB pathway supports the expression of extracellular matrix molecules (ECMs), suggesting that these molecules are required for maintaining the undifferentiated state of hESCs. Moreover, activin/nodal pathway maintains pluripotency through the activation of intracellular proteins known as SMADs. SMADs belong to a family of proteins similar to the gene products of the *Drosophila* (Mad) and *C. elegans*, which are collectively referred to as Sma proteins. When nodal binds to activin receptors on the cell membrane, SMAD2/3 are phosphorylated. SMAD2/3 then form a complex with SMAD4 before translocating to the nucleus to promote transcription of Oct3/4 (Oh and Li, 1997; Gu et al., 1999; Song et al., 1999). Previous findings discovered that inhibition of SMAD2/3 phosphorylation led to the loss of Oct3/4 expression in hESC (James et al., 2005a). However, there was no decrease in expression of Oct3/4 in the *in vitro* culture of mESC (James et al., 2005b).

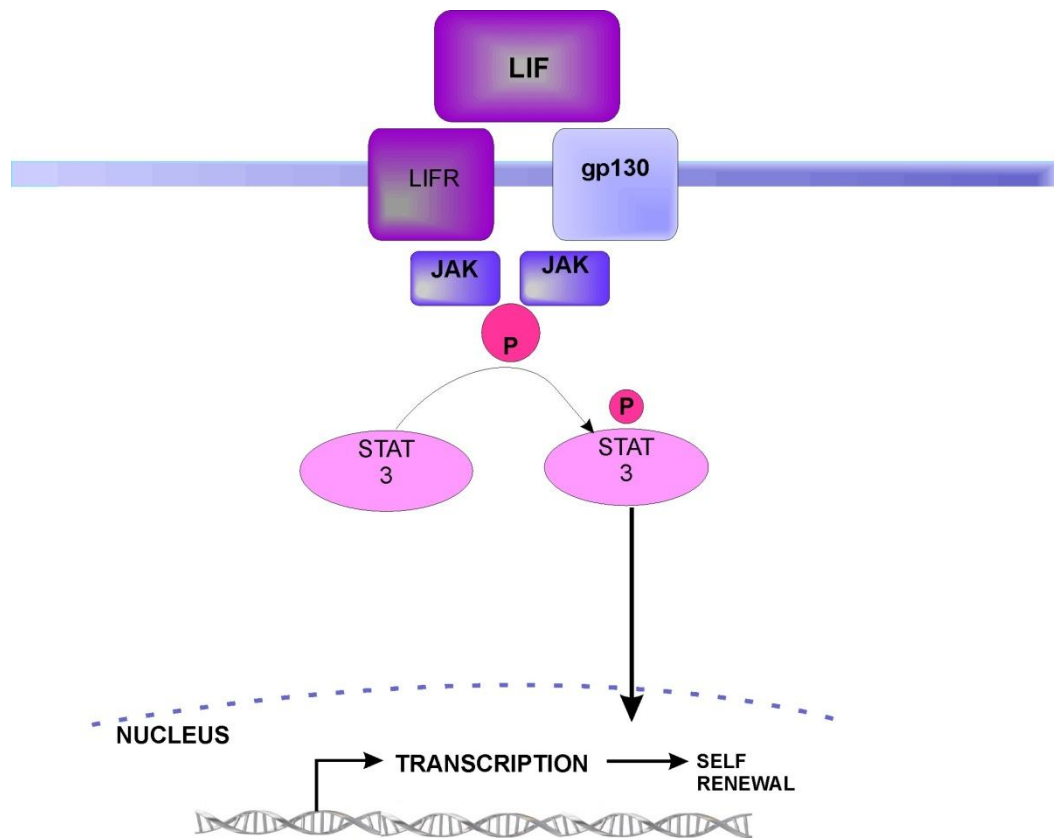


**Figure 1.8 Effect of LIF on pluripotency of hESCs**

The binding of LIF to its receptor complex initiates the recruitment of JAK kinases which activate the STAT3 signalling pathway and promote transcription of self-renewal genes.

Other reports have shown a decrease in levels of Oct3/4 in mESC due to the loss of SMAD2/3 or nodal (Conlon et al., 1994;Gendall et al., 1997a;Robertson et al., 2003;Vallier et al., 2004), but the disparity in the reports has been attributed to the differences between gene expression *in vitro* and *in vivo*.

Several genes have been used to characterise the pluripotency of mESCs and hESCs such as alkaline phosphatase (AP) and telomerase (Thomson et al., 1998f). However, a major difference between mESCs and hESCs is the expression of stage specific embryonic antigen, SSEA1. Like mouse EC cells, the expression of SSEA1 in mESCs denotes their undifferentiated state while the opposite is true in hESCs. Other genes that have been used to identify undifferentiated hESCs are tumour rejection antigens TRA-1-60 and -81, along with expression of proteins, SSEA3/4 and octamer transcription factor, Oct4 (Adewumi et al., 2007f).

Oct4 is a nuclear factor that binds specifically to the promoter region of DNA expressed in undifferentiated cells (Rosner et al., 1990), positively promoting the transcription of the octamer motif found on genes such as Nanog (Kuroda et al., 2005), FGF4 (Yuan et al., 1995;Ambrosetti et al., 2000) and UTF1 (Nishimoto et al., 1999). Nanog is a transcription factor present in the ICM, undifferentiated mESC and hESCs. It is important for maintaining the ICM *in vivo* and ESCs *in vitro*. Knockdown of Nanog has resulted in the upregulation of transcription factors Gata4/6, which are required for endoderm differentiation (Rossant, 2004). Oct4 has been detected in both ovary and testis because they contain totipotent cells, with the ability to differentiate into any cell type. Expression of Oct4, therefore, indicates the capability of cells to remain undifferentiated.

SSEA3 and SSEA4, expressed in hESCs and not in mESCs, are cell surface antigens which have been found on human and also primate ESCs. Previous work determined these antigens to be carbohydrates and changes in their carbohydrate structure appear to influence the development of pre-implantation embryos (Shevinsky et al., 1982;Andrews et al., 1982b).

Unlike SSEA3/4, TRA-1-60 is a proteoglycan and has been found expressed by EC cells (Andrews et al., 1984a;Badcock et al., 1999). It is associated with a keratan sulfate, representing a terminal modification of the protein core. Later studies identified that TRA-1-60 and TRA-1-81 were epitopes of the protein, podocalyxin, which is expressed by hEC and hESCs (Schopperle and DeWolf, 2007a). Podocalyxin is an integral membrane protein with one transmembrane domain, a small cytoplasmic domain and a large extracellular domain containing five putative *N*-linked glycosylation sites, three glycosaminoglycan sites, and a 270-amino acid mucin domain (Schopperle

and DeWolf, 2007b). Differentiation of hEC or hESCs causes the glycosylation of podocalyxin, resulting in the loss of binding affinity to and lack of expression of TRA-1-60/81 (Schopperle and DeWolf, 2007c). This loss of expression of TRA-1-60/81 is similar to what occurs to the expression of SSEA1 in mECs or mESCs following differentiation (that is, loss of SSEA1 expression), suggesting that all three membrane proteins have comparable roles in early embryo development (Avner et al., 1985).

### 1.5.3.1 Acquisition and use of hESCs

Due to the ethical issues regarding the use of human embryos, research involving hESCs remains a controversial issue and therefore heavily regulated. Consent must be given by patients who have undergone *in vitro* fertilisation (IVF) to use any surplus embryos for research purposes. This is regulated by the Human Fertilisation and Embryology Act (HFEA) (Hunt, 2007). In addition, the UK requires all stem cell lines derived to be deposited to the UK Stem Cell Bank (UKSCB) to ensure that the cell lines are well characterised and made available for research (Healy et al., 2005b). All cell line deposits and applications to acquire cells from the UKSCB must be approved by the UK Steering Committee which oversees all activities involving hESCs (Healy et al., 2005a; Hunt, 2007). So far, all hESC lines currently in the UK Stem Cell Bank are only for research and not clinical use (Hunt, 2007) but there is progress toward eliminating animal components from the routine culturing of the cells (Richards et al., 2004a; Ellerstrom et al., 2006a), making them more useful for therapeutic purposes. Increasingly, there is a switch from using mouse fibroblasts as feeder layers and using human foreskin fibroblasts instead (Inzunza et al., 2005c).

There has also been a push towards the use of autologous stem cells, which are obtained from a patient's own body and will avoid the occurrence of rejection after transplant (graft versus host disease, GVHD) (Tyndall and Gratwohl, 1996; Tamm et al., 1996). This has already occurred with HSCs where the stem cells have been instrumental for blood regeneration and treatment of diseases which require a high dose of chemotherapy such as neuroblastoma (McElwain et al., 1979) and Hodgkin's disease (Laurence and Goldstone, 1999). However, the quantity of stem cells that can be retrieved from a patient may be inadequate for the treatment that is required. There is also an issue of the differentiation capacity of autologous stem cells as they are not pluripotent, and therefore may have limited number of cell types into which they can differentiate, making ESCs more advantageous.

#### 1.5.4 *Induced pluripotent stem cells (iPSCs)*

In order to avoid the ethical issues and post-transplant rejection associated with the use of hESCs, it is now possible to induce pluripotency in somatic cells by the introduction of up to four transcription factors, namely Oct3/4, Sox2, c-Myc, and Kruppel-like transcription factor, Klf4 (Takahashi and Yamanaka, 2006). This was first carried out in mouse fibroblasts and later in adult human fibroblasts (Yu et al., 2007c;Takahashi et al., 2007c;Masaki et al., 2008;Park et al., 2008b).

The roles of Oct3/4 in maintaining pluripotency has been previously described in section 1.5.4. Sox2, like Oct4, is associated with promoter regions of genes in hESCs (Boyer et al., 2005a). It encodes transcription factors that promote the transcription of self-renewal genes (Boyer et al., 2005b). In murine ESCs, Oct4 and Sox2 act synergistically to activate transcription of genes for pluripotency (Ambrosetti et al., 1997;Remenyi et al., 2004). c-Myc functions to enhance cell proliferation (Adhikary and Eilers, 2005) and it may also induce a global histone acetylation which allows more specific binding of Oct3/4 and Sox2 to their target proteins (Fernandez et al., 2003). Klf4 also promotes proliferation by binding to the promoter region of the p53 gene, which is known to activate apoptosis (Rowland et al., 2005). It has also been shown to repress Nanog during differentiation (Lin et al., 2005). However, overexpression of Klf4 activates p21 which induces apoptosis and therefore suppresses proliferation (Zhang et al., 2000). This antiproliferation function of Klf4 can be inhibited by c-Myc (Seoane et al., 2002); thereby the use of Klf4 and c-Myc must be balanced to ensure effective reprogramming of somatic cells into pluripotent cells.

The combination of Oct4, Sox2, Nanog, and LIN28 has also been identified in achieving pluripotency in human mesenchymal and human cord blood (Yu et al., 2007d;Haase et al., 2009a). Nanog has been found to increase the reprogramming efficiency (Silva et al., 2006) and cloning efficiency of hESCs (Darr et al., 2006). LIN28 is an mRNA-binding protein that is found in ESCs, ECs, neurons and epithelia but is down-regulated in most adult tissues with the exception of skeletal and cardiac muscles (Richards et al., 2004b). It is comprised of two RNA-binding motifs, namely the cold shock domain that binds single nucleic acids and a retroviral-type zinc finger motif (Moss and Tang, 2003b). Due to its post-transcriptional function, LIN28 is required for the regulation of development during embryogenesis and therefore affects sex determination, and also the differentiation of cells into specific lineages (Yang and Moss, 2003;Moss and Tang, 2003a). As a result of their roles in maintaining the pluripotent status of cells and inducing proliferation, Oct3/4, Sox2, Nanog, LIN28, c-Myc and Klf4 are employed for the transformation of somatic cells into pluripotent cells.

Success has also been achieved in generating iPS cells from mouse embryonic fibroblasts (Feng et al., 2009). Further advances have been made to replicate pluripotency induction with the aid of two factors instead of four (Zhao et al., 2008; Kim et al., 2008a). Recently, human cord blood has been found to produce iPS cells using only Oct4 and Sox2 (Giorgetti et al., 2009b). Similarly, MEFs have been reprogrammed into iPS cells using Oct4 and Klf4 combined with small chemical compounds (Shi et al., 2008a; Shi et al., 2008b).

To characterise the pluripotency of iPS cells, expression of ES markers such as SSEA3/4, TRA-1-60 and TRA-1-81 has been investigated (Takahashi et al., 2007b; Lowry et al., 2008; Giorgetti et al., 2009a; Haase et al., 2009b). Moreover, iPS cell potential has been demonstrated by injecting the cells into severe compromised immunodeficient (SCID) mice to verify that they form teratomas as is the case with ESCs and ECs (Park et al., 2008a; Kim et al., 2008b; Okita et al., 2008b). The formation of EBs and subsequent replating onto tissue culture dishes have also been used to characterise cell plasticity which is shown by the presence of cells representative of the three germ layers (Wernig et al., 2007; Takahashi et al., 2007a; Kim et al., 2008c). Human and mouse somatic cells induced to become pluripotent cells were found to have similar characteristics to their ES counterpart, indicating that reprogramming mechanisms are conserved across species. As a result, human iPS cells express the same genes found in hESCs and do not express SSEA1 as in mES cells.

iPS cells are advantageous because an individual's somatic cells could be induced to become more embryonic in nature and then differentiate into the cells of interest. This eliminates the issue of immune rejection because a patient would be treated with their own cells rather than cells from another individual. However, there are concerns regarding the introduction of extra genes through retroviruses which may cause mutations in the genome (Yu et al., 2007a). Furthermore, c-Myc is oncogenic and could lead to tumour growth (Nakagawa et al., 2008; Okita et al., 2008a). It would be more clinically beneficial if the genes responsible for maintaining an embryonic status can be activated in adult/differentiated cells instead of adding further genes by viral transfer. However, before this can be achieved, the mechanisms of embryonic development need to be more thoroughly understood.

## **1.6 Current cryopreservation protocols for SCs**

In order to preserve these highly useful cells, an essential storage method such as cryopreservation should be utilised. This reduces the cost of maintaining cells in culture and also provides a way in which cell lines can be made widely available to researchers.

It is important to note that cryopreservation media containing serum are generally used for the preservation of various types of cells and has been found to increase the recovery rate of intact and functional cells after thawing (Grilli et al., 1980b; Ellington et al., 1999). Freezing of cells in the presence and absence of serum in freeze media showed that cells in the presence of serum survived better than in medium without serum (Grilli et al., 1980a). Additionally, serum growth, and survival factors required by cells to proliferate in culture and exhibit essential function (Stojkovic et al., 2005a). Although the importance of LIF in growth medium has been discussed, experiments show that LIF can only maintain self renewal of mESCs *in vitro* in the presence of serum, which suggests it may contain additional factors that contribute to self-renewal (Berger and Sturm, 1997; Gendall et al., 1997b). However, there are published reports showing that hESCs can be maintained in serum-free media with the combination of serum-replacement media with human feeders (Inzunza et al., 2005d) or the addition of bone morphogenic protein 4 (BMP4) to growth medium (Ying et al., 2003a). BMP4 induces the transcription of *Id* genes which suppress differentiation through the SMAD pathway (Ying et al., 2003b). This development of serum-free conditions will make hESCs more clinically useful due to the lack of animal components.

### 1.6.1 Cryopreservation of HSCs

Since HSCs are beneficial for clinical treatments of diseases such as leukaemia, lymphoma and aplastic anaemia, storage methods for bone marrow and blood have become important in order to ensure availability for use when required.

Following initial murine models, cell concentrations of  $5.6 \times 10^8$  cells/mL were frozen with cell recovery of 75% post-thaw (Rowley et al., 1994d). However, cell concentrations of up to  $200 \times 10^6$  have been routinely used in cryopreserving peripheral blood stem cells (PBSCs) and umbilical cord blood (Rowley et al., 1994c; Gluckman, 2001; Villalon et al., 2002). Cell density, as described in section 1.3.4, is important to cell survival as there is greater probability of damage occurring in densely packed cells due to recrystallisation.

The discovery of the protective action of glycerol on spermatozoa (Polge et al., 1949a) led to its use in the freezing of bone marrow. Using a concentration of 12%, bone marrow was cooled at a rate 1°C/min to -15°C, then at 5°C/min to -40°C, and then cooled to -79°C or -196°C at any convenient rate. However, this was not an optimal cryopreservation method because it was determined that cell survival rate decreased as cooling rate was increased subsequent to freezing occurring. Moreover, 10-12% (v/v) Me<sub>2</sub>SO was found to increase the effectiveness of bone marrow which was shown by the improvement of haematological recovery in irradiated mice (Ashwood-Smith,

1961), but other published data indicated that glycerol was still a better CPA (Lewis and TROBAUGH, Jr., 1964a). The introduction of hydroxyethyl starch (HES) to a reduced concentration of Me<sub>2</sub>SO (6% HES and 5% Me<sub>2</sub>SO) has also been found to improve post-thaw recovery and prevent the occurrence of cell clumping (Stiff et al., 1983a; Stiff et al., 1983b). Both glycerol and Me<sub>2</sub>SO are widely used in the cryopreservation of human and mouse HSCs and HPCs.

Two methods of thawing frozen bone marrow have been tested (Lewis and TROBAUGH, Jr., 1964b). One involved the serial dilution of glycerol using CPA-free medium at 37°C, which resulted in damaged cells. Rapid thawing, however, resulted in better cell recovery (74%, expressed as percentage of cells in the same volume of unfrozen bone marrow) with characteristic morphology and motility (Lewis and TROBAUGH, Jr., 1964c). Consequently, rapid thawing is a preferred method for the post-freeze manipulation of bone marrow. Post-thaw recovery between 75 and 85% has been generally achieved, indicating that the cryopreservation methods developed for HSCs and HPCs produce comparable results (Linch et al., 1982; Rowley et al., 1994b; Fleming and Hubel, 2006a).

Similar cryopreservation procedures have been applied for storage of peripheral blood and umbilical cord blood with some modifications, including the use of a lower concentration of Me<sub>2</sub>SO (Abrahamsen et al., 2002b; Abrahamsen et al., 2004; Fleming and Hubel, 2006b), combining CPA with hydroxyethyl starch (HES) or other sugars (Moezzi et al., 2005; Rodrigues et al., 2008), and the sole use of sugars (Buchanan et al., 2004).

### 1.6.2 Cryopreservation of mESCs

Mouse ESCs (mESCs) have been cryopreserved by several methods, including in-situ freezing of the colonies in multi-well plates using culture medium that contained 10% Me<sub>2</sub>SO (Chan and Evans, 1991c; Ure et al., 1992b; Udy and Evans, 1994). However, the commonly used protocol is equilibrium or slow cooling method with medium containing 10% Me<sub>2</sub>SO, 50% foetal bovine serum (FBS) and culture medium. The cells are transferred into cryovials and cooled to -80°C at a cooling rate of 1°C/min (Kashuba Benson et al., 2008a). The cells are then plunged into liquid nitrogen (-196°C) from -80°C. Thawing of the cells was carried out using pre-equilibrated medium at 37°C. It is important to note that these protocols have been utilised based on basic cryobiological tenets of avoidance of injury by exclusion of intracellular ice through slow freezing and rapid thawing.

Results of post-thaw recovery ranged from 10% to 90% survival and varied widely between cell lines (Kashuba Benson et al., 2008b). It has been suggested that less than 50% of cells in most mESC lines survive the cryopreservation process (Kashuba Benson et al., 2008c). Recently, a study was carried out to optimise current mESC cryopreservation protocol by determining cryopreservation variables such as  $V_b$ ,  $L_p$ ,  $P_s$  and osmotic tolerance limits that are required for the modelling of an optimal protocol (Kashuba Benson et al., 2008d). The designed protocol used 1M PG instead of 1.3M  $\text{Me}_2\text{SO}$  combined with 50% FBS in culture medium. Cells were cooled at  $1^\circ\text{C}/\text{min}$  to  $-41^\circ\text{C}$  before being plunged into liquid nitrogen (Kashuba Benson et al., 2008e). Subsequent thawing of the cells occurred at room temperature with culture medium added drop-wise, resulting in post-thaw recovery of 64% of cells (measured by percentage of cells with intact membranes) which was a significant improvement over standard methods.

### 1.6.3 Cryopreservation of iPSCs

Similar cryopreservation protocols used in hESC storage have also been employed for the preservation of iPSCs (Yu et al., 2007b; Claassen et al., 2009a; Mollamohammadi et al., 2009f; Baharvand et al., 2010). The iPSC colonies are dissociated into single cells before being suspended in freeze medium containing 90% foetal calf serum (FCS), 10%  $\text{Me}_2\text{SO}$  and ROCK inhibitor, Y27632. The cell suspension is then cooled to  $-80^\circ\text{C}$  in a freezing container before being transferred into liquid nitrogen (Mollamohammadi et al., 2009e). Reported post-thaw recovery rates for iPSCs have been over 80% (Claassen et al., 2009b; Mollamohammadi et al., 2009d).

### 1.6.4 Cryopreservation of hESCs

Unlike mESCs, optimisation of the cryopreservation methods for hESCs has not been carried out due to the lack of biophysical data on these cells. Hence, protocols based on those utilised for the preservation of mESCs and human embryos are currently in use, which were initially developed from methods used for other cells such as lymphocytes and T cells (Leibo, 1986). Subsequent modifications of these protocols have been developed for the preservation of hESCs. However, these protocols cannot be deemed optimal because biophysical data of hESCs may be very different to those of mESCs and mouse or human embryos. The current protocols being used for the storage of hESCs at low temperature are slow cooling and vitrification (Reubinoff et al., 2001c; Ha et al., 2005a; Ware et al., 2005f). Until now, different stem cell laboratories have improved the preservation procedure by adding sugars to the CPA medium (Ji et al., 2004a; Wu et al., 2005e) and cytokine inhibitors such as Rho-associated kinase inhibitor (ROCK), Y-27632 (Martin-Ibanez et al., 2008f); others have tested cooling

rates and concluded that a rate of 1°C/min is optimal for hESCs (Heng et al., 2005b; Heng et al., 2006c; Katkov et al., 2006d); yet others have chosen the vitrification approach instead of slow cooling (Reubinoff et al., 2001d; Zhou et al., 2004c; Ware et al., 2005e; Li et al., 2010b).

There has also been research investigating in-situ cryopreservation of hESCs which involves freezing of hESCs while adhered to the feeder layer or matrigel-coated tissue culture plastic (Ji et al., 2004b; Heng et al., 2005a; Heng et al., 2006f). Results indicated that virtually all hESC colonies remained intact following cryopreservation and there was less differentiation found in the adherent colonies than in hESCs frozen as a suspension (Ji et al., 2004c). However, this method of cryopreservation demands larger storage space in order to produce banks of cells that would be large enough for research or clinical purposes. Furthermore, the fact that a feeder layer might be required prevents such cells being utilised for clinical purposes. More recently, work has been published which studied the in-situ cryopreservation of cells in clinical 'cassettes' that adhere to Good Manufacturing Practice (Amps et al., 2010). Although similar post-thaw results were achieved compared to cells cryopreserved on matrigel, the feeder cells will need to be eliminated in order for the cells to be used in the clinic.

The vitrification methods used for hESCs are based on cryopreservation of bovine ova and embryos which are labour intensive, comprising the incubation of the cells in vitrification solutions for a few seconds at a time and then a final immersion in liquid nitrogen (Hunt and Timmons, 2007). The time-limited procedure introduces variability when carried out by different individuals and therefore creates the possibility of the cell material not vitrifying correctly. In addition, only about 12 colony fragments can be vitrified simultaneously which means that the procedure must be repeated a number of times in order to yield a substantial number of cells. Cell survival rates reported for vitrified cells range from below 15% to 81% (Reubinoff et al., 2001e; Zhou et al., 2004b; Wu et al., 2005d).

Similarly, slow cooling methods have resulted in poor post-thaw survival rates as low as 1% (Ware et al., 2005d; Suemori et al., 2006). Various approaches to improve the slow cool procedure include freezing of hESCs while they are still adhered to the mouse fibroblast feeder layer (Ji et al., 2004d), the addition of sugars like trehalose (Wu et al., 2005c) and the addition of caspase inhibitors to the cryoprotective medium (Heng et al., 2006b; Heng et al., 2007). More recent research has cryopreserved hESCs as a single cell suspension which allows the cryopreservation of much larger numbers of hESCs than the vitrification methods and is a much quicker and easier process to perform (Martin-Ibanez et al., 2008e).

The number of hESC lines being derived has increased dramatically in recent years; about 144 lines from various countries have been or will be deposited into the UK stem cell bank (Personal communication). In order to make these hESCs available to researchers, stocks of cells must be cultured and cryopreserved in order to make their dispatch to different locations an easier process (Hunt, 2007). However, there are issues to be resolved with the cryopreservation methods used which currently are suboptimal due to the wide range of post-thaw recovery achieved by various stem cell laboratories.

Currently, each cell line dispatched by the UK stem cell bank is accompanied by a vial of MEFs and protocols for hESC propagation and cryopreservation. These protocols are usually the same as those used by the depositing laboratory.

## 1.7 Summary of cryopreservation protocols

Table 1.1 lists the current preservation protocols used for mouse and human HSCs, EC cells, mouse and human ESCs, and iPSCs. All cell types in the listed protocols were subjected to rapid warming in pre-equilibrated medium at 37°C because it has been shown that recrystallisation or devitrification can be avoided.

Although all cell types listed were cryopreserved using variations of slow cooling, hESC lines can also be vitrified. The base medium (BM) used in all vitrification solutions comprises of 89% (v/v) 25mM 4-(2-hydroxyethyl)-1-piperazineethanesulfonic acid (HEPES) buffered Dulbecco's Modified Eagle's medium (DMEM), 10% (v/v) FBS and 1% non-essential amino acids. The composition for the first and second vitrification solutions, VS1 and VS2, are detailed in the table legend. It is clear that cells are gradually introduced to increasing solute concentration in order to minimise extensive cell volume shrinkage when cells with isotonic volumes come in contact with hypertonic media. Similarly, CPA is gradually diluted from cells by initial exposure to the first thawing solution (TS), TS1, which contains 80% (v/v) BM and 20% (v/v) BM with 1M sucrose, while TS2 contains 50% (v/v) TS1 and 50% BM. TS1 contains greater solute concentration than TS2 in order to induce gradual cell volume expansion.

The protocols listed in table 1.1 have been developed according to cryobiological principles but without consideration of cells' physical properties which impact on the transport of water and CPA.

**Table 1.1 Current cryopreservation protocols for various cell types**

Cell type	Freezing technique	Cryopreservation medium	Cooling rate	References
mESC	Slow freezing	Culture medium + 1.3M Me <sub>2</sub> SO + 50%FBS	1°C/min	(Chan and Evans, 1991b;Ure et al., 1992a;Kashuba Benson et al., 2008f)
		Culture medium + 1M PG + 50%FBS		(Kashuba Benson et al., 2008g)
iPSC	Slow freezing	90% FCS + 10% Me <sub>2</sub> SO + ROCK inhibitor	1°C/min	(Claassen et al., 2009c;Mollamohammadi et al., 2009c)
Mouse HSC and Human HSC	Slow freezing	10-12% Me <sub>2</sub> SO in medium	1°C/min to -15°C; -5°C/min to -40°C; plunge in liquid nitrogen	(Ashwood-Smith, 1961)
		20% Me <sub>2</sub> SO	1°C/min to -40°C; 10°C/min to -80°C	(Rowley et al., 1994a)
		5% Me <sub>2</sub> SO + 6%HES	1°C/min to -80°C; plunge in liquid nitrogen	(Stiff et al., 1983c)
EC	Slow freezing	90% FCS + 10% Me <sub>2</sub> SO	1°C/min	UK Stem Cell Bank
hESC	Slow freezing	90% FCS + 10% Me <sub>2</sub> SO	1°C/min	(Hunt and Timmons, 2007)
	Vitrification	VS1, VS2 (1) 1min in VS1; 25sec in VS2 twice	plunge in liquid nitrogen	(Hunt and Timmons, 2007)

(1) VS1- 80% (v/v) base medium with 1M sucrose + 10% (v/v) Me<sub>2</sub>SO + 10%(v/v) EG. VS2 is comprised of 50% (v/v) base medium with 1M sucrose + 10% (v/v) base medium + 10% (v/v) Me<sub>2</sub>SO + 10% (v/v) EG

## 1.8 Project objectives

Although protocols used for hESC storage were adapted from well known methods used to preserve other cell types, it is clear that advances to cryopreservation methods have improved the recovery rates of hESCs. However, these modified protocols have been developed empirically through experimentation of components that can improve the cryopreservation process. There is also the fundamental issue that cells of the same or different species have been found to possess different physical properties which affect the efficiency of their storage as is the case with mouse and bovine oocytes (Ruffing et al., 1993;Benson and Critser, 1994). It was found that the blastocyst stage of embryos for mouse and cattle have the respective surface areas of  $1.7 \times 10^4 \mu\text{m}^2$  and  $7.1 \times 10^4 \mu\text{m}^2$ , with corresponding volumes of  $2.2 \times 10^5 \mu\text{m}^3$  and  $17.7 \times 10^5 \mu\text{m}^3$  (Whittingham et al., 1972;Hochi et al., 1996b). As a result, their surface area to volume ratio differs greatly, which determines how quickly cell water effluxes when the embryos are in a hypertonic solution. This phenomenon is also true in the case of human oocytes where significant differences in osmotic properties have been found (Van den Abbeel et al., 2007). As a result, there may be differences in the properties of the embryos formed from these oocytes, and subsequently in ESCs derived from the embryos.

It is therefore the aim of this PhD study to determine the physical properties of each cell type to be cryopreserved in order to establish a method which is optimal for its preservation. These properties include the cells' non-osmotic volume, surface area, hydraulic conductivity ( $L_p$ ) and solute permeability ( $P_s$ ) (Pegg and Diaper, 1990), which are necessary to prevent osmotic stress and for modelling protocols for the best mode of adding and removing CPAs. The step-by-step approach to designing a cryopreservation protocol has been employed for the storage of various cell types including mESCs, bone marrow, haematopoietic progenitors, oocytes and haematopoietic stem cells from umbilical cord blood (Hubel, 1997;Paynter et al., 1999a;Hunt et al., 2006;Kashuba Benson et al., 2008h;Son et al., 2010). However, this approach has not been applied to hESCs.

## 1.9 Optimal cryopreservation protocol for hESCs

Establishing the basic physical properties of hESCs will enable the optimisation of current cryopreservation protocols by identifying the variables contributing to the damage of cells during the process of preservation which could be a result of osmotic damage, CPA toxicity or freezing injury.

In addition, growth and membrane integrity assays will be carried out to assess the effect of various anisotonic conditions. This will indicate the range of osmolalities and volume excursions (that is, shrinkage and expansion) that the cells will tolerate before becoming damaged. Once these parameters have been established, they can be used to model different cryopreservation protocols to establish the best procedure for addition and removal of CPA which allows osmotic excursions within the cells' tolerance limits. The method of CPA introduction is important because of the effect of its toxicity and the length of exposure which must be minimised. Careful elution of the CPA is also essential as water will enter the cell causing it to expand; excessive swelling can also be damaging to the cells.

Furthermore, the effectiveness of the protocol will be assessed by examining the membrane integrity by the exclusion of propidium iodide (PI); the functionality of the cells will also be tested by their ability to adhere to the MEF layer *in vitro* and form colonies; thirdly, formation of embryoid bodies (EBs) will be performed to assess the differentiation capability of the cells. Surface marker expressions of the hESCs will also be tested.

Experiments were initially carried out on the human embryonal carcinoma cell line, 2102Ep, because these cells possess similar markers to those found on human embryonic stem cells such as TRA-1-60, TRA-1-81, Oct4, and SSEA3/4 (Andrews, 2002b). They can also be cultured easily because they do not require a feeder layer. The effect of freezing on gene expression can therefore be studied due to similar expression patterns between 2102Ep and hESCs.

This research will be carried out to test the following hypothesis: that a systematic approach to designing a cryopreservation protocol, which is based on the biophysical properties of cells, combined with experimental analyses produces a better optimised procedure than methods derived only by empirical analyses. For hESCs, it includes the following aims:

- Establishing basic biophysical properties

- Identifying variables which lead to cell injury during the cryopreservation process by carrying out CPA toxicity assays, cooling rate experiments, growth and membrane integrity assays
- Using physical properties and optimal cryopreservation conditions to model cryopreservation protocols best suited to the cell lines
- Carrying out experimental analysis to determine the efficacy of the cryopreservation protocol designed by carrying out growth and membrane integrity assays, replating cryopreserved cells in culture and analysing hESC colonies for characteristic gene expression and cell pluripotency.

## **Chapter 2**

# **MATERIALS AND METHODS**

## 2.1 Cell culture

All cells were incubated at 37°C and 5% CO<sub>2</sub>.

## 2.2 Mycoplasma testing

Cells were mycoplasma tested during cell culture to ensure absence of infection. First the cells were washed three times with phosphate buffered saline (PBS) (Invitrogen). 200µL of methanol was added to the cells and allowed to fix for 5 minutes before they were washed again with PBS. The cells were incubated with 200µL of 4',6-diamidino-2-phenylindole (DAPI) for a further 5 minutes at room temperature. DAPI binds to the DNA in the cells and can be detected with a fluorescence microscope. Non-infected cells will have DAPI staining only in the nucleus while infected cells will have DAPI staining both in the nucleus and cytoplasm.

## 2.3 Human embryonic stem cell lines used in project

Consequently, this work aims to use a systematic approach in determining the biophysical properties of two different hESC lines, namely, SHEF3 and RH1. SHEF3 cell line (University of Sheffield) was manually passaged, meaning each colony was separated from the feeder layer using a dissecting tool which was used to eliminate any differentiated areas before transfer into a new culture vessel (Reubinoff et al., 2000d). RH1 (Roslin institute, Edinburgh), however, was maintained *in vitro* by trypsinisation into single cells before transfer onto a new feeder layer. Single cell dissociation is now widely applied for the culture of hESCs and provides a less laborious means of up-scaling (Rosler et al., 2004b; Hasegawa et al., 2006a; Ellerstrom et al., 2007d).

## 2.4 Transportation of hESC lines and MEFs between UKSCB and University of York

Both SHEF3 and RH1 hESC lines and MEFs were transported as frozen vials stored on dry ice in a Styrofoam box. These vials were then stored at -80°C for short-term storage or in the vapour phase of liquid nitrogen for longer-term storage.

## 2.5 2102Ep cell culture

The embryonal carcinoma cell line, 2102Ep, were cultured in Dulbecco's Modified Eagle's medium (DMEM) (Invitrogen) with 10% foetal bovine serum (FBS). Cells were trypsinised

using 0.25% trypsin/EDTA, neutralised with growth medium and subcultured every 2-3 days.

## **2.6 Mouse embryonic fibroblast (MEF) culture**

Mouse embryonic fibroblasts (MEFs) were cultured in 10% FBS/DMEM. They were passaged using 0.25% trypsin/EDTA every 3-4 days at a ratio of 1:3.

### *2.6.1 Inactivation of mouse embryonic fibroblasts*

MEFs were inactivated using 10µg/mL of mitomycin C (Sigma) in DMEM/FBS. MEF monolayers were washed three times with phosphate buffered saline (PBS) and incubated with 5mL of mitomycin C (10µg/mL) at 37°C for 2-3 hours. Mitomycin C was removed, the cells washed three times with PBS, trypsinised, and either frozen in 10% v/v dimethyl sulphoxide (Me<sub>2</sub>SO) in FBS or plated out as required on gelatinised tissue culture flasks.

## **2.7 Human embryonic stem cell (hESC) culture**

### *2.7.1 Derivation of human embryonic stem cells and acquisition of cell lines*

Human embryonic stem cells (hESCs) are derived from the inner cell mass of blastocysts of embryos which are genetically disadvantaged or are no longer required for *in vitro* fertilisation. All embryos used for the derivation of hESC lines are patient-approved. The hESC lines used in this project were approved by the UK steering committee to be used for the intended research and also by the ethics committee at the University of York which agreed the use of human derived cells in the laboratory. Frozen vials of mitotically-inactivated mouse embryonic fibroblasts (MEFs) and 2102Ep were also acquired from the UK Stem Cell Bank (UKSCB) for the support of hESC growth *in vitro*.

### *2.7.2 hESC in vitro culture*

hESC colonies, begin to appear between 10 days and 2 weeks post-thaw. Once the colonies are in culture for a period of time, they begin to differentiate around the periphery displaying a 'fried-egg' appearance where the cells become less cohesive. Passaging the colonies should occur while still undifferentiated but detecting the right time is subjective and requires experience with the culture of these cells.

The manual passaging of hESC colonies through the use of collagenase is routinely used by researchers. Although it is time-consuming, it ensures the transfer of mostly hESCs and not the inactivated feeders that support their undifferentiated growth. Moreover, the use of

trypsin-EDTA proved unsuccessful for disaggregating hESC colonies. However, quicker and less laborious methods have been developed which dissociate hESC colonies into single cells and have been shown to result in subsequent formation of colonies (Hasegawa et al., 2006b; Ellerstrom et al., 2007c). Although an easier method of passaging, the single-cell dissociation of hESCs results in the transfer of both hESCs and MEFs. Human embryonic stem cell lines (hESCs), RH1 and SHEF3, were cultured on a MEF feeder layer in a growth medium containing knockout DMEM, 20% knockout serum, 1% non-essential amino acids, 1% glutamine, 0.2% betamercaptoethanol and 0.2% basic fibroblast growth factor (bFGF) (See table 2.1). The medium was changed every 2-3 days. The cells were passaged using recombinant trypsin (TrypLE Invitrogen); 1mL of TrypLE was used to wash each well of a 6 well plate and removed to leave only trace amounts of the enzyme on the cells. The cells were incubated for 1-2 minutes while monitored closely to ensure disaggregation of the hESC colonies, which were then washed off the feeder layer using the growth medium. All medium components were purchased from Invitrogen.

**Table 2.1 hESC Medium components**

	<i>hESC Medium</i>	
	<b>50mL</b>	<b>25mL</b>
Knockout DMEM	38.4mL	19.4mL
Knockout serum	10mL	5mL
Non essential amino acids (NEAA) 100X (final concentration: 1X)	500µL (1%)	250µL
Glutamax 100X (final concentration: 1X)	500µL (1%)	250µL
B-mercaptoethanol, 100mM	100µL (0.1mM)	50µL
bFGF, 10µg	100µL (4ng/mL)	50µL

## 2.8 MTT Assay

This assay was performed in order to optimise the concentration of Mitomycin C used for inactivation of mouse embryonic fibroblasts (MEFs). Currently, 10µg/mL is used. For the assay however, four other concentrations were tested- 2.5, 5, 25 and 50µg/mL- and there was a control sample not treated with mitomycin C. MEF cells were seeded onto wells of a 96-well plate (1280 cells per well and 7 replicates per concentration) and incubated

overnight to allow the cells to adhere to the culture vessel. 100 $\mu$ L of Mitomycin C was added to each well, except for the control sample, and incubated for 3 hours. The cells were washed 3 times with PBS, media was added to cells before an overnight incubation. The medium was replaced with 100 $\mu$ L of fresh medium and 25 $\mu$ L of 5mg/mL MTT (3-(4,5-dimethylthazol-2-yl)-2,5-diphenyl tetrazolium bromide) solution added, followed by incubation at 37°C for 3 hours. The medium was then replaced with 200 $\mu$ L acidic isopropanol to dissolve the formazan and pipetted up and down several times. Absorbance was measured on an ELISA plate reader at a wavelength of 570nm.

## 2.9 RNA Extraction

Cells were washed with PBS which was then aspirated completely from the culture vessel. An appropriate volume of TRIZOL reagent (Invitrogen) was added to the cells- 0.5mL per well of a 6-well plate or T25 flask, 1mL per T75 or 2mL per T175- and incubated at room temperature for 5minutes. 200 $\mu$ L of chloroform per 1mL of TRIZOL was added to the cell samples and placed on a vortex for 15 seconds. Samples were allowed to incubate for 5minutes at room temperature before undergoing centrifugation at 12000g for 20 minutes at 4°C. The upper aqueous layer was carefully transferred into a new tube. 0.5mL of 100% isopropanol per 1mL of TRIZOL was subsequently added to the tube and mixed by brief vortexing. The sample was incubated for 30minutes at room temperature or 4°C. Centrifugation at 12000g for 15minutes at 4°C followed before the isopropanol was removed from the RNA pellet. The pellet was washed in 1mL of 75% ethanol and vortexed briefly. Another centrifugation step followed at 12000g for 5minutes. The ethanol was removed and the pellet allowed to air dry briefly. The pellet was resuspended in RNase/DNase-free water. Quantification of the concentration of RNA was carried out using a spectrophotometer (Nanodrop).

## 2.10 DNase treatment of RNA

A 20 $\mu$ L DNase digestion reaction was prepared by combining a set amount of RNA in water with 2 $\mu$ L of RNase-free DNase 10X reaction buffer and 1unit per microgram RNA of RNase-free DNase. Nuclease-free water was added to the mixture to a final volume of 20 $\mu$ L and resuspended gently by pipetting. Incubation followed at 37°C for 30 minutes. 1 $\mu$ L of DNase Stop solution was added to terminate the reaction. The cell sample was then incubated at 65°C for 10 minutes to inactivate the DNase enzyme. Reagents for DNase treatment were purchased from Promega.

## 2.11 cDNA synthesis

The following reagents were added to two eppendorf tubes: oligo dt primer, 10mM dNTPs and water; one for cDNA synthesis and another for a no-RT control. The resulting mix was then incubated at 65°C for 5 minutes and chilled on ice for 2 minutes. While on ice, a master mix was prepared comprising a first strand buffer, 0.1M DTT and water, which was added to the cDNA and control samples. The mix was incubated at 42°C for 1hour, and then incubated at 70°C for 15 minutes in order to inactivate reverse transcriptase. RNase H was added to each sample and incubated at 37°C for 20 minutes. The cDNA and no-RT product were diluted to a yield of about 0.5µg.

## 2.12 Reverse Transcription-polymerase chain reaction (RT-PCR)

RNA was extracted using Trizol according to the manufacturer's instructions. Chloroform was added to the Trizol lysate to separate RNA from DNA. 100% isopropanol was added to the sample and incubated at 4°C for 30 minutes in order to precipitate RNA. The resulting RNA pellet was washed in 75% ethanol and precipitated by centrifugation at 12000g for 5 minutes. All traces of ethanol were then removed. DNase/RNase-free water was added to dissolve the RNA product. Subsequently, the RNA was treated with DNase using Ambions DNA-free kit. 0.1 volume of the DNase inactivation reagent was added to RNA, incubated for 2 minutes at room temperature, and centrifuged for 1 minute to pellet the inactivation reagent. Absorbance was measured using a Nanodrop spectrophotometer.

## 2.13 Characterisation by surface marker expression using flow cytometry

$5 \times 10^5$  cells/mL resuspended in cold buffer (0.2% BSA and 5mM EDTA in PBS) was used for each analysis (100µL/sample). Each primary antibody- TRA-1-60, TRA-1-81, SSEA3/4, and SSEA1- was added to each cell sample (1:100) except for the negative controls, and then placed on ice in the dark for 45 minutes. 1mL of buffer was added to all the tubes which were spun for 5minutes at 450xg at 4°C. 100µL of FITC-conjugated secondary antibody was then added (1:50 dilution) and the tubes incubated on ice in the dark for 45 minutes. Cells were centrifuged and resuspended in 100µL buffer and analysed by flow cytometry (Cyan, Beckman Coulter).

## 2.14 Coulter counter

There are various ways in which biophysical properties of cells can be determined. Photomicrography is a direct method of monitoring volume but can only analyse a small number of cells while the Coulter counter is an indirect method of measuring volume changes and allows for a large number of cells to be analysed (Mazur, 2007).

The Coulter counter is an electronic particle sizer comprising a glass tube which has a small orifice through which cells can pass. There are electrodes inside and outside the tube between which a current flows and the apparatus causes a constant current to pass through the orifice. As the cells enter the glass tube and are pulled through suction, they displace a certain amount of buffer thereby causing the resistance of the orifice to change. The result is a voltage peak in the output.

The Coulter Principle states that the voltage output is directly proportional to the three dimensional volume of the particle that produced it. Thus, the larger the amount of electrolyte displaced, the larger the voltage output and pulse; small cells will produce small pulses; larger ones, larger pulses (McGann et al., 1982). The Coulter counter is advantageous because it allows for a large number of cells to be analysed and has upper and lower threshold settings which eliminate particle sizes of extreme values, leading to more accurate results.

Many studies utilised the Coulter counter in cell size measurements which will also be employed in this PhD project (Liu et al., 1995; Woods et al., 2000b; Si et al., 2006; Kashuba Benson et al., 2008i). The Coulter counter (model ZM) was equipped with a 100 $\mu$ m orifice through which each cell sample passes. The counter is attached to a standard PC which runs an ADWIN™ 1MHz A/D converter program (Keithley) that converts the volume data from the cell sample into a voltage pulse. Time files are first created by the user and are used by the Coulter to record data at specific time intervals. Data for 1000 cells are collected for each run performed and saved for subsequent analysis by a purpose-written PASCAL computer program. The software places the values for the cell volume and puts them in order, recording the modal value from each data set.

All cells that passed through the Coulter counter were suspended in PBS<sup>+</sup> (0.5% bovine serum albumin in PBS); no adjustments were made for different solutions because the current that passes through the equipment is constant. The only change that occurs is in

the voltage pulse produced which is influenced by the size of the cell passing through the current flow.

## 2.15 Preparation of anisotonic conditions

Isotonic medium was first prepared which contained 0.5% bovine serum albumin in PBS (PBS<sup>+</sup>). Hypertonic and hypotonic solutions were then prepared by the addition of sucrose or ultrapure water to the isotonic solution (300mOsm/kg). The hypertonic solutions ranged from 500 to 1200mOsm/kg while the hypotonic were between 150 and 300mOsm/kg. A freezing point osmometer was used to confirm the osmolality of each solution. Each solution was prepared at 2X the required final concentration.

## 2.16 Cell Volume Analysis

Cell volume changes in response to anisotonic conditions were analysed by a Coulter counter technique.

## 2.17 Membrane integrity assay

Propidium iodide (PI) exclusion was used to determine the effect of anisotonic conditions on the cell membrane. The cells were exposed to varied osmolalities for 5 minutes before being centrifuged and resuspended in buffer solution comprising 0.2%BSA and 5mM EDTA in PBS. The fluorescent dye, PI, was added to the cell suspension at a concentration of 0.6µg/mL; cells with damaged membranes uptake the dye while those with intact membranes exclude the dye. In order to provide quantitative data, fluorescent beads at a concentration of 1080beads/µL were added to the cell sample to aid in provide absolute cell counts. Samples were analysed by flow cytometry. The number of cells per µL was determined using the formula given by the manufacturer:

(Number of cell events counted/ Number of beads counted) x Bead concentration x Dilution factor

## 2.18 Assessment of cell growth

The cells were trypsinised as previously described. The cell suspension was centrifuged at 1200rpm for 5 minutes.  $1.74 \times 10^4$  cells were exposed (in triplicate) to different anisotonic conditions (150, 225, 500, 800, 1200mOsm/kg plus isotonic control). After treatment, the cells were centrifuged at 1200rpm for 5 minutes, resuspended in at  $5.8 \times 10^3$  cells/replicate,

and seeded onto 3 wells of a 6 well plate. After 48 hours in culture, the cells were trypsinised and counted using a haemocytometer.

### **2.19 Adhesion assay**

The cells were trypsinised as previously described and the cell suspension centrifuged at 1200rpm for 5 minutes. Equal numbers of cells were then subjected to different anisotonic conditions (75, 150, 225, isotonic, 500, 800, 1200mOsm/kg).  $5 \times 10^4$  cells were seeded in 6 wells of a 96 well plate (6 replicates per condition). After 4 hours, the cells were gently washed with PBS. The adherent cells were fixed in 70% ethanol in PBS for 15 minutes. The ethanol solution was discarded and the cells stained at RT overnight with 0.1% crystal violet in 95% ethanol in PBS. Stained cells were lysed with 2% SDS in PBS for 15 minutes in order to release the dye, and absorbance was read at 570nm.

### **2.20 Membrane Integrity assessment**

The cells were trypsinised as earlier described. Equal cell concentrations were exposed to anisotonic conditions. In sucrose solutions, the exposure time was 5 minutes while in solutions with either  $\text{Me}_2\text{SO}$  or PG the exposure time was 15 minutes. The cell suspensions were pelleted by centrifugation at 1200rpm for 5 minutes before being resuspended in fresh PBS<sup>+</sup>. PI was then added to each cell sample and placed on ice before analysis through flow cytometry.

### **2.21 Statistical analysis**

All data were collated and plotted using Excel or SigmaPlot. The error bars were standard error of mean (SEM). Statistical analysis was performed using the statistics package SPSS. Tests applied included the normality test, Levene's test of equality of variance, one way analysis of variance (ANOVA), post-hoc test and Student's t-test to analyse the data and make comparisons between data sets.

## **Chapter 3**

# **BIOPHYSICAL PROPERTIES OF HUMAN EMBRYONIC STEM CELLS**

## 3.1 INTRODUCTION

This chapter focuses on the fundamental properties required to design an optimal cryopreservation protocol for hESCs. Although several studies have been carried out on the cryopreservation of hESCs with varied outcomes, the protocols developed have been largely empirical with exceptions in studies of optimal cooling rates (Ha et al., 2005b; Ware et al., 2005c). The current methods have been based on those used for other cell types and not on systematic derivation which combines theoretic predictions of optimal conditions with experimental analysis. It is in such a case that any protocol can be described as 'optimal'. The physical properties that will be determined in this chapter include nonosmotic volume ( $V_b$ ), hydraulic conductivity ( $L_p$ ) and solute permeability ( $P_s$ ).

### 3.1.1 Nonosmotic volume ( $V_b$ )

Initially, in the presence of CPAs, the extracellular solution possesses a higher solute concentration than the intracellular space which increases the osmotic pressure exerted on the cell membrane, causing the movement of water from the inside of the cell to the suspending medium (van't Hoff, 1887). Simultaneously, there is a concentration gradient formed that then causes the influx of CPA into the cell in order to re-establish equilibrium across the cell membrane; water simultaneously enters the cell in response to the increased osmotic pressure. This process continues until there is no more movement of solute or water between the intra- and extracellular compartments; the cell can now be described as being in equilibrium with the suspending medium. Figure 3.1 shows the sequential occurrence of these events; (a) water moves out of the cell in response to osmotic pressure; (b) the CPA begins moving into the cell in response to the concentration gradient; (c) the movement of solute and water continues until there is osmotic and concentration equilibrium.

Van't Hoff's equation for pressure describes the relation between solute concentration and cell volume,

$$V^{\text{rel}} = 1/M^{\text{rel}},$$

$V^{\text{rel}}$  is cell volume relative to the initial volume and  $M^{\text{rel}}$  is the solute concentration. This equation supports the fact that when osmotic pressure (which is proportional to solute concentration) increases, the cell reduces in volume.

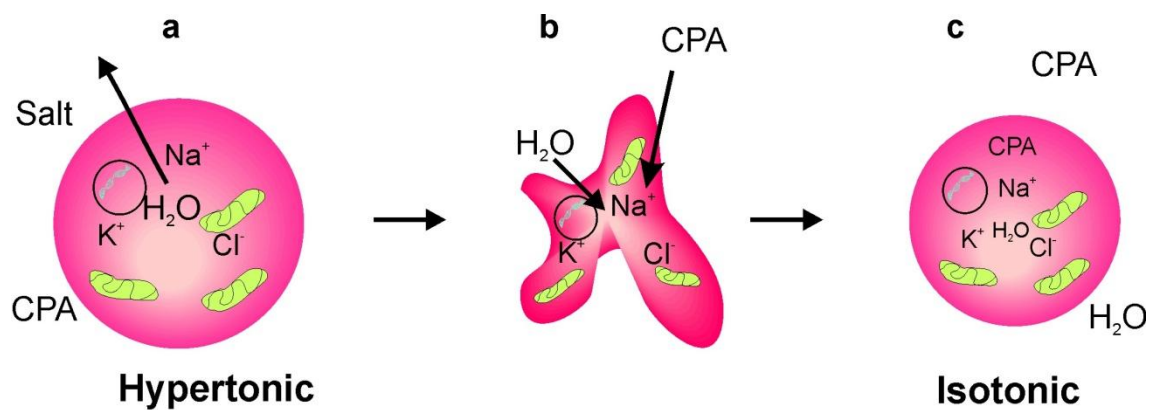


**Figure 3.1 Cell response in medium CPA-containing medium**

Illustration of a cell freezing in a multi-solute system. The arrows indicate the direction of movement of cryoprotectant (CPA) and water. (a) First water moves out of the cell in response to the hypertonic medium which results in cell shrinkage. (b) Water and CPA then move into the cell to maintain osmotic and concentration balance. (c) Cell regains its isotonic volume and is considered to be in equilibrium.

While the cell experiences a volume flux, there is a part of the volume which does not experience any change and it is referred to as the nonosmotic volume; it is also known as the nonsolvent volume or the volume of water that is unavailable to dissolve solutes. The nonosmotic volume has been found to include water bound to solids such as proteins and cellular organelles (Cook, 1967a). Understanding of this volume has come mainly from the work on erythrocytes which have been regarded as “perfect osmometers,” shrinking in volume when in solutions of high solute concentrations and then swelling in order to maintain solute concentration and osmotic equilibrium (Jacobs, 1962b).

Determining the nonosmotic volume of a cell can be achieved by several methods including desiccation, submergence in an electrolyte or non-electrolyte solution. Desiccation is useful in providing the volume of cell water but it does not illustrate the osmotic behaviour of the cell while the other methods do. However, one disadvantage of submerging cells in an electrolyte solution is that it may affect the equilibrium state of the already present ions in the cells (Jacobs, 1962a). For example, when a cell is submerged in a saturated sodium chloride solution, the permeability of the cell membrane to ions increases. Therefore, using a non-electrolyte solute like sucrose, which remains impermeable to the cell membrane, will provide the osmotically active water volume without affecting the equilibrium state of ions in the cell. The osmotic properties of various cells have been determined using sucrose to make the hypertonic solutions (Gilmore et al., 1995a; Wu et al., 2005h; Seki et al., 2007).

Passing the cells in anisotonic solutions through the Coulter counter produces voltage outputs which correspond to cell volume. The voltage output can be plotted against the reciprocal osmolality to generate a linear plot known as the Boyle van't Hoff plot, named after the British physicist, Robert Boyle, and Dutch chemist, Jacobus van't Hoff. The equation for the line is,

$$V^{\text{rel}} = V^{\text{int}} + (1 - V^{\text{int}}) / M_e^{\text{rel}},$$

where  $V^{\text{rel}}$  is the cell volume relative to the isotonic cell volume,  $V^{\text{int}}$  is the non-osmotic volume and  $M_e^{\text{rel}}$  is the isotonic osmolality.

Although cell suspensions that will pass through the Coulter counter will mostly contain hESCs, there is a probability of cross-over of MEF cells, which is why modal cell volumes will be used rather than mean cell volumes in order to eliminate any outlying data from MEFs. Mode, in comparison to mean, is unaffected by outlying data in cell suspensions with varied cell sizes (Pegg and Lancaster, 1998). The resulting Boyle van't Hoff plots generated from the cell volume measurements will be modal cell

volumes plotted against the inverse osmolality. Extrapolation of the linear plot (to the y-intercept) estimates a value for the non-osmotic cell volume since the y-intercept represents a value for cell volume at infinite osmolality. Determination of the nonosmotic volume establishes the volume of osmotically active water. In addition, cell volume measurements of latex beads with known volumes make it possible to calculate cell volume of hESCs. If it is assumed that the shape of the cells is spheroidal, the formula for volume of a spheroid can be used to determine the radius of the each cell which then means the cell surface area can be calculated using the mathematical formula for calculating the area of a sphere ( $A = 4\pi r^2$ ).

### 3.1.2 Membrane permeability properties ( $L_p$ and $P_s$ )

The surface area to volume ratio (S/V) is important in determining how rapidly a cell will lose its osmotically active water in an anisotonic solution or, in other words, its hydraulic conductivity ( $L_p$ ). A small cell with a large S/V ratio will therefore allow a more rapid flow of water due to the availability of more membrane for water to permeate than a large cell which has a smaller S/V ratio (Dumont et al., 2004). Rapid water movement across the cell membrane may be attributed to the presence of aquaporins in the membrane which aid in the transport of water. In fact, aquaporins have caused a 10-fold increase in osmotic water permeability in xenopus oocytes (Ishibashi et al., 1994c). Edashige et al, in measuring the  $L_p$  and activation energies of mouse morulae and embryo, found they possessed high water permeability and low activation energy which suggested transport of water through facilitated diffusion (Edashige et al., 2006b). Immunocytochemical analysis revealed aquaporin 3 was the protein responsible for water transport in mouse morulae. Cells with high permeability to water, therefore, have the ability to equilibrate quicker and can be cooled at high cooling rates without the occurrence of intracellular ice.

Aquaporins have also been shown to be involved in the transport of some CPAs. Reports by Yamagi et al. showed aquaporin 3 also responsible for the transport of glycerol, ethylene glycol, propylene glycol and dimethyl sulfoxide in xenopus oocytes (Yamaji et al., 2006a). Another member of the aquaporin family, aquaporin 9, has been shown to transport neutral solutes including purines, polyols and carbamides across the cell membrane (Tsukaguchi et al., 1998). Other published data have shown that water, glycerol and ethylene glycol permeate mouse morulae through channel-dependent means (Edashige et al., 2006a). However, it was determined that simple diffusion was responsible the transport of water and solutes across mouse embryo membrane due to measured values  $L_p$  being low and high for activation energy (Edashige et al., 2007a). It has been suggested, then, that permeability may be

dependent on the stage of embryo development and responsible for the difference in tolerance to cryopreservation at these stages. Studies by Mazur and colleagues demonstrated this phenomenon, showing that permeability of mouse embryos to glycerol increased from oocytes and 1-cell zygotes to 8-cell embryos (Mazur et al., 1976; Jackowski et al., 1980).

Although the S/V ratio and the presence of aquaporins affect the values of  $L_p$  and  $P_s$  in cells, permeability is also dependent on temperature and type of CPA. It is evident in biological processes that the lower the temperature, the slower the rate of water and solute movement. Moreover, the nature of CPA impacts how easily or rapidly they are able to permeate the cell membrane because each CPA differs in its molecular weight and viscosity.

To determine the  $L_p$  and  $P_s$  of cells in this chapter, a curve-fitting approach will be adopted (Higgins and Karlsson, 2010) where hypothetical values of  $L_p$  and  $P_s$  are adjusted until the curve produced by the values fit the experimental data for cell volumes at various time points. Similar approach has been utilised in studies for other cell types including human and mouse oocytes, spermatozoa, chondrocytes and CD34<sup>+</sup> cells from umbilical cord blood (Noiles et al., 1993; Woods et al., 1999b; Paynter et al., 1999e; Woods et al., 2000a; Paynter et al., 2001a; Xu et al., 2003b; Hunt et al., 2003j; Wu et al., 2005g). The statistical calculation of Chi-square,  $X^2$ , which measures the goodness of fit, was used to determine the best-fit curve. The  $L_p$  and  $P_s$  of each cell line will be determined while the cells are suspended in two different CPAs, Me<sub>2</sub>SO and PG, and at two different temperatures, RT and +2°C. This is in order to carry out a comparative study of any effect the CPAs might have on the plasma membrane and also the permeability of the cells to each solute to determine the better CPA.

### 3.1.3 PG and Me<sub>2</sub>SO

Throughout this study, PG and Me<sub>2</sub>SO will be the only CPAs tested in various assays. Me<sub>2</sub>SO is widely used in preserving various cell types and is the only CPA used in slow cooling protocols for hESCs. However, PG is a more stable glass former than Me<sub>2</sub>SO and EG (the second CPA used in vitrifying hESCs) (Baudot et al., 2000; Baudot and Odagescu, 2004), which means it vitrifies more easily. It can also be utilised in lower concentrations and can produce a greater depression in the temperature at which ice forms, suggesting PG possesses the potential to reduce the occurrence of intracellular ice during cooling and recrystallisation during warming. For the cryopreservation of mESCs, it was found that PG was the optimum CPA compared to Me<sub>2</sub>SO and EG (Kashuba Benson et al., 2008j). On the contrary, 2,3-butanediol which is also a stable glass former has been shown to be more toxic than PG (Wusteman et al., 2002). As a

result, PG has been chosen, in this study, as a second CPA in the cryopreservation of hESCs. Its toxicity to the cell lines will be assessed and compared to that of Me<sub>2</sub>SO.

In addition, the effect of each CPA on the stabilisation of phospholipids in the membrane of each hESC line will be analysed using PI exclusion to test for membrane integrity. Me<sub>2</sub>SO has been found to stabilise liposomes in concentrations higher than 1M through interaction with polar headgroups of phospholipids in the cell membrane (Anchordoguy et al., 1987b). However, disaccharides such as trehalose and sucrose conferred greater protection through hydrophobic interactions with phospholipids (Anchordoguy et al., 1987a) but their impermeability to the cell membrane means they are unable to maintain osmotic and concentration equilibrium in cells. The ability of PG to protect cell membranes and the concentration at which it does so will be crucial in determining whether it is a better membrane stabiliser at concentrations which are non-damaging to the cells.

### 3.2 Chapter aims

- Determine whether hESCs act as 'perfect osmometers'.
- Establish the basic physical properties of hESCs ( $V_b$ ,  $L_p$  and  $P_s$ ) and comparing any differences between the two hESC lines.
- Compare the effect of two CPAs, PG and Me<sub>2</sub>SO, on the permeability of each hESC line at two different temperatures, at room temperature (RT) and on ice (+2°C).

### 3.3 Materials and Methods

#### 3.3.1 Volume calibration

Prior to using the Coulter Counter, volume calibrations had to be carried out using latex beads (Beckman Coulter) measuring 5 $\mu$ m and 10 $\mu$ m in diameter. The beads were added to isotonic PBS<sup>+</sup> solution and passed through the Coulter counter to determine their modal voltages. There were five blocks of data per run and 6 replicates for each set of beads. The data were then used to plot a standard line; the y-intercept corresponded to the instrument offset voltage which will either be subtracted or added to the measured cell volumes.

#### 3.3.2 Non-osmotic cell volume ( $V_b$ )

Cells were trypsinised and resuspended in PBS<sup>+</sup> (300mOsm/kg). 100 $\mu$ L of cells were added to 20mL of each anisotonic condition for 5 minutes and analysed by the Coulter counter ZM (Beckman Coulter) at 10 second intervals for 90 seconds (150, 225, 300, 500, 800, and 1200mOsm/kg). The duration of cells in anisotonic medium was chosen to be 5 minutes as an initial duration of 10 minutes appeared to be damaging to the cells and a linear plot for the Boyle van't Hoff graph could not be achieved. For each of the experiments, 1000 cells were analysed per run and 10 runs for each condition. As cells passed through the 100 $\mu$ m aperture of the Coulter counter, an amount of PBS<sup>+</sup> is displaced leading to an emission of a voltage pulse equivalent to the cell volume. A PASCAL program was utilised to calculate modal voltages at the different osmolalities from the range of voltage outputs produced by the Coulter Counter. The average modal voltages for each anisotonic condition were then calculated. These modal values were plotted on a Boyle van't Hoff plot.

#### 3.3.3 Adhesion assay

The cells were trypsinised as previously described and the cell suspension centrifuged at 1200rpm for 5 minutes. Equal numbers of cells were then subjected to different anisotonic conditions (75, 150, 225, isotonic, 500, 800, 1200mOsm/kg).  $5 \times 10^4$  cells were seeded in 6 wells of a 96 well plate (6 replicates per condition). After 4 hours, the cells were gently washed with PBS. The adherent cells were fixed in 70% ethanol in PBS for 15minutes. The ethanol solution was discarded and the cells stained at RT overnight with 0.1% crystal violet in 95% ethanol in PBS. Stained cells were lysed with 2% sodium dodecyl sulphate (SDS) in PBS for 15 minutes in order to release the dye, and absorbance was read at 570nm.

### 3.3.4 Timecourse experiments

The 2102Ep and hESCs were trypsinised as previously described and exposed to either 10% (v/v) Me<sub>2</sub>SO or 5% (v/v) PG at one of two temperatures (+2°C and +20°C). Using the ADWIN program, a timing file was created for each temperature to allow the program to record modal voltages. At +20°C, the timing file was 2 second intervals for the first 10 seconds and increasing intervals for 3 minutes; and at +2°C, 5 second intervals and increased to 18 minutes. For the experiments carried out at +2°C, all CPA solutions were immersed in ice until fully-equilibrated. 19mL of CPA in isotonic PBS<sup>+</sup> was aliquotted into a container and placed onto the Coulter stand so that the orifice was fully immersed in the solution. A trigger mechanism was activated at the same time as 1mL of cell suspension was added to the solution close to the orifice. 1000 cells were collected for each interval and the data for cells at RT and at +2°C were recorded. The modal voltages were then normalised to the average modal voltage for the isotonic control and plotted against time.

### 3.3.5 $L_p$ and $P_s$ determination

Following generation of the shrink-swell curves from the timecourse experiments, two programme files were created: a data file that contained all the experimental data from the timecourse experiment and a parameter file which contained the cells' physical properties and hypothetical values for  $L_p$  and  $P_s$ . The cell volumes over the time course were fitted to a two parameter model (Kedem and Katchalsky, 1958d) using the following equations,

Volume flux of water =  $-L_p (\Pi^e - \Pi^i)$ , where  $J_{v_w}$  is the volume flux;  $\Pi$  is the external and internal osmolality (or internal and external osmotic pressure); and  $L_p$  is the hydraulic conductivity;  $(\Pi^e - \Pi^i)$  can also be defined as  $(C^e - C^i) \times RT$ , where  $R$  is the universal gas constant (Joules/mol/K) and  $T$  is temperature (in Kelvin, K). The equation then becomes

$$\text{Volume flux of water} = -L_p (C^e - C^i) \times RT$$

Volume flux of CPA =  $V_s \times P_s (C^e - C^i)$ , where  $P_s$  is the solute permeability,  $V_s$  is the partial molar volume of CPA and  $C$  is the internal and external concentration of CPA in mol/L. The partial molar volume was calculated by dividing the molecular weight of CPA by its density; for Me<sub>2</sub>SO,  $V_s = 71\text{cm}^3$ , while for PG  $V_s = 73.5\text{cm}^3$ .

With all other variables known in the equations except for  $L_p$  and  $P_s$ , hypothetical values for the unknowns were utilised in order for a curve to be generated. A purpose-written computer program, TWOPSTEP, which simultaneously calculates the 2P

formula, plots the corresponding shrink-swell curve onto the experimental data. Manual iteration of the values for  $L_p$  and  $P_s$  was performed until the best curve to fit the experimental data was achieved which was indicated by the value of chi-square value,  $\chi^2$  (Bevington, 1969); the lower the value of  $\chi^2$ , the better the fit. This approach to determining permeability values has been applied in other studies (Walcerz et al., 1995; Hunt et al., 2003i).

### 3.3.6 *Growth and propidium iodide exclusion assays*

The effect of anisotonic conditions were tested by studying the effects of various osmolalities using methods described in the previous chapter.

## 3.4 Results

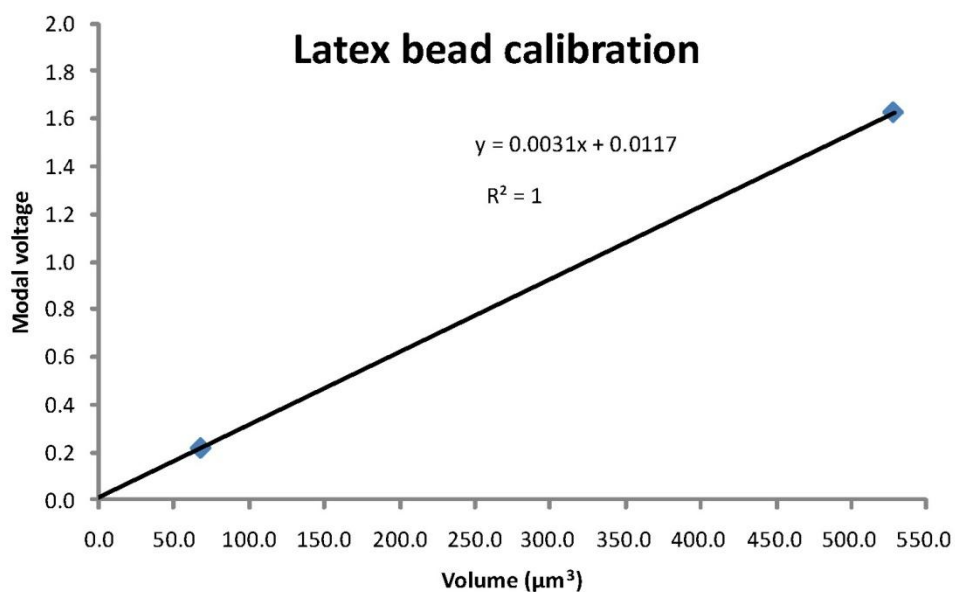
### 3.4.1 *Determination of offset voltage*

In order to determine the offset voltage of the Coulter counter with a 100 $\mu$ m orifice, latex beads of known volume and which are within 5-20% of the size of the orifice were utilised. Hence, it was appropriate to use 5 $\mu$ m and 10 $\mu$ m latex beads for the calibration of the apparatus. Performing runs with the beads in isotonic PBS<sup>+</sup> and repeating this process 6 times produced average modal voltages of 0.22V and 1.62V for the 5 $\mu$ m and 10 $\mu$ m beads respectively (Table 3.1). These modal voltages along with their known volumes produced a standard curve with the y-intercept of +0.0117V (Figure 3.2), which represents the value of error in the voltage readings the equipment produces. This value was subtracted from all other modal voltages retrieved from the Coulter counter to make the data more accurate.

**Table 3.1 Volume calibration using latex beads**

Known volume of polystyrene latex beads and their corresponding modal voltage.

Particle size	Volume $\mu\text{m}^3$	Average modal Voltage (n=6)	Standard deviation	Standard error of mean
5 $\mu\text{m}$	68.28	0.22	0.0097	0.0039
10 $\mu\text{m}$	528.33	1.62	0.019	0.0076

**Figure 3.2 Standard line for latex bead volume**

Standard line from the modal voltages of 5 and 10 $\mu\text{m}$  polystyrene beads at preset gain setting of 4 and attenuation setting at 8. Each set of latex beads had 6 replicates. The standard deviation (SD) values for the 5 and 10 $\mu\text{m}$  polystyrene beads were 0.019 and 0.010 (n=6), respectively. The error bars are not visible because of very low SD values. y-intercept revealed an offset voltage 0.011V.

### 3.4.2 Determination of non-osmotic volume ( $V_b$ )

2102Ep cells were initially used in all experiments performed in order to become familiar with the protocol before using the hESCs, RH1 and SHEF3. It was evident from the volume response of all the cells to the various anisotonic conditions that they acted as osmometers.

Cell volume measurements from the Coulter counter were recorded as voltages which were then adjusted by subtracting the value of the offset voltage (+0.0117V) determined earlier from the latex bead measurements. The voltages were then plugged into the equation for the line produced from the latex bead calibration to determine the actual value for cell volume for the different cell lines. The equation for the standard curve was  $y = 0.0031x + 0.0117$ , where  $y$  is the modal voltage (V) and  $x$  is the corresponding cell volume ( $\mu\text{m}^3$ ).

The Boyle van't Hoff plots generated showed extrapolation of the linear regression to the y-axis produced a  $V_b$  for 2102Ep cells of 0.25volts (or cell volume equalling  $81\mu\text{m}^3$ ) (Figure 3.3), while those for RH1 and SHEF3 were 0.22volts ( $61\mu\text{m}^3$ ) and 0.19volts ( $68\mu\text{m}^3$ ), respectively (Figure 3.4-3.5).

It should be noted that for all three cell lines, there was a shift from linearity for cells in 500mOsm solution, which may be the result of an error in the preparation of the stock solution which may have been more hypertonic than required.

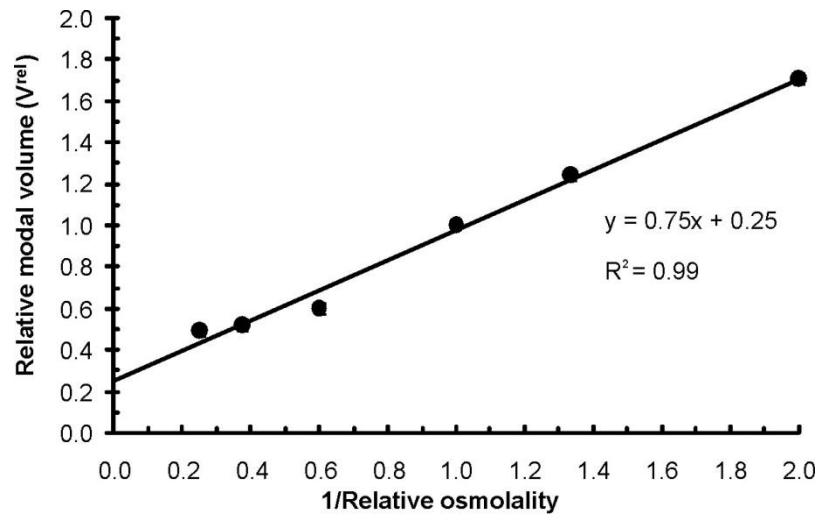


**Figure 3.3 Boyle van't Hoff plot for 2102Ep**

Human embryonal carcinoma cell line, 2102Ep, was trypsinised and centrifuged at 1200rpm. The cell pellet was resuspended in PBS<sup>+</sup>. 1mL of cell suspension was added to 19mL of each of the hypo- or hypertonic solutions made up in PBS<sup>+</sup> solution and left in solution for 5 minutes. The cells were then passed through the Coulter counter for subsequent volume measurements. Boyle van't Hoff plot indicated that the value for its non-osmotic volume,  $V_b$ , was 0.25. Cell volume measurements were normalised to the isotonic cell volume. Data are means  $\pm$ SEM (n=6).

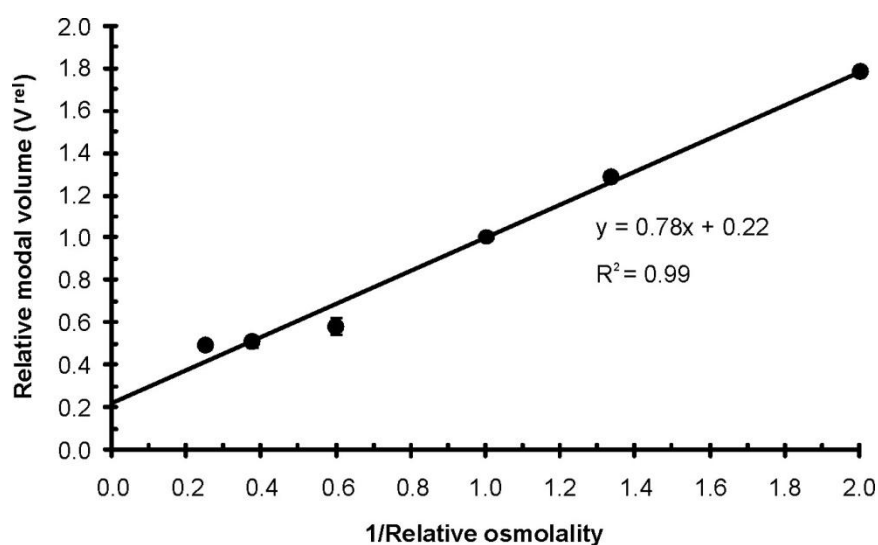


**Figure 3.4 Boyle van't Hoff plot for RH1**

Human embryonic stem cell line, RH1, was trypsinised and centrifuged at 1200rpm. The cell pellet was resuspended in PBS<sup>+</sup>. 1mL of cell suspension was added to 19mL of each of the hypo- or hypertonic solutions made up in PBS<sup>+</sup> solution and left in solution for 5 minutes. The cells were then passed through the Coulter counter for subsequent volume measurements. Boyle van't Hoff plot indicated that the value for its non-osmotic volume,  $V_b$ , was 0.22. Cell volume measurements were normalised to the isotonic cell volume. Data are means  $\pm$ SEM (n=6).

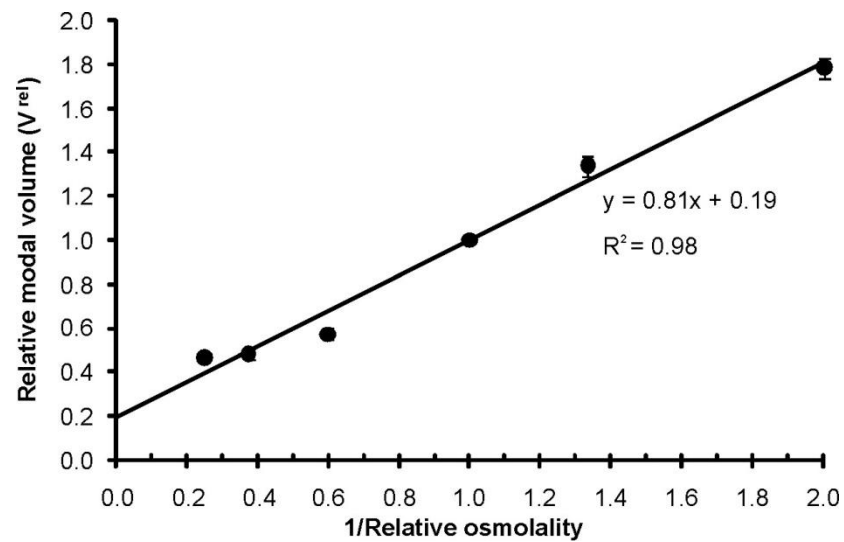


**Figure 3.5 Boyle van't Hoff plot for SHEF3**

Human embryonic stem cell line, RH1, was trypsinised and centrifuged at 1200rpm. The cell pellet was resuspended in PBS<sup>+</sup>. 1mL of cell suspension was added to 19mL of each of the hypo- or hypertonic solutions made up in PBS<sup>+</sup> solution and left in solution for 5 minutes. The cells were then passed through the Coulter counter for subsequent volume measurements. Boyle van't Hoff plot indicated that the value for its non-osmotic volume,  $V_b$ , was 0.19. Cell volume measurements were normalised to the isotonic cell volume. Data are means  $\pm$ SEM (n=4).

### 3.4.3 Basic cell properties

Some relevant biophysical properties of the three cell types are listed in table 3.2. The cell volumes were measured using the Coulter counter with the instrument offset correction shown in Fig. 3.2. The cells were assumed to be spherical and the radius was calculated from the standard formula for the volume of a sphere ie  $\text{Volume} = 4/3\pi r^3$ , where  $r$  is the radius of the sphere. The surface area of each cell was then calculated from the formula for the surface area of a sphere,  $\text{Area} = 4\pi r^2$ . The osmotic volume of each cell type was calculated from the relevant Boyle van't Hoff plot ( $\text{Osmotic volume} = 1 - V_b$ ).

The water content of the cells was assumed to be 87% (or 0.87) of total cell volume, following Dick's work on the measurement of the water content of erythrocytes in comparison to several different cell types (Dick, 1966). It was found that cell water content did not vary widely between different cell types and were comparable to that of erythrocytes. Water volume was measured using dehydration, and calculating cell volume before and after dehydration was carried out. Erythrocytes, compared to other cell types, are less complex because they mainly contain haemoglobin which is a well-characterised protein for which osmotic data is available, and lack a nucleus and membrane-bound organelles (Dick, 1969). In contrast, other cells contain organelles and several proteins which may be known but are less characterised and lack osmotic data. As a result, osmotic data from erythrocytes provide a more accurate estimate of cell water volume than other cell types. Water volume in a similar study on umbilical cord blood cells has also used Dick's value of 0.87 (Hunt et al., 2003h). Assuming this value for the proportion of cell volume occupied by water, therefore, the actual volume of cell water can be calculated (ie  $0.87 \times \text{Cell volume}$ ).

### 3.4.4 Adhesion assay

The first assay performed to assess the effect of anisotonic solutions on the different cell lines was an adhesion assay was carried out on 2102Ep cells. Results showed a larger percentage of cells in hypotonic media adhered to the tissue culture plastic compared to cells in isotonic or hypertonic media (Fig. 3.6) but there were no significant differences between the various anisotonic conditions tested. As a result, this assay was not carried out on any of the hESC lines because it was not helpful in determining the osmotic tolerance of the cells.

**Table 3.2 Biophysical properties of hEC and hESCs.**

Basic cell properties for embryonal carcinoma cell line, 2102Ep, and human embryonic stem cell lines, RH1 and SHEF3.

<i>Cell Identity</i>	<i>Cell isotonic volume (<math>\mu\text{m}^3</math>)</i>	<i>Cell surface area (<math>\mu\text{m}^2</math>)</i>	<i>Non-osmotic volume (<math>V_b</math>)</i>	<i>Osmotic water volume (<math>1 - V_b</math>)</i>	<i>Proportion of total cell water volume (1)</i>
2102Ep	1035	494	0.25	0.75	0.87
RH1	2901	984	0.21	0.79	0.87
SHEF3	2097	792	0.19	0.81	0.87

(1) See (Dick, 1966)

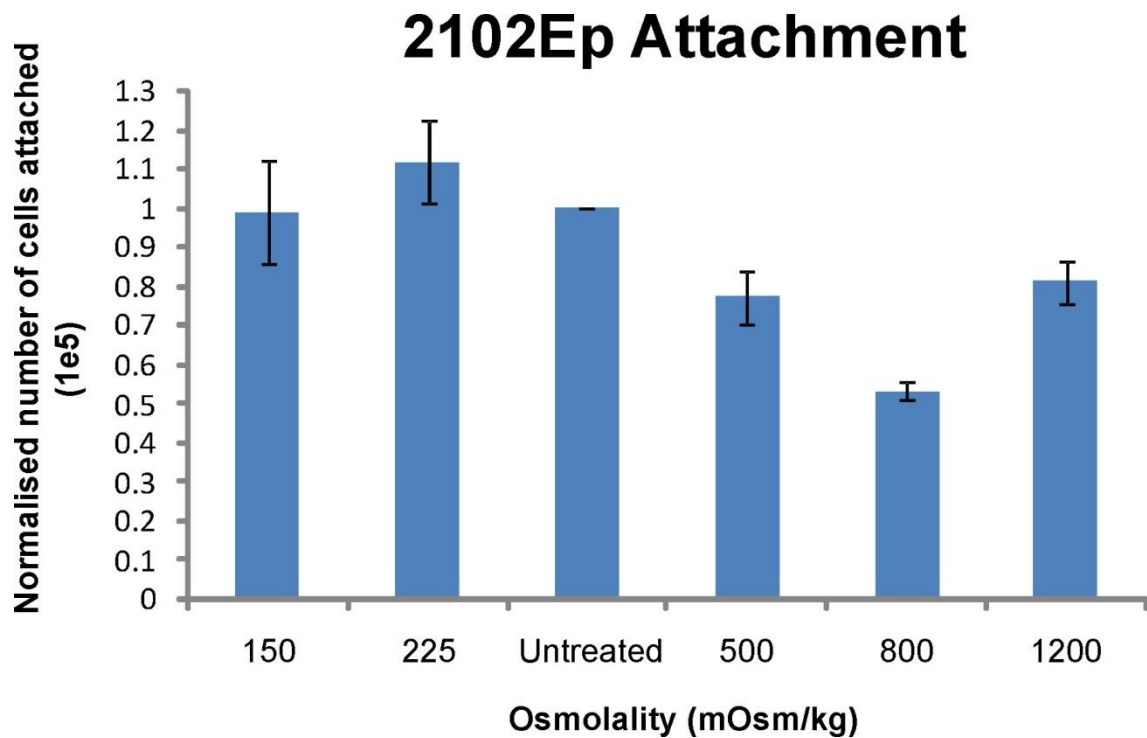


**Figure 3.6 2102Ep cell adhesion following exposure to anisotonic media**

2102Ep cells exposed to hypo- and hypertonic media did not show significant difference in the number of cells that attached to tissue culture plastic compared to cells in isotonic media. The y-axis shows number of cells attached normalised to cells in isotonic media. Data are means  $\pm$ SEM ( $n = 3$ ).

### 3.4.5 Determination of tolerance limits

Due to the results of the adhesion assay, the osmotic tolerance of each cell line was tested using PI exclusion and cell growth assays. The isotonic control for each assay was treated in the same way as all other conditions. All percentages in the PI exclusion assays are shown in relation to the number of cell input, but the cells that might have floated off during the assay were not accounted for because the aim of the assay was to compare the results of each anisotonic condition with the isotonic control.

For the 2102Ep cells, there was a significant difference in cell growth under hypertonic conditions (Fig. 3.7A) compared to the isotonic control, indicating the cells' sensitivity to these treatments and, more importantly, to volume shrinkage. There were no significant differences between the hypotonic treatments and the isotonic control. Following calculation of the percentage of cells that excluded PI dye through flow cytometer analysis, there were significant responses in solutions measuring 75 and 150mOsm/kg (Fig. 3.7B). Significant damage was also observed at each of the hypertonic conditions tested (500-1200mOsm/kg).

For the RH1 cells, significant damage was experienced at 75 and 1500 mOsm/kg (Fig. 3.8) while damage was experienced at 75, 150 and 1500 mOsm/kg in the SHEF3 cells (Fig. 3.9). The equations for the lines in the Boyle van't Hoff plots were used to calculate the modal voltage that corresponds to the osmolality where damage was induced. This voltage was then plugged into the equation of the standard curve from the latex bead calibration to calculate the cell volumes in each anisotonic solution which caused damage. This volume was then divided by the cell volume in isotonic medium to calculate the extent of expansion and shrinkage each cell line could withstand.

As a result, it was determined that 2102Ep cells could tolerate shrinkage of up to 60% and expansion by 70% of isotonic volume. For RH1 cells, the volume excursion limit was shrinkage by 60% and expansion of up to 30% or 60-130% of isotonic volume. SHEF3 cells could tolerate between 60-170% of their isotonic volume.

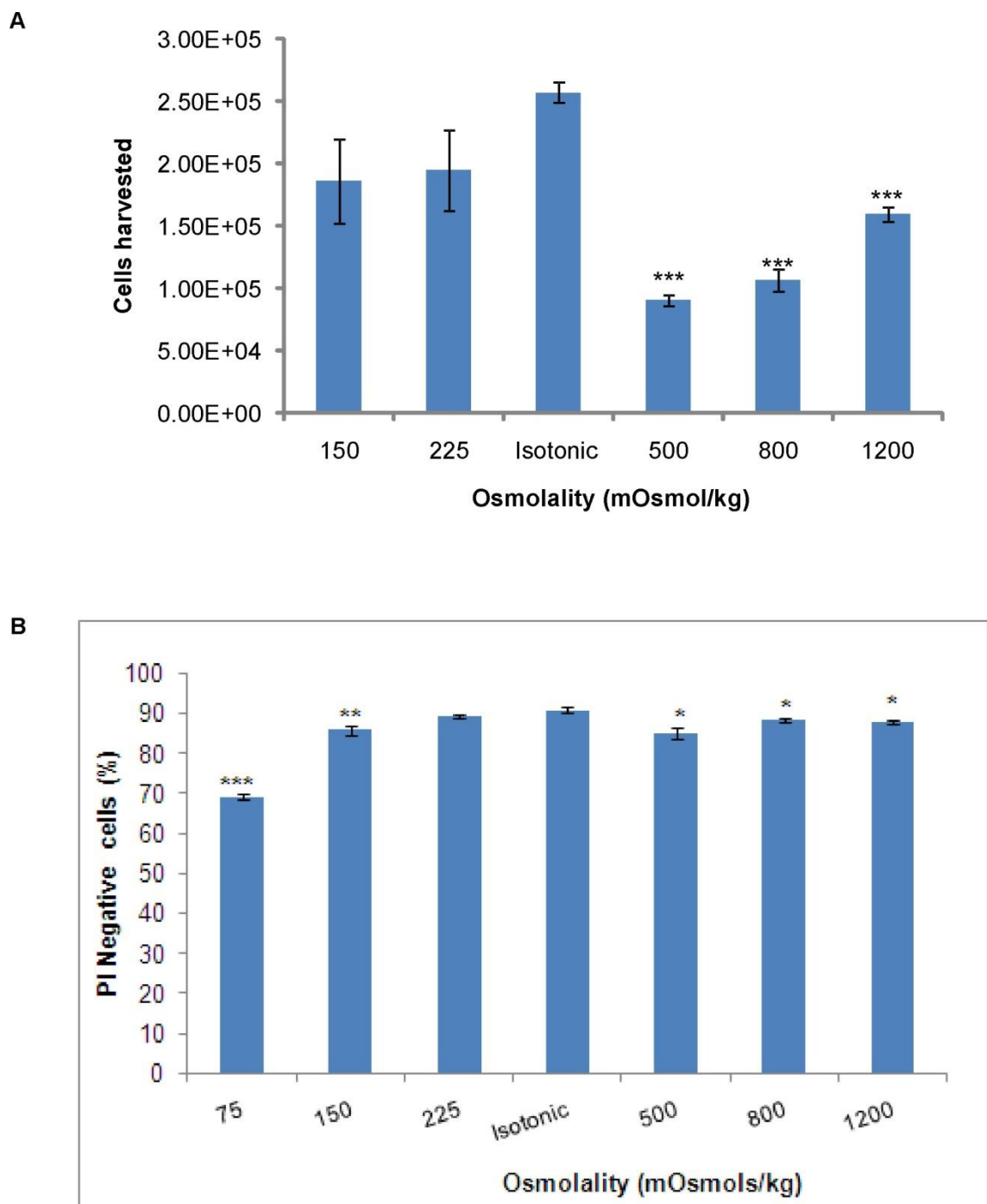


### Figure 3.7 Cell volume excursion limits for 2102Ep

Assessment of the osmotic tolerance of human embryonal carcinoma cell line, 2102Ep. (A) Growth assessment of 2102Ep cells after on day 3 after exposure to anisotonic conditions revealed damage in all hypertonic solutions. (B) Assessment of membrane integrity by exclusion of propidium iodide dye also showed some damage at all anisotonic conditions except 225mOsm. Data are mean  $\pm$ SEM. Statistical analysis was carried out using Levene's test for variance and Student's t-test (\* $p < 0.05$ , \*\* $p < 0.01$ , \*\*\* $p < 0.001$ ) ( $n=3$ ). Using the Boyle van't Hoff data, the damage at 150mOsm and 500mOsm correspond to shrinkage beyond 60% and expansion beyond 170% which gives a volume flux tolerance between 60-170% of isotonic volume.

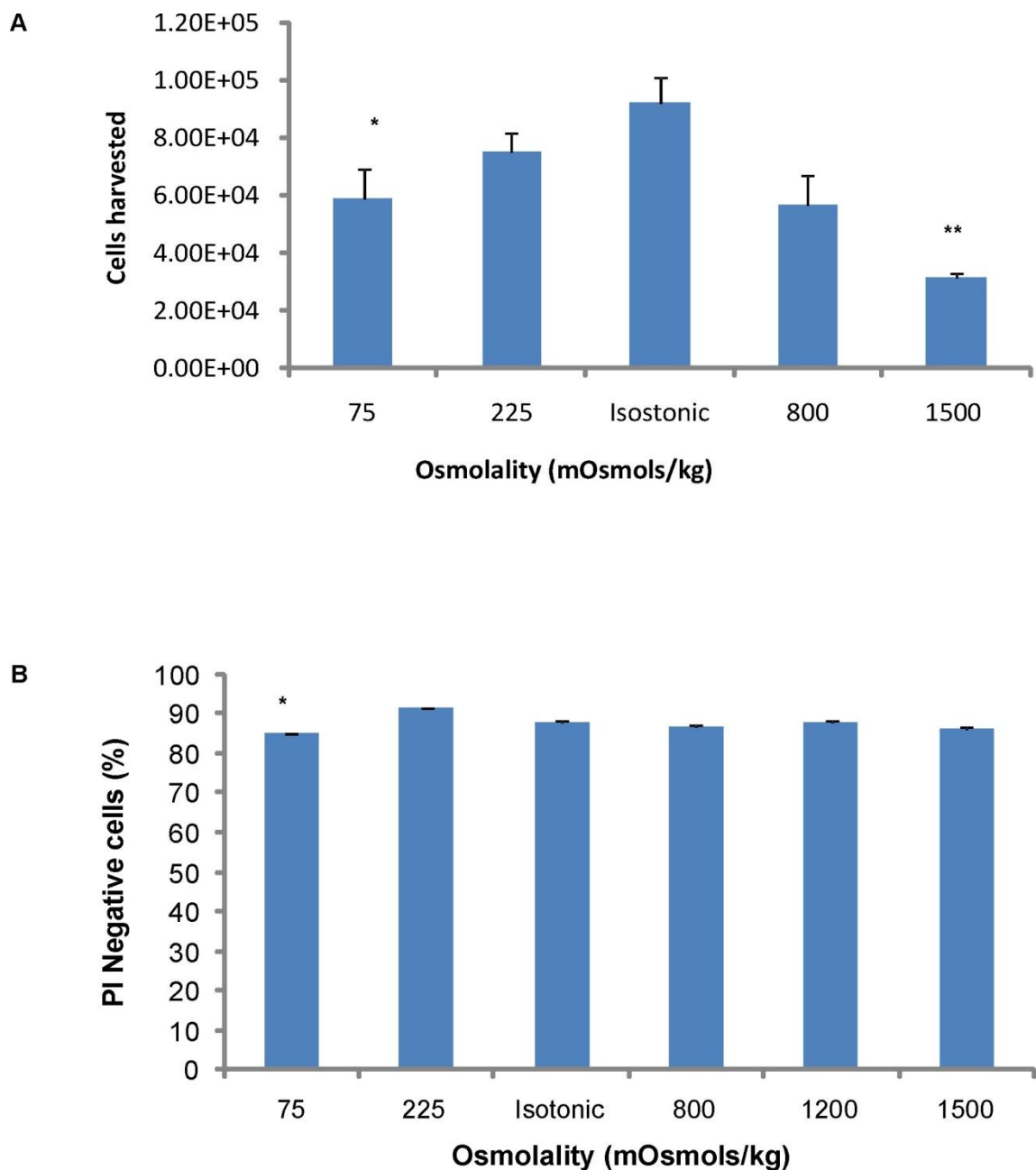


**Figure 3.8 Cell volume excursion limits for RH1**

(A) Growth assessment of RH1 cells after on day 3 after exposure to anisotonic conditions showed damage at 75 and 1500mOsm. (B) Assessment of membrane integrity by exclusion of propidium iodide dye only showed damage at 75mOsm. Data are mean  $\pm$  SEM. Statistical analysis was carried out using Levene's test for variance and Student's t-test (\* $p < 0.05$ , \*\* $p < 0.01$ , \*\*\* $p < 0.001$ ) ( $n = 3$ ). Using the Boyle van't Hoff data, the damage at 75mOsm and 1500mOsm correspond to shrinkage by 60% and expansion of up to 30% or a volume flux tolerance between 60-130% of isotonic volume.

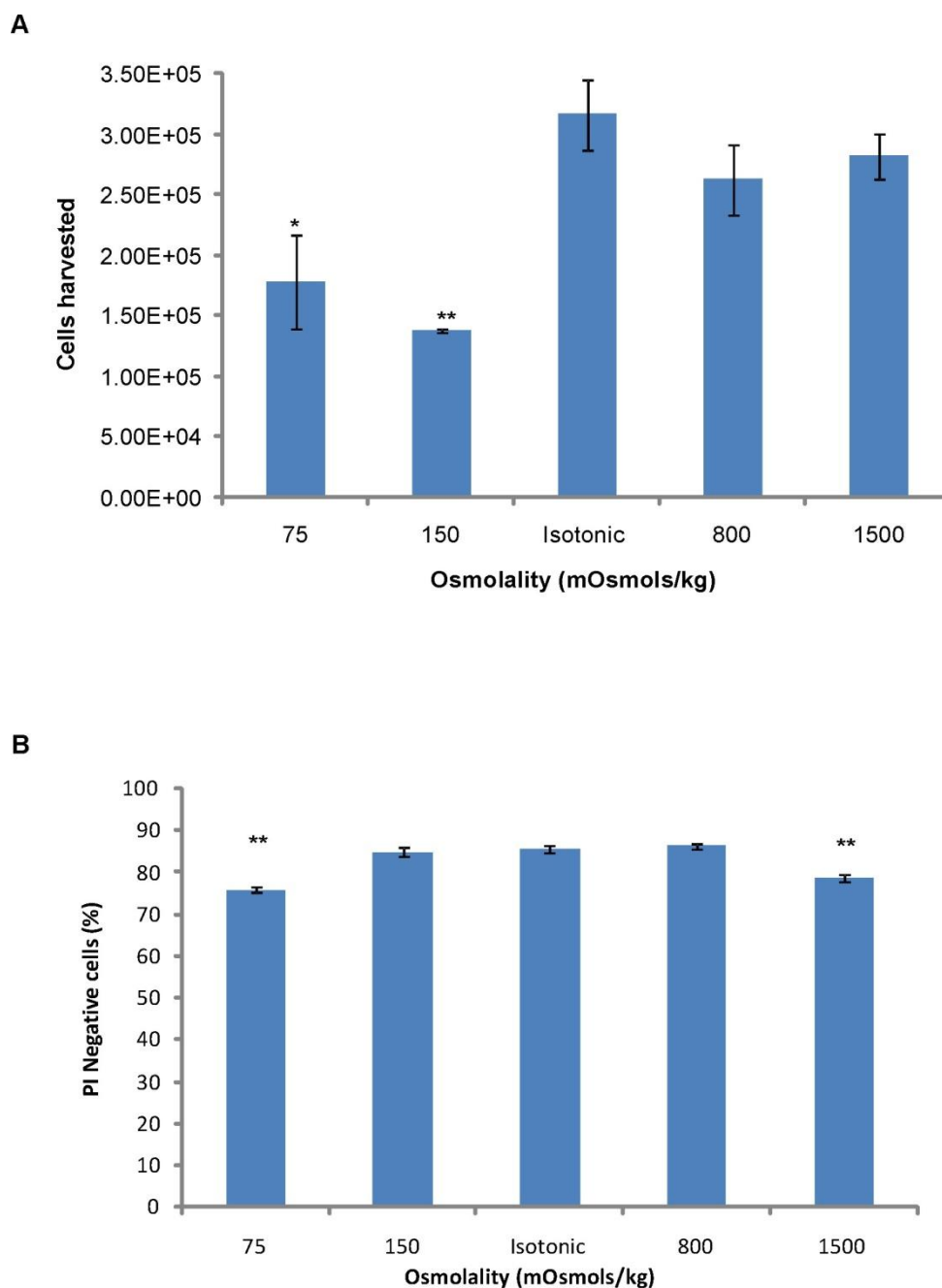


**Figure 3.9 Cell volume excursion limits for SHEF3**

(A) Growth assessment of SHEF3 cells after on day 3 after exposure to anisotonic conditions only showed damage in hypotonic media. (B) Assessment of membrane integrity by exclusion of propidium iodide dye showed significant damage at 75 and 1500mOsm. Data are mean  $\pm$ SEM. Statistical analysis was carried out using Levene's test for variance and Student's t-test (\* $p$ <0.05, \*\* $p$ <0.01, \*\*\* $p$ <0.001) ( $n$ =3). Using the Boyle van't Hoff data, the damage at 150mOsm and 1500mOsm correspond to shrinkage by 60% and expansion up 70% or a volume flux tolerance between 60-170% of isotonic volume.

#### *3.4.6 Effect of anisotonic medium on hESC colony morphology*

Further attempt to analyse the effect of anisotonic media on hESCs was carried out by assessing colony morphology. However, exposure to each of the anisotonic conditions did not inhibit the ability of the hESCs to adhere to the feeder layer and produce colonies with characteristic hESC morphology- closely packed cells in the undifferentiated core and a defined periphery that separates the colony from the MEF layer. The colonies in hypotonic media appeared with less closely packed cells than the hypertonic or isotonic conditions (Fig. 3.10). However, no further analyses were carried out on the morphology such as size measurements of colonies produced in each anisotonic medium because the aim of the assay was to assess whether certain anisotonic conditions affect the adherence and subsequent colony formation of replated cells.

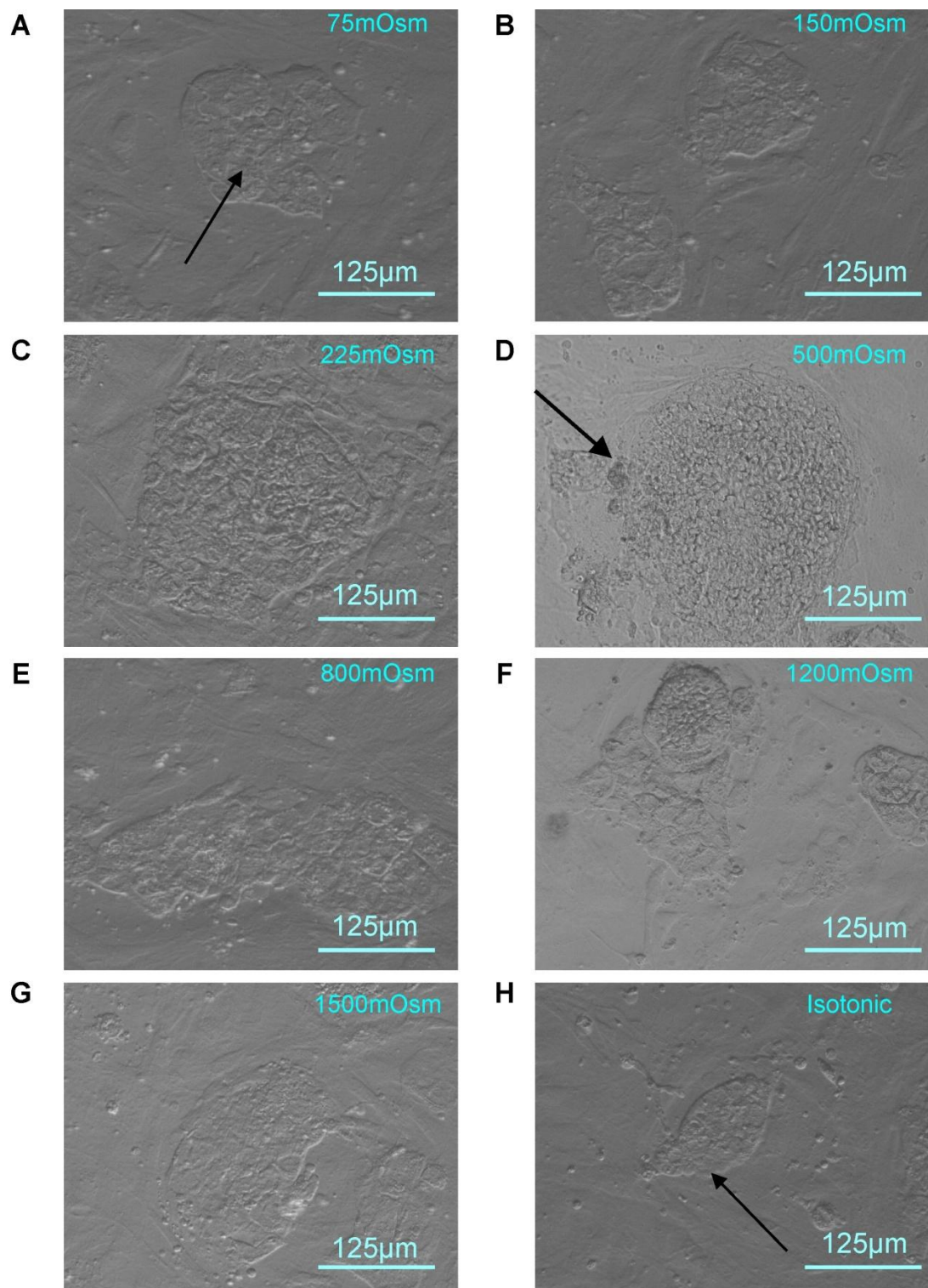


**Figure 3.10 Phase contrast images of colonies in anisotonic conditions**  
hESC colonies at a magnification of 10X in hypotonic conditions (A-C) while those in hypertonic media are shown in D-G. All colonies exhibit characteristic morphology with tightly packed cells on the core and a defined periphery between the colony and the MEF layer which can be clearly seen in the isotonic medium. The arrow in D indicates some area of differentiation. (n = 3 for each condition)

### 3.4.7 *Timecourse responses of cells to CPAs*

Analysis of the effect of PG and Me<sub>2</sub>SO on each cell line was carried out. 2102Ep cells shrank and regained their isotonic volume in Me<sub>2</sub>SO at RT (Fig. 3.11A) while cells required more than 20 minutes to equilibrate in Me<sub>2</sub>SO at +2°C (Fig. 3.11B). However, 2102Ep responded similarly in PG at both temperatures (Fig. 3.12).

The RH1 ESC line in Me<sub>2</sub>SO shrank by 50% and 30% at RT and +2°C, respectively, and regained their isotonic volume; volume shrinkage experienced was within their tolerable limits of volume flux (Fig. 3.13 A&B). On the contrary, longer time periods were required for isotonic cell volume to be restored in PG at each temperature (Fig. 3.14 A&B).

In contrast, SHEF3 required a much longer duration than RH1 to regain isotonic cell volume for all conditions except in PG at RT (Figs. 3.15 and 3.16). Both Me<sub>2</sub>SO and PG caused greater osmotic responses in SHEF3 than in RH1 cells which may indicate greater susceptibility of SHEF3 cells to damage. SHEF3 may also possess a lower permeability than RH1 to the CPAs which may be the reason for its inability to regain isotonic cell volume. In addition, shrinkages experienced in Me<sub>2</sub>SO exceeded the tolerance limit (>60% of isotonic cell volume) determined earlier while shrinkage in PG was close to tolerable limits. This suggests that Me<sub>2</sub>SO may have damaged the cell membrane and PG may be a preferable CPA for SHEF3.

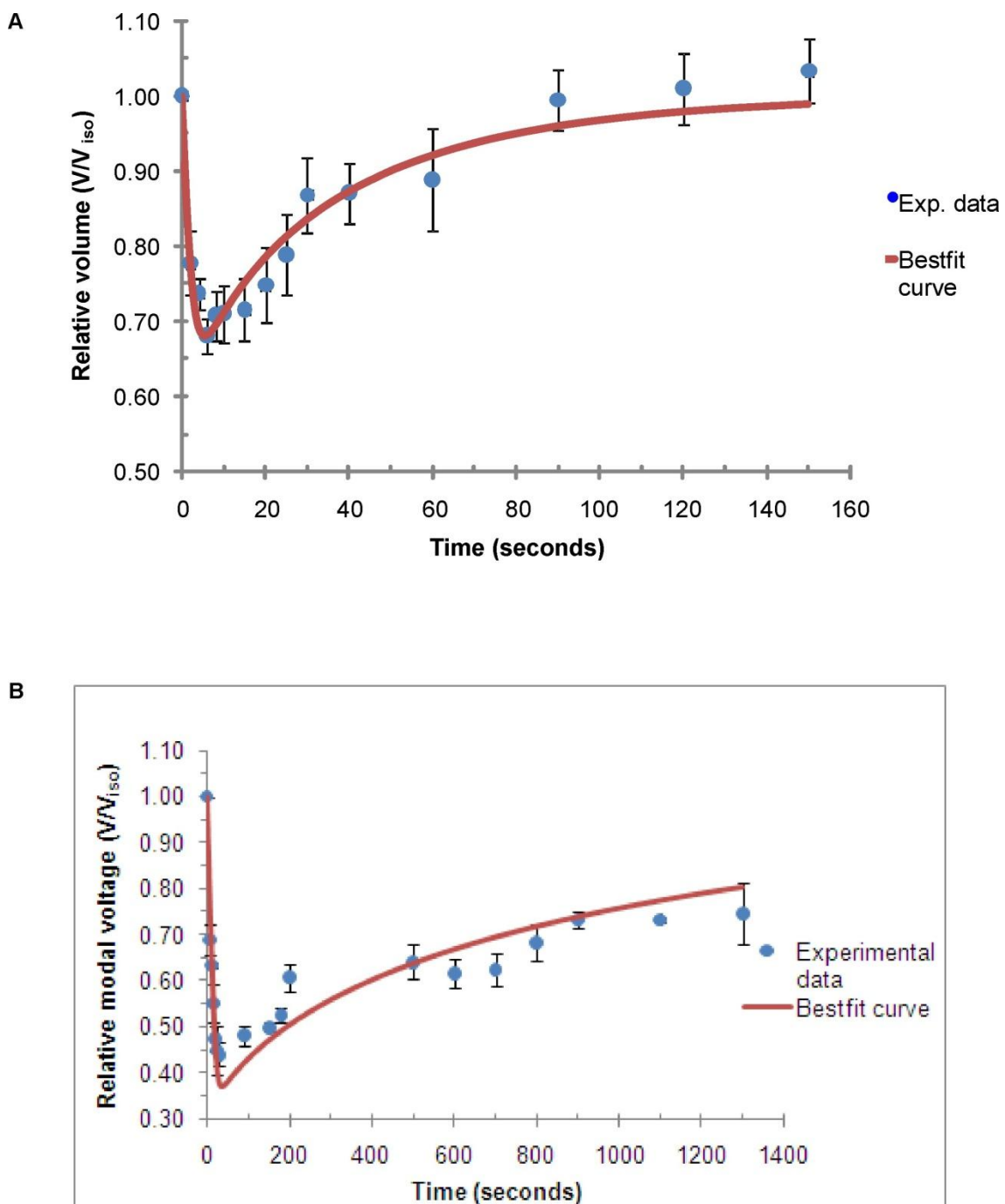


**Figure 3.11 Best-fit curves for 2102Ep in Me<sub>2</sub>SO**

Cells were exposed to 1.225M Me<sub>2</sub>SO for 5 minutes before cell volume was measured using the Coulter counter. Timecourse responses of the human embryonal carcinoma cell line, 2102Ep, to a single exposure to at (A) RT and (B) +2°C. Data are means  $\pm$ SEM (n = 4).

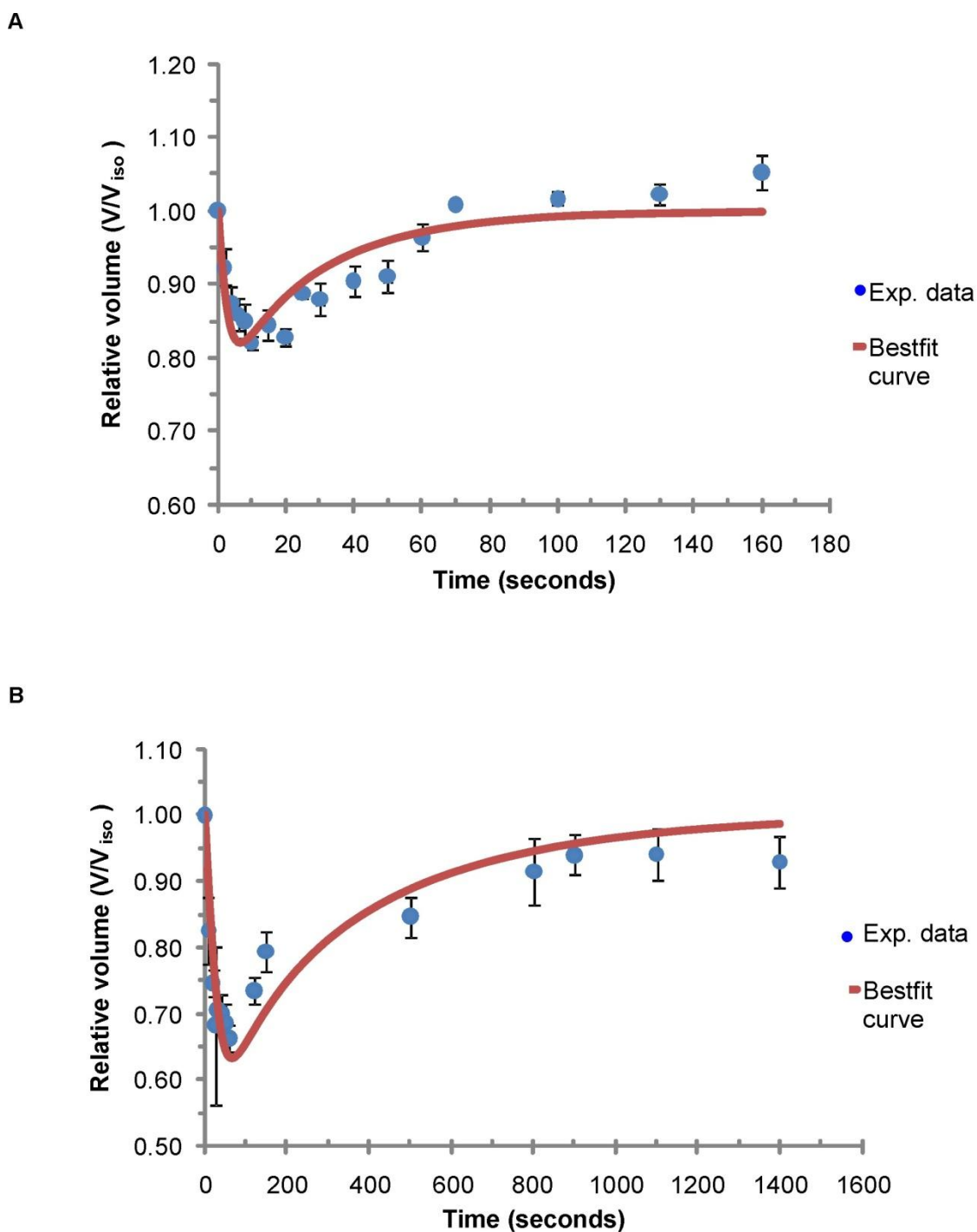


**Figure 3.12 Best-fit curves for 2102Ep in PG**

Timecourse responses of the human embryonal carcinoma cell line, 2102Ep, to a single exposure to 0.66M PG at (A) RT and (B) +2°C. Data are means  $\pm$ SEM ( $n = 4$ ). 500 $\mu$ L of cells were added to 19.5mL of 0.66M PG solution and left for 5 minutes at each temperature before measuring cell volume response on the Coulter counter.

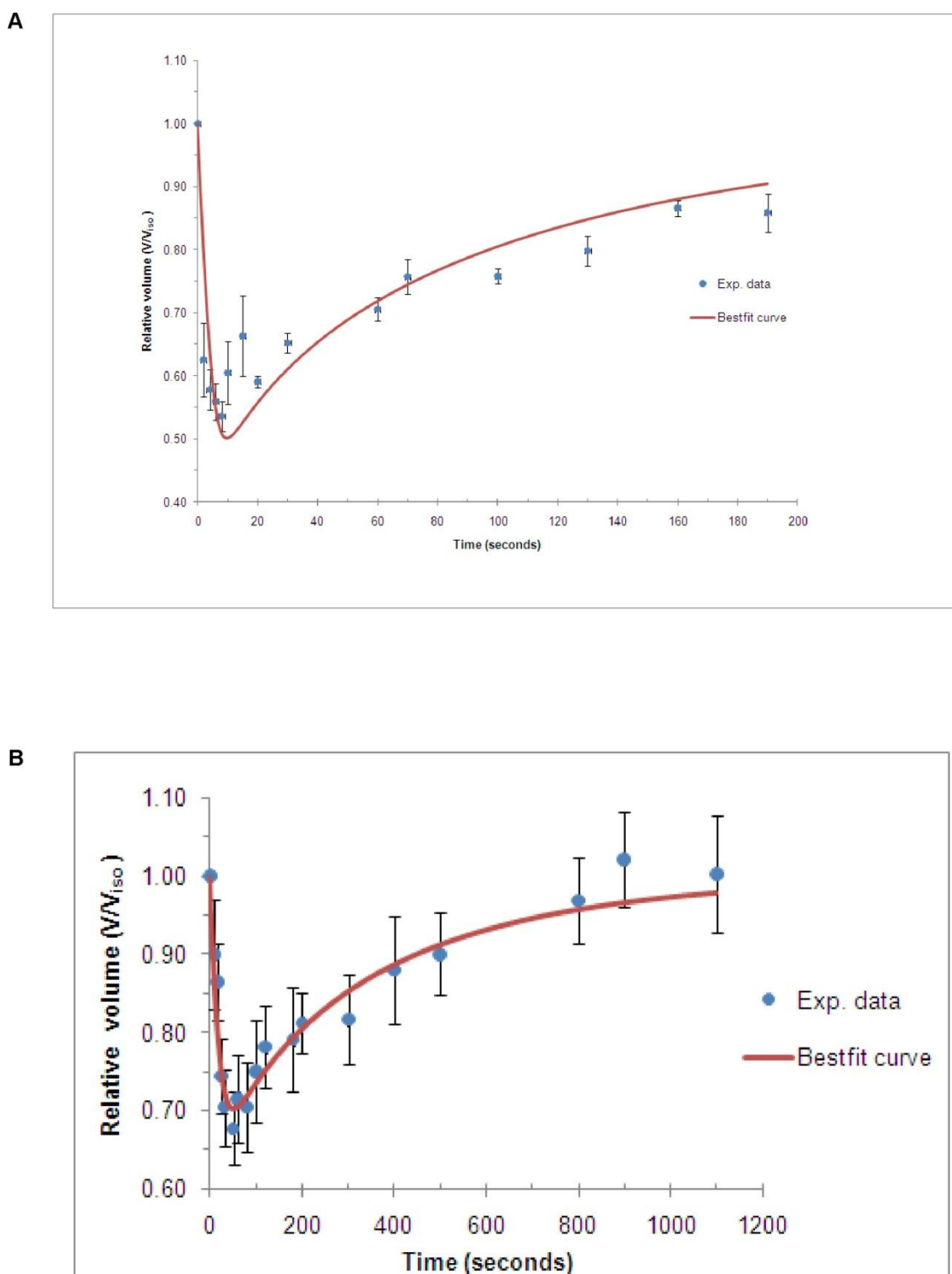


**Figure 3.13 Best-fit curves for RH1 in Me<sub>2</sub>SO**

Timecourse responses of the hESC line, RH1, to a single exposure to 1.225M Me<sub>2</sub>SO at (A) RT and (B) +2°C. Data are means  $\pm$ SEM ( $n = 4$ ). 500 $\mu$ L of cells were added to 19.5mL of 1.225M Me<sub>2</sub>SO solution and left for 5 minutes at each temperature before measuring cell volume response on the Coulter counter.

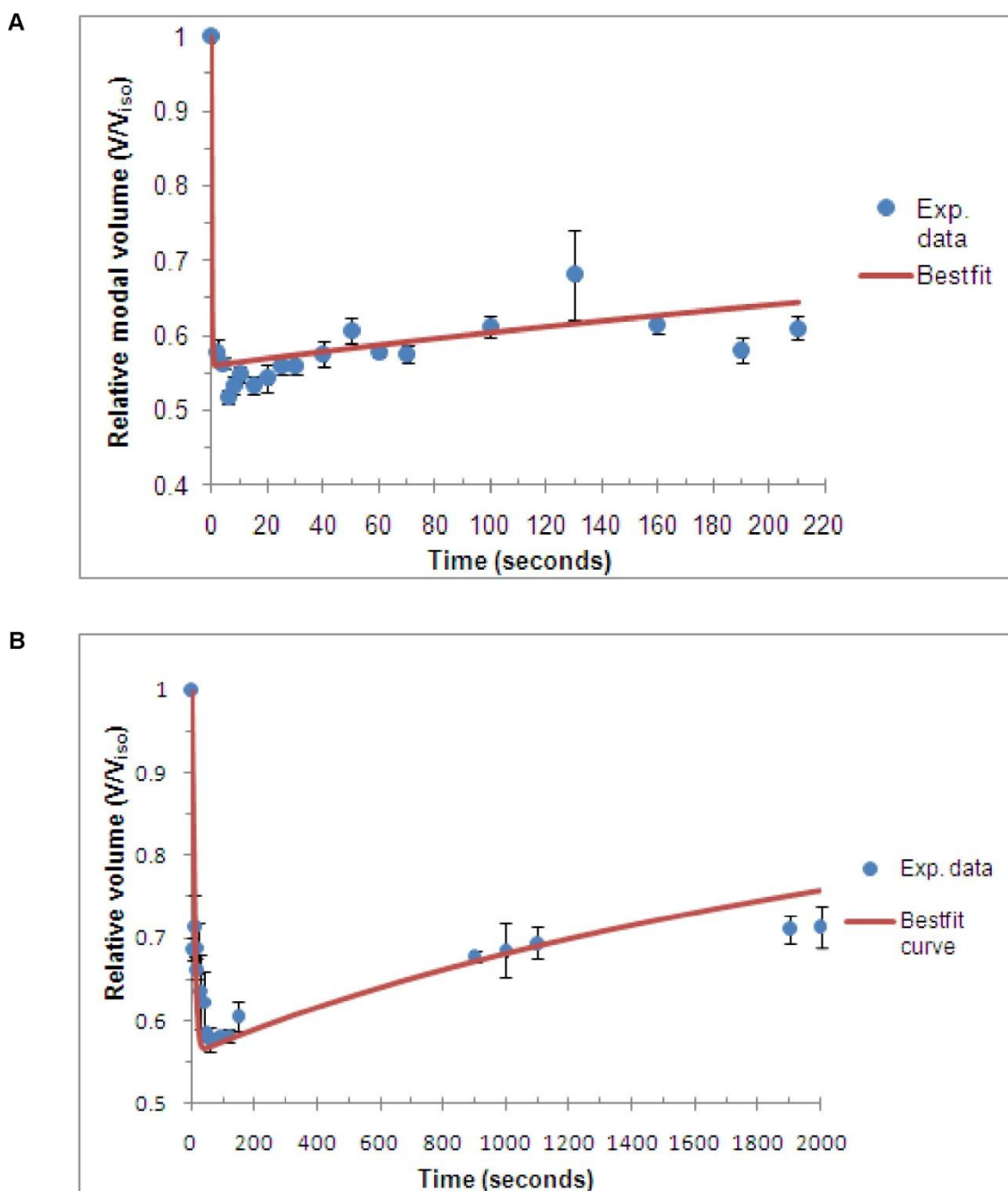


**Figure 3.14 Best-fit curves for RH1 in PG**

Timecourse responses of the hESC line, RH1, to a single exposure to 0.33M PG at (A) RT and (B) +2°C. 500 $\mu$ L of cells were added to 19.5mL of 0.33M PG solution and left for 5 minutes at each temperature before measuring cell volume response on the Coulter counter. Data are means  $\pm$ SEM ( $n = 4$ ).

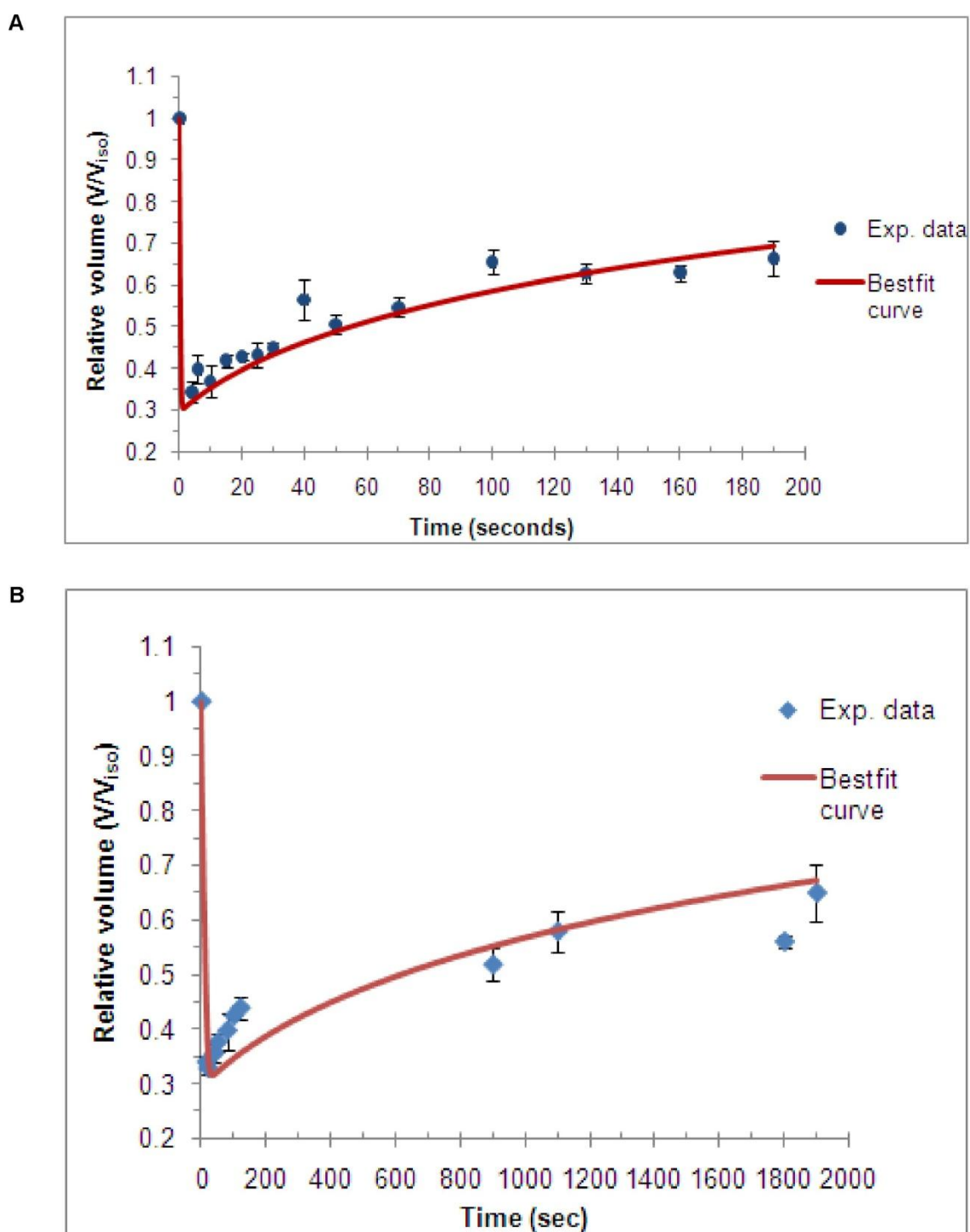


**Figure 3.15 Best-fit curves for SHEF3 in  $Me_2SO$**

Timecourse responses of the hESC line, SHEF3, to a single exposure to 1.225M  $Me_2SO$  at (A) RT and (B) +2°C. 500 $\mu$ L of cells were added to 19.5mL of 1.225M  $Me_2SO$  solution and left for 5 minutes at each temperature before measuring cell volume response on the Coulter counter. Data are means  $\pm$ SEM (n = 4).

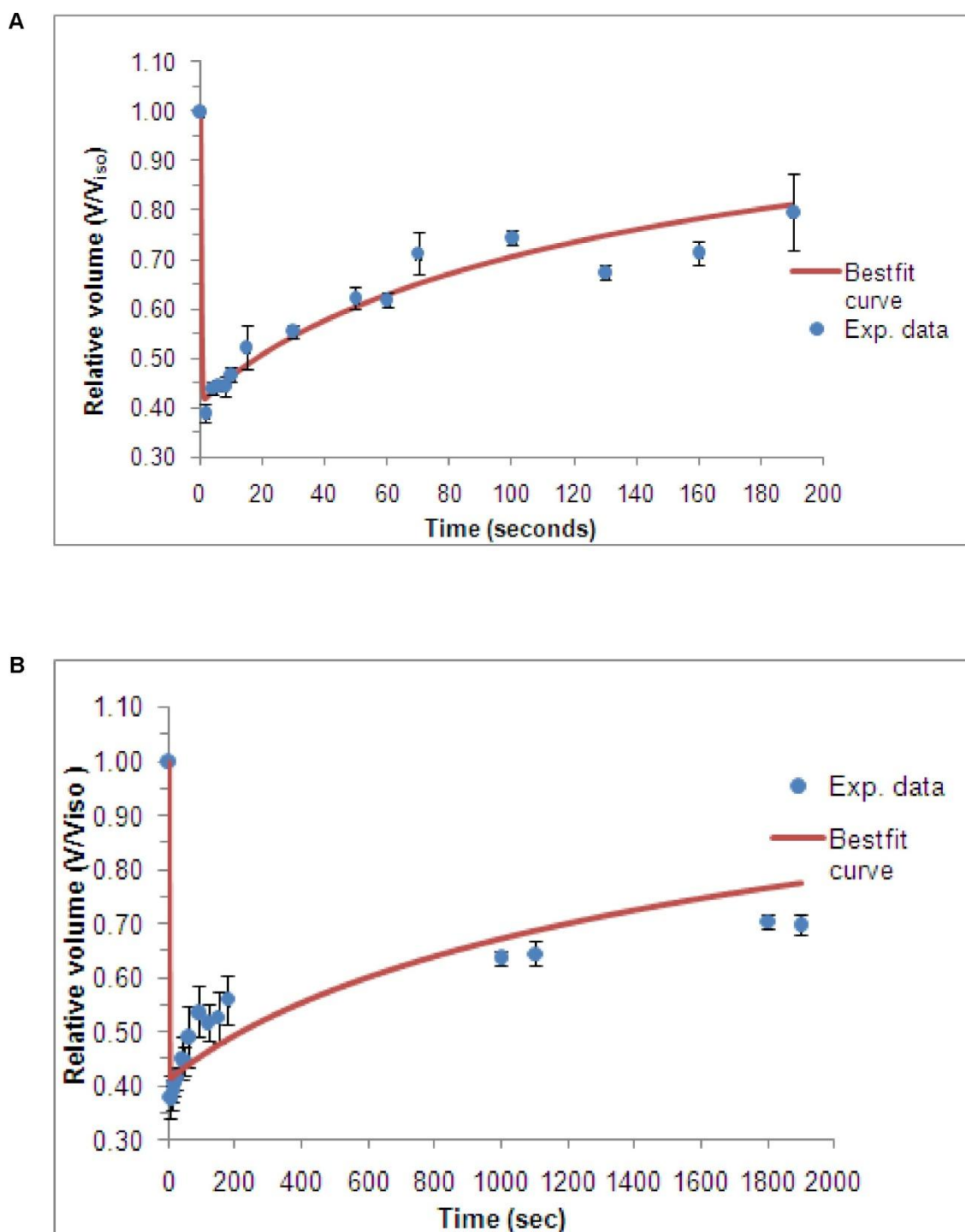


**Figure 3.16 Best-fit curves for SHEF3 in PG**

Timecourse responses of the hESC line, SHEF3, to a single exposure to 0.66M PG at (A) RT and (B) +2°C. 500 $\mu$ L of cells were added to 19.5mL of 0.66M PG solution and left for 5 minutes at each temperature before measuring cell volume response on the Coulter counter. Data are means  $\pm$ SEM ( $n = 4$ ).

### 3.4.8 Summary of data from curve-fitting

2102Ep- Cells recovered their isotonic cell volume in Me<sub>2</sub>SO at RT compared to +2°C. However, cells recovered isotonic volume in the presence of PG at either temperature, indicating that PG may be a more appropriate CPA if exposure is carried out on ice due to its ability to permeate the cells more rapidly than Me<sub>2</sub>SO at low temperatures.

RH1- Cells recovered isotonic volume in Me<sub>2</sub>SO at both RT and +2°C but failed to recover in PG at either temperature, indicating that this cell line is more permeable to Me<sub>2</sub>SO than to PG.

SHEF3- Similar recovery of isotonic volume occurred in Me<sub>2</sub>SO and PG at either temperature but cells appeared damaged in Me<sub>2</sub>SO due to cell volume shrinkage which exceeded tolerable limits of the cells. In contrast to RH1 cells, SHEF3 may possess lower permeability to either CPAs due to not regaining isotonic cell volume in similar exposure times.

### 3.4.9 Permeability variables determined

A summary of the permeability parameters for 2102Ep, RH1 and SHEF3 is shown in table 3.3. It is clear that all values for  $L_p$  and  $P_s$  are higher at RT than +2°C and therefore the recovery of the isotonic cell volume is slower and requires a much longer time period at +2°C. Subsequently, the cells are exposed to the toxic effects of the CPA for a longer period of time at +2°C. The effect of CPA on the cells' permeability and the differences between the cells are also illustrated.

Similar values of  $P_s$  were established for 2102Ep cells in either CPA at RT while  $P_s$  at +2°C was higher for PG than for Me<sub>2</sub>SO, which support the findings from the timecourse experiments that either CPA will be appropriate except if exposure was carried out at very low temperatures.

For the RH1 cells, similar  $L_p$  values were attained for both CPAs but  $P_s$  values were one order of magnitude higher for Me<sub>2</sub>SO at both temperatures than for PG. Although cells lost water at the same rate, isotonic cell volume was either not regained or required a longer time period in PG due to the cells' lower permeability to this CPA.

Furthermore, similar permeability values for CPA were established for SHEF3 illustrating why similar cell recovery occurred within the same time period (33 minutes). However, the higher recovery of cell volume in PG at RT can be explained by the higher value for  $L_p$  which means more water entered the cells during volume recovery.

It also confirms that PG may be more suitable and less toxic to SHEF3 cells than Me<sub>2</sub>SO.

**Table 3.3. Hydraulic conductivity and solute permeability**

Permeability properties for 2102Ep, RH1 and SHEF3 cells for Me<sub>2</sub>SO and PG at RT and +2°C.

Cell identity	Cryoprotectant	L <sub>p</sub> (cm/atm/s)		P <sub>s</sub> (cm/s)	
		RT	+2°C	RT	+2°C
2102Ep	Me <sub>2</sub> SO	1.05x10 <sup>-6</sup>	2.2x10 <sup>-7</sup>	3.88x10 <sup>-5</sup>	6x10 <sup>-7</sup>
	PG	7x10 <sup>-7</sup>	2.0x10 <sup>-7</sup>	3.0x10 <sup>-5</sup>	2.08x10 <sup>-6</sup>
RH1	Me <sub>2</sub> SO	1.3x10 <sup>-6</sup>	1.52x10 <sup>-7</sup>	1.9x10 <sup>-5</sup>	6.48x10 <sup>-6</sup>
	PG	2.5x10 <sup>-6</sup>	5.0x10 <sup>-7</sup>	4.5x10 <sup>-6</sup>	3.0x10 <sup>-7</sup>
SHEF3	Me <sub>2</sub> SO	8x10 <sup>-6</sup>	3x10 <sup>-7</sup>	3x10 <sup>-6</sup>	2.53x10 <sup>-7</sup>
	PG	2x10 <sup>-5</sup>	4x10 <sup>-6</sup>	2.75x10 <sup>-6</sup>	2.5x10 <sup>-7</sup>

### 3.5 Discussion

Biophysical properties of various cell types have been investigated and published but such data are unavailable for hESCs. Previous cryopreservation studies have mostly been based on increasing post-thaw survival and not deriving an optimal cryopreservation method that requires fundamental physical properties of cells to be known. In order for these properties to be determined, it first had to be established whether hESCs behaved as perfect osmometers, responding to anisotonic media by the shrinking and expanding in cell volume; and secondly, their various physical properties could be determined. It was the aim of this chapter, therefore, to utilise hESC lines which had undergone different culturing methods in the early stages following derivation to assess whether the culturing techniques may affect their membrane properties and therefore how each responds to cryopreservation.

Due to their colony forming nature *in vitro* and in order to obtain accurate data for membrane properties, single cell suspensions were required which were attained by the trypsinisation of hESC colonies using the recombinant trypsin, TrypLE (Invitrogen). TrypLE has been shown to dissociate hESCs colonies successfully into single cells with subsequent regeneration of new colonies *in vitro* (Ellerstrom et al., 2007b). This trypsin is gentler and more effective for cells that have been manually passaged or enzymatically treated as was the case with the hESC lines, SHEF3 and RH1, respectively. The human embryonal carcinoma cell line, 2102Ep, was used in preliminary experiments because it is of the same species as SHEF3 and RH1, it has been shown to express similar cell surface markers as hESCs, and lastly, can be easily cultured without the need for a feeder layer to maintain an undifferentiated state (Andrews, 2002a; Adewumi et al., 2007e).

Exposure of all cell lines to anisotonic media revealed that 2102Ep, SHEF3 and RH1 behaved as perfect osmometers over the range of 150-1200mOsm/kg as illustrated in the Boyle van't Hoff plots produced for each cell line. However, the data point at 500mOsm/kg for each cell line deviated from linearity compared to other data points. This could have been due to error in the preparation of the stock solution which may have been more concentrated than 500mOsm/kg and caused greater shrinkage than expected. However, the  $R^2$  values for all three cell lines showed that the linearity of the plots was unaffected by the inclusion or exclusion of the data point;  $V_b$  values, therefore, remain good estimates. Similar deviation from linearity occurred with CD34<sup>+</sup> cells at 140mOsm/kg with the value of  $V_b$  unaffected (Hunt et al., 2003g). Extrapolation of the plot indicated that the nonosmotic volume for 2102Ep, SHEF3 and RH1 were 0.25, 0.19 and 0.22, respectively, which are comparable to the nonosmotic volumes for

various cell types, including CD34<sup>+</sup> cells from the umbilical cord blood (0.27) (Hunt et al., 2003f), human oocytes (0.20) (Paynter et al., 1999b) and human haematopoietic progenitors from bone marrow (0.205) (Gao et al., 1998). However, the  $V_b$  values were much lower than those reported for mouse embryonic stem cells (0.497) (Kashuba Benson et al., 2008k) human chondrocytes (0.414) (Wu et al., 2005i) and human spermatozoa (0.50) (Gilmore et al., 1995c). Interestingly, cell volume measurements for human haematopoietic progenitors from bone marrow were measured using both optical and electronic particle sizer methods, resulting in cell volumes which were not significantly different from each other. It may be more efficient therefore to carry out volume measurements of hESCs using video microscopy because of the smaller cell sample required which will allow hESCs to be used for other assays.

The assays used in this chapter to test the effect of anisotonic media were membrane integrity test through the exclusion of PI, cell adhesion to the feeder layer and growth assay to assess functionality by the production of colonies in culture. The adhesion assay did not produce any significant differences between the various osmolalities, which led to only the membrane integrity and cell growth assays to be utilised in determining the extent of shrinkage and swelling the cells can tolerate before experiencing osmotic damage. Li et al performed cell adhesion assays post-thaw using H9 hESCs to compare cells which were treated with a p160-Rho-associated coiled-coil kinase (ROCK) inhibitor, Y-27632, and those that were untreated (Li et al., 2008e). The cells were disrupted into single cells, replated onto Matrigel-coated plates, and incubated for 12 hours, yielding marked difference between the two groups of cells. Although the role of ROCK is not well understood, it has been shown to induce apoptosis and is involved in the regulation of cell motility and cell proliferation (Riento and Ridley, 2003). In hESCs, dissociation of the colonies activates ROCK and therefore apoptosis (Ohgushi et al., 2010a). As a result, the addition of a ROCK inhibitor such as Y-27632 will be beneficial for hESC survival (Narumiya et al., 2000;Watanabe et al., 2007b).

Membrane integrity and cell growth assays provided more useful information on osmotic tolerance, indicating that the volume excursion limit for each of the cell lines was 60-170% of the isotonic volume for 2102Ep cells and SHEF3 cells, while that of RH1 cells was 60-130%. Each cell line could tolerate a greater shrinkage than that of umbilical cord blood cells (45-140% of isotonic volume) (Hunt et al., 2003e) and sea urchins (Adams et al., 2003) but were more comparable to mouse ES cells (63-153% of isotonic volume) (Kashuba Benson et al., 2008l), which may indicate the greater stress capacity of embryonic cells compared with more differentiated cell types. It is evident that shrinkage beyond 40% of initial volume induced osmotic stress in SHEF3

cells exposed to Me<sub>2</sub>SO. This shrinkage limit is similar to that of human oocytes which are able to maintain membrane integrity following shrinkage of up to 40% (McWilliams et al., 1995).

The establishment of the osmotic tolerance limits of the cells made it possible to calculate water and solute permeability in the presence of CPA. Although the Kedem and Katchalsky formalism (Kedem and Katchalsky, 1958c) is commonly used in calculating these parameters, Kleinhan's 2P formalism (Kleinhan, 1998c) provides a simpler means by excluding the reflection coefficient and assuming the transport of water and solute through different membrane channels. This simpler formalism was used in this chapter to generate curves to fit the experimental shrink-swell curves produced by each cell line. Manual iteration occurred by changing the values of each permeability parameter until the best-fit curve was achieved. The resulting  $L_p$  and  $P_s$  determined were at least an order of magnitude higher at RT than at +2°C, indicating the faster movement of water and solutes through the cell membrane at the higher temperature which confirms that biological processes occur more rapidly at higher temperatures than lower temperatures.

For all cell lines,  $L_p$  values were an order of magnitude greater in Me<sub>2</sub>SO than that of mESCs (Kashuba Benson et al., 2008m). In PG, however, 2102Ep cells possessed the same  $L_p$  value of  $7 \times 10^{-7}$  cm/atm/s at RT as mESCs while those of RH1 and SHEF3 were one and two orders of magnitude higher than the value for mESCs, respectively, indicating that these hESC lines were more permeable to water and may possess more water channels than their mouse counterparts. SHEF3 also possessed higher  $L_p$  values in Me<sub>2</sub>SO and PG than human white blood cells and Pacific oyster oocytes (McGann et al., 1984; Salinas-Flores et al., 2008). It can be suggested that aquaporin 3 may be present on hESC membranes and responsible for the facilitated diffusion of water across the cell membrane which is the case various cell types (Ishibashi et al., 1994d; Ishibashi et al., 1997c; Edashige et al., 2000a). Consequently, a further investigation into the expression of aquaporin 3 and other members of the aquaporin family should be carried out because there are currently no reports that hESC membranes possess these proteins.

$P_s$  value in Me<sub>2</sub>SO for RH1 was an order of magnitude higher than SHEF3 cells at both temperatures while permeability to PG was similar for both cell lines at either temperature. However, it is clear that either cell line required a much longer time period to regain isotonic cell volume in PG which may subject the cells to the toxic effects of the CPA. For SHEF3, however, PG appears the more suitable CPA due to the damage experienced in Me<sub>2</sub>SO and the greater restoration of isotonic cell volume in PG. PG

has also been found to be the optimal CPA for mESCs (Kashuba Benson et al., 2008n) and is widely used in cryopreserving human oocytes (Paynter et al., 2001b; Paynter et al., 2005b). However, its effect on cellular physiology should be considered as it has been shown that PG causes cellular degeneration and hardening of the zona pellucida in human oocytes (Larman et al., 2007b). In contrast to SHEF3, RH1 was more permeable to Me<sub>2</sub>SO as it only gained about 60% of its isotonic volume at both RT and +2°C in PG. Human oocytes, however, regained isotonic cell volume quicker in PG than Me<sub>2</sub>SO (Paynter et al., 1999c; Paynter et al., 2001c). Although similar permeability to PG was determined for SHEF3 and RH1, surface area to volume (S/V) ratio may provide an explanation why SHEF3 was more permeable to PG than RH1 in the same exposure period. Using the calculated volume and area of each cell line, SHEF3 has an S/V ratio of 0.38 compared to 0.33 for RH1 which suggests that more water and solute will permeate the SHEF3 membrane than the RH1 membrane.

The damage experienced by SHEF3 in Me<sub>2</sub>SO may provide an explanation for hESC susceptibility to differentiation post-thaw. Katkov et al. found reduced expression of Oct4 in hESC when Me<sub>2</sub>SO was used in slow-cooling procedures (Katkov et al., 2006c). Hence, loss of membrane integrity pre-cooling may be related to the down-regulation of pluripotent genes and increased differentiation post-thaw. Since loss of pluripotency has been found connected to deficiency in intercellular interaction in ES cells (Wong et al., 2004; Todorova et al., 2008), it can be suggested that hESCs which have experienced stress due to extensive shrinkage or swelling may lose the ability to form colonies *in vitro* because they lack the necessary GAP junctions through which they communicate. Wong and colleagues identified that hESCs express connexin 43 and connexin 45 which are involved in cell proliferation, cell differentiation and apoptosis (Wong et al., 2004). Consequently, hESCs can lose the potential to grow in culture, form EBs in suspension cultures or develop teratomas when injected into immunodeficient mice. Loss of GAP junctions can also cause hES cells to be vulnerable to apoptosis, which has been linked to the loss of E-cadherin dependent intercellular contact that stimulates ROCK (Wong et al., 2006; Ohgushi et al., 2010b). This confirms why the addition of a ROCK inhibitor to cryoprotective medium improves survival of hESCs post-thaw (Li et al., 2008d; Li et al., 2008i; Claassen et al., 2009d). Moreover, damage on the cell membrane may facilitate the growth of ice in the intracellular space due to extracellular ice acting as a nucleus for the supercooled water in the cytoplasm to form ice during cooling (Mazur, 1965a). Furthermore, there is an indication that the single or one-step addition of 10% Me<sub>2</sub>SO is a sub-optimal method of CPA addition to SHEF3 but this cannot be verified until further analysis is carried out in the next chapter.

Differences between RH1 and SHEF3 indicate that membrane physiology may differ from one cell line to another, which may be a result of what stage in embryo development they were derived. This may impact on how permeable the membrane of each cell line is to water and CPAs as increases in permeability were evident in mouse at later stages of development compared to earlier stages (Mazur et al., 1976). Again, the presence of protein channels that may be involved in transporting CPAs across the cell membrane should be investigated because they may possess different channels which may be selective for specific CPAs. Disparities in the response to cryopreservation have been reported for cells of the same species as is the case for spermatozoa from different males (McLaughlin et al., 1992; Thurston et al., 2002; Leibo et al., 2007). As a result, a uniform protocol may not be possible for hESC lines, which suggests that a routine measurement of the physical characteristics of each hESC line is essential in achieving optimal survival of cells.

This chapter has demonstrated the biophysical properties of 3 cell types and their influence on cell response to sudden changes in osmolality, which in turn affects the choice of CPA that should be used in cryopreserving the cells, the temperature at which the solute should be introduced, and the length of exposure that would prevent osmotic stress. The membrane integrity and cell growth assays have also revealed the effects of damage on the potential of hESCs post-thaw, and prove good measures of the consequences of anisotonic conditions. As a result, these assays will be carried out throughout the rest of the study. The tolerance limits of cell volume shrinkage and expansion established in this chapter can be used to model protocols that allow the addition and elution of CPA without inducing osmotic damage with the aim of developing optimal criteria for the cryopreservation of hESCs.

# **Chapter 4**

**PROTOCOL**

**MODELLING AND DESIGN**

## **4.1 Introduction**

One of the advantages of a systematic approach to designing a cryopreservation protocol is that each source of damage to cells is identified and can therefore be eliminated or the effect minimised in order to optimise cell survival. This chapter considers sources of damage such as CPA toxicity, osmotic effects and the likelihood of intracellular ice. Each cryopreservation criterion will be combined with biophysical properties established in the previous chapter to model a variety of protocols in order to ascertain the procedure that is optimal for each hESC line.

#### 4.1.1 Cryoinjury

Other forms of cell damage include membrane lysis and exposure to damaging concentrations of salts inside and outside the cell (Lovelock, 1953f; Pegg and Diaper, 1988; Muldrew and McGann, 1990a; Muldrew and McGann, 1994). It has been hypothesised that the excessive loss of water affects the organisation of organelles in the cytoplasm (Litvan, 1972) due to the lack of water that normally exists between each organelle. Furthermore, ice crystals forming inside the cells cause damage by unknown mechanisms- presumably mechanical. The formation of ice crystals is dependent on the membrane permeability of cells to water and the rate of cooling.

In order to avoid IIF, it is important to use CPAs that will protect cells from damage, and this is also dependent on the cells' permeability to the CPA. Various CPAs are available for preserving cells at low temperatures. Each of these CPAs permeates the membrane at a different rate depending on the cell type as has been shown in previous studies such as those involving human spermatozoa, bovine chondrocytes, and human platelets (Gilmore et al., 1995e; Woods et al., 1999a; Xu et al., 2003a). The rate of CPA permeation through the cell membrane depends on the biophysical properties of the particular cell type (Lovelock, 1954; Wu et al., 2005j) and the temperature at which the additive is introduced (Mazur et al., 1974; Agca et al., 1998).

Mathematical formulae have been developed to measure the permeability characteristics of cell membranes to water and solutes (Jacobs, 1933b; Kedem and Katchalsky, 1958b). The KK formalism assumes the co-transport of water and solutes through a common channel and introduces a reflection coefficient,  $\sigma$ , which is the degree of interaction between the solute and solvent (Kedem and Katchalsky, 1958a). Conversely, the 2P formalism assumes the independent transport of solute and solvent through separate channels (Kleinans, 1998b). Both of these formalisms have been used in modelling the transport of water and cryoprotectant through the cell membrane (Jacobs, 1933a; Gilmore et al., 1995b; Paynter et al., 1999f; Hunt et al., 2003d; Chaveiro et al., 2004). It has been found that the values for hydraulic conductivity ( $L_p$ ) and solute permeability ( $P_s$ ) were similar with either formalism (Kleinans, 1998a).

It is also important to consider the toxicity of CPAs to cells. Results in chapter 3 have shown that the hESC lines possess varying permeabilities to Me<sub>2</sub>SO and PG. In this chapter, the protective abilities of each CPA were compared in the cryopreservation of hESCs by evaluating their effect on the membrane integrity and functional capabilities of the cells following exposure to each CPA.

#### *4.1.2 Cryopreservation protocol design*

The determination of  $L_p$  and  $P_s$  for each hESC line in the previous chapter is used to model various CPA addition and removal protocols, which can then be used in cooling experiments to test different cooling rates and assess the effectiveness of the protocols. Similar steps have been carried out in the design of a cryopreservation procedure for articular cartilage and umbilical cord blood stem cells (Pegg and Diaper, 1990; Woods et al., 2003a). The resulting methods of adding and eluting CPA can minimise osmotic damage that may occur from the extensive shrinkage or expansion in volume that the cells may experience. However, the results of modelling only provide theoretical predictions of how the cells should react. Hence, experimental testing such as toxicity assays must accompany the freezing tests to ensure that non-toxic concentrations of CPA are utilised for the preservation of the cells. The ideal CPA concentration would be high enough to reduce the concentration of damaging salt concentrations and low enough to remain non-toxic to the cells (Lovelock, 1953g; Mazur et al., 1981b). Finally, cooling experiments where several cooling rates are tested can be performed to reduce damage that may occur from solution effects or intracellular ice formation (see Fig. 1.4). Optimised protocols can then be compared to the current slow cooling protocol used in cryopreserving hESCs which will also be modelled. Figure 4.1 illustrates the steps for designing an optimal cryopreservation protocol.

The aim of this chapter is to investigate each of the cryopreservation variables that may cause cell damage in order to determine the optimal conditions, which will be used in designing a cryopreservation protocol that can be easily executed in a laboratory and which minimises the length of exposure to CPA.

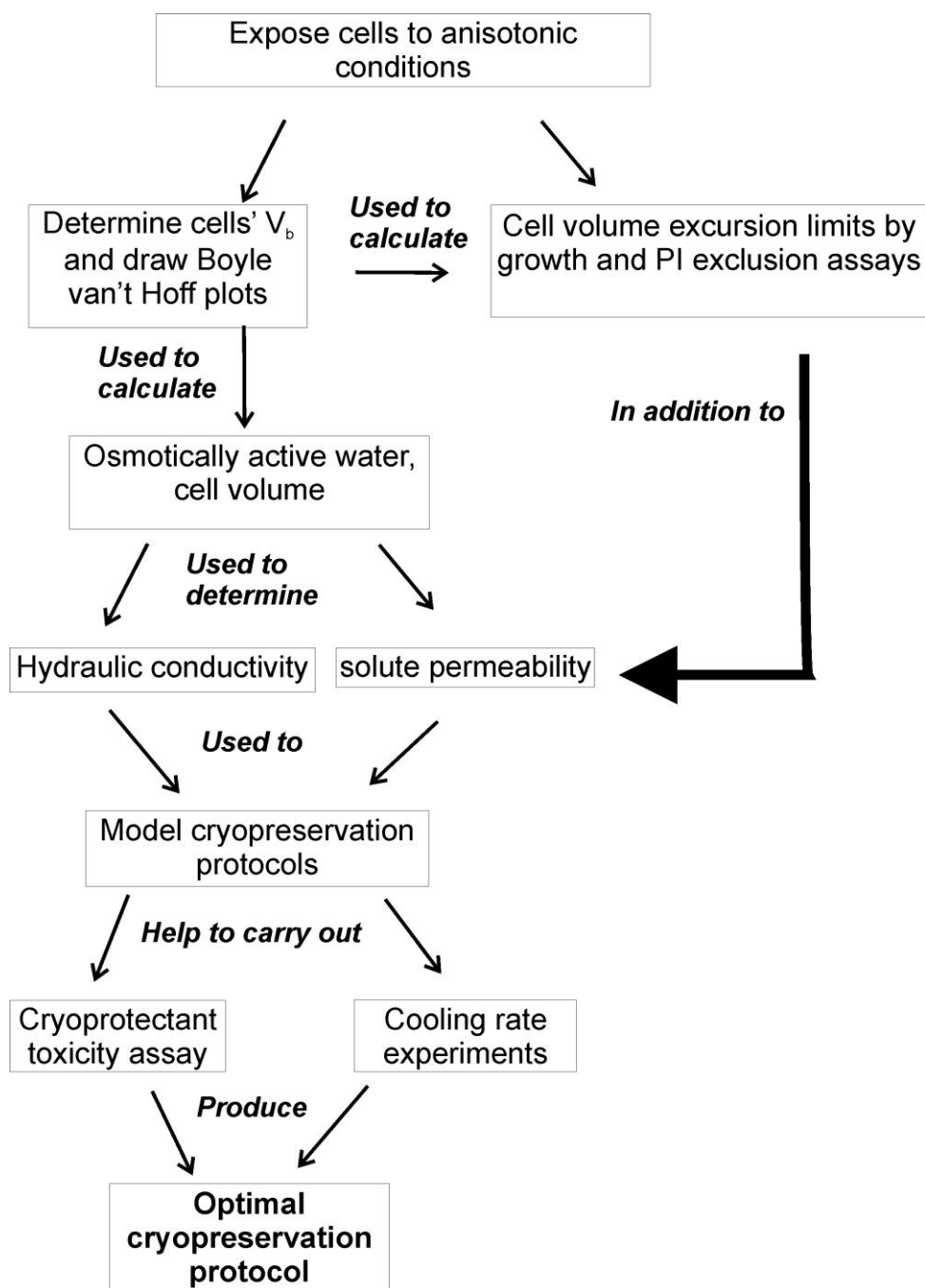


**Figure 4.1 Schematic diagram of designing a cryopreservation protocol**

Illustration of the steps required in designing a cryopreservation protocol. First, nonosmotic volume and biophysical properties are determined. Secondly, osmotic tolerance of each cell type is established. Thirdly, the 2P formalism is used to model CPA addition and removal. Lastly, CPA toxicity and cooling rate assays provide optimal CPA concentration and cooling rate. Theoretical protocol is assessed using membrane integrity and cell growth assays.

## 4.2 Chapter aims

- Use established biophysical properties and osmotic tolerance limits of each cell line (from chapter 3) to model protocols for adding and eluting CPA.
- Carry out CPA toxicity assays to determine optimal CPA by assessing effect of varying concentrations on membrane integrity and *in vitro* cell growth.
- Perform cooling rate assay to determine optimal cooling rate.
- Define optimal protocol for each hESC line based on the assays carried out and assess whether a uniform protocol is possible for both hESC lines.

### **4.3 Materials and Methods**

#### 4.3.1 Toxicity after exposure to cryoprotectant

The toxicity of Me<sub>2</sub>SO and PG to the cells was assessed by using the addition protocols modelled for adding CPA which was then followed by a further 15minutes of exposure. The cells were either replated onto MEF feeders to investigate their colony-forming capabilities or underwent a propidium iodide (PI) assay to assess their membrane integrity. Cell counts were carried out using a haemocytometer while flow cytometry was used to calculate the percentage of cells that excluded PI.

#### 4.3.2 Stepwise addition of PG

0, 2.5, 5, 10, 15% PG were added to the cells following the modelled protocols in order to ascertain the highest CPA concentration each cell line can tolerate before experiencing damage.

#### 4.3.3 Stepwise elution of PG

PG was eluted from RH1 cells using PBS<sup>+</sup> solution and allowing 10 minutes between each dilution step. However, a solution of PBS<sup>+</sup> and D-mannitol was used in diluting PG from SHEF3 cells whilst allowing 10 minutes between intermediate steps (see Tables 4.2 & 4.10).

#### 4.3.4 Stepwise addition of Me<sub>2</sub>SO

0, 5, 10, 15, and 20% Me<sub>2</sub>SO were tested using the addition protocol in order to determine the optimal concentration that does not induce damage to the cells.

#### 4.3.5 Stepwise elution of Me<sub>2</sub>SO

For the RH1 cells and SHEF3 cells, the CPA was removed in a stepwise fashion using a solution of PBS<sup>+</sup> containing 2% (w/w) D-mannitol. D-mannitol is a non-permeable osmoticant which was added to the thawing medium to restrict the degree of swelling the cells experienced. The duration for each intermediate step was 4 and 15minutes for RH1 and SHEF3 cells, respectively (see Tables 4.4 & 4.6).

#### 4.3.6 Addition and elution modelling

The permeability parameters and the biophysical properties determined for the hESCs and the hECs were entered into a purpose-written program, *PLOTSTEP*. The program uses the physical properties- internal and external osmolalities, L<sub>p</sub>, P<sub>s</sub>, and the partial

molar volume of CPA- to solve the Kleinhan's two parameter modelling equation for volume flux and change in concentration of CPA. With all of the variables known, the volume flux experienced by the cells can be calculated. The PLOTSTEP program allows for the addition of CPA to occur in one or more steps. Manual iteration of the internal and external concentrations was then carried out until the volume flux experienced by the cells lay within their tolerance limits. The modelling was carried out using 10% (v/v) Me<sub>2</sub>SO and 5% (v/v) PG as the target concentrations at two different temperatures for each of the cell lines. In addition, modelling of currently used protocols for each cell line was performed which involves addition of 10% Me<sub>2</sub>SO at RT in a single step. Although some add 10% Me<sub>2</sub>SO in a dropwise fashion, there is no published data that states the equilibration period allowed between each drop. However, it was difficult to model the current elution protocol because the amount of elution medium and the length of time that cells remain in the medium vary between technicians.

#### *4.3.7 Cooling*

Cells were trypsinised as earlier described and subsequently subjected to the addition protocols for adding 10% PG or 10% Me<sub>2</sub>SO. The cell suspensions were then aliquotted into 2mL cryovials, placed into a rate-controlled freezer and cooled at 0.3, 1, 3, or 10°C/min to -50°C. The cryovials were subsequently transferred into the vapour phase of a liquid nitrogen Dewar until thawed.

#### *4.3.8 Thawing*

Cells were thawed in a 37°C water-bath until all ice was melted. The CPA was then eluted in a stepwise fashion as earlier mentioned. The cells were subsequently centrifuged at 1200rpm to remove the CPA completely and resuspended in isotonic media.

## **4.4 Results**

#### 4.4.1 Addition modelling data

The modelling of CPA addition to each cell type was carried out in order to determine whether the current cryopreservation protocol used for hESCs was adequate or required optimisation.

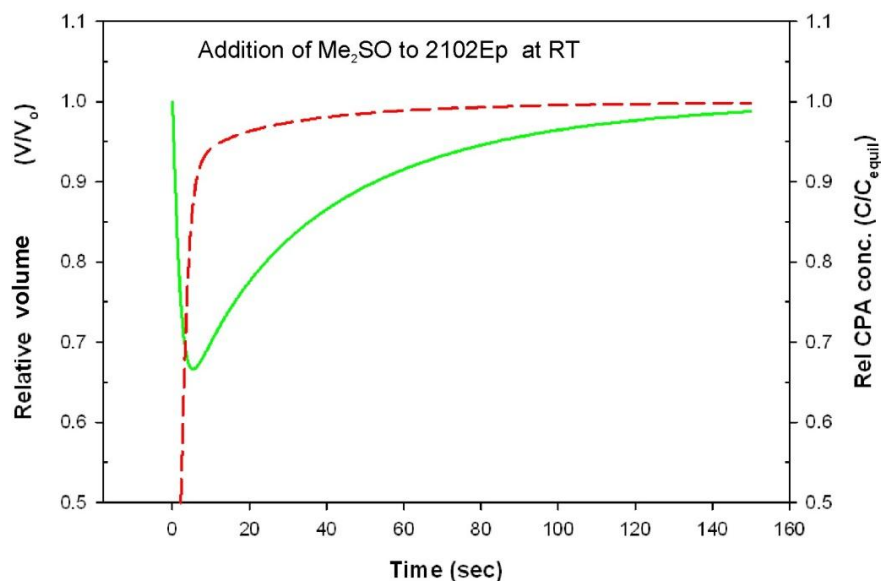
For the hEC cells, the addition of 10% (v/v) Me<sub>2</sub>SO (1.29M) and 5% (v/v) PG (0.66M) at RT could be completed in a single step with the cell volume flux remaining within the tolerable limits of shrinkage (<60%) (Figs. 4.2A & 4.3A). However, the addition of Me<sub>2</sub>SO and PG at +2°C had to be done in four and two steps, respectively; it would require twice the time for the cells to equilibrate in 1.29M Me<sub>2</sub>SO than in 0.66M PG (Fig. 4.2B & 4.3B).

The addition of PG to the RH1 cells, however, had to be carried out in two steps at each temperature (Fig. 4.4). In order for the cell volume and concentration of CPA inside and outside the cells to be equilibrated, a period of 10 minutes and one hour had to be allowed at RT and +2°C, respectively. On the other hand, the single addition of 10% Me<sub>2</sub>SO was adequate at both RT and +2°C (Fig. 4.5).

As with the RH1 cells, the addition modelling showed that 0.66M PG is best added to SHEF3 cells in two steps at RT (Fig. 4.6A) and in five separate steps at +2°C with 50minute equilibration periods (Fig. 4.6B). Me<sub>2</sub>SO had to be added in four steps at both temperatures in order for the cells to avoid osmotic damage; equilibration periods of 17 and 50 minutes had to be incorporated at RT and +2°C, respectively (Fig. 4.7).

Modelling the currently used protocols for each of the cell lines (Fig. 4.8) revealed that the theoretic modelling did not provide a different method for adding Me<sub>2</sub>SO at RT to 2102Ep and RH1. However, the current method of adding Me<sub>2</sub>SO to SHEF3 shows that the cells experience shrinkage beyond their tolerable limits which suggests they must already be damaged before being subjected to cooling.

A



B

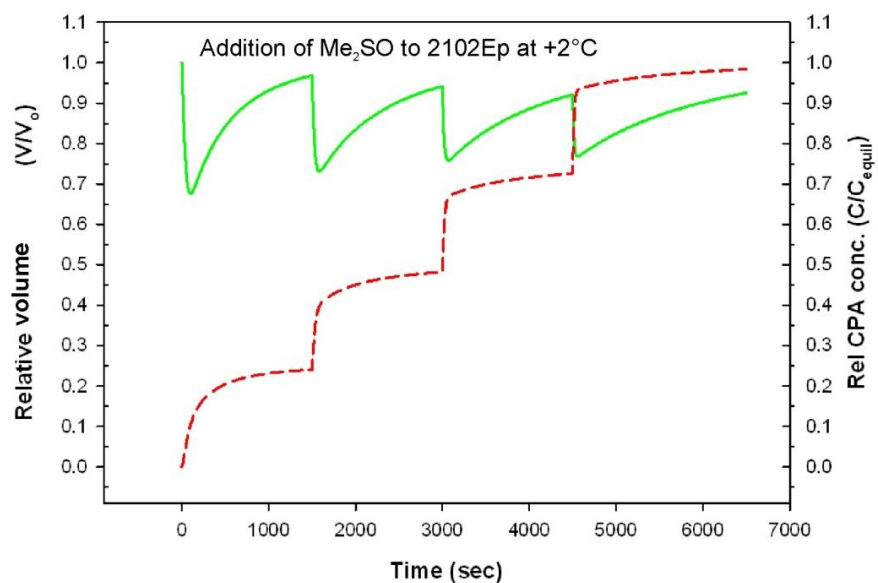


### Figure 4.2 Modelled protocols for addition of Me<sub>2</sub>SO to 2102Ep cells

Modelling addition of 1.29M Me<sub>2</sub>SO to human embryonal carcinoma cell line, 2102Ep at (A) RT and (B) +2°C. At RT, the CPA addition occurred in a single step while at +2°C, it would have to occur in 4 steps at increments of 0.3M in order to maintain the extent of volume expansion and shrinkage the cells could tolerate. The osmotically induced volume excursions (solid line) and intracellular CPA concentration (dashed line) are displayed.



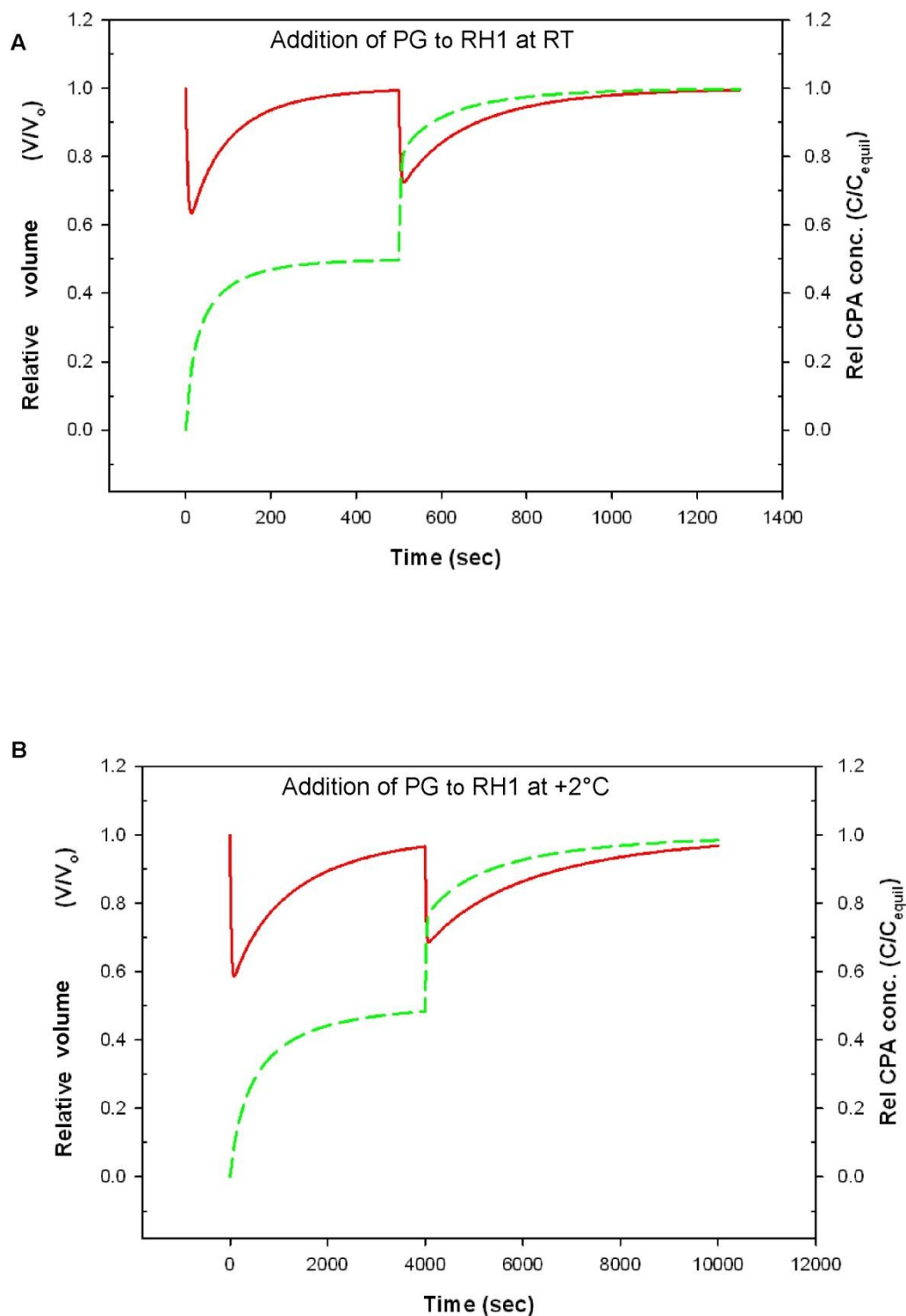
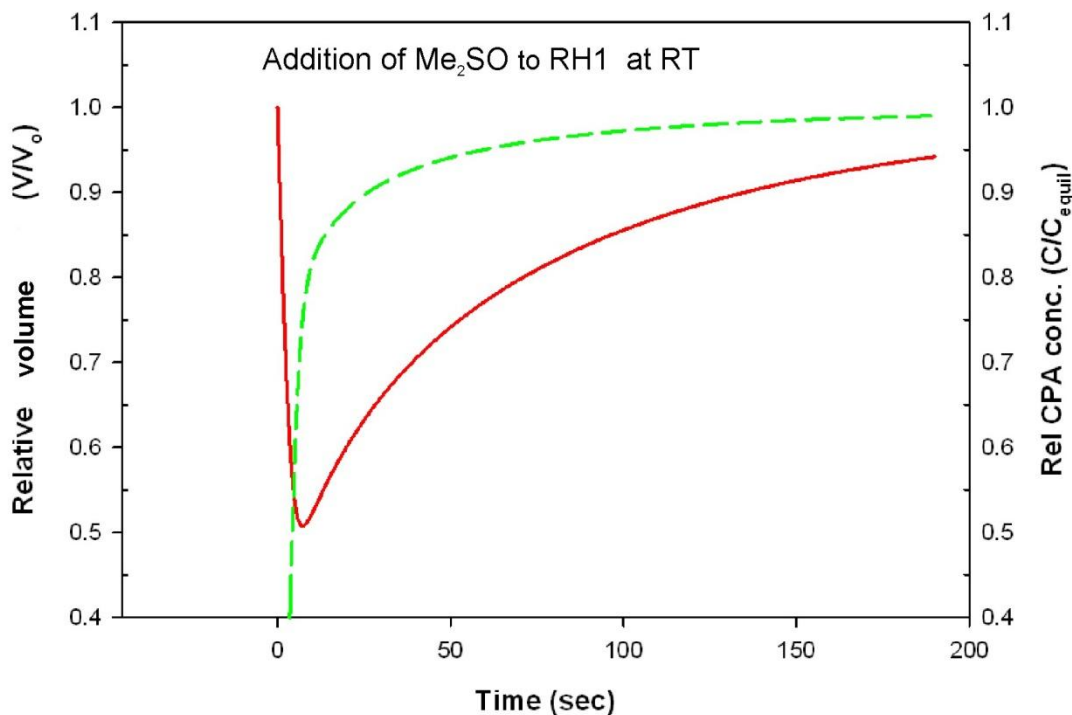


**Figure 4.4 Modelled protocols for addition of PG to RH1 cells**

Modelling addition of 0.66M PG to human embryonic cell line, RH1 at (A) RT and (B) +2°C. At RT and +2°C, the CPA addition occurred in two steps in increments of 0.3M to maintain the tolerable volume excursion of the cells. The osmotically induced volume excursions (solid line) and intracellular CPA concentration (dashed line) are displayed.

A



B

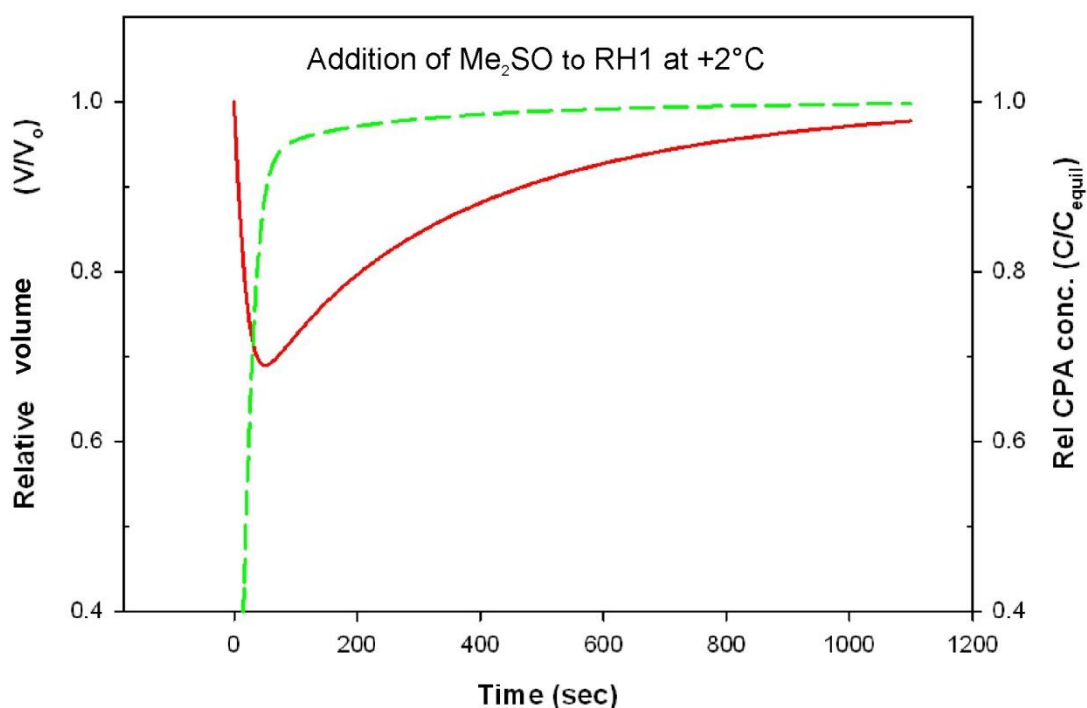


**Figure 4.5 Modelled protocols for addition of Me<sub>2</sub>SO to RH1 cells**

Modelling addition of 1.29M Me<sub>2</sub>SO to human embryonic cell line, RH1 at (A) RT and (B) +2°C. At RT and +2°C, the CPA addition occurred in a single step to maintain the tolerable volume excursion of the cells. The osmotically induced volume excursions (solid line) and intracellular CPA concentration (dashed line) are displayed.

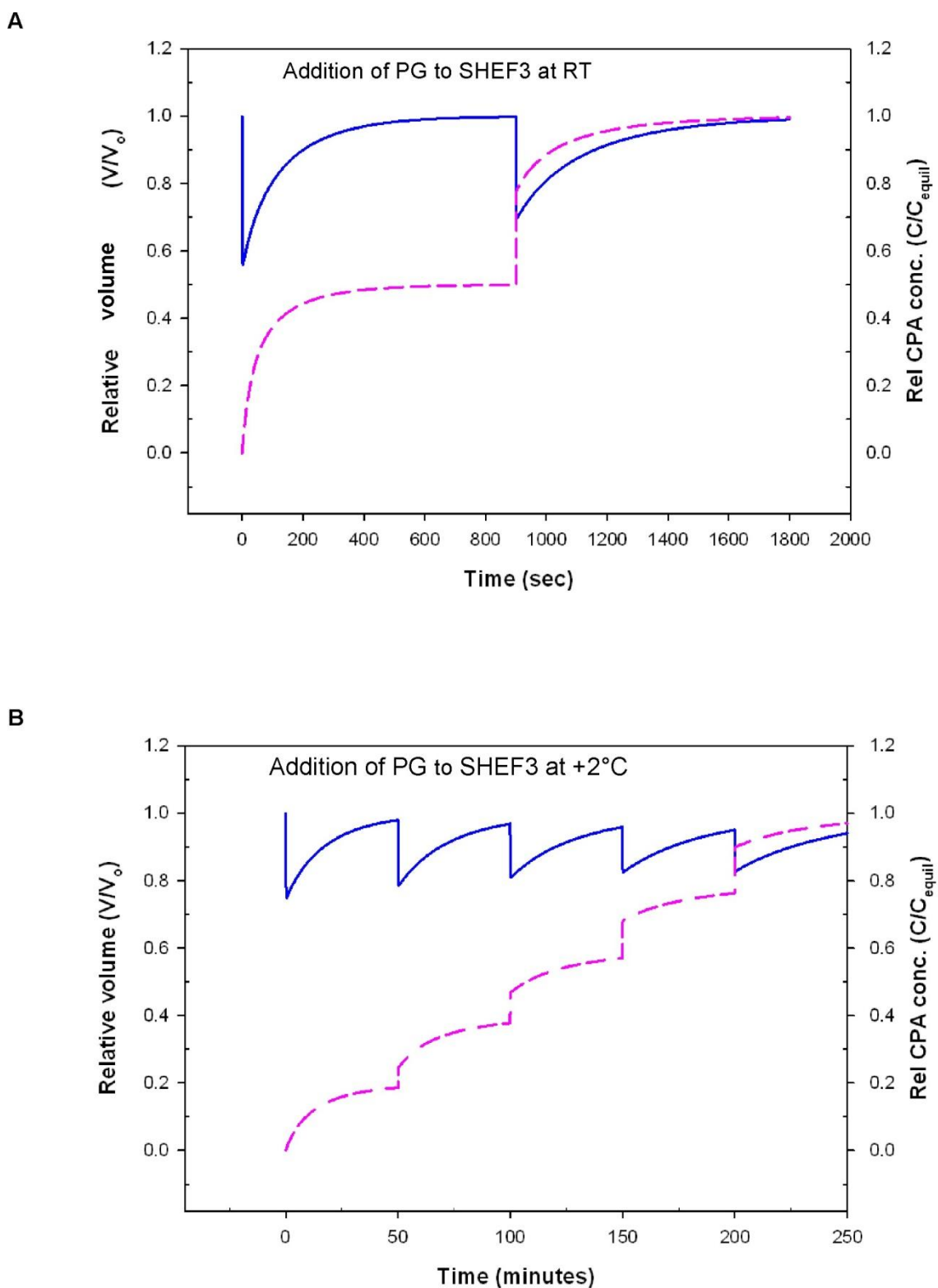
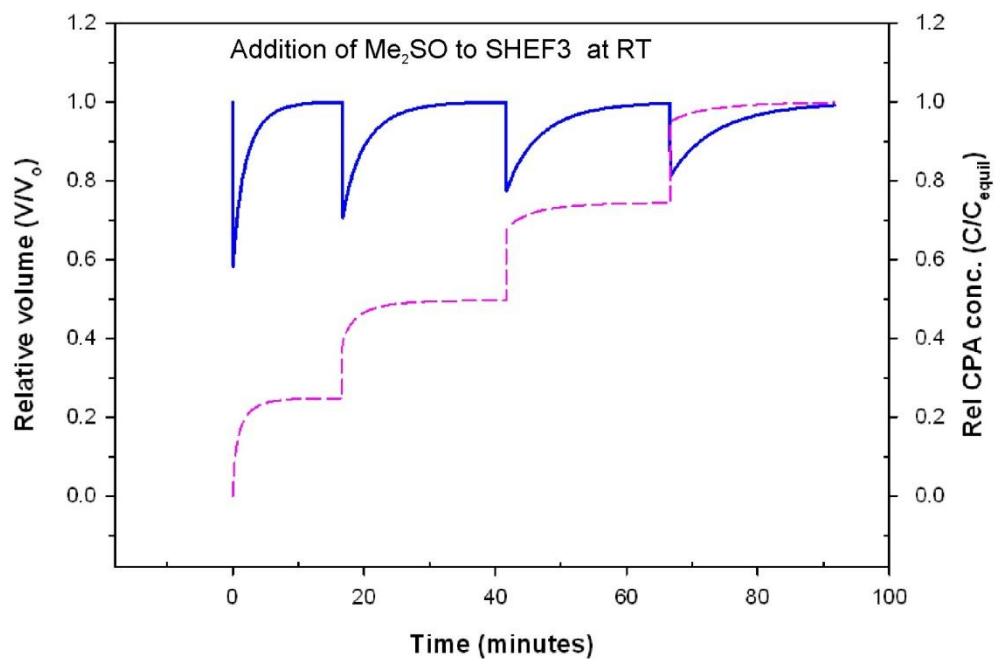


**Figure 4.6 Modelled protocols for addition of PG to SHEF3 cells**

Modelling addition of 0.66M Me<sub>2</sub>SO to human embryonic cell line, SHEF3 at (A) RT and (B) +2°C. At RT, the CPA addition occurred in two separate steps in increments of 0.33M, and in 5 steps at +2°C in increments of 0.13M to maintain the tolerable volume excursion of the cells. The osmotically induced volume excursions (solid line) and intracellular cryoprotectant concentration (dashed line) are displayed.

A



B

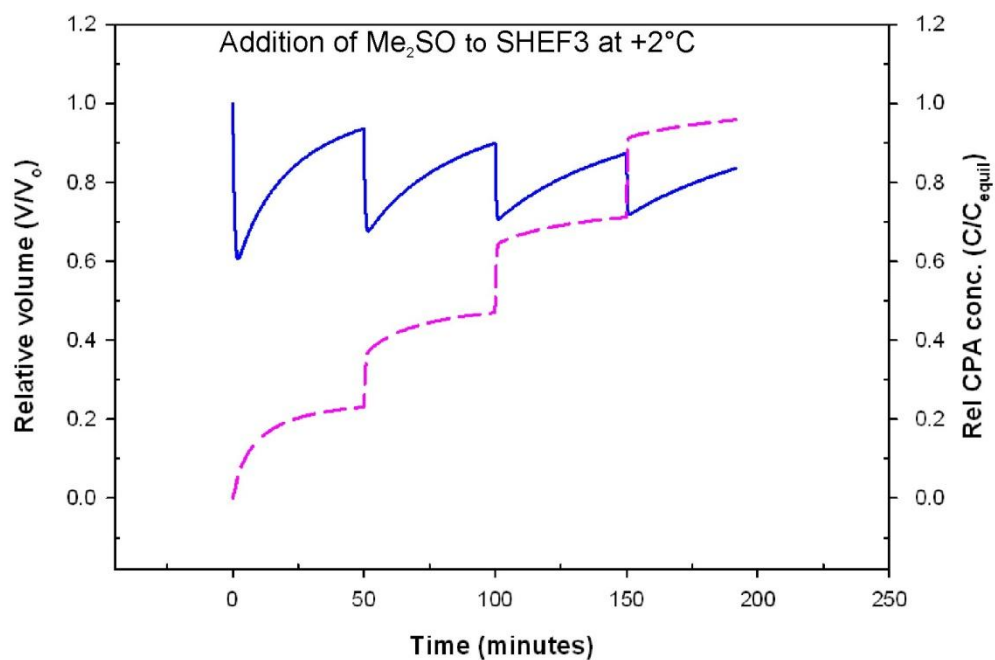


**Figure 4.7 Modelled protocols for addition of Me<sub>2</sub>SO to SHEF3 cells**

Modelling addition of 1.29M Me<sub>2</sub>SO to human embryonic cell line, SHEF3 at (A) RT and (B) +2°C. At RT and +2°C, the CPA addition occurred in four separate steps in increments of 0.3M to maintain the tolerable volume excursion of the cells. The osmotically induced volume excursions (solid line) and intracellular CPA concentration (dashed line) are displayed.

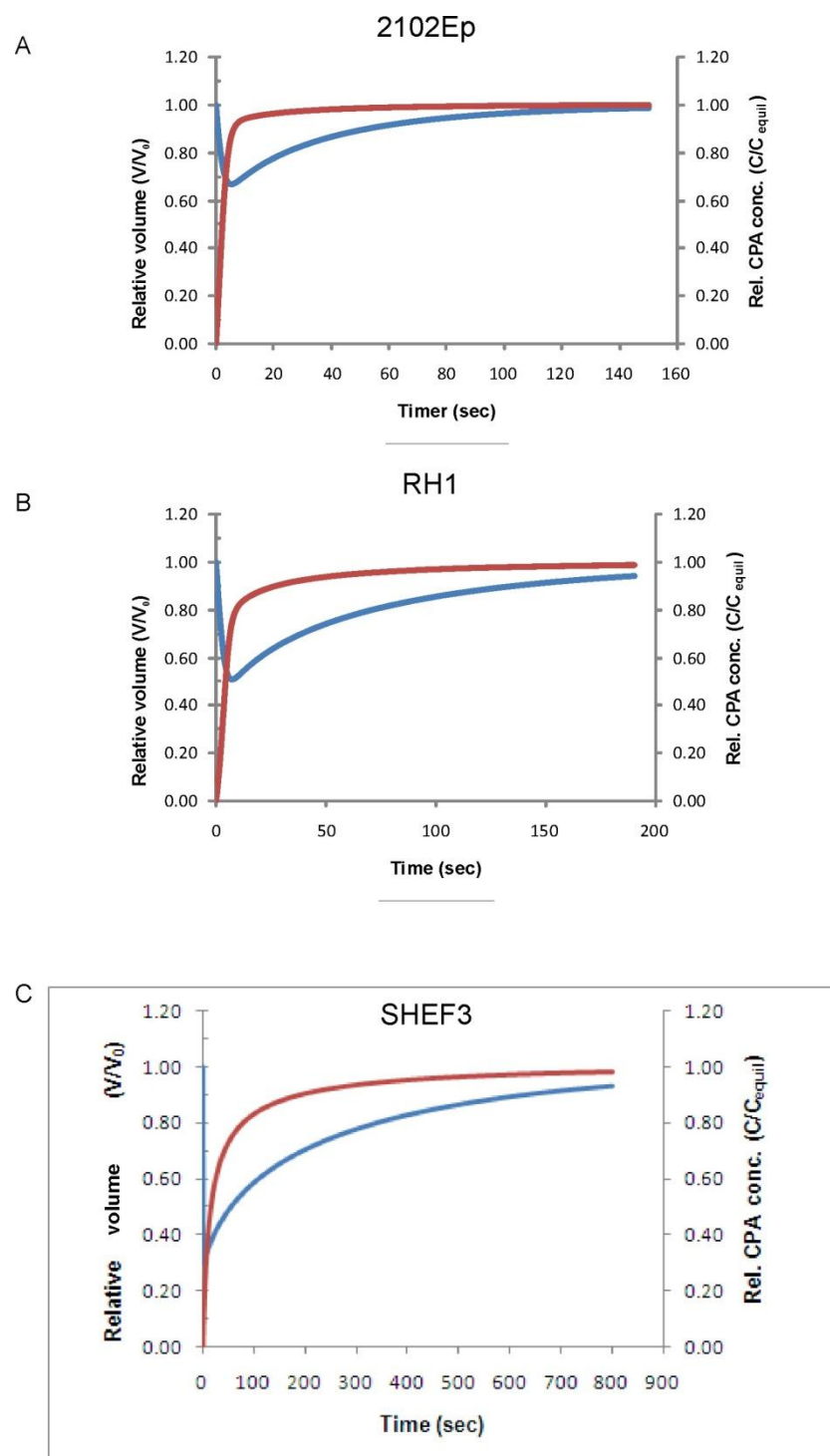


**Figure 4.8 Standardised CPA addition protocol modelled using 2-parameter formalism**

Modelling addition of 1.29M  $\text{Me}_2\text{SO}$  at RT to (A) hEC line, 2102Ep, hESC lines (B) RH1 and (C) SHEF3. The osmotically induced volume excursions (blue solid line) and intracellular CPA concentration (red solid line) are displayed. Modelling of these protocols showed that adding 1.29M  $\text{Me}_2\text{SO}$  at RT to 2102Ep and RH1 causes volume excursions that stay within the cells' tolerable limits while these conditions cause SHEF3 to exceed its tolerable volume shrinkage limits (shrinking below 40% of the isotonic volume).

#### 4.4.2 Summary of modelling for CPA addition

2102Ep- Me<sub>2</sub>SO should be added to cells in a single step at RT and 4 separate steps at +2°C. PG is best added in one step at RT and 2 steps at +2°C. It should be noted that protocols carried out at +2°C take about 18 hours and 8 hours for Me<sub>2</sub>SO and PG, respectively, while CPA addition can be performed in about 2 minutes at RT.

RH1- Me<sub>2</sub>SO should be added to cells in a single step at either temperature while PG addition should occur in 2 steps at either temperature. However, it will take more than 24 hours for cells to equilibrate in PG at +2°C. The quickest protocol was the addition of Me<sub>2</sub>SO at RT which only required about 3 minutes.

SHEF3- Me<sub>2</sub>SO should be added to cells in 4 steps at either temperature with equilibration times of 18 minutes at RT and 50 minutes at +2°C. PG should be added in 2 steps at RT with equilibration times of 2.5 hours, while 5 steps at +2°C were required with equilibration periods of 50 minutes. Similar to RH1, the quickest protocol was the addition of Me<sub>2</sub>SO at RT which could be carried out in 1.5 hours.

Standardised protocol for addition of Me<sub>2</sub>SO agreed with theoretical prediction for addition of Me<sub>2</sub>SO to 2102Ep and RH1 but showed that SHEF3 cells undergo osmotic stress when Me<sub>2</sub>SO is added in a single step.

#### 4.4.3 Elution modelling data

The same formula used in modelling CPA addition was used to model how each CPA should be removed from each cell line at each temperature, the concentrations of CPA used were 1.29M (10% v/v) for Me<sub>2</sub>SO and 0.66M (5% v/v) for PG.

At RT, the 2102Ep cells only needed a single step of dilution for Me<sub>2</sub>SO to be eluted (Fig. 4.9A) while three dilution steps were required for Me<sub>2</sub>SO to be removed from the hECs at +2°C (Fig. 4.9B). However, removal of PG from the cells could be carried out in a single step at either temperature while staying within the tolerable limits of cell volume expansion (Fig. 4.10).

At RT, PBS<sup>+</sup> containing 2% mannitol was also required for the removal of Me<sub>2</sub>SO from RH1 cells in three steps (Fig.4.11A) while the elution of Me<sub>2</sub>SO from RH1 cells at +2°C (Fig. 4.11B) was possible in a single step. 2% mannitol was added to the dilution medium in order to restrict the expansion in cell volume that the cells would experience in isotonic medium. Mannitol made the medium hypertonic exerts shrinkage in cell volume. Mannitol was also added to the dilution medium for the elution of PG at RT while two steps were required to remove PG at +2°C (Fig. 4.12).

The SHEF3 cells also required 2% mannitol in isotonic medium for the removal of either CPA at both temperatures (Figs. 4.13 & 4.14).

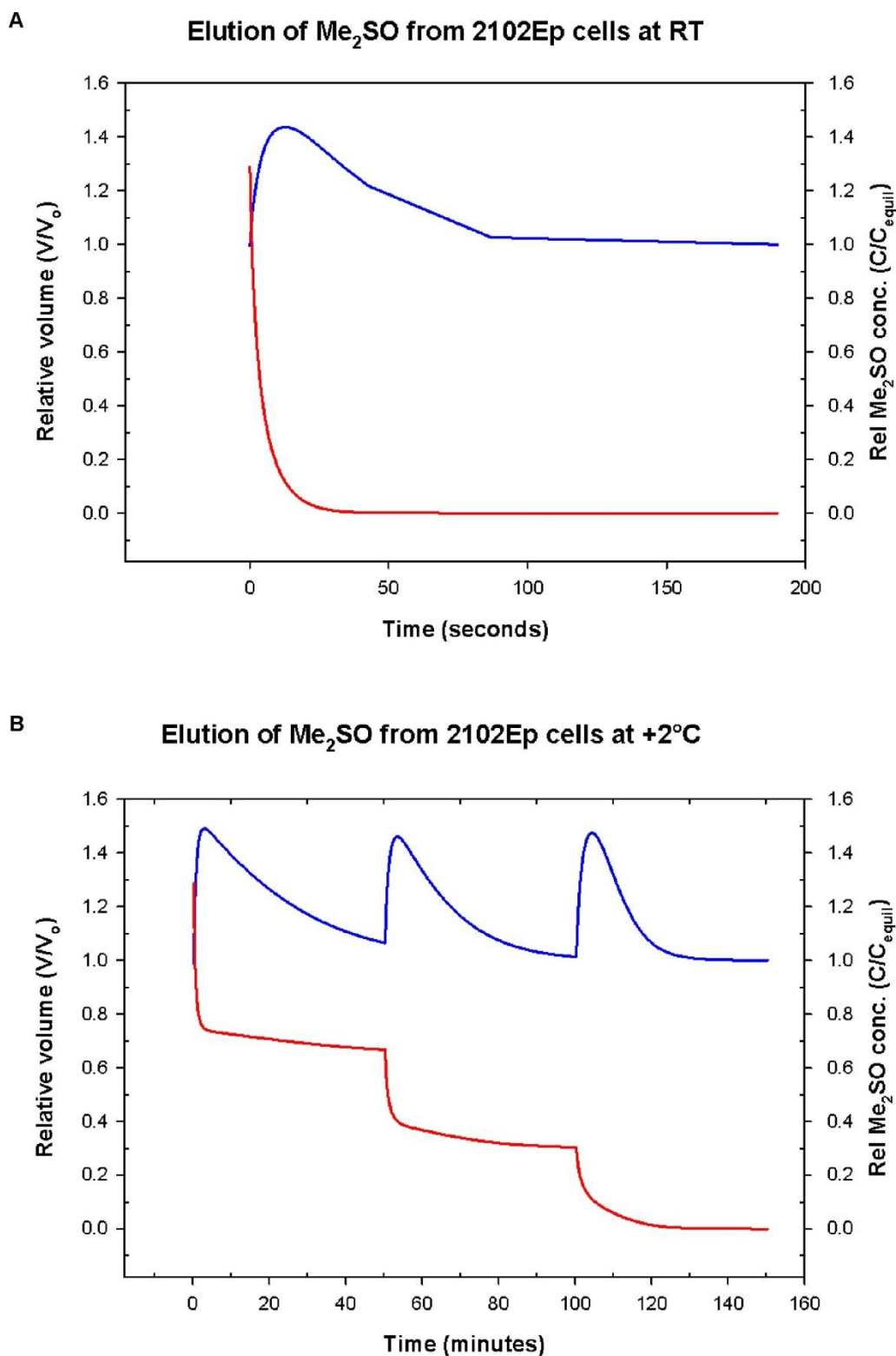


**Figure 4.9 Modelled protocols for elution of Me<sub>2</sub>SO from 2102Ep cells**  
 Modelling removal of 1.29M Me<sub>2</sub>SO from human embryonal carcinoma cell line, 2102Ep at (A) RT and (B) +2°C. The osmotically induced volume excursions (solid line) and intracellular CPA concentration (dashed line) are displayed.

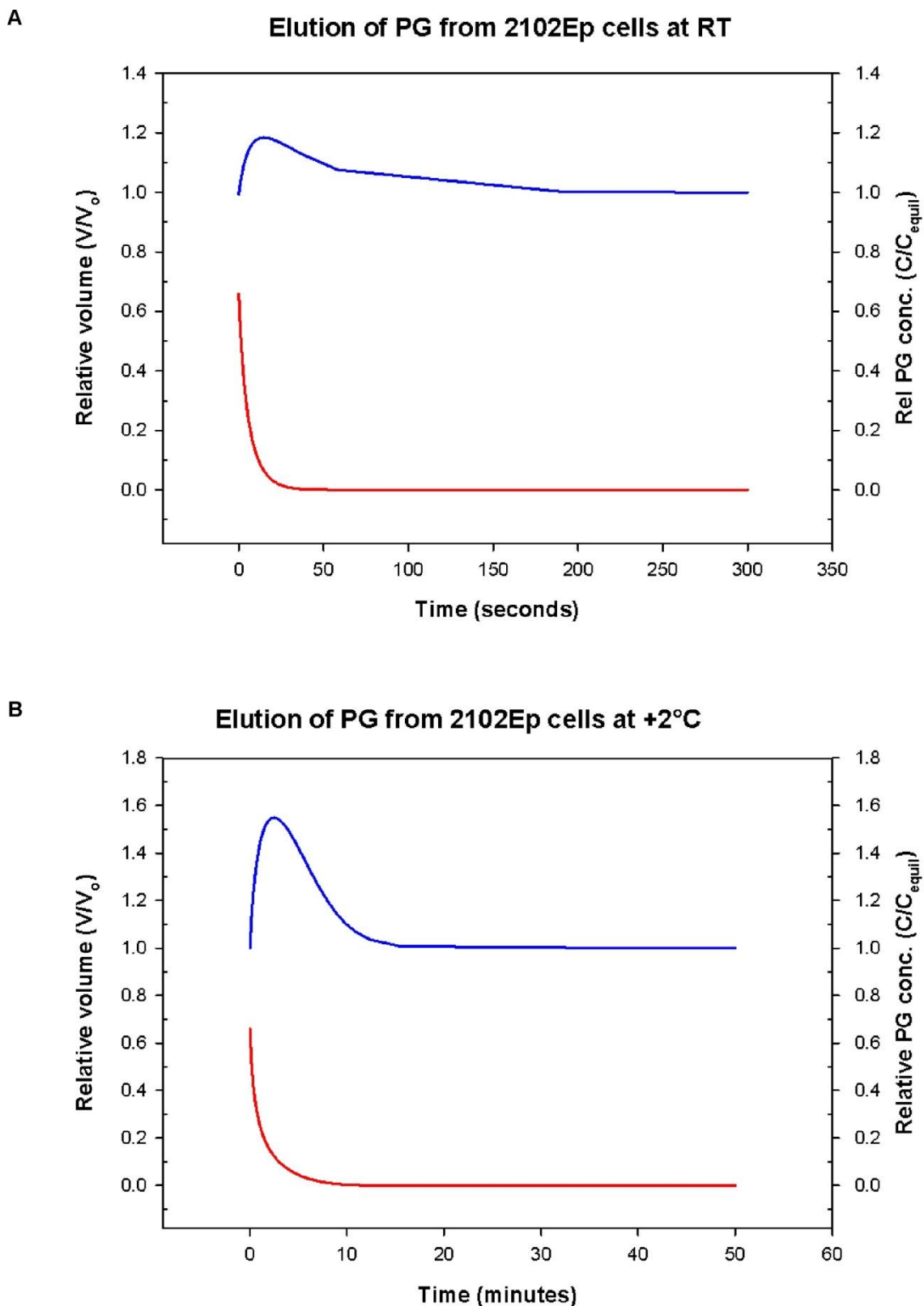


**Figure 4.10 Modelled protocols for elution of PG from 2102Ep cells**

Modelling removal of 0.66M PG from human embryonal carcinoma cell line, 2102Ep at (A) RT and (B) +2°C. The osmotically induced volume excursions (solid line) and intracellular CPA concentration (dashed line) are displayed.

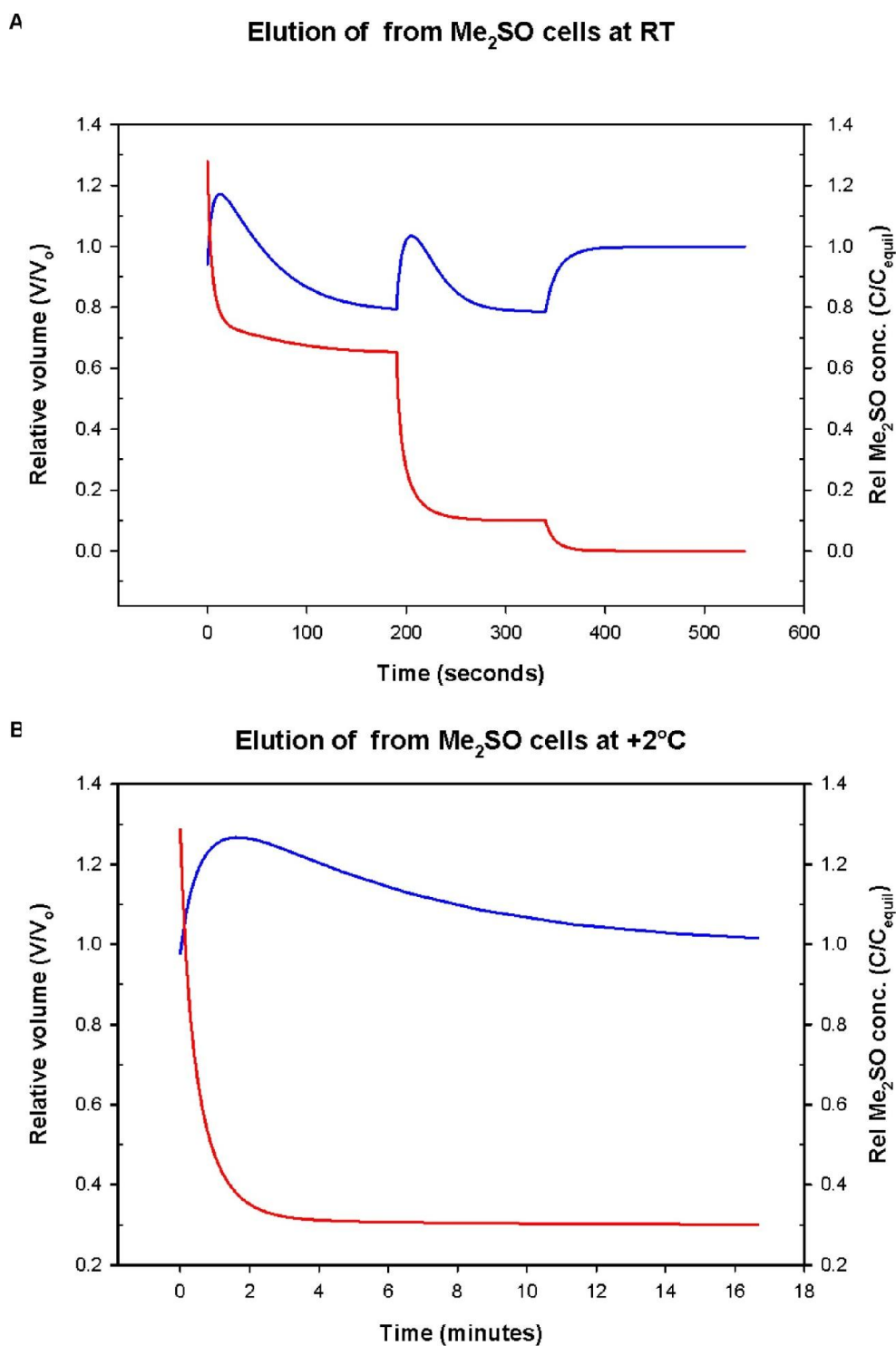


**Figure 4.11 Modelled protocols for elution of Me<sub>2</sub>SO from RH1 cells**

Modelling removal of 1.29M Me<sub>2</sub>SO from human embryonic cell line, RH1 at (A) RT and (B) +2°C. Mannitol was added in the elution medium to reduce the cell volume expansion experienced by the cells. The osmotically induced volume excursions (solid line) and intracellular CPA concentration (dashed line) are displayed.

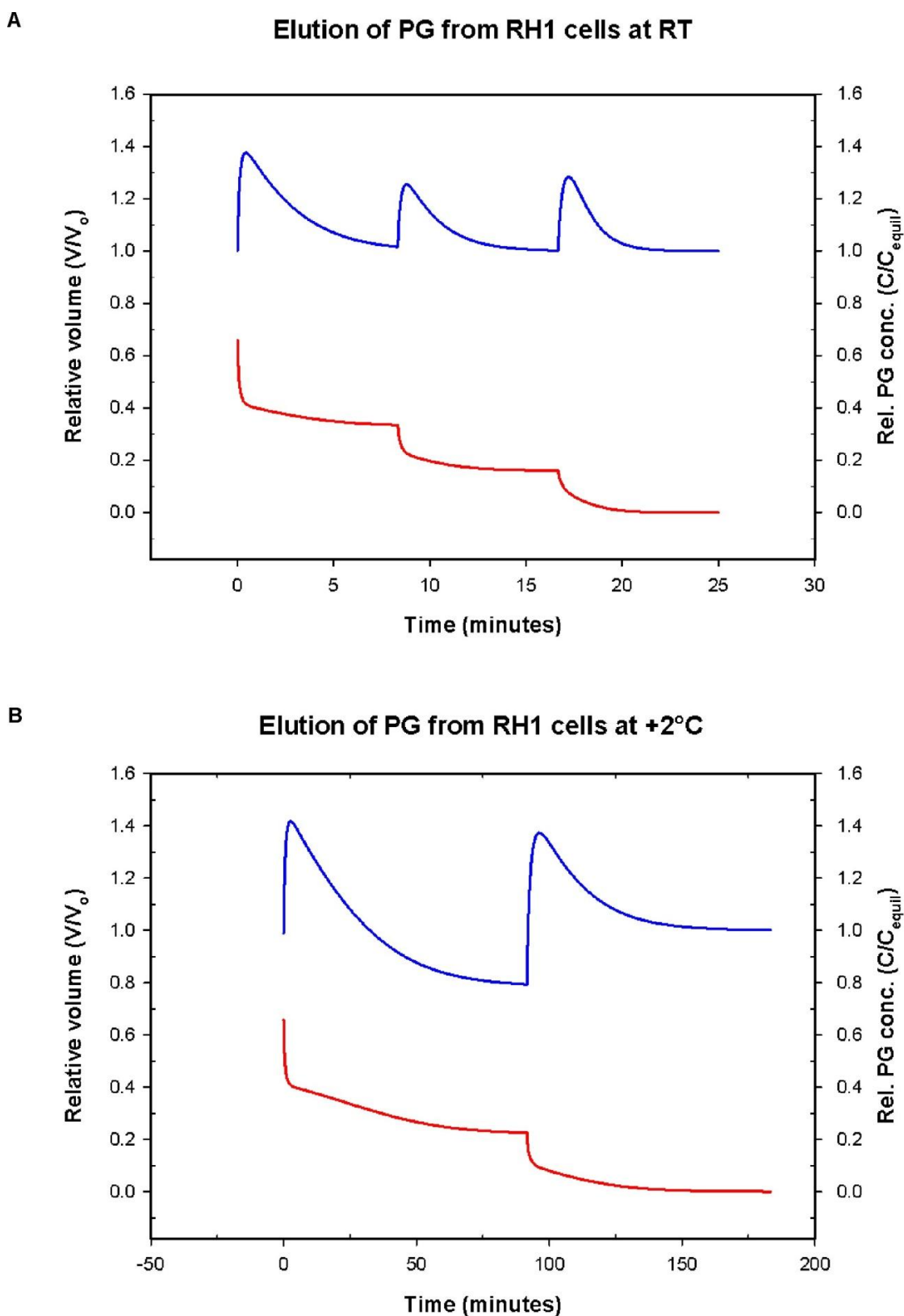


**Figure 4.12 Modelled protocols for elution of PG from RH1 cells**

Modelling removal of 0.66M PG from human embryonic cell line, RH1 at (A) RT and (B) +2°C. Mannitol was added in the elution medium to reduce the cell volume expansion experienced by the cells. The osmotically induced volume excursions (solid line) and intracellular CPA concentration (dashed line) are displayed.

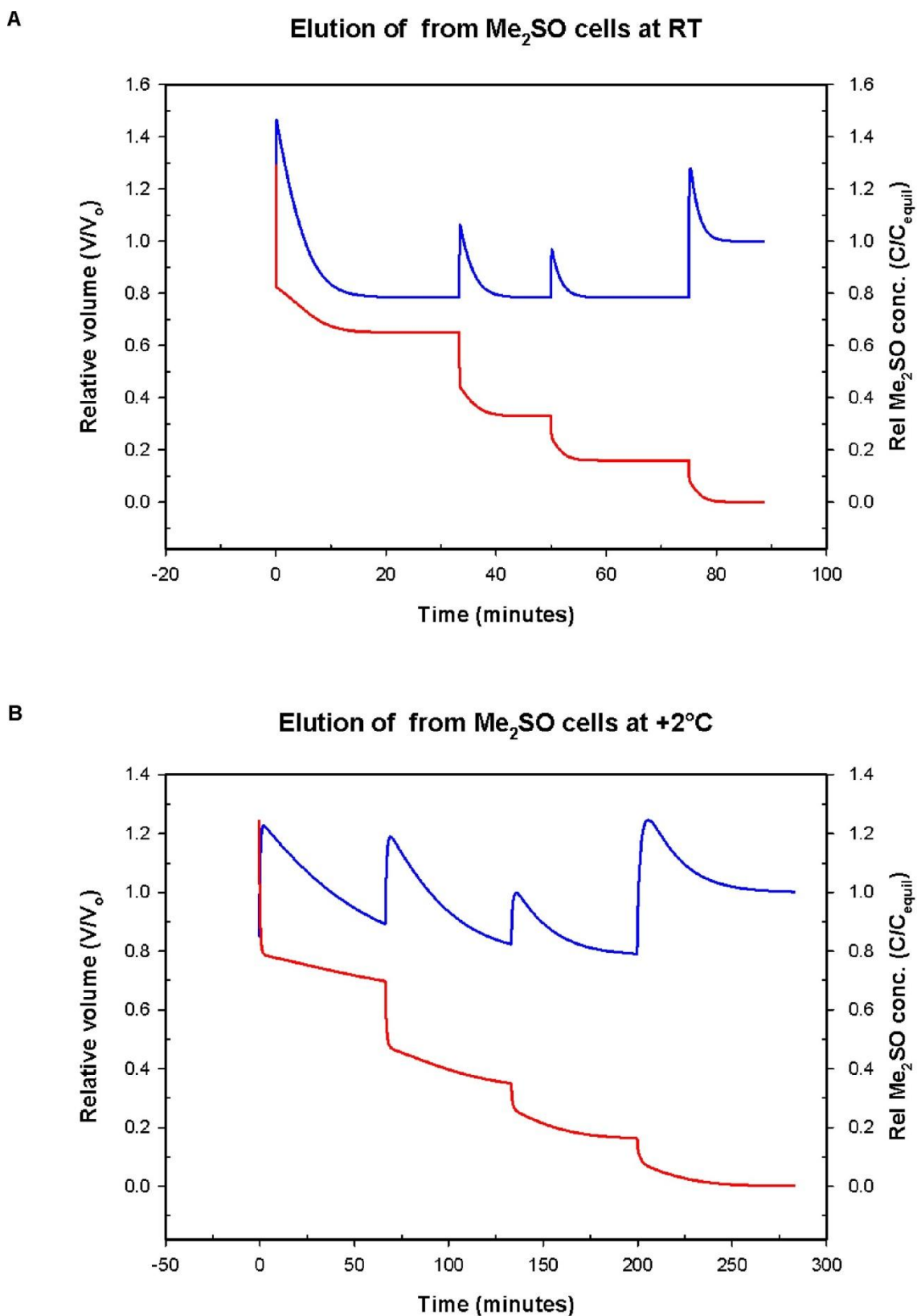


**Figure 4.13 Modelled protocols for elution of Me<sub>2</sub>SO from SHEF3 cells**

Modelling removal of 1.29M Me<sub>2</sub>SO from human embryonic cell line, SHEF3 at (A) RT and (B) +2°C. The osmotically induced volume excursions (solid line) and intracellular CPA concentration (dashed line) are displayed.

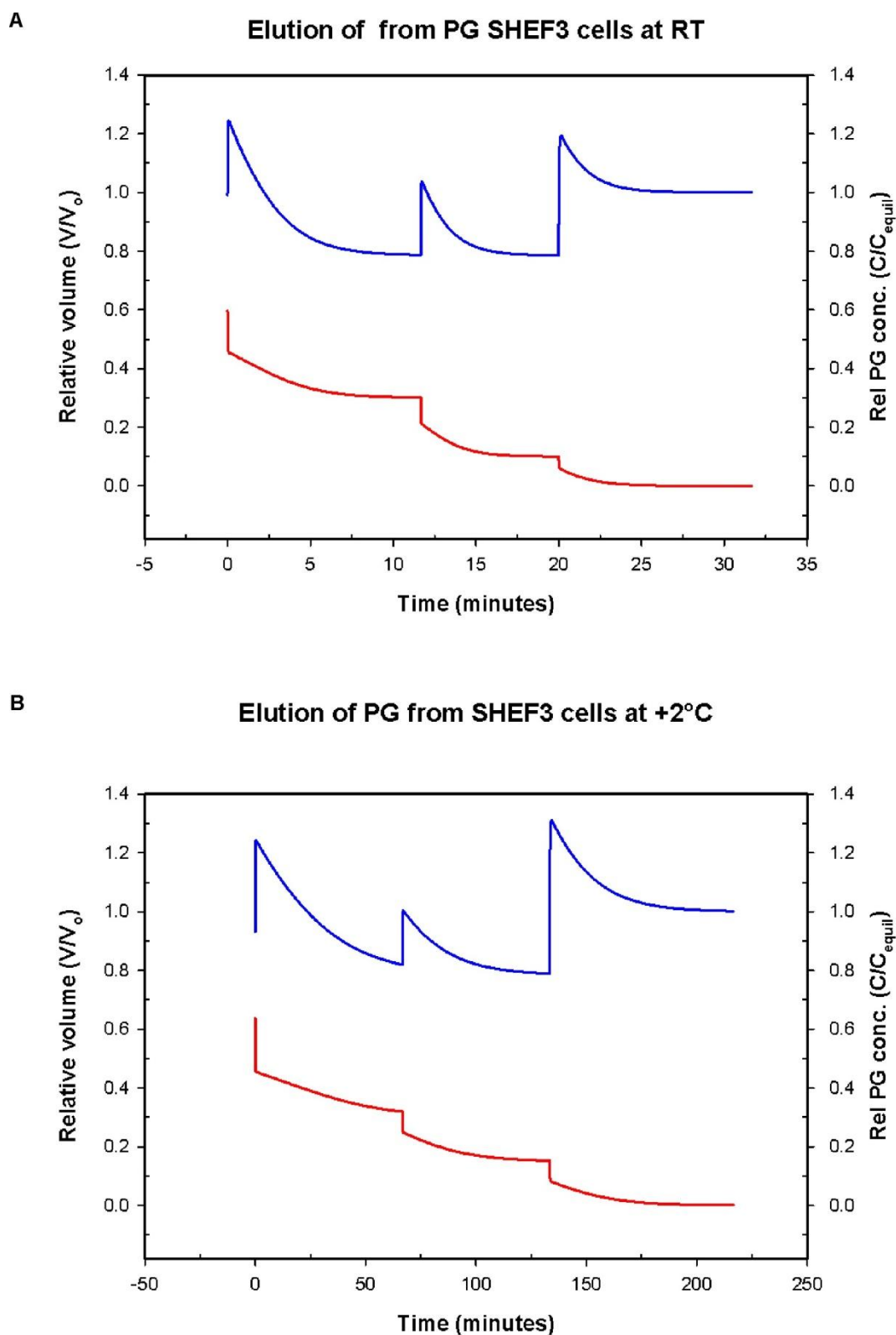


**Figure 4.14 Modelled protocols for elution of PG from SHEF3 cells**

Modelling removal of 0.66M PG from human embryonic cell line, SHEF3 at (A) RT and (B) +2°C. The osmotically induced volume excursions (solid line) and intracellular CPA concentration (dashed line) are displayed.

#### 4.4.4 Summary of modelled protocols for elution of PG and Me<sub>2</sub>SO

The same concentrations of CPA were used in modelling how each CPA should be removed from each cell line at each temperature. The summary of the findings are as follows:

2102Ep- Me<sub>2</sub>SO could be diluted in one step at RT and in three steps at +2°C while one step was required for the dilution of PG at either temperature.

RH1- three-step dilution of Me<sub>2</sub>SO was required at RT and one step at +2°C. For the removal of PG from the cells, 3 steps were required at RT and 2 steps at +2°C.

SHEF3- A four-step dilution was required for the removal of Me<sub>2</sub>SO from the cells at either temperature. However, 3 steps were required for the dilution of PG at either temperature. Dilution of Me<sub>2</sub>SO at RT would require 1.5hours to perform compared to 30minutes required for the dilution of PG at the same temperature. Similar time period (about 4hours) would be required for the dilution of either CPA at +2°C.

Based on the modelling of the addition and elution protocols, therefore, the procedures which are most practical and easily carried out in the laboratory are as follows:

- 1) Addition and removal of PG for RH1 at RT
- 2) Addition and elution of Me<sub>2</sub>SO at RT for both SHEF3 and RH1, and
- 3) Addition and removal of PG or Me<sub>2</sub>SO at RT for 2102Ep

It is clear that protocols carried out at +2°C are impractical and cannot be carried out conveniently in a laboratory. As a result, only the practical methods will be illustrated in tables 4.1 to 4.8 which show how each protocol can be carried out by giving the concentration of CPA that should be present at each step until the target concentration is achieved. Only protocols for the hESCs have been illustrated.

It can also be said that the predictions from the modelling support earlier findings in the previous chapter where there were indications that either PG or Me<sub>2</sub>SO may be used in cryopreserving 2102Ep cells while Me<sub>2</sub>SO remains the preferable CPA for both SHEF3 and RH1. However, it was interesting that RH1 cells equilibrated quicker in PG at RT than SHEF3 cells which agrees with timecourse responses in chapter 3 but contradicts the permeability values determined which shows similar P<sub>s</sub> values for both hESC lines.

**Table 4.1**

Table of the molar Me<sub>2</sub>SO concentrations at each intermediate step during the addition of cryoprotectant to SHEF3 at RT up to the end concentration

Intermediate molar Me <sub>2</sub> SO concentrations (w/w)								Final w/w% Me <sub>2</sub> SO
Step 1	Step 2	Step 3	Step 4	Step 5	Step 6	Step 7	Step 8	
0.32 (2.5%)	0.64 (5%)							5%
0.32 (2.5%)	0.64 (5%)	0.96 (7.5%)	1.28 (10%)					10%
0.32 (2.5%)	0.64 (5%)	0.96 (7.5%)	1.28 (10%)	1.60 (12.5%)	1.92 (15%)			15%
0.32 (2.5%)	0.64 (5%)	0.96 (7.5%)	1.28 (10%)	1.60 (12.5%)	1.92 (15%)	2.24 (17.5%)	2.56 (20%)	20%

Each step was designed to restrict shrinkage to  $\geq 40\%$  cell volume. Equilibration period for each step was 15 mins.

**Table 4.2**

Table of the molar Me<sub>2</sub>SO concentrations and wt% of D-mannitol at each intermediate step during the elution of cryoprotectant to SHEF3 at RT up to the end concentration

Starting molar Me <sub>2</sub> SO concentration	Intermediate molar Me <sub>2</sub> SO concentration + wt% D-mannitol						Resuspension in Me <sub>2</sub> SO /mannitol-free PBS <sup>+</sup> medium
	Step 1	Step 2	Step 3	Step 4	Step 5	Step 6	
5%	0.32 (2.5%)+ 2%	0.16 (1.25%)+ 2%					0 + 0%
10%	0.64 (5%) + 2%	0.32 (2.5%) + 2%	0.16 (1.25%)+ 2%				0 + 0%
15%	1.28 (15%) + 2%	0.64 (10%)+ 2%	0.32 (5%) + 2%	0.16 (2.5%) + 2%			0 + 0%
20%	1.92 (20%) + 2%	1.28(15%) + 2%	0.64 (10%) + 2%	0.32 (5%) + 2%	0.16 (2.5%) + 2%		0 + 0%

Centrifugation (1200rpm, 5mins)

Each step was designed to restrict swelling to ≤170% cell volume. Equilibration period for each step was 20 mins

**Table 4.3**

Table of the molar Me<sub>2</sub>SO concentrations at each intermediate step during the addition of cryoprotectant to RH1 at RT up to the end concentration

Intermediate molar Me <sub>2</sub> SO Concentrations		Final w/w% Me <sub>2</sub> SO
Step 1	Step 2	
0.64 (5%)		5%
1.28 (10%)		10%
1.28 (10%)	1.92 (15%)	15%
1.28 (10%)	2.56 (20%)	20%

Each step was designed to restrict shrinkage to  $\geq 40\%$  cell volume. Equilibration period for each step was 4 mins.

**Table 4.4**

Table of the molar Me<sub>2</sub>SO concentrations and wt% of D-mannitol at each intermediate step during the elution of cryoprotectant from RH1 at RT up to the end concentration

Starting molar Me <sub>2</sub> SO concentration	Intermediate molar Me <sub>2</sub> SO concentration (w/w) + wt% D-mannitol					Resuspension in Me <sub>2</sub> SO/mannitol-free PBS <sup>+</sup> medium
	Step 1	Step 2	Step 3	Step 4	Step 6	
5%	0.32 (5%) + 2%					0 + 0%
10%	0.64 (5%) + 2%	0.32 (2.5%) + 2%				0 + 0%
15%	1.28 (10%) + 2%	0.64 (5%) + 2%	0.32 (2.5%) + 2%			0 + 0%
20%	1.92 (15%)+ 2%	1.28 (10%) + 2%	0.64 (5%) + 2%	0.32 (2.5%) + 2%		0 + 0%

Centrifugation (1200rpm, 5mins)

Each step was designed to restrict swelling to ≤130% cell volume. Equilibration period for each step was 4 mins

**Table 4.5**

Table of the molar Me<sub>2</sub>SO concentrations at each intermediate step during the addition of cryoprotectant to RH1 at +2°C up to the end concentration

Intermediate molar Me <sub>2</sub> SO Concentrations (w/w)		Final w/w% Me <sub>2</sub> SO
Step 1	Step 2	
0.64 (5%)		5%
1.28 (10%)		10%
1.28 (10%)	1.92 (15%)	15%
1.28 (10%)	2.56 (20%)	20%

Each step was designed to restrict shrinkage to ≥40% cell volume. Equilibration period for each step was 20 mins.

**Table 4.6**

Table of the molar Me<sub>2</sub>SO concentrations at each intermediate step during the elution of cryoprotectant from RH1 at +2°C up to the end concentration

Starting molar Me <sub>2</sub> SO concentration	Intermediate molar Me <sub>2</sub> SO concentration (w/w)					Resuspension in Me <sub>2</sub> SO/mannitol-free PBS <sup>+</sup> medium
	Step 1	Step 2	Step 3	Step 4	Step 6	
5%	0.32 (2.5%)					0
10%	0.64 (5%)					0
15%	1.28 (10%)					0
20%	1.28 (10%)	0.64 (5%)				0

Centrifugation (1200rpm, 5mins)

Each step was designed to restrict swelling to ≤130% cell volume. Equilibration period for each step was 20 mins

**Table 4.7**

Table of the molar PG concentrations at each intermediate step during the addition of cryoprotectant to RH1 at RT up to the end concentration

Intermediate molar PG Concentrations (w/w)						Final w/w% PG
Step 1	Step 2	Step 3	Step 4	Step 5	Step 6	
0.33 (2.5%)						2.5%
0.33 (2.5%)	0.66 (5%)					5%
0.33 (2.5%)	0.66 (5%)	0.99 (7.5%)	1.32 (10%)			10%
0.33 (2.5%)	0.66 (5%)	0.99 (7.5%)	1.32 (10%)	1.65 (12.5%)	1.98 (15%)	15%

Each step was designed to restrict shrinkage to  $\geq 40\%$  cell volume. Equilibration period for each step was 8 mins and 13mins for the last step.

**Table 4.8**

Table of the molar PG concentrations at each intermediate step during the elution of cryoprotectant from RH1 at RT up to the end concentration

Intermediate molar PG concentrations								Resuspension in Me <sub>2</sub> SO-free PBS <sup>+</sup> medium
	Step 1	Step 2	Step 3	Step 4	Step 5	Step 6	Step 7	
2.5%								0
5%	0.33 (2.5%)	0.16 (1.25%)						0
10%	0.99 (7.5%)	0.66 (5%)	0.33 (2.5%)	0.16 (1.25%)				0
15%	1.64 (12.5%)	1.32 (10%)	0.99 (7.5%)	0.66 (5%)	0.33 (2.5%)	0.16 (1.25%)		0

Centrifugation (1200rpm, 5mins)

Each step was designed to restrict swelling to  $\leq 130\%$  cell volume. Equilibration period for each step was 10 mins

#### 4.4.5 *Effect of cryoprotectant on membrane integrity and functionality of the cells*

Due to results in the previous chapter that showed rapid permeation of CPA through the cell membrane at RT, toxicity of Me<sub>2</sub>SO and PG was analysed only at this temperature in order to minimise exposure to damaging effects of each CPA. Consequently, short-term exposure of the hESCs to varying concentrations of Me<sub>2</sub>SO and PG at RT was carried out following the protocols in the tables earlier displayed in order to determine the highest CPA concentration the cells can tolerate. The results of the PI exclusion assays indicated that damage to the RH1 and SHEF3 cell membranes was induced at Me<sub>2</sub>SO concentrations ranging from 10-20% (v/v) (Figs. 4.15A and 4.16B). However, 10% Me<sub>2</sub>SO was acceptable because the percentage of cells with membrane damage was not much lower than that of cells in isotonic medium or 5% Me<sub>2</sub>SO. Moreover, there was considerable cell growth for both RH1 and SHEF3 cells in 10% Me<sub>2</sub>SO compared to the untreated cells (Figs. 4.15B & 4.16A).

The dye exclusion assay indicated significant damage to RH1 cell membrane compared to isotonic, but the actual percentage of cells in 10 and 15%PG were not much lower compared to the untreated cells (Fig. 4.17B). Furthermore, the results showed significant damage to the growth of SHEF3 cells which were exposed to 15%PG (Fig. 4.18).

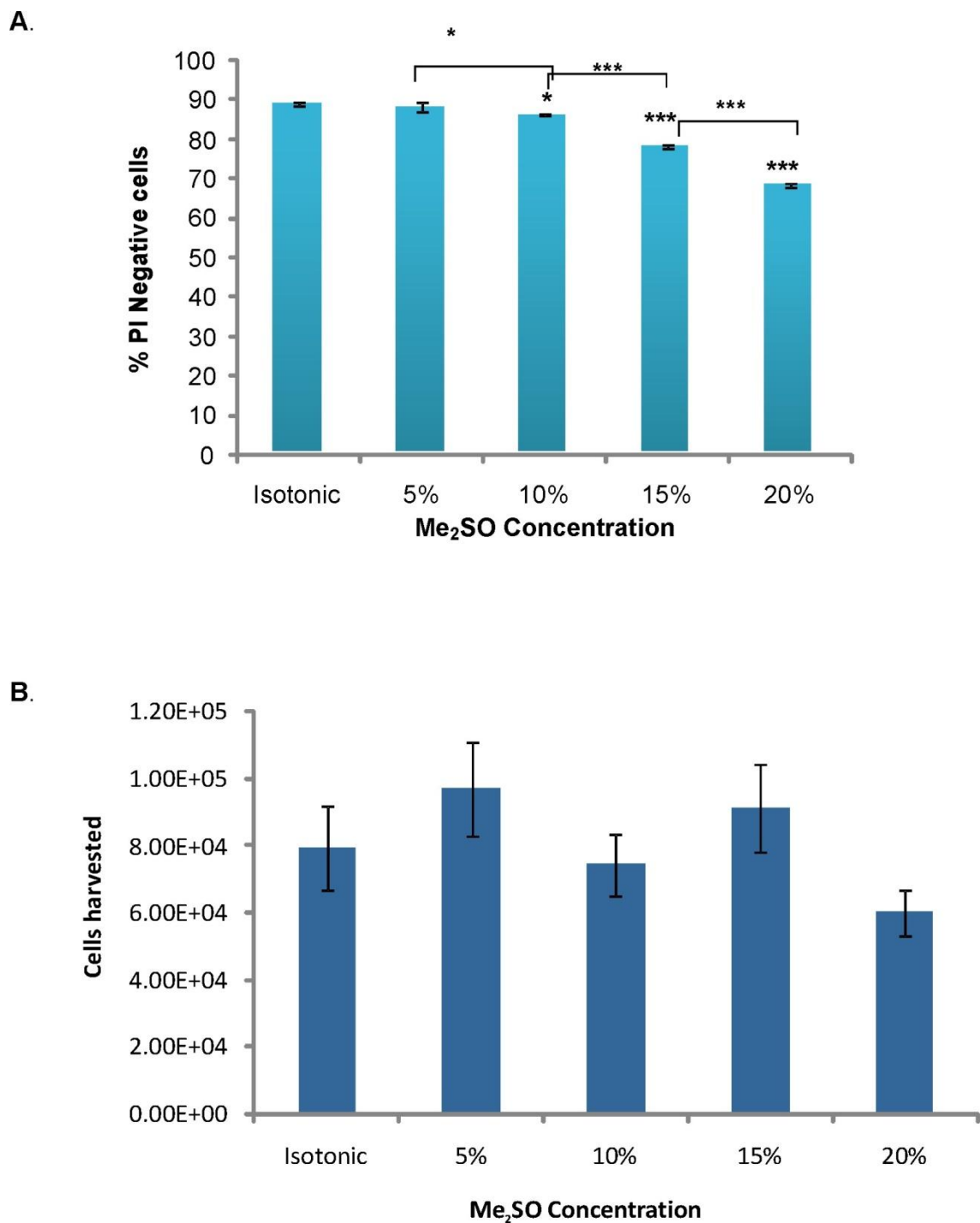
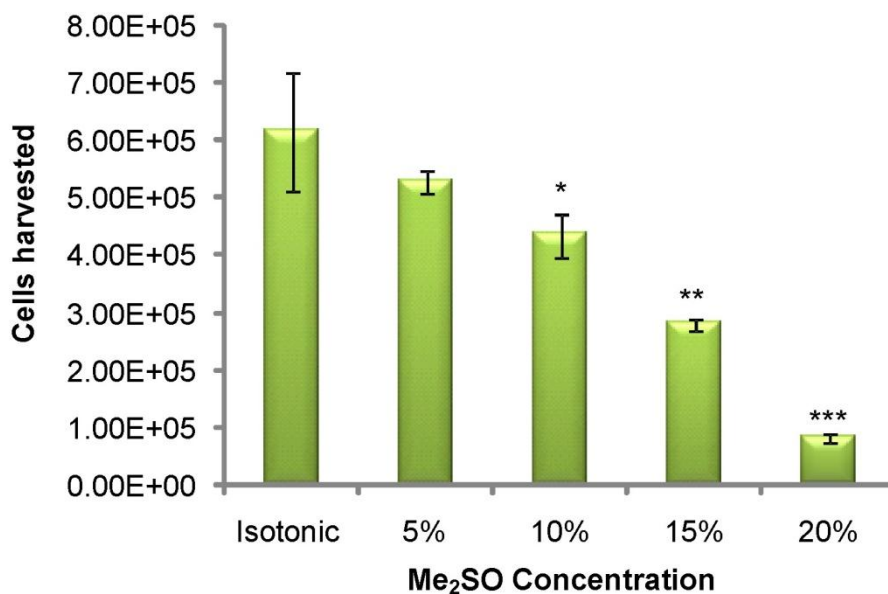


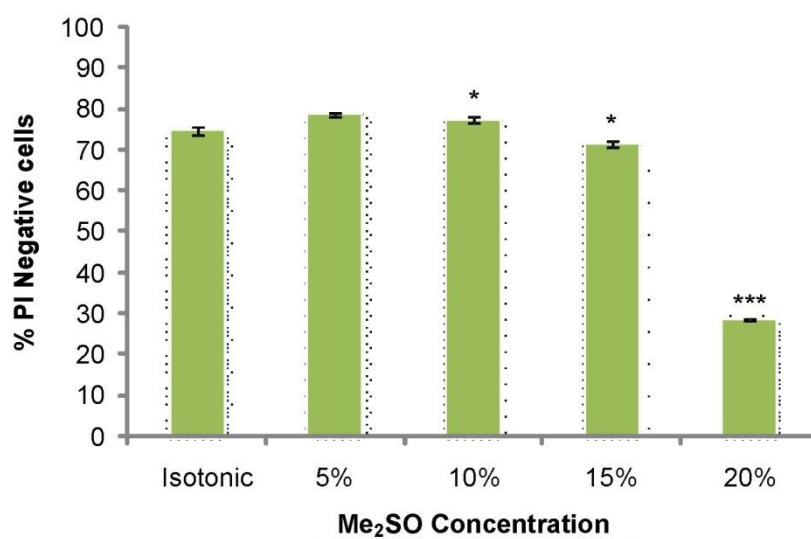
**Figure 4.15 Effect of exposure to Me<sub>2</sub>SO on RH1 cells**

(A) Results of membrane integrity assay using propidium iodide showed damage was highest at the highest concentration of Me<sub>2</sub>SO. (B) Cell growth assessment of human embryonic stem cell line RH1 after 15 minutes exposure to varying concentrations of Me<sub>2</sub>SO at RT following modelled protocol. Data are mean  $\pm$  SEM ( $n = 4$  for A and  $n = 3$  for B). Statistical analysis was carried out using the ANOVA test (\* $p < 0.05$ , \*\* $p < 0.01$ , \*\*\* $p < 0.001$ ).

A.



B.

**Figure 4.16 Effect of exposure to Me<sub>2</sub>SO on SHEF3 cells**

(A) Cell growth assessment of human embryonic stem cell line SHEF3 after 15 minutes exposure to varying concentrations of Me<sub>2</sub>SO at RT following modelled protocol. Cell growth was lowest at the highest concentration of Me<sub>2</sub>SO (B) Results of membrane integrity assay using propidium iodide showed damage was highest at the highest concentration of Me<sub>2</sub>SO. Data are mean ± SEM (n = 4 for A and n = 3 for B). Statistical analysis was carried out using the ANOVA test (\*p<0.05, \*\*p<0.01, \*\*\*p<0.001).

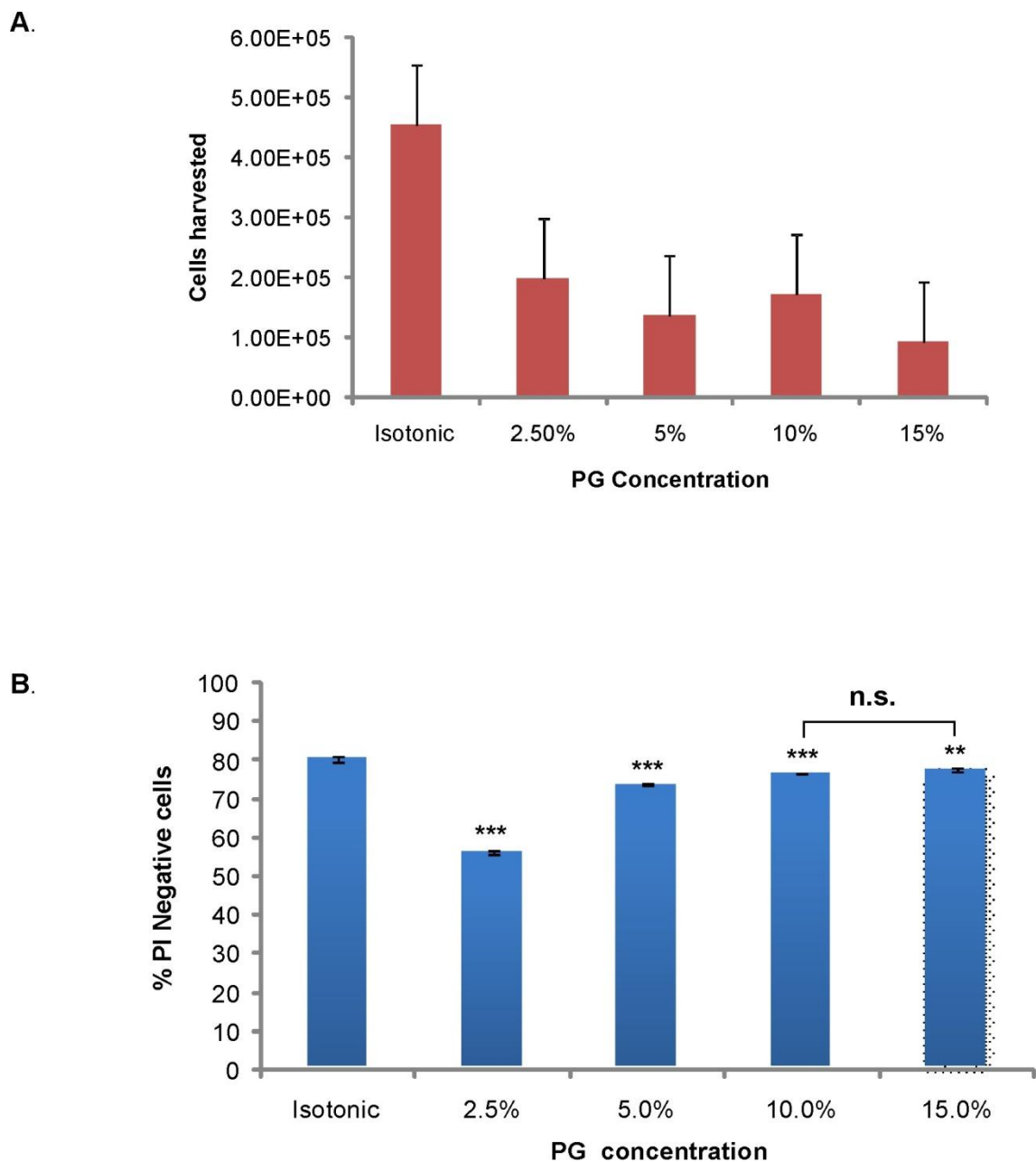


**Figure 4.17 Effect of exposure to PG on RH1 cells**

(A) Cell growth assessment of human embryonic stem cell line RH1 after 15 minutes exposure to varying concentrations of PG at RT following modelled protocol. (B) Results of membrane integrity assay using propidium iodide showed highest degree of damage at the lowest concentration of PG. Data are mean  $\pm$  SEM ( $n = 4$  for A and  $n = 3$  for B). Statistical analysis was carried out using the ANOVA test (\* $p < 0.05$ , \*\* $p < 0.01$ , \*\*\* $p < 0.001$ ).

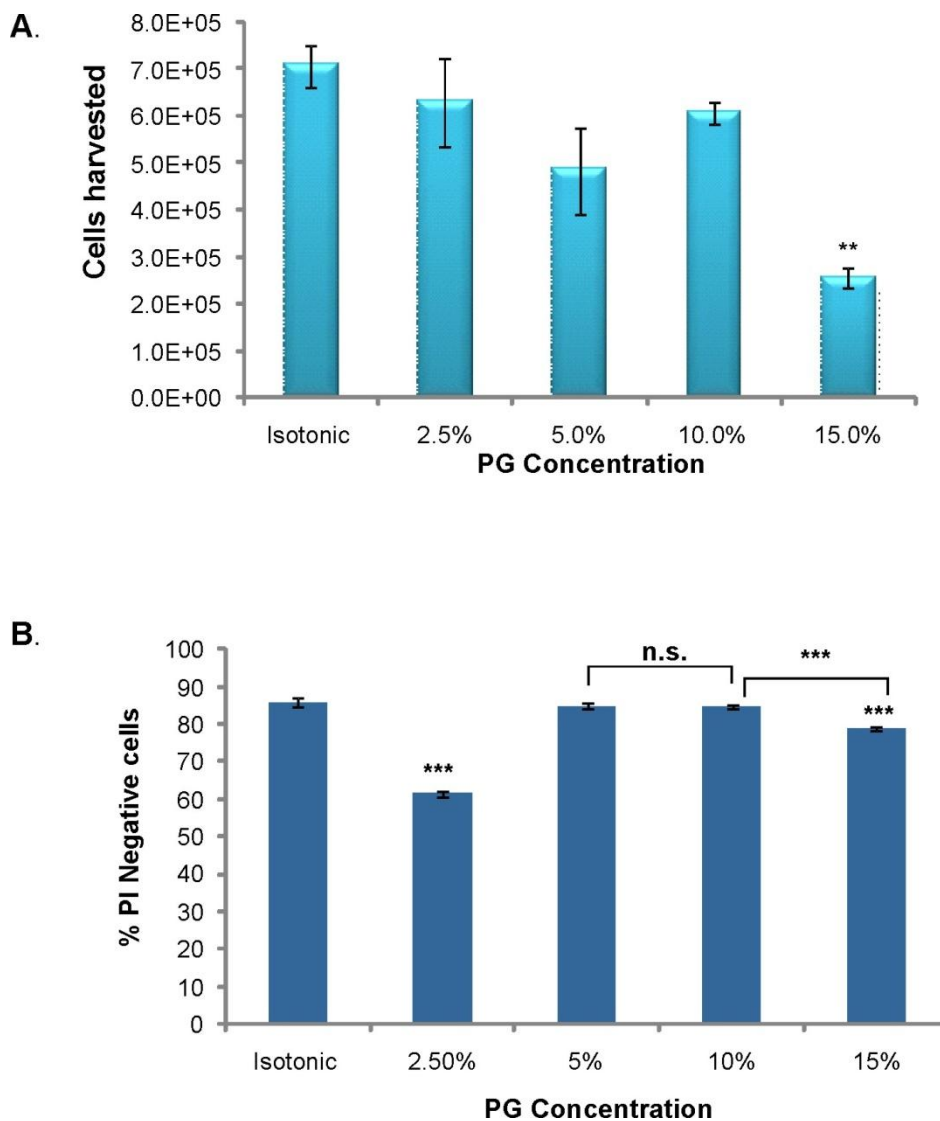


**Figure 4.18 Effect of exposure to PG on SHEF3 cells**

(A) Cell growth assessment of human embryonic stem cell line SHEF3 after 15 minutes exposure to varying concentrations of PG at RT following modelled protocol. (B) Results of membrane integrity assay using propidium iodide showed significant damage at the lowest and highest concentrations of PG. Data are mean  $\pm$  SEM ( $n = 4$  for A and  $n = 3$  for B). Statistical analysis was carried out using the ANOVA test (\* $p < 0.05$ , \*\* $p < 0.01$ , \*\*\* $p < 0.001$ ).

#### 4.4.6 *Effect of cooling rate*

Following the results of the toxicity assay, the optimal CPA concentrations determined when using Me<sub>2</sub>SO and PG were utilised in cooling rate experiments. As a result, 10% PG and 10% Me<sub>2</sub>SO were added to each hESC line at RT. PI dye exclusion assay showed significant damage to RH1 cells in 10%PG (v/v) occurred at cooling rates of 0.1°C/min and 10°C/min while no significant damage occurred between 0.3-3°C/min (Figs. 4.19 & 4.20). Freezing the cells at various cooling rates showed significant membrane damage to SHEF3 cells frozen in 10% Me<sub>2</sub>SO at rates between 0.3-10°C/min (Figs. 4.21 & 4.22A). The number of cells harvested for the cooling rate of 1°C/min showed the highest cell growth compared to the untreated cells and those frozen at other rates (Figs. 4.22B).

Similarly, in 10% Me<sub>2</sub>SO (v/v), RH1 cells were best frozen at a cooling rate of 1°C/min due to the highest proportion of intact cells at this rate (Figs. 4.23 & 4.24).

So far, then, the toxicity and cooling rate assays suggest that 10% Me<sub>2</sub>SO and a cooling rate of 1°C/min are optimal conditions for the cryopreservation of RH1 and SHEF3. The only difference in protocol is the method of adding and removing the CPA to each cell line.

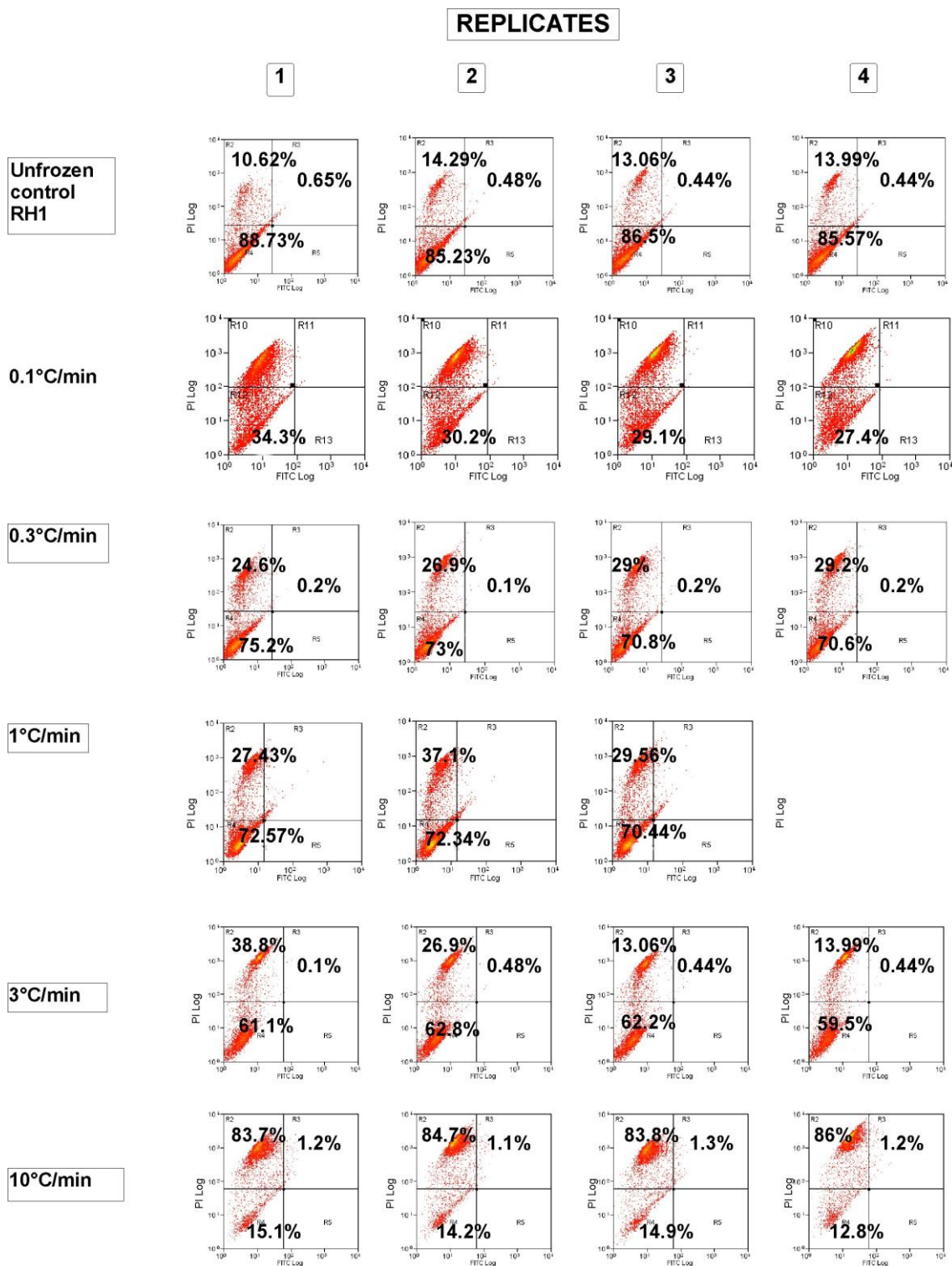


**Figure 4.19 Membrane integrity of RH1 cells in 10%PG at +20°C.** Flow cytometry analysis of RH1 cells that excluded propidium iodide following freezing at cooling rates from 0.1 to 10°C/min.

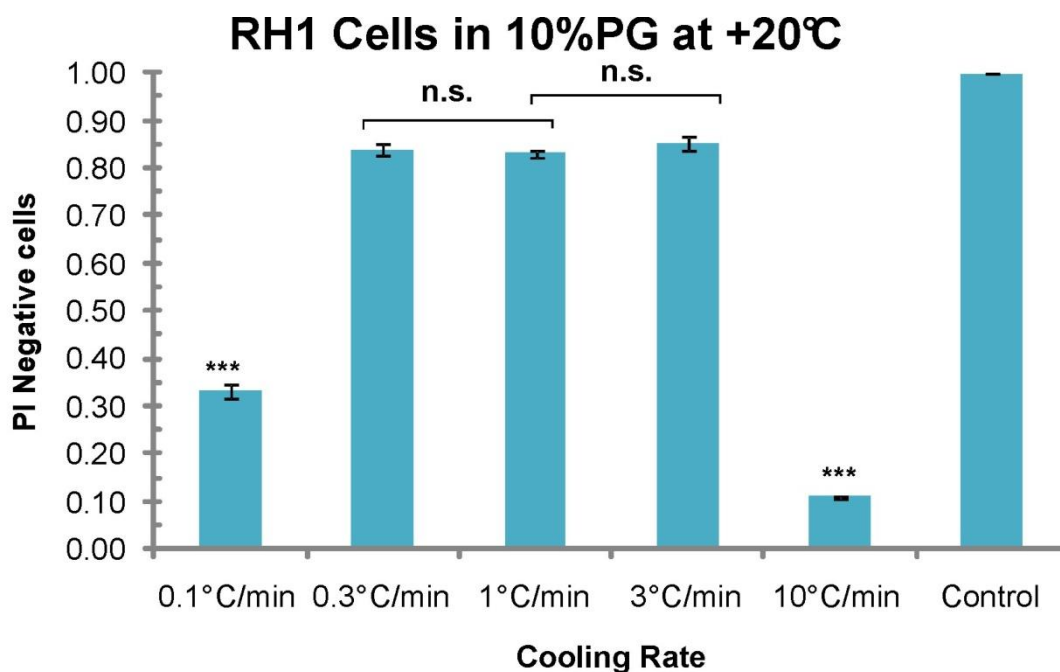


**Figure 4.20 Post-thaw results RH1 frozen in 10%PG.**

Effect of freezing hES cell line, RH1, at the cooling rate 0.1°C/min. Analysis of membrane integrity using flow cytometry and PI dye to identify membrane intact cells. Recovery of PI negative cells is expressed relative to unfrozen control. Data are mean  $\pm$  SEM (n = 4).

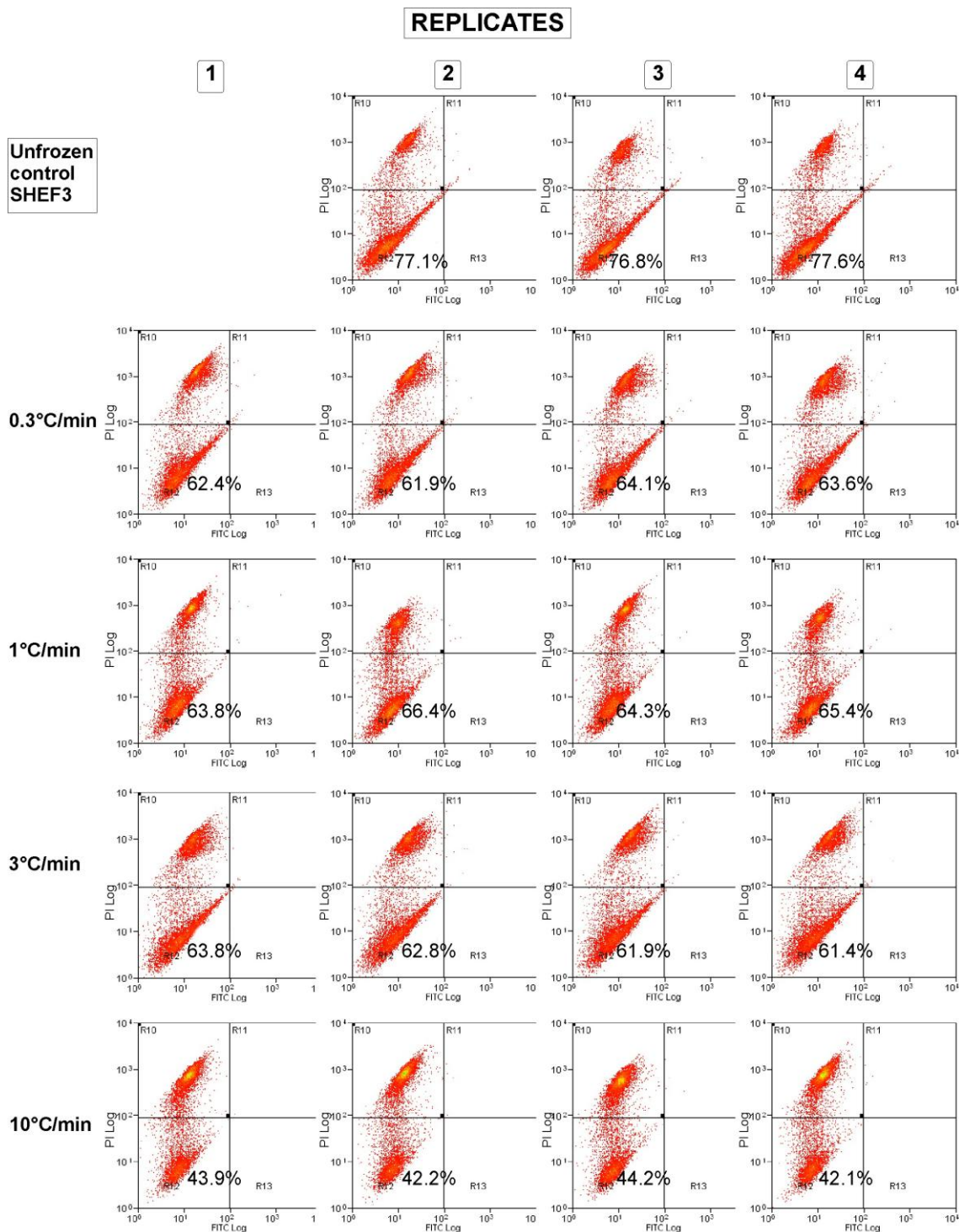


**Figure 4.21 Membrane integrity of SHEF3 cells in 10% Me<sub>2</sub>SO at RT.**

Flow cytometry analysis of SHEF3 cells that excluded propidium iodide following freezing at cooling rates from 0.3 to 10°C/min.

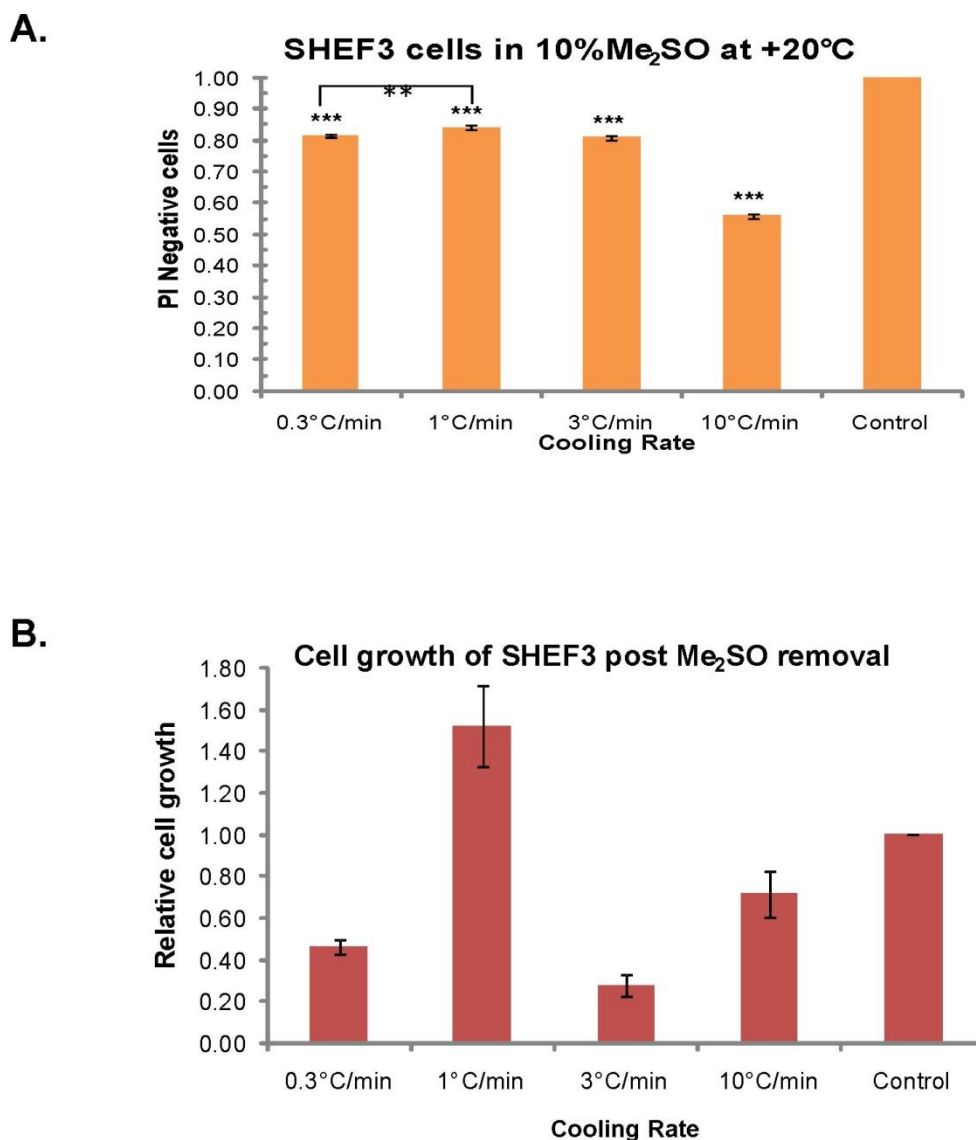


**Figure 4.22 Graphical representation of post-thaw results SHEF3 frozen in 10% Me<sub>2</sub>SO.**

Effect of freezing hES cell line, SHEF3, at cooling rates ranging from 0.3 to 10°C/min.

(A) Analysis of membrane integrity using flow cytometry and PI dye showed significant damage to cell membrane at all cooling rates compared to the unfrozen control.

Recovery of PI negative cells is expressed relative to unfrozen SHEF3 cells. (B) Growth assay showed the optimal cooling rate to be 1°C/min. Recovery is expressed as number of cells relative to unfrozen control. Data are mean  $\pm$  SEM (n = 4 for (A) and n = 3 for (B)). Statistical analysis was carried out using the ANOVA test (\*\*p<0.001).

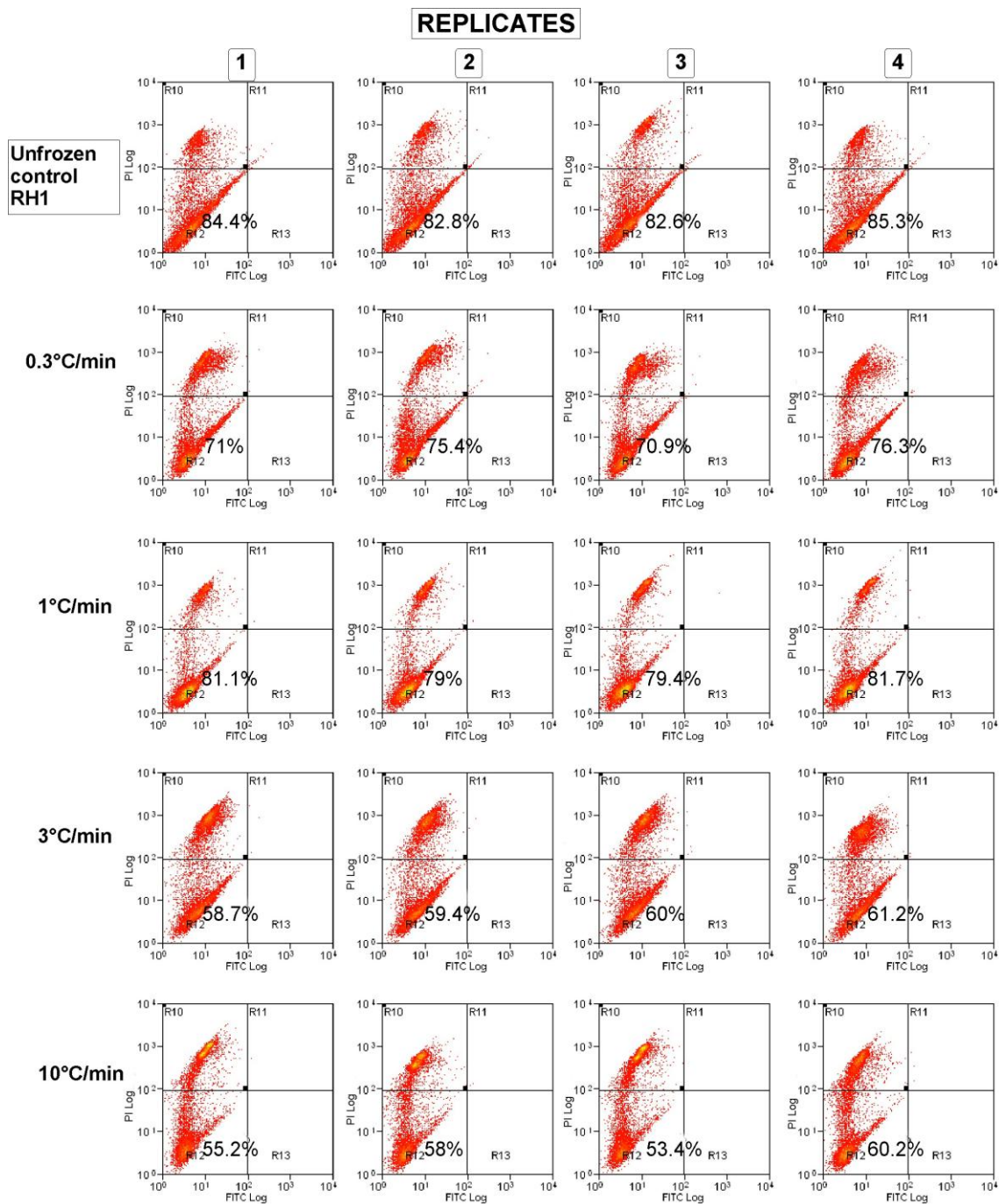


**Figure 4.23 Membrane integrity of RH1 cells in 10%Me<sub>2</sub>SO at RT.**  
Flow cytometry analysis of RH1 cells that excluded propidium iodide following freezing at cooling rates from 0.3 to 10°C/min.

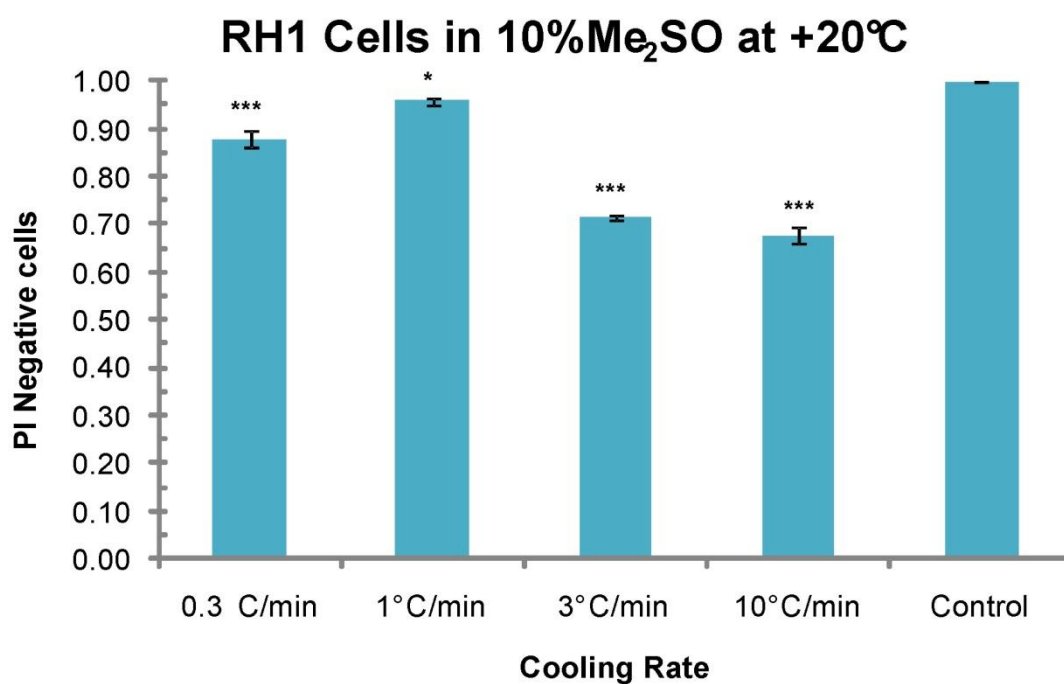


**Figure 4.24 Post-thaw results RH1 frozen in 10%Me<sub>2</sub>SO.**

Effect of freezing hES cell line, RH1, at the cooling rate 0.1°C/min. Analysis of membrane integrity using flow cytometry and PI dye to identify membrane intact cells. Recovery of PI negative cells is expressed relative to unfrozen control (that is, cells in culture). Data are mean ± SEM (n = 4).

## 4.5 Discussion

Following the establishment of the necessary physical properties and tolerable osmotic limits in chapter 3, the work in this chapter uses that biophysical data to demonstrate the optimal concentration of CPA which is least toxic to the cells and the most favourable mode of adding and removing the solute. In addition, the freezing experiments carried out determined the optimal cooling rate for freezing down each hESC line in Me<sub>2</sub>SO and PG.

In order to investigate the best method of adding and diluting CPA to/from each of the three different cell types, a purpose-written computer program which uses Kleinhan's two parameter formalism was employed to experiment with various protocols. The software calculates volumetric water flux and the volumetric flux of CPA using the  $L_p$  and  $P_s$  of the cells that have already been determined in known concentrations of CPA. The computer program allowed the modelling of a single or multistep addition/removal of the CPAs to/from the cells. This same methodology was used for designing the protocols for chondrocytes (Pegg et al., 2006) and CD34<sup>+</sup> cells from umbilical cord blood (Hunt et al., 2003c).

It has emerged through the modelling of addition protocols that the hESCs and the hEC line achieve their isotonic cell volume as long as they do not experience beyond 50% shrinkage which agreed with already determined osmotic limits. Similar volume excursion limits have been found for human oocytes (Paynter et al., 2005a). The extent of shrinkage permitted by each of the cells is slightly different in the various CPAs.

This work is the first report of an investigation into the addition and elution steps involved in cryopreserving and thawing hES cells. Current cryopreservation procedures for hESCs have not taken into account the method of adding and eluting CPAs. Existing slow cooling protocols for hESCs involve the single addition of 5-20% Me<sub>2</sub>SO to cell clusters or cell suspensions and then cooling at rates between 1-2°C/min (Richards et al., 2004a; Heng et al., 2005c; Hunt, 2007). The freezing of cell clusters rather than a single cell suspension poses the problem of the CPA unable to permeate equally into all cells in a colony. Cells on the periphery encounter the CPA before those in the core which will lead to some cells having greater or lesser volume than their isotonic volume because they have not had enough time to equilibrate. Such cells are more susceptible to damage when subjected to freezing due to the possibility of intracellular ice formation which has been proven to be more damaging in an organised array of cells in a cluster than in a cellular suspension (Jacobsen et al., 1984). As a result, it is advantageous to freeze hESCs as a single cell suspension rather than clusters where every cell can be equally equilibrated in medium containing CPA before

being subjected to freezing. However, it is evident that a single addition of 10% Me<sub>2</sub>SO was only appropriate for the RH1 cell suspension; it was best added in 4 separate steps for the SHEF3 cell line, indicating that various stem cell lines may require different protocols for CPA addition. This was confirmed through modelling of currently used protocol where addition of 10% Me<sub>2</sub>SO to RH1 caused a cell response that was within the determined osmotic tolerance while SHEF3 cells experienced shrinkage beyond tolerable limits. Theoretical modelling of CPA addition methods was useful in identifying that it was the mode of adding 10% Me<sub>2</sub>SO which induced excessive shrinkage in SHEF3 cells rather than the chemical toxicity of the compound. Further evidence to support this was revealed in the toxicity assays that showed 10% Me<sub>2</sub>SO as an optimal concentration for SHEF3 cells.

Vitrification is another method of hESC cryopreservation that has been employed, using brief exposure times to concentrated vitrification solutions of 60 and 25 seconds at either room temperature or 37°C (Hunt, 2007). This increases the probability of osmotic stress and damage from the pre-cooling process because much longer equilibration times may be required but timecourse experiments like those in the previous chapter combined with addition modelling will need to be carried out to determine appropriate exposure times. In addition, current exposure times to vitrification solutions (which generally contain high concentrations of Me<sub>2</sub>SO and ethylene glycol) may subject cells to the toxic effects of the high CPA concentration; they are also considered impractical because of high probability of technical variability in execution of the protocol but studies have not been carried out to assess the time required for the CPAs to successfully permeate hESCs and avoid damage. Moreover, rapid cooling through the plunging of hESC clusters into liquid nitrogen may be damaging to the cells and a cause of poor post-warming recovery. The membrane integrity and functional assays along with freezing experiments carried out in this chapter have shown that damage occurs in hESCs at the slowest and most rapid cooling rates, a phenomenon which has historically been demonstrated and analysed by Mazur (Mazur et al., 1972). Hence, the modelling of various protocols was important in reducing osmotic damage and made it possible to investigate the length of exposure to CPA which is safe for the cells.

Recent work by Higgins proposed a mathematical strategy that challenged the idea that the shortest exposure to CPA minimises toxicity. Two approaches were considered for minimising toxicity; one used a constant rate of toxicity with the assumption that it was independent of CPA concentration while the second approach assumed that toxicity was proportional to the square of the intracellular CPA concentration (Higgins, 2010a). The results of this work found that the second approach produced minimal

damage by using a hypotonic vehicle solution during CPA addition and removal, which caused the cells to swell to the maximum tolerable volume and minimised the intracellular CPA concentration (Higgins, 2010b). It must be noted that while these results are interesting, they are theoretical and will need to be tested experimentally.

Based on the modelling of diverse protocols for adding and diluting CPAs, it was determined that adding and removing Me<sub>2</sub>SO at RT was optimal for both RH1 and SHEF3 cell lines. Both cell lines also required the addition of 2% mannitol to the dilution medium in order to minimise the cell volume expansion that the cells experience. Addition of compounds such as mannitol during the dilution of CPA has been used for human oocytes to increase post-thaw recovery (Bernard and Fuller, 1996). The time required in carrying out the addition and removal of Me<sub>2</sub>SO at RT was not excessive and can be routinely executed in a laboratory. For RH1 and SHEF3, addition of Me<sub>2</sub>SO at RT required 3 minutes and 1 hour, respectively; dilution of the CPA from each cell line required 8 minutes and 1 hour, respectively.

Toxicity data achieved in this chapter showed that cell growth of the SHEF3 cells relative to isotonic control was about 80% after exposure to 10%PG (1.3M) and about 60% after exposure to 10% Me<sub>2</sub>SO (1.28M). Similar results were realised with the cryopreservation of mouse ESCs where higher post-thaw recovery was achieved in cells cryopreserved in 1M PG than in 1M Me<sub>2</sub>SO (Kashuba Benson et al., 2008o). However, this is inconsistent with the results for RH1 cells which indicated that cell growth was much higher in Me<sub>2</sub>SO than in PG, which suggests that different hESC lines require diverse CPAs for optimal post-thaw survival. The addition modelling showed that SHEF3 required 5 hours to equilibrate in 5%PG which means twice the amount of time would be required for 10%PG to permeate the cell membrane, an impractical method for routine purposes but which may be considered for long-term storage of the cells.

When using Me<sub>2</sub>SO, however, both SHEF3 and RH1 were best frozen using a cooling rate of 1°C/min which is concurrent with the cooling rate that has been used for the cryopreservation of hESCs in Me<sub>2</sub>SO (Ware et al., 2005b; Nishigaki et al., 2009) and other types of stem cells such as cord blood stem cells and human dental pulp-derived stem cells (Woods et al., 2006; Woods et al., 2009). The cooling rate of 10°C/min was most detrimental to both hESCs in both CPAs. Similarly, the lowest survival for CD34<sup>+</sup> cells in Me<sub>2</sub>SO was found at 10°C/min (Hunt et al., 2003k). Although exposure times vary for these hESC lines, there is uniformity in the concentration of CPA utilised and cooling rate required.

---

The step-by-step procedure of cryopreserving the hESCs in this work is outlined in section 4.6, detailing how the serial addition and elution of CPA should be carried out for RH1 and SHEF3 in Me<sub>2</sub>SO. Such detailed steps have only been published for the vitrification of hESCs where equilibration steps in each of the vitrification solutions used were stated (Hunt and Timmons, 2007).

This chapter has shown that investigating each of the variables necessary for cryopreservation is important for designing an optimal cryopreservation protocol. Theoretical modelling of protocols in addition to performing membrane integrity and functional tests have contributed to ensuring that the designed protocols are optimal for cell survival. As a result, 10% Me<sub>2</sub>SO and a cooling rate of 1°C/min remain suitable for cryopreserving hESCs but equilibration times in CPAs differ from conventional methods and should be adapted for increased cell survival.

## 4.6 Designed cryopreservation protocols

### Freezing SHEF3 using 10% Me<sub>2</sub>SO as a cryoprotectant.

1. Add cryoprotectant in increments of 2.5% allowing cells to equilibrate for 18 minutes.
2. Transfer cells into a cryovial.
3. Place cryovial into a rate-controlled freezer and set cooling rate to 1°C/min. Cool cells to -50°C and transfer into a liquid nitrogen dewar.

### Thawing SHEF3 frozen in 10% Me<sub>2</sub>SO

1. Add medium containing 2% mannitol to dilute the concentration to 5% Me<sub>2</sub>SO. Then carry out subsequent dilutions until the concentration is 1.25% (each dilution step should reduce CPA concentration to half the initial concentration). Allow 35 minutes after for first step and 15 minutes for subsequent steps for cells to equilibrate.
2. Pellet the cells by centrifuging at 1200rpm for 5 minutes.
3. Resuspend cells in growth medium.

### Freezing RH1 using 10% Me<sub>2</sub>SO as a cryoprotectant.

1. Add 10% Me<sub>2</sub>SO to the cells allowing an equilibration period of 4 minutes.
2. Transfer cells into a cryovial.
3. Place cryovial into a rate-controlled freezer and set cooling rate to 1°C/min. Cool cells to -50°C and transfer into a liquid nitrogen dewar.

### Thawing RH1 frozen in 10% Me<sub>2</sub>SO

1. Add medium containing 2% mannitol to dilute the concentration to 5% Me<sub>2</sub>SO. Then carry out subsequent dilutions until the concentration is 2.5% (each dilution step should reduce CPA concentration to half the initial concentration). Allow 4 minutes for cells to equilibrate after each dilution step.
2. Pellet the cells by centrifuging at 1200rpm for 5 minutes.
3. Resuspend cells in growth medium.

## **Chapter 5**

# **PROTOCOL ASSESSMENT**

## 5.1 Introduction

This chapter focuses on evaluating the effect of the designed cryopreservation protocol for both RH1 and SHEF3 on pluripotency, gene expression and cell survival post-thaw; advantages of the designed protocol will be identified and compared to the conventional slow cooling protocol which is in general use.

A cryopreservation study by Katkov and colleagues compared the pluripotency of control cells (unfrozen cells) with H9 hESC line containing Oct4 promoter driven, enhanced green fluorescent protein (EGFP) that had been subjected to freeze/thawing (Katkov et al., 2006b). Flow cytometry analysis, after 3 days in culture, showed that control cells, which were passaged on the same day as the frozen cells were thawed, had majority of the cells being EGFP-positive, while thawed cells were only 10% EGFP-positive. Although Oct4-positive expression increased after 7 days, there were large numbers of EGFP-negative cells within each hESC colony in the control and thawed cell populations. Similar decreases in post-thaw expression of Oct4 were found in other studies (Richards et al., 2004a). Since Oct4 is widely used as a marker for pluripotency (Thomson et al., 1998e; Reubinoff et al., 2000c; Boyer et al., 2005c; Adewumi et al., 2007d), a loss in expression may suggest a loss of pluripotency and/or increased differentiation. However, Oct4-positive cells increased after 7 days in culture, which raises the debate whether loss of Oct4 is a reversible process. In addition, cells which lost Oct4 expression were also found to be non-viable through PI staining (Katkov et al., 2006a), however these cells were not shown to be either necrotic or apoptotic. Heng and colleagues identified that loss of viability in cells of the H1 hESC line that have undergone slow-cooling was due to apoptosis rather than necrosis (Heng et al., 2006d). In this study, 98% of cells appeared viable immediately after warming, but survival decreased after incubation at 37°C; deterioration of the cells was found to be slowed by keeping the cells at 4°C. Terminal deoxynucleotidyl transferase (TdT)-mediated dUTP nick-end-labeling (TUNEL) assay confirmed apoptosis-induced nuclear DNA fragmentation combined with immunocytochemistry analysis which detected caspase-3 staining, another marker for apoptosis. Research by Baust and colleagues also identified the apoptotic pathway in frozen-thawed hESCs as a major contributor to cell death along with necrosis and cell lysis; these three modes of cell death were collectively referred to as cryopreservation-induced delayed-onset cell death (CIDOCD) (Baust, 2002b). Previous work on frozen-thawed human fibroblasts showed an up-regulation of transcriptional and proteolytic activity of caspase-3 (Baust et al., 2002). Further up-regulation of transcriptional activity of caspase-8 and -9 was also found (Baust et al., 2002).

Caspases can be classed into initiator and effector caspases based on structure and function. Their structure consists of an N-terminal regulatory prodomain of varying lengths followed by a catalytic domain at their core (Fig. 5.1). They are activated by the cleaving of other caspases and cellular proteins, thereby forming an apoptotic cascade. Initiator caspases (caspases 3, 6 and 7) are first activated through the binding of adaptor molecules and then subsequently activate effector caspases (caspases 8, 9 and 10) which cause apoptosis to occur (Fig. 5.2) (Thornberry et al., 1997). Apoptosis can occur either through the intrinsic or extrinsic pathway. The intrinsic pathway is initiated by stimuli (for example, irradiation and proapoptotic drugs such as staurosporine) which cause the release of cytochrome c in the intermembrane mitochondrial space. Cytochrome c moves into the cytosol where it binds apoptotic protease-activating factor 1 (Apaf-1) to form a complex that activates caspase-9 and in turn activates caspase-3. However, the extrinsic pathway begins by the binding factors to a death domain-containing receptor on a cell's surface, which activates caspase-8 or -9 and stimulates caspase-3, -6 or -7. Knowledge of apoptotic events in frozen-thawed hESCs, therefore, has initiated the use of caspase inhibitors in freezing and thawing media in order to maximise cell survival.

In this chapter, the roles of necrosis and apoptosis will be assessed using Annexin V-FITC and PI dyes. The incorporation of both dyes indicates apoptotic activity while the detection of PI alone shows membrane-damaged and necrotic cells. Similar dual staining have also been utilised in determining cell viability (Yang et al., 1998; Tijssen et al., 2000; Abrahamsen et al., 2002a; Li et al., 2008c; Wagh et al., 2011). Yet other studies have used the exclusion of single dyes such as trypan blue or PI to evaluate cell viability (Katkov et al., 2006e; Guan et al., 2008).

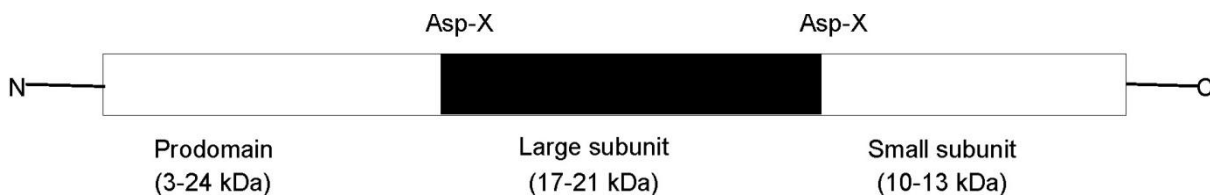


### Figure 5.1 Caspase structure

Characteristic structure of caspases, showing a catalytic core (the dark middle region) and an N-terminal prodomain. Cleavage at the aspartate (Asp) sites activates the enzyme to induce apoptosis.

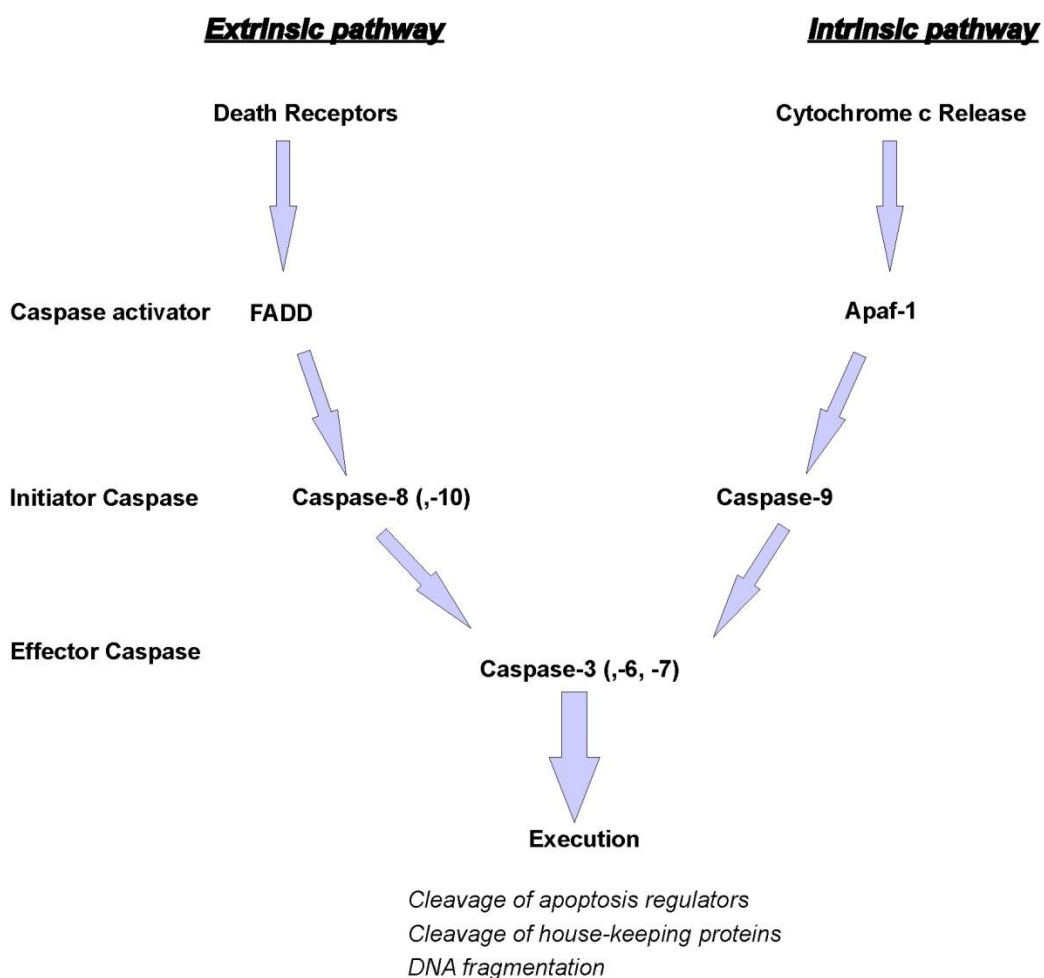


### Figure 5.2 Two main apoptotic pathways.

The extrinsic pathway involves the association of death receptors through death domain proteins (such as Fas-associated death domain, FADD) which activates caspase-8 or-10. The intrinsic pathway begins with the release of cytochrome c in the mitochondria which moves into the cytosol. It then binds Apaf-1 which activates caspase-9. Both of the pathways lead to the activation of effector caspases (3, 6 and 7) which result in cell death.

### *5.1.1 Post-thaw assessment of cell survival*

Cell survival has been evaluated differently through gene expression and occurrence of apoptotic events, but insufficiently defined for hESCs that have undergone cryopreservation. It is adequate to say that hESC survival post-thaw can be assessed by their functionality which has been characterised by their ability to remain undifferentiated, express known surface and nuclear markers, and capable of differentiating into specific lineages. However, due to the many possible lineages that the cells could differentiate into, such a basis to classify cell survival is inadequate. In addition, use of the term 'viability' in various studies has also been questioned due to lack of an exact scientific meaning. Having viability clearly defined, therefore, will determine the kind of assays that will be used in characterising post-thaw cell survival (Pegg, 1989).

### *5.1.2 Functionality of Human Embryonic Stem Cells*

The international stem cell initiative (ISCI) was a thorough investigative study with the objective to define characteristics that stem cell lines may have in common such as gene expression profiles, hence providing a standard for characterising hESCs (Adewumi et al., 2007c). 59 hESC lines from different laboratories were analysed for this work. Although there were some commonalities in expression of cell surface markers and protein antigens, variations were still observed between various cell lines (Adewumi et al., 2007b). Other studies have examined plasma membrane proteins that may be similarly expressed between hESC lines (Josephson et al., 2006; Dormeyer et al., 2008).

The attractive feature of hESCs is their ability to become any cell type, thus it is essential that this capability be maintained before and after cryopreservation. As a result, hESCs must be maintained in an undifferentiated state in order to differentiate into a desired lineage. The work in this chapter sets out to differentiate each hESC line used in the study into the osteogenic lineage. Similar attempts have been carried out by other groups who have differentiated hESCs into osteoblasts (Andrews et al., 1994; Cao et al., 2005d). Moreover, others have differentiated hESCs into hepatocytes (Rambhatla et al., 2003), haematopoietic progenitors (Ng et al., 2005b), and cardiomyocytes (Mummery et al., 2003a; Bielby et al., 2004c; Passier et al., 2005a; Passier and Mummery, 2005b). All of these differentiation procedures were performed with an initial step of forming aggregates of hESCs called embryoid bodies (EBs). These spheroidal structures are created by disaggregating hESC colonies and introducing them to a feeder-free culture system where they exist in suspension. Subsequent manipulation, involving the addition of necessary factors, promotes the

EBs to differentiate into the desired cell type. For example, a cocktail of dexamethasone, ascorbic acid and  $\beta$ -glycerolphosphate has been added to EBs to promote osteogenic differentiation (Bielby et al., 2004b;Cao et al., 2005a). It has also been found that EBs in suspension medium can spontaneously differentiate into the three germ layers (Thomson et al., 1998d;Reubinoff et al., 2000b).

hESCs have also been differentiated without the requirement for EB formation, for example in the generation of haematopoietic colony forming cells (Kaufman et al., 2001b) which was achieved by the co-culture of hESC colonies with irradiated mouse bone marrow stromal cells or mouse yolk-sac endothelial cells (Kaufman et al., 2001a). Differentiation into neural progenitors has been found in hESC colonies following a 3-4 week culture of hESC colonies without replacing the MEF layer (Reubinoff et al., 2001a).

Markers such as  $\alpha$ -fetoprotein, brachyury and nestin represent endoderm, mesoderm and ectoderm, respectively, and have been detected using assays such as RT-PCR and immunocytochemistry (Reubinoff et al., 2000a;Itskovitz-Eldor et al., 2000c).

A major challenge regarding the differentiation of hESCs is the lack of a standardised protocol, making it difficult to reproduce the results from one laboratory to another. It also introduces variability in the success of the procedure. It is evident that uniformity is required in executing differentiation protocols and that hESCs must maintain their ability to remain undifferentiated in culture, forming characteristic colonies with appropriate morphology (Fig. 5.3). However, assessing colony morphology is also a subjective process and requires a standardised morphology which can be used to identify undifferentiated and differentiated colonies.

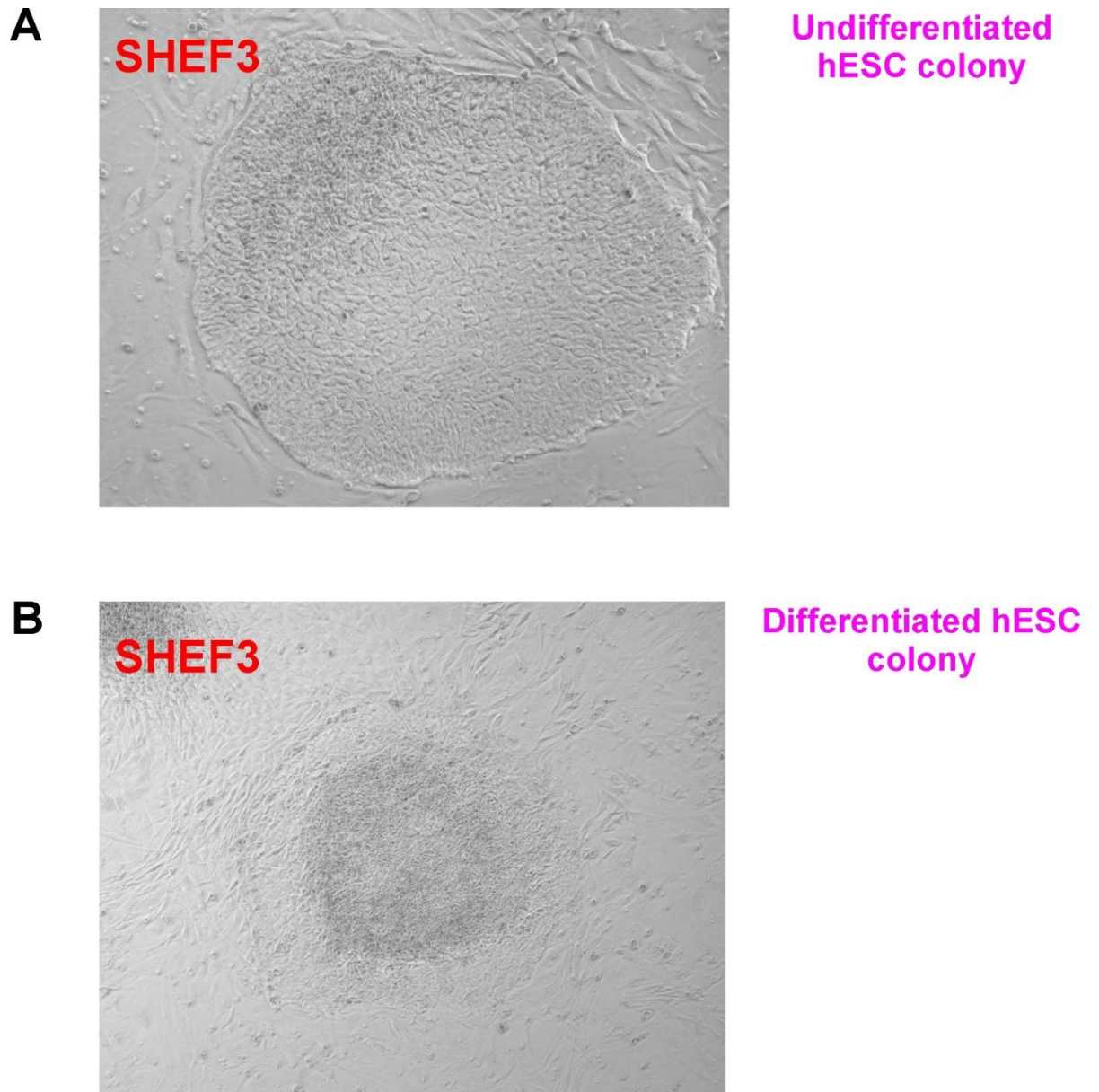


**Figure 5.3 SHEF3 Colonies**

(A) Undifferentiated colony with a defined edge and tightly packed cells in the core; there is a clear separation between the colony and surrounding feeder layer of mouse embryonic fibroblasts. (B) Differentiated colony with a 'fried-egg' appearance; the edge of the colony is less defined than that of an undifferentiated colony.

### 5.1.3 *Criteria for testing optimal cryopreservation protocol*

In this chapter, four criteria will be used in assessing hESC survival following cryopreservation in 10% Me<sub>2</sub>SO according to the designed protocol in the previous chapter. Cryopreservation in 10% PG will also be carried out to compare its effect to that of 10% Me<sub>2</sub>SO and the conventional or unoptimised protocol. The four criteria for assessment of hESC survival are as follows:

- Ability of the hESC lines to form colonies in culture post-thaw.
- Expression of the characteristic cell surface markers TRA-1-60, TRA-1-81, SSEA4 which indicate undifferentiated cell population.
- Ability of hESCs to form EBs and differentiate into a specific cell lineage
- Reduction in apoptotic events in cells that have undergone the designed protocol compared to those cryopreserved under the unoptimised protocol.

## 5.2 Chapter aims

- Characterise hESCs by surface marker expression pre-freeze which would be analysed by flow cytometry.
- Assess effectiveness of designed protocols from chapter 4 by comparing surface marker expression after freeze-thaw to expression prior to freezing, EB formation and subsequent expression of markers specific for each germ layer.
- Test differentiation capability of freeze-thawed cells by carrying out osteogenic differentiation.
- Compare the effect of PG and Me<sub>2</sub>SO on cell survival by apoptotic assay involving staining with annexin V-FITC and PI.

Each of the set objectives above will be carried out to prove the study hypothesis that a systematic approach to designing a cryopreservation protocol produces a more optimal procedure than one designed through an empirical approach.

## 5.3 Materials and Methods

### 5.3.1 Preparation of embryoid body (EB) medium

For 100mL,

84mL  $\alpha$ -MEM (1.5 g/l glucose) with Glutamax

15 ml FBS (final: 15%)

1 ml 100x penicillin/streptomycin (final: 1x)

### 5.3.2 Embryoid body formation

RH1 and SHEF3 colonies were washed with 1X PBS, which was then aspirated. 500  $\mu$ l 1 mg/ml collagenase Type IV (GIBCO) solution was added for each well of a 6-well plate and incubated for 5 minutes at 37°C. 1mL of hESC growth medium was added to each well and colonies were gently detached from the MEF feeder layer using a 1000  $\mu$ l pipet tip. Colonies were then transferred into a 50mL tube (2 6-well plates per 50mL tube) and allowed to settle by gravity. Suspending medium was gently pipetted out of the tube. hESC medium was added to colonies for a second wash.

### 5.3.3 Surface Marker Expression profiles

The following surface markers were assessed in 2102Ep, RH1 and SHEF3 cells: TRA-1-60, TRA-1-81, SSEA4, and SSEA1 using flow cytometry as described earlier (See sections 2.5 and 2.7 for culturing methods, and section 2.13 for flow cytometry procedure). Expression of SSEA3 was not tested due to unavailability of the appropriate isotype control and secondary antibody at the time the assay was carried out.

### 5.3.4 Differentiation potential of hESCs

In order to assess the potency of RH1 and SHEF3, two approaches were considered: spontaneous differentiation and directed differentiation, which both require the initial formation of EBs. Both approaches have been utilised in characterisation studies involving hESCs (Itskovitz-Eldor et al., 2000b; Conley et al., 2004b; Bhattacharya et al., 2005; Ng et al., 2005a; Cao et al., 2005b).

#### 5.3.4.1 Primer design

Two genes that represented each germ layer (Table 5.1) were chosen in order to carry out RT-PCR analysis of spontaneous differentiation in RH1 and SHEF3. Human mRNA sequences of each gene of interest were acquired from the National Center for

biotechnology information (NCBI) database. Primer sequences were chosen from the mRNA sequence and compared with the mouse mRNA using a sequence alignment program, ClustalW2, in order to increase binding specificity to human genes. This was useful to carry out because the hES cell suspensions contained mouse cells from the inactivated mouse feeder layer.

#### **5.3.4.2 Gene expression of embryoid bodies from SHEF3 and RH1**

EBs remained in suspension cultures for 10 days before being disaggregated using either recombinant trypsin, TrypLE (Invitrogen) or 1.2units/mL of liberase (Roche). RNA was extracted from disaggregated EBs and used to generate cDNA as described in sections 2.7 and 2.8. Each primer pair (Table 5.1) was added to the cDNA product for each cell line in order to run a PCR reaction. NCAM and GFAP were used as markers of the endoderm; GATA6 and SOX7 represented the ectoderm while brachyury and  $\alpha$ -fetoprotein represented the mesodermal germ layer.

**Table 5.1 RT-PCR primers for germ layer detection**

Primers are markers for endoderm, mesoderm and ectoderm

PRIMER	ANNEALING TEMP (°C)	ELONGATION TIME (seconds)	SIZE (bp)	PRIMER SEQUENCE
NCAM	59	30	814	Forward: TGTCATCTACGGTTAACATCAGCGCG Reverse: CCTGAACCGAGTCCATCATCCAAG
GFAP	59	30	89	Forward: TCAAGTGTCTCAGTCCACCTGAGC Reverse: CAAGTGCTGAGAATCAAGCTCCCAC
GATA6	59	30	649	Forward: CCCAAGAGGCTTGCTGAAAGAGTG Reverse: ACAATCCAAGCCGCCGTGATGAAG
SOX7	59	30	230	Forward: ACGGTGGCTCACGCCTGTAATC Reverse: GCAATCTCAGCTCACTGCAACCTC
BRACHYURY	59	30	241	Forward: ACGTCACCGCCTTAGGATTCGAC Reverse: ACATCTGCTGACGTCATCGTGACG
α-FETOPROTEIN	59	30	127	Forward: AGAGGAGATGTGCTGGATTGTCTGC Reverse: ATTGACCACGTTCCAGCGTGGTC

### 5.3.4.3 Osteogenic differentiation

Day 5 EBs were transferred into a tube before being washed twice with 5mL of 1X PBS under slight agitation and disrupted using either recombinant trypsin, TrypLE (Invitrogen) or 1.2units/mL of liberase (Roche). EBs were incubated at 37°C for 30 minutes with shaking every 10 minutes. EB medium was added to the tube and resuspended using a 5mL pipet. Cell count was carried out using a haemocytometer.  $1 \times 10^5$  cells were seeded onto each well of a 6 well plate and allowed to adhere overnight. Medium was changed from EB medium to osteogenic medium containing hESC medium supplemented with 10mM  $\beta$ -glycerophosphate, 50 $\mu$ g/mL L-ascorbic acid-2-phosphate and 1 $\mu$ M dexamethasone.

### 5.3.5 Cell viability assay using conventional Annexin-V/PI

hESCs were frozen using the optimal cooling rates that were earlier determined and stored in liquid nitrogen vapour phase for 7 days. The cells were then thawed and CPA diluted according to the designed protocols. hESC concentration was adjusted to  $1 \times 10^6$  cells/mL. Then cells were incubated for 30 minutes at 37°C. 0.5mL of cell suspension from both samples were placed in microfuge tubes and centrifuged for 5 minutes at 1000xg. Cells were resuspended in 0.5mL cold PBS. Centrifugation was repeated and the cells resuspended in 0.5mL cold binding buffer. 1.25 $\mu$ L of annexin V-FITC (Calbiochem) was added to the cells and incubated for 15 minutes at room temperature in the dark. Again, the cells were centrifuged and resuspended in 0.5mL cold binding buffer. Lastly, 10 $\mu$ L of propidium iodide (PI) was added to the samples and which kept on ice and in the dark. Analysis by flow cytometry followed shortly thereafter. Phosphatidylserine which is normally on the cytoplasmic surface of the cells translocates to the cell surface when apoptosis is induced. Annexin V has a strong affinity to phosphatidylserine and therefore binds to apoptosed cells. Figure 5.4 shows a schematic which is used to identify necrotic and apoptotic cells.

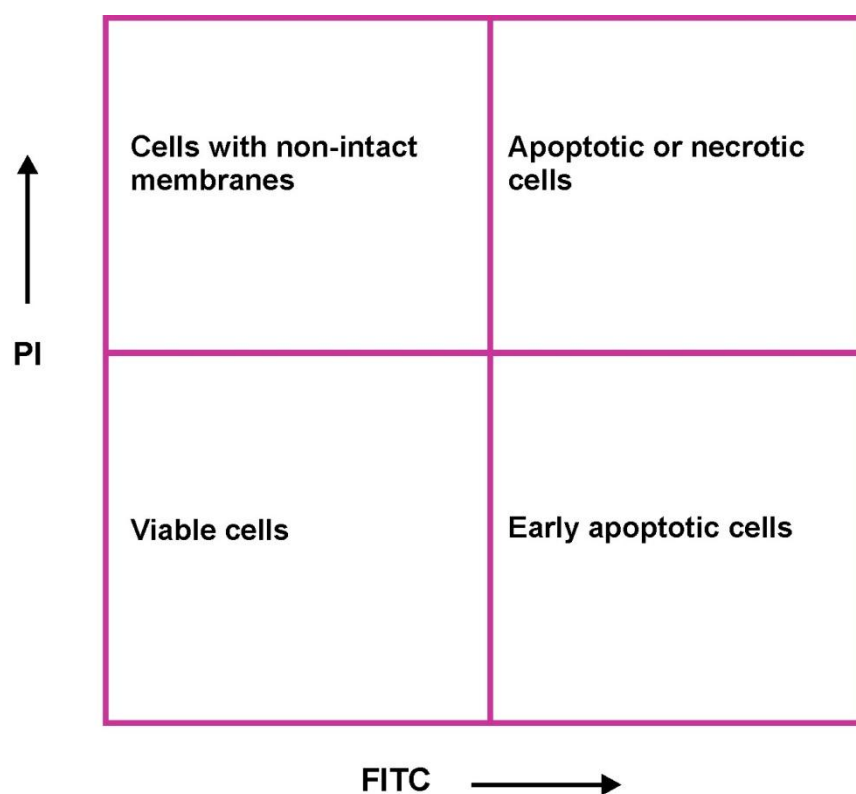


**Figure 5.4 Schematic diagram of viability assessment by Annexin V-FITC and PI**  
The upper right hand quadrant shows cells which are stained with both PI and Annexin V-FITC and are apoptotic. However, the bottom left-hand quadrant indicates cells which have not been stained with either PI or Annexin V-FITC and are considered viable and membrane intact.

## 5.4 Results

### 5.4.1 *Surface marker expression prior to freeze-thaw process*

Characterisation of the surface marker expressions of the hEC line, 2102Ep, and hESCs RH1 and SHEF3 was carried out by flow cytometry to ensure that an undifferentiated cell population was being utilised in subsequent analyses that would be performed. Results showed characteristic marker expression in all cell lines (Figs. 5.5-5.7). All cells lacked expression of SSEA1 and showed positive expression of SSEA4, TRA-1-60, and TRA-1-81.

### 5.4.2 *Formation of embryoid bodies (EBs) and spontaneous differentiation*

In order to test the potential of each hESC line without injecting immunodeficient mice with a cell suspension of pluripotent material, an alternative assay which has been utilised in studies involving hESCs combines the formation EBs in suspension cultures with either an assay to detect markers from the three germ layers through spontaneous differentiation or directed differentiation into a specific lineage. RH1 and SHEF3 colonies formed EBs when in suspension culture with each of the three-dimensional structures displaying a darkened differentiated core (Fig. 5.8). However, further analysis to examine the presence of cells from the different germ layers was performed by expression of various genes through RT-PCR but SOX7 was the only gene detected in both hESCs (Fig. 5.9). This may be an indication that RT-PCR is not the best method of detecting genes of the three germ layers because they may be expressed at very low levels.

### 5.4.3 *Osteogenic differentiation*

Following the results of the RT-PCR, an attempt to carry out directed differentiation using the EBs generated yielded no results because disrupted EBs failed to attach to the tissue culture plastic. Several attempts at disrupting EBs with TrypLE or collagenase IV and seeding the cells to perform osteogenic differentiation also yielded no results. Assay was repeated over a period of 6 months without success.

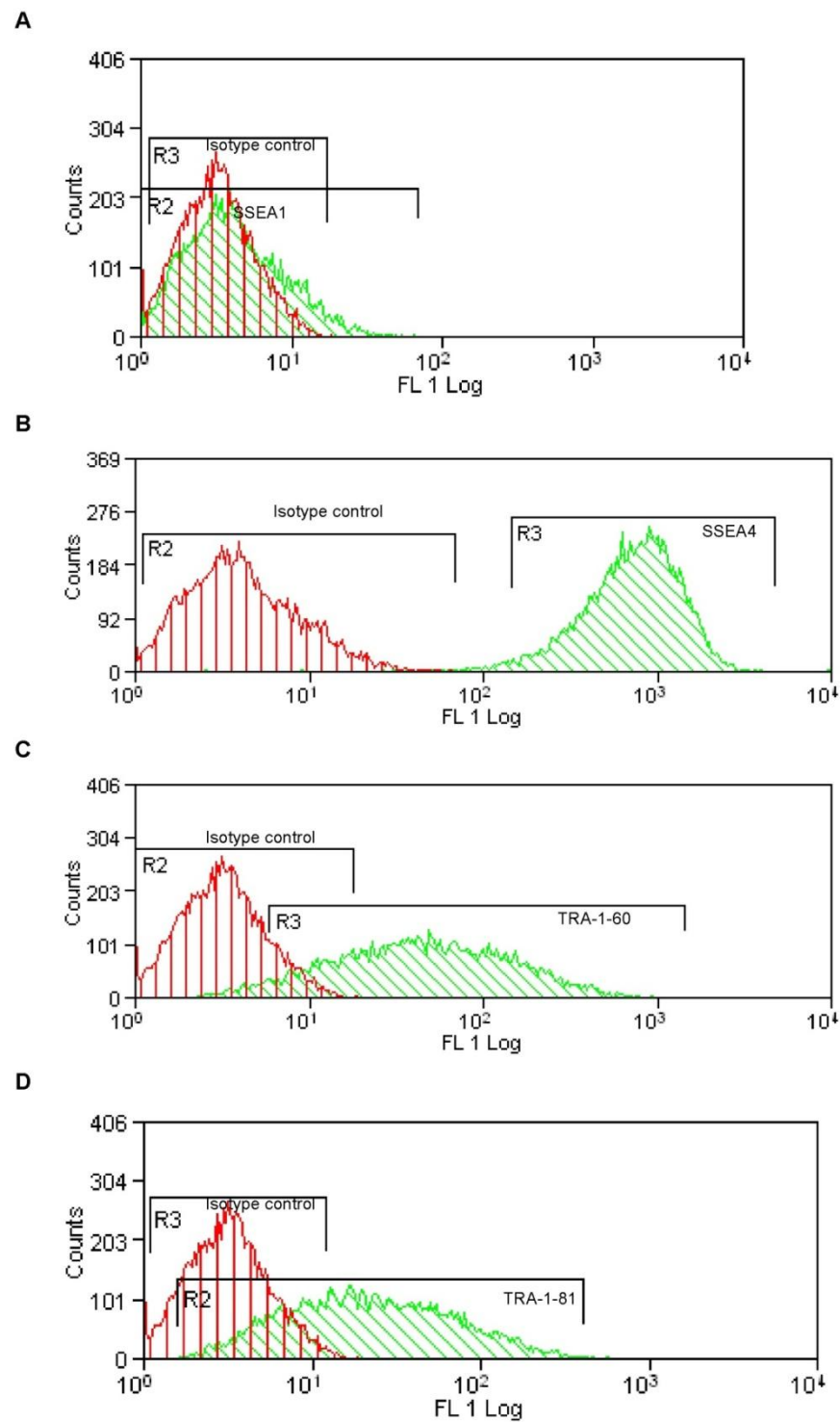
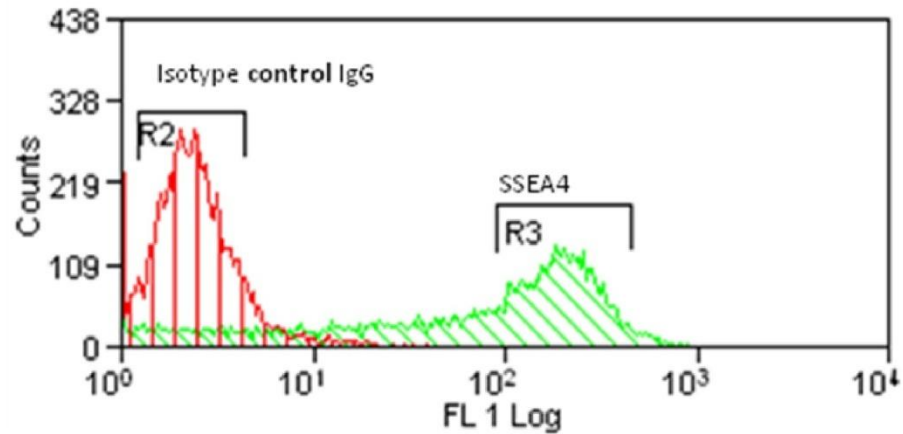


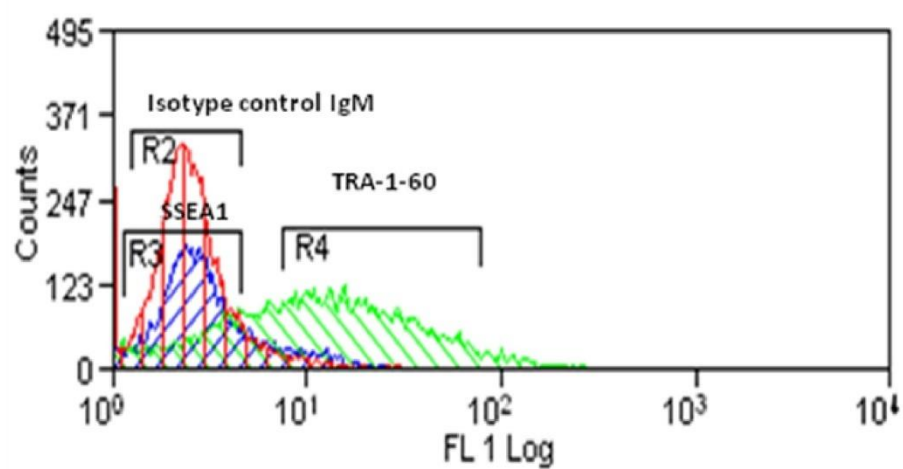
### Figure 5.5 Surface marker expression of 2102Ep cells

The hEC line, 2102Ep showed (A) Negative expression to SSEA1, a marker for differentiation. Positive expression was detected for (B) SSEA4 and TRA-1-60, and also (D) TRA-1-81. Red histograms indicate antibody controls. The y-axis indicates the cell count on a logarithmic scale.

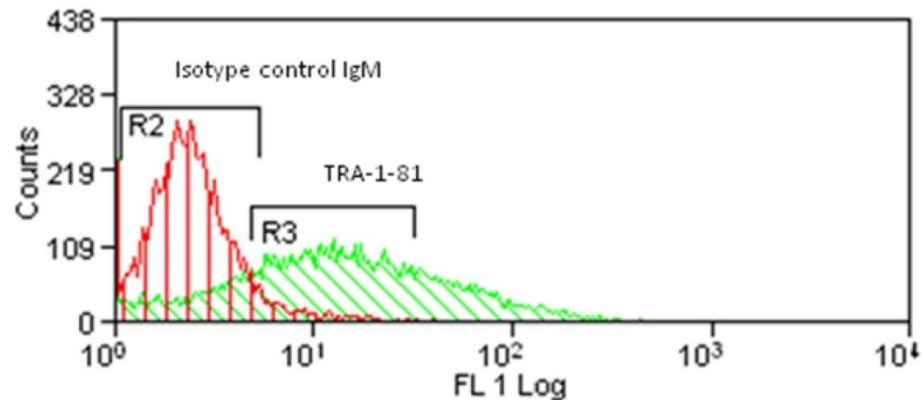
A



B

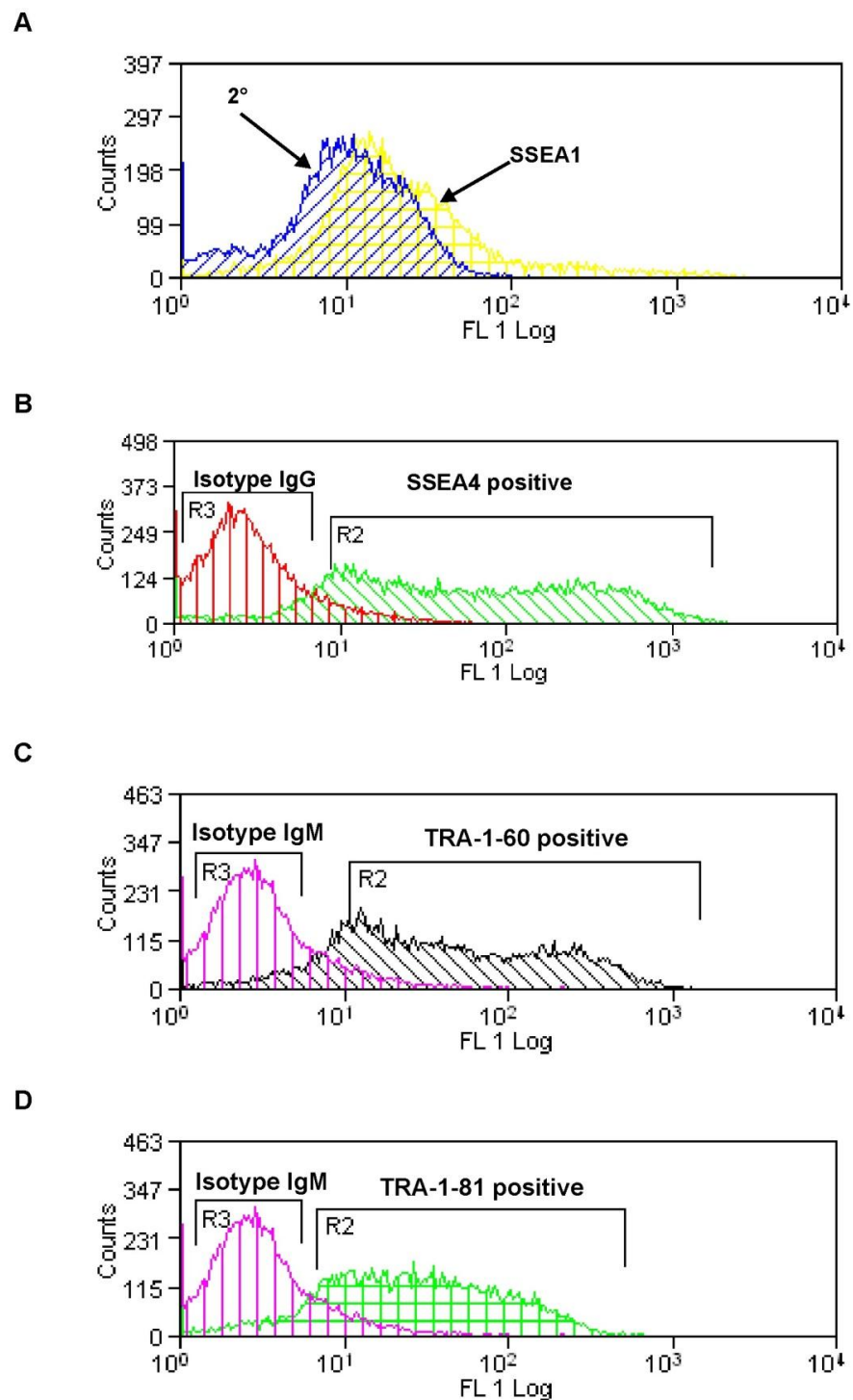


C



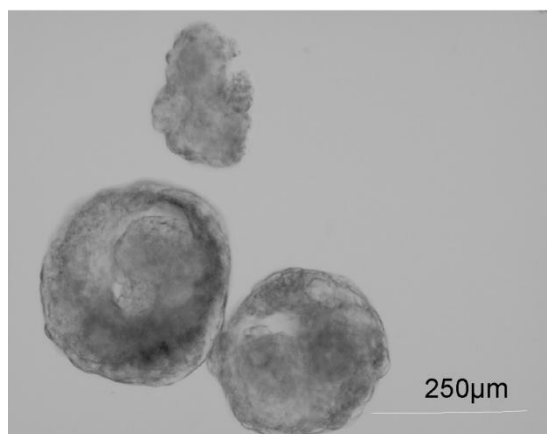
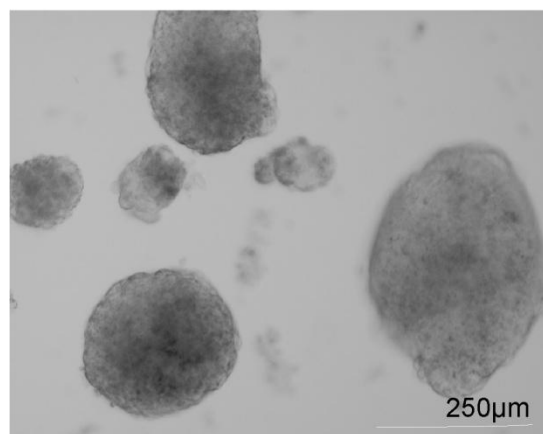
**Figure 5.6 Surface marker expression of RH1 cells.**

Flow cytometry analysis indicated (A) Positive expression of SSEA4 (B) No expression of SSEA1, a marker for differentiation and positive expression of TRA-1-60 and (C) positive expression of TRA-1-81. Red histograms indicate antibody controls while blue and green histograms represent gene expression. The y-axis indicates the cell count on a logarithmic scale.



**Figure 5.7 Surface marker expression of SHEF3 cells.**

Flow cytometry analysis of hESC line, SHEF3, showed (A) Negative expression to SSEA1, a marker for differentiation. Positive expression was detected for (B) SSEA4 and TRA-1-60, and also (D) TRA-1-81. Red, purple and blue histograms indicate antibody controls, while green and black histograms represent gene expression. The y-axis indicates the cell count on a logarithmic scale.

**RH1****SHEF3****Figure 5.8. Embryoid bodies**

Disaggregated RH1 and SHEF3 colonies possess the ability to form EBs in suspension cultures. The EBs were of varied sizes.

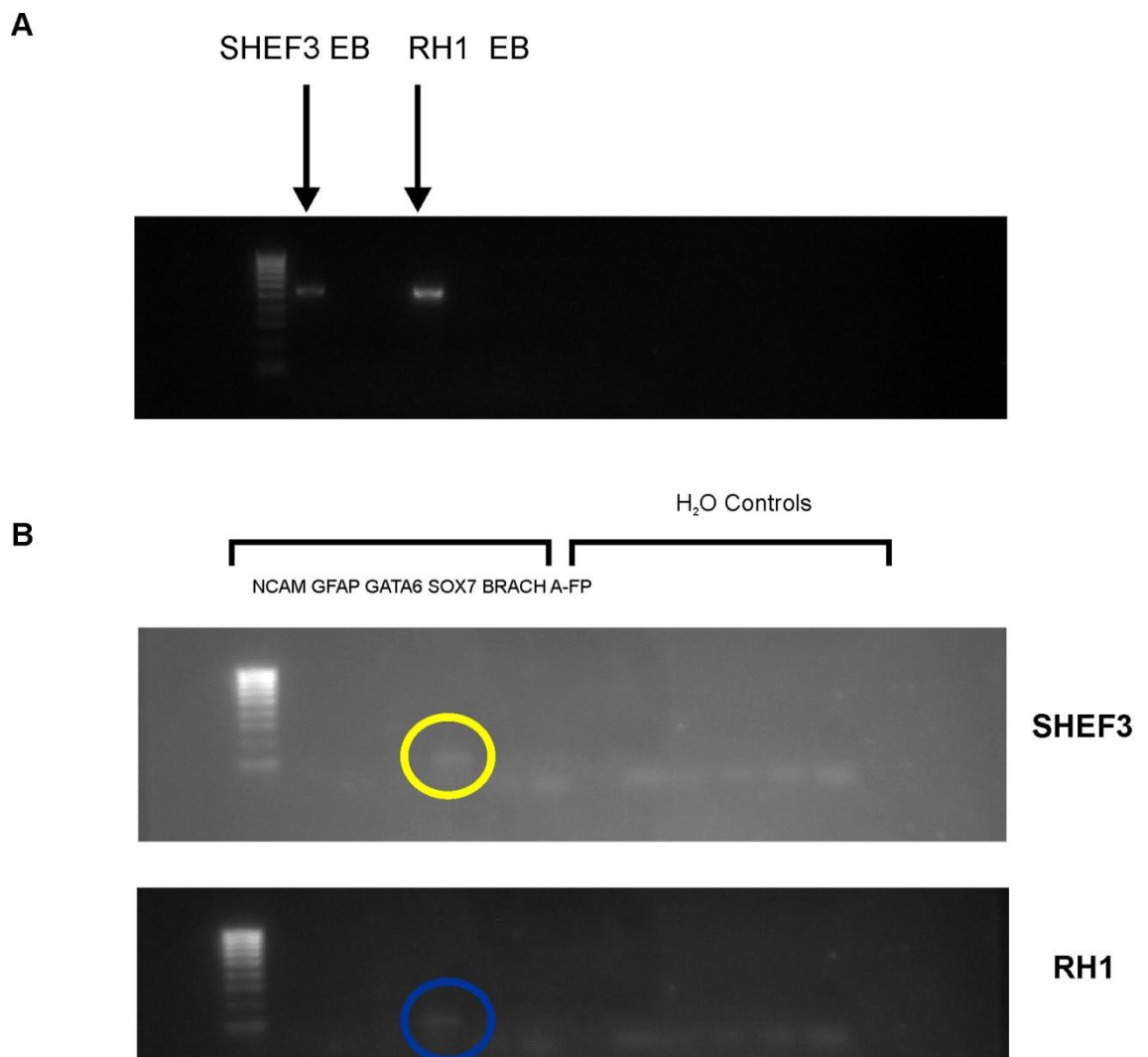


**Figure 5.9 RT-PCR analysis of hESC gene expression**

PCR images of (A) expression of house-keeping gene, GAPDH, for RH1 and SHEF3 EBs, and marker expression for each of the three germ layers in (B) SHEF3 and RH1. SOX7 was the only gene detected in both RH1 and SHEF3 EBs.

#### *5.4.4 Analysis of colony morphology*

Post-thaw analysis of hESC colonies after undergoing freezing in Me<sub>2</sub>SO and PG showed characteristic morphology with defined periphery and tightly packed undifferentiated cells in the core of the colony (Fig. 5.10) but size measurement of the colonies was not carried out.

#### *5.4.5 Post-thaw marker expression*

Following freeze-thaw in Me<sub>2</sub>SO and PG using the designed cryopreservation protocol and rapid warming in a 37°C water bath, SHEF3 cells were characterised for expression of pluripotent markers in order to ensure that pluripotency was maintained during the process. Flow cytometry analysis showed positive expression to TRA-1-60/81 and SSEA4 indicating their undifferentiated state (Fig. 5.11). There were no post-thaw results for RH1 due to contamination that occurred while the cells were in culture.

#### *5.4.6 Comparative analysis of cell survival using Annexin V/PI*

Cell survival according to flow cytometry analysis was higher for hESCs cryopreserved with the designed protocols for PG and Me<sub>2</sub>SO than those frozen using the conventional protocol (Figs. 5.12 and 5.13). Significantly higher numbers of necrotic and apoptotic cells were found in cells under the conventional protocol compared to the designed protocols. Although there were no significant differences between cells frozen in PG and Me<sub>2</sub>SO, the scatter plots show a high proportion of the cell population which were Annexin V-positive in cells frozen in PG than in Me<sub>2</sub>SO. This was also the case with cells frozen using the conventional protocol.

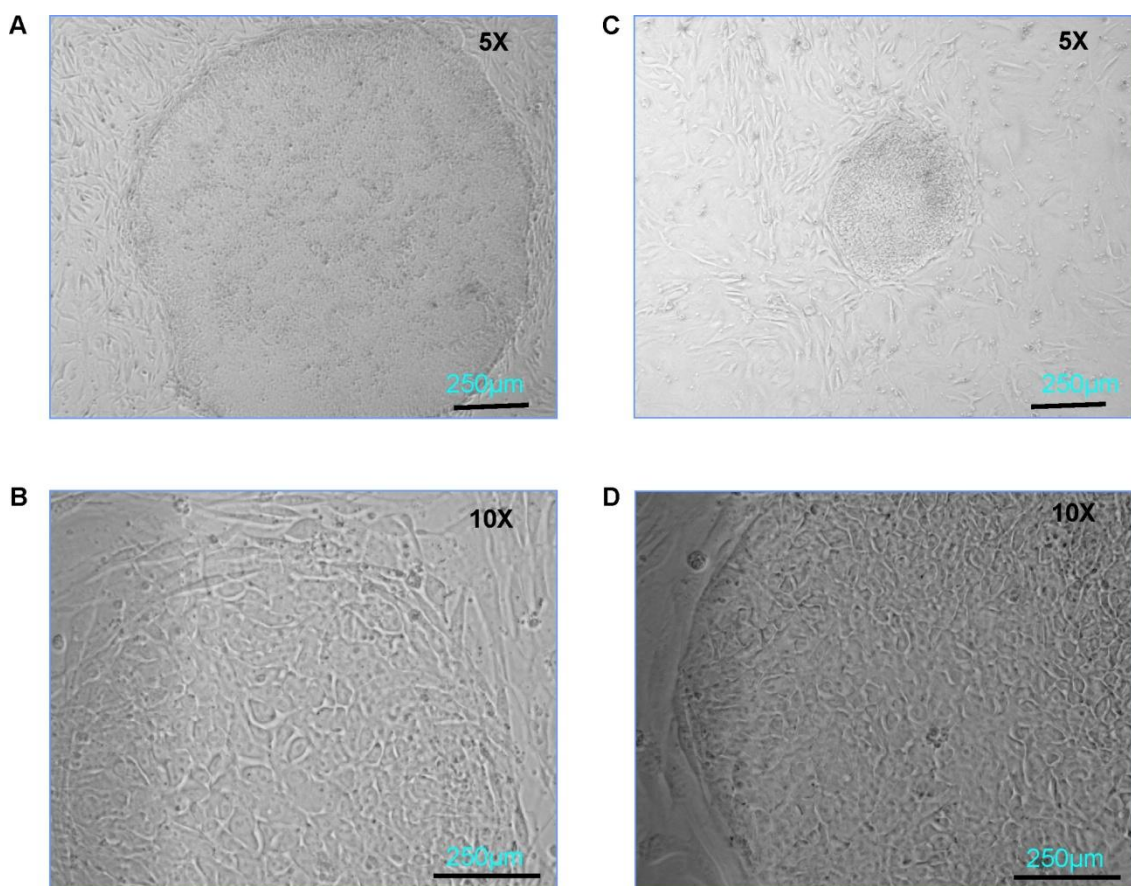


**Figure 5.10 Post-thaw analysis of SHEF3 colonies in Me<sub>2</sub>SO and PG**

Images of hESC colonies *in vitro* following freeze-thaw process (n = 5). In Me<sub>2</sub>SO, 5X (A) and 10X (B), and in PG at magnification of 5X (C) and 10X (D). Images show tightly packed cells in each colony with defined peripheries that distinguishes the colony from the MEF feeder layer.

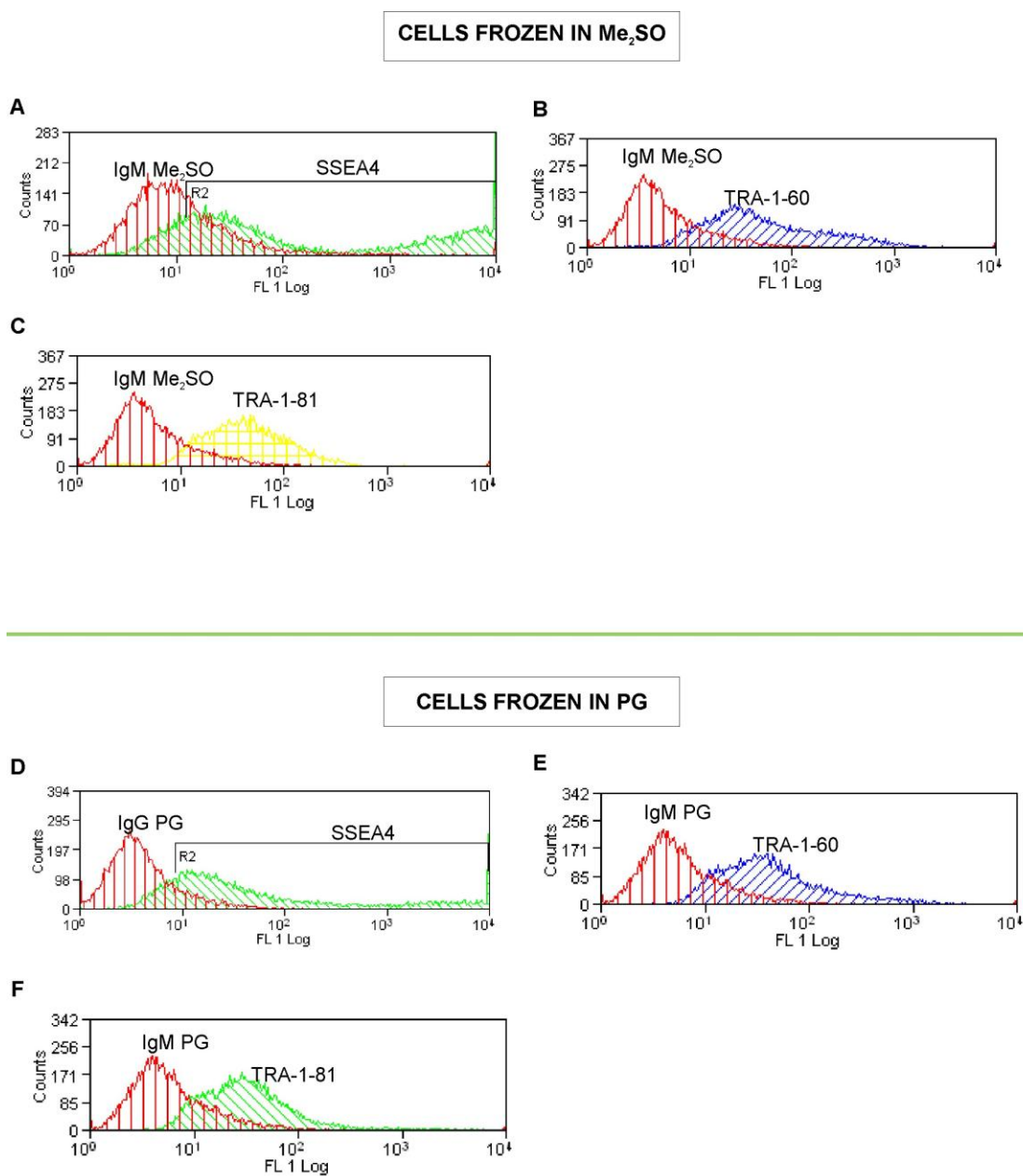
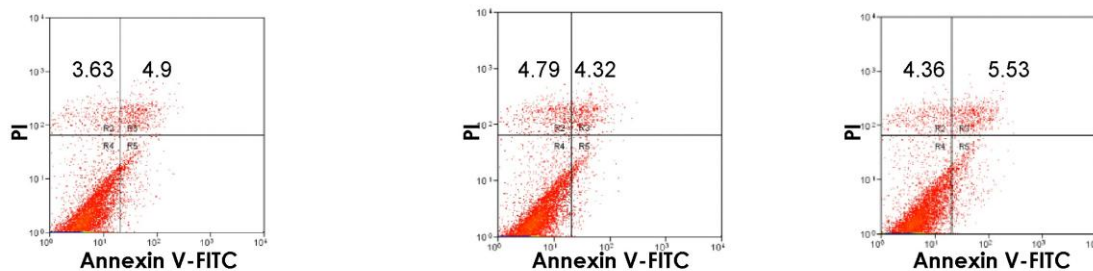


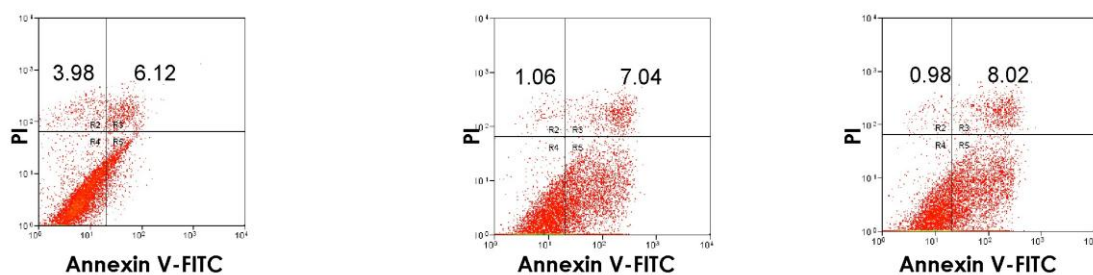
**Figure 5.11 Surface marker expression of SHEF3 after undergoing freezing in Me<sub>2</sub>SO and PG.**

hESCs maintained expression of SSEA4, TRA-1-60 and TRA-1-81 following freezing and thawing using the designed cryopreservation and thawing protocols when using PG or Me<sub>2</sub>SO. Red histograms indicate antibody controls. The y-axis indicates the cell count on a logarithmic scale.

## CELLS FROZEN IN DMSO



## CELLS FROZEN IN PG



## CELLS FROZEN IN CONVENTIONAL PROTOCOL

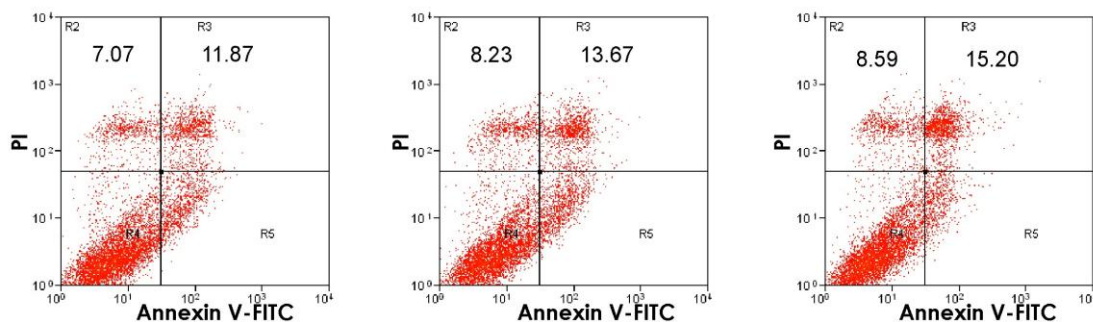


**Figure 5.12** Flow cytometry analysis of apoptosis in SHEF3 following freeze-thaw using designed and unoptimised protocols.

Flow cytometry scatter plots show necrotic, apoptotic and viable SHEF3 cells after staining with Annexin V-FITC and PI dye. Necrotic and apoptotic cells were higher in the conventional protocol compared to the designed protocols for adding and removing 10%Me<sub>2</sub>SO and 10%PG. Early apoptotic cells appear highest in both cells frozen in 10%PG and conventional protocols.

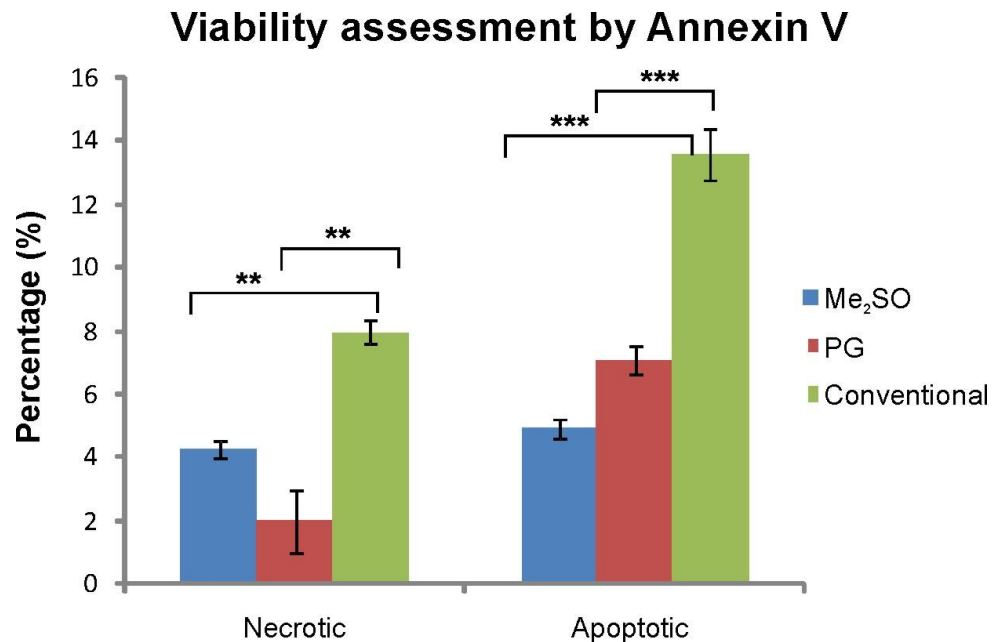


**Figure 5.13 Post-thaw analysis of apoptotic events in SHEF3.**

Apoptotic and necrotic events were lower in the cells cryopreserved under the designed protocols for Me<sub>2</sub>SO and PG than under the conventional protocol (single addition of 10% Me<sub>2</sub>SO). There were no significant differences in the number of necrotic and apoptotic cells in cells cryopreserved in either Me<sub>2</sub>SO or PG while significant differences were observed between cells which had undergone the designed protocols compared to the conventional protocol. Data are means  $\pm$ SEM (n = 3). Significance analysis was carried out using the ANOVA test (\*\*p<0.01, \*\*\*p<0.001).

## 5.5 Discussion

In this chapter, the designed protocols for cryopreserving hESCs in PG and Me<sub>2</sub>SO, and eluting the CPAs post-thaw were assessed for their effectiveness in maintaining hESC characteristics. The influence of each CPA on apoptotic events was also measured and compared in order to determine which CPA was better in improving cell survival.

Initial characterisation of each hESC line showed that the cells expressed characteristic surface markers prior to being frozen. The hEC cells, 2102Ep, and hESC lines, RH1 and SHEF3, all expressed pluripotent markers which were part of a panel of markers used in the international stem cell initiative project to characterise hESC lines (Adewumi et al., 2007a; Wright and Andrews, 2009). Although a specific function of the surface antigens SSEA3/4 is not clear, they have been found to be involved in early embryo development. Therefore, the lack of expression of these antigens signifies a less primitive status (Damjanov et al., 1994). In addition, the SSEA1 antigen which is associated with the induction of differentiation in human teratocarcinoma and hESCs, is normally not expressed in such cells (Kannagi et al., 1983). It has been shown that differentiation leads to a diminished expression of the SSEA3 antigen and the positive expression of SSEA1 (Andrews et al., 1982a); TRA-1-60/81 expression also disappears. Although SSEA3 expression was not assessed in this study, SSEA4 is closely related to SSEA3, and it can be concluded that its expression also diminishes upon differentiation (Fenderson et al., 1987).

SHEF3 and RH1 also formed EBs in suspension as expected but disaggregating the EBs to perform osteogenic differentiation was problematic. A therapeutically useful hESC line should not only be free of reagents sourced from animals, it should also be capable of being differentiated into a desired cell type. Both RH1 and SHEF3 cells displayed the capability of creating EBs, but did not express the lineage-specific markers chosen to represent the three germ layers in this work. This might have been due to the length of time that the EBs were in culture. The EBs in this project were in suspension culture for 14 days because it has been shown that there is reduced marker expression in day 21 EBs compared to day 14 EBs (Bhattacharya et al., 2005). It is possible that the chosen markers may have been expressed in such low levels that they would not be detected by RT-PCR. As a result, quantitative PCR (qPCR) might have been a more appropriate method because it is able to detect low level expression of markers that may not be identified by RT-PCR (Moore et al., 2010). Other assays such as immunocytochemistry have also been used in identifying lineage-specific markers (Thomson et al., 1998c; Reubinoff et al., 2000g; Carpenter et al., 2003). This

chapter has shown that the spontaneous differentiation of hESCs is not an optimal method of assessing their pluripotency. The attempt to perform osteogenic differentiation following current procedures (Bielby et al., 2004a;Cao et al., 2005c) was also unsuccessful, proving that the need for more robust differentiation protocols to be developed. Currently, available osteogenic differentiation methods vary in the number of days that the EBs should be in suspension and in the means that the EBs should be disaggregated.

All post-thaw analyses were carried out on SHEF3 cells due to contamination of RH1 cells in culture which meant there were not enough cells to carry out required assays. Hence, post-thaw results cannot be compared between hESC lines for lack of necessary data. After undergoing freeze-thaw in each CPA, the morphology of SHEF3 cells compared to conventional hESC morphology (Thomson et al., 1998b;Reubinoff et al., 2000h;Ellerstrom et al., 2006b), with each colony possessing an undifferentiated core and differentiated cells on the periphery. Colony scoring was not performed due to the variability in the size of colonies even when similar cell numbers are replated from a single cell suspension. Ji and colleagues found that colony size varied by as much as a factor of three (Ji et al., 2004e). The cryopreservation of cell clusters or clumps has also been found to generate colonies of different sizes because some clumps divide into smaller clumps during the freeze-thaw process (Hunt and Timmons, 2007). Advances to generate uniform sized colonies are existent where hESCs are propagated by plating single cell suspensions on micropatterned extracellular matrix islands (Peerani et al., 2007b;Bauwens et al., 2008). It has been found that colony size is involved in maintaining an undifferentiated phenotype in hESCs (Peerani et al., 2007a). Larger colonies, which have higher cell densities than smaller colonies, maintained an undifferentiated state by suppressing activation of SMAD1 (see section 1.5.3 that describes activation of SMAD2/3 maintains pluripotency) (Peerani et al., 2007c). It may therefore be possible to identify undifferentiated colonies by measuring their sizes. Additionally, the length of time allowed before passaging may be determined in order to avoid hESC colonies from differentiating and ensuring the replating of undifferentiated colonies. Although the effect of PG and Me<sub>2</sub>SO on hESC proliferation may be determined as a result of colony scoring, it does not necessarily provide information on the phenotype of the colonies because sections of undifferentiated colonies have been found to contain differentiated cells (Ware et al., 2005a;Ha et al., 2005c).

Several cryopreservation studies involving hESCs have therefore utilised colony morphology only as part of evaluating cryopreservation methods (Reubinoff et al., 2001f;Zhou et al., 2004a;Wu et al., 2005b;Ha et al., 2005d;Li et al., 2008h). The

subjectivity of identifying cells which are undifferentiated, therefore, required more tests to be performed in this study to ensure that the cells possessed pluripotency markers such as SSEA4, TRA-1-60 and TRA-1-81. Similar tests have been used in other cryopreservation studies to prove the undifferentiated state of hESC lines (Reubinoff et al., 2001g;Wu et al., 2005a). SHEF3 cells maintained expression of earlier mentioned markers, identifying the cells as a pluripotent population, which suggests that the appropriate concentration of either PG or Me<sub>2</sub>SO does not affect expression of surface markers. Yet other studies have carried out karyotype analysis in order to detect chromosomal changes as a result of cryopreservation methods with many finding no abnormal changes (normal karyotype, diploid) (Richards et al., 2004a;Ji et al., 2004f;Wu et al., 2005f;Martin-Ibanez et al., 2008d). Chromosomal changes have been observed in long-term culture of hESCs where there has been a gain of chromosome 17q and 12 (Draper et al., 2004). It has been suggested that the gain of chromosome 17q may confer proliferative advantage on hESCs by inhibiting apoptosis and differentiation through the expression of inhibitor genes which lie on the chromosome (Chiou et al., 2003). Chromosome 12 has been shown to be associated with Nanog in mESCs (Chambers et al., 2003) and hECs (Mostert et al., 1998). Although karyotype analysis was not performed in this study, it may influence the choice of CPA used in cryopreservation based on its effect on phenotype and proliferation.

This chapter showed SHEF3 possessed an undifferentiated phenotype after freeze-thaw, but a more definitive evaluation of cell survival was determined by carrying out an apoptotic assay using PI and annexin V conjugated with FITC. Assessment of apoptotic and necrotic events showed that cell death by necrosis was generally lower than by apoptosis, an agreement with published data by Heng et al, which stated that loss of viability during freeze-thaw was due to apoptosis rather than necrosis (Heng et al., 2006a). Apoptosis was assessed by terminal deoxynucleotidyl transferase (Tdt)-mediated dUTP nick-end-labeling (TUNEL) assay which detects apoptosis-induced fragmentation of nuclear DNA (Heng et al., 2006e). Baust and colleagues also found that loss of viability of peripheral blood mononuclear cells (PBMCs) was largely due to apoptotic events (Baust et al., 2007b).

Interestingly, this PhD study found early apoptotic cells which were only positive for annexin V in cells cryopreserved with PG, suggesting that these cells could have apoptosed if more time was allowed before analysis. A study by Baust and colleagues showed that though PBMCs were 80-90% viable immediately post-thaw, further incubation at 37°C resulted in significant decline in viability due to increase in necrotic and apoptotic events in the cells but more largely due to apoptosis (Baust et al., 2007a). This discovery of early apoptotic cells may provide an explanation for why the

toxicity assay in chapter 4 showed a higher percentage of cell numbers for SHEF3 in 10%PG than in 10%Me<sub>2</sub>SO. Although there were no significant differences in the number of necrotic and apoptotic cells between cells frozen in 10%PG or in 10%Me<sub>2</sub>SO, the presence of early apoptotic cells in 10%PG confirms that Me<sub>2</sub>SO remains the optimal CPA for SHEF3 cells and produced more viable cells. Other studies have measured cell viability by trypan blue exclusion (Reubinoff et al., 2001h;Baust, 2002a;Martin-Ibanez et al., 2008c;Mollamohammadi et al., 2009b), counting cells that exclude the dye on a haemocytometer. It is not an optimal assay because it does not discriminate between cells which have membrane damage from cells which are necrotic and can no longer proliferate. The analysis of necrotic cells by the trypan blue method is also skewed and based on the individual carrying out the analysis. Using the annexin V dye to distinguish between necrotic cells and apoptotic cells is a better means of analysis. A study by Li and colleagues used Annexin V-FITC to detect apoptosis in single cell suspensions of hESCs which had undergone five rounds of freeze-thaw (Li et al., 2008b). hESCs cryopreserved in medium supplemented with Rho-associated kinase inhibitor (ROCK) were found to produce more colonies and proliferated at a faster rate than hESCs frozen without the ROCK inhibitor (Li et al., 2008a). The results of cell survival in this chapter agree with earlier results of toxicity assays previously discussed in chapter 4, which indicated the use of 10% Me<sub>2</sub>SO as the optimal CPA concentration to be applied for cryopreservation of RH1 and SHEF3. Moreover, the shorter time period required for the addition and elution of Me<sub>2</sub>SO at RT, determined by theoretical modelling also demonstrated best methods because hESCs would have shorter exposure times to Me<sub>2</sub>SO than to PG. The measure of apoptotic events in the cells was evaluated to ensure and provide additional evidence that the designed cryopreservation protocols were more optimal by producing significantly higher numbers of undamaged cells than the cells cryopreserved under the conventional protocol.

This chapter highlights the importance of using an optimised cryopreservation protocol for the storage of hESCs. First, it proves that the cryopreservation and CPA removal protocols designed in this work maintained the expression of pluripotent markers TRA-1-60, TRA-1-81 and SSEA4 in the hESCs. Secondly, this chapter provides an optimised cryopreservation method using Me<sub>2</sub>SO which has not been published before. Post-thaw analysis of the cells indicated significantly higher post-thaw recovery in cells cryopreserved using the designed protocol for 10% Me<sub>2</sub>SO than the unoptimised protocol for adding 10% Me<sub>2</sub>SO. It is important to note that Me<sub>2</sub>SO has been shown to cause differentiation in hESCs through the loss of Oct4 expression (Katkov et al., 2006f), but it has not been concluded that the lack of expression of this marker is necessarily related to the loss of pluripotency.

In conclusion, knowledge of the biophysical properties of hESCs has enabled the design of a cryopreservation protocol which considers and minimises damage that each parameter for cryopreservation may induce. As a result, better post-thaw results were produced than current slow cool methods. Following the freeze-thaw process using the designed cryopreservation procedures in this chapter, the hESCs showed expression of pluripotent markers, high cell viability, and the ability to form EBs.

# **Chapter 6**

## **GENERAL DISCUSSION**

The pluripotency of hESCs makes them potentially useful for clinical therapies and for basic research, for example, into developmental regulation and onset of disease (Draper and Andrews, 2002; Gerecht-Nir and Itskovitz-Eldor, 2004; Davila et al., 2004). However, a lot more research needs to be carried out. Each stem cell line that has been derived requires a storage method in order for expansion to occur. Cryopreservation is one such method where hESCs can be stored and resurrected when required. As a result, many studies have been performed to find the optimal cryopreservation method for hESCs (Katkov et al., 2006g; Li et al., 2008j). This work offers a different perspective in such research by providing the fundamental properties of hESCs which are necessary to design an optimal cryopreservation protocol. This is the first time a systematic approach has been applied to the research of hESC cryopreservation.

## 6.1 Challenges

The first challenge in carrying out this cryopreservation study was the colony-forming nature of hESCs *in vitro* since single cell suspensions were required in order to establish biophysical properties of the cells. Gap junction proteins such as Connexin 43 and 45 (Wong et al., 2004; Huettner et al., 2006) have been found in hESCs and are required for electrical and chemical signals to be passed from one cell to another within a colony. These gap junctions have been shown to be necessary for the maintenance of pluripotency in mouse (Egashira et al., 2004) and human ESCs (Carpenter et al., 2004; Wong et al., 2004). They are also involved in maintaining self-renewal properties in somatic cells such as neural stem cells (Cai et al., 2004) and mesenchymal stem cells (Valiunas et al., 2004; Lin et al., 2007). There is, therefore, a risk of differentiation when hESC colonies are disaggregated into single cells. However, evidence exists in published literature for successful dissociation of hESCs into single cells which possessed high replating efficiency and maintained an undifferentiated state in sub-culture populations (Hasegawa et al., 2006c; Ellerstrom et al., 2007a). As a result, each hESC line used in this study was dissociated into single cells before each assay was carried out.

Although single cell dissociation of hESCs is now routinely carried out for many hESC lines, dissociation-induced apoptosis should be considered because Ohgushi and colleagues showed that the loss of E-cadherin-dependent intercellular contact in hESC colonies activates Rho proteins which are regulators of apoptosis (Ohgushi et al., 2010c). Since Rho-dependent protein kinase (ROCK) induces apoptosis in hESCs, ROCK inhibitors have been added to culture media to improve plating efficiency and even cryopreservation media to improve cell survival. ROCK inhibitors were not added

to any of the media used in culturing or cryopreserving hESCs in this study, but may prove beneficial to hESCs which are cryopreserved using the designed protocol developed in this work.

Another challenge in this study was the use of MEF feeders to subculture each hESC line. Although feeder-free hESC culture existed, it was not well-established at the beginning of this study and problems existed such as an adaptation period that had to be allowed for the cells to adjust when transferred from a feeder layer to feeder-free system (Xu et al., 2001c; Rosler et al., 2004a; Amit and Itskovitz-Eldor, 2006; Mallon et al., 2006). Consequently, hESC populations used in our study were a heterogeneous population of hESCs and some MEFs. As a result, modal values for cell volume were used rather than mean values because mode has been shown to be unaffected by outlying data when there is a broad distribution of data (Pegg and Lancaster, 1998). Modal values represent the most frequently occurring cell volumes during measurement which are more representative of the cell population.

## 6.2 Achievements

The hEC line, 2102Ep, was used in preliminary experiments due to its expression of similar surface markers to RH1 and SHEF3. This PhD study identified that 2102Ep possessed similarities in biophysical properties to hESCs. The biophysical and gene expression data were evidence that not only can 2102Ep be used as a reference cell line for biochemical study of hESCs (Josephson et al., 2007) but can also be employed for cryopreservation studies.

Although differences were discovered in biophysical data established for RH1 and SHEF3, there were similarities in membrane permeability values to those of human spermatozoa and human oocytes (Gilmore et al., 1995d; Paynter et al., 1999d) which may indicate that cells from the same species may be categorised into a set range of values for  $L_p$  and  $P_s$ . However, further studies to acquire biophysical data for every hESC line derived are required and should be documented to assess the variation in permeability to water and CPAs.

It was clear that the cell populations used in the assays performed had pluripotent characteristics from the surface marker expressions of each hESC line. RH1 and SHEF3 expressed characteristic markers before and after freezing using the slow cool method designed in this work. Similar to this study, post-thaw characterisation of the undifferentiated state of hESCs has been carried out using flow cytometry to analyse their expression of cell surface markers such as SSEA4, TRA-1-60 and TRA-1-81 (Martin-Ibanez et al., 2008b; Li et al., 2008g; Amps et al., 2010). However, a real-time

PCR analysis of the level of expression of each gene would provide information on whether the genes were up or down-regulated compared to cells under the conventional cooling protocol. Proteomic analysis has been employed to analyse oocyte proteins which were either up or down-regulated after the freeze-thaw process (Larman et al., 2007a). This method of analysis may identify the difference in the level of protein expression between hESCs before and after freezing and provide more information on the effect of PG and Me<sub>2</sub>SO on gene expression. Although PG and Me<sub>2</sub>SO did not affect surface marker expression of SHEF3, earlier chapters have shown that PG induces osmotic stress to the cells and also requires much longer equilibration periods than Me<sub>2</sub>SO. In a comparative study by Katkov and colleagues, ethylene glycol (EG) was found to maintain pluripotency similarly to Me<sub>2</sub>SO but better than PG, and was also found to be less toxic than both PG and Me<sub>2</sub>SO (Katkov et al., 2011). 10% was chosen for the concentration of EG used in the study because conventional slow cooling protocols for hESCs use 10% Me<sub>2</sub>SO (Katkov et al., 2011). Another study has shown the possibility of hESC cryopreservation without using Me<sub>2</sub>SO (Nishigaki et al., 2009). Instead, a combination of 40% (v/v) EG and 10% (v/v) PEG was used to cryopreserve the Japanese hESC line, Khes1, resulting in higher cell recovery compared to the cells that were preserved with cryoprotective medium containing Me<sub>2</sub>SO (Nishigaki et al., 2009). This study has shown that an investigation into the CPA permeability into hESC membranes and a toxicity assay would provide more certain results of the optimal concentration and mode of addition and removal of CPA to/from hES cells.

The aim of this work was not only to design an optimal cryopreservation protocol for hESCs, but also to contrast the difference between adopting a trial and error approach and a systematic approach. Based on the CPAs tested, results achieved showed that 10% Me<sub>2</sub>SO remains an optimal concentration and 1°C/min an optimal cooling rate for slow cooling of hESCs which are similar to conventional protocols. More importantly, this study showed a distinct difference in the mode of CPA addition and elution between each hESC line. For RH1, a single step addition of 10% Me<sub>2</sub>SO and three step elution were most suitable, while a four step addition and removal method were the optimal protocols for SHEF3 cells. Further analysis of the effect of CPA on apoptotic events in SHEF3 cells showed the highest occurrence in cells cryopreserved using conventional protocols compared to the designed protocols. The designed protocol for 10% Me<sub>2</sub>SO produced the lowest numbers of apoptotic cells, which supports earlier findings that it is a better CPA than PG.

Many studies exist which have taken different approaches to optimise cryopreservation procedures for various cell types. A theoretical approach based on computer

simulations or mathematical formulae has been applied to spermatozoa, peripheral blood HPCs and umbilical cord blood (Tijssen et al., 2000; Hunt et al., 2003a; Woods et al., 2003b; Woelders and Chaveiro, 2004) while an empirical or 'trial and error' approach was taken for optimising hESC cryopreservation methods (Chan and Evans, 1991a; Chen et al., 2009a; Mollamohammadi et al., 2009a; Amps et al., 2010) produced better results than existent protocols. However, this study combined the use of a theoretical approach using of the 2 parameter formula to determine osmotic properties of hESCs, and an empirical approach by choosing two commonly used CPAs and carrying out timecourse responses of the cells to each using a time period of 5 minutes.

The work in this thesis presents novel data because none of the cryopreservation variables have been determined for any of the hESC lines currently available. Determination of physical parameters and tests of functionality produced a more optimal cryopreservation protocol for hESCs than the conventional or less optimised protocol, hence proving the hypothesis. It should become routine practice that the biophysical data for each hESC line be determined as part of the characterisation process.

### **6.3 Future Work**

The designed protocols in this study have shown that damage to hESCs is significantly minimised compared to currently used cryopreservation protocols. However, there are possible ways to further optimise the final protocols designed for RH1 and SHEF3 in this study such as investigating warming rates and adding caspase inhibitors to cryopreservation and thawing media. More differentiation protocols also need to be tested and modified accordingly in order to successfully achieve directed differentiation. Additionally, knowledge of the role of aquaporins in solute transport may be useful in the selection of CPAs that can be used for cryopreserving various hESCs.

#### *6.3.1 Warming rate experiments*

Experiments studying the effect of various warming rates will be valuable due to their role in recrystallisation which was previously discussed in the introductory chapter. Although cooling rates were investigated in this study, the frozen cells were warmed in a 37°C water bath which was assumed to provide rapid warming that will avoid the occurrence of recrystallisation. It has been stated that this method of warming thawed frozen cells equates to a rate of  $120^{\circ}\text{C} \pm 7^{\circ}\text{C}/\text{min}$  (Hunt et al., 2003b). However, using a cryomicroscope to visualise the events occurring during thaw may result in the choice of a more optimal warming rate. The effect of cooling and warming rates have been tested on the survival of hamster tissue culture cells (Mazur et al., 1969b), porcine and

bovine embryos (Hochi et al., 1996a; Sanchez-Osorio et al., 2010), human erythrocytes (Pegg et al., 1984b) and human spermatozoa (Henry et al., 1993).

### 6.3.2 Addition of caspase inhibitors to optimised CPA media

The Annexin-V results showed that both designed protocols using PG and Me<sub>2</sub>SO produced fewer numbers of necrotic and apoptotic cells post-thaw than the unoptimised cryopreservation protocol. In the future, therefore, caspase inhibitors can be incorporated in the designed cryopreservation procedure in order to enhance survival because they have been shown to reduce the occurrence of apoptosis and also differentiation (Watanabe et al., 2007a; Van Hoof et al., 2008a; Martin-Ibanez et al., 2008a; Li et al., 2008f; Claassen et al., 2009e).

### 6.3.3 Improvement of differentiation protocols

The formation of EBs prior to performing directed differentiation has been used as an assay for the pluripotency of hESCs (Itskovitz-Eldor et al., 2000a; Conley et al., 2004a; Bhattacharya et al., 2005) but attempts to differentiate hESCs into osteogenic cells following EB formation were unsuccessful despite using available differentiation protocols. Another possible differentiation assay is cardiomyocyte differentiation which is also not reproducible as it is partly dependent on the occurrence of spontaneous events. EBs are cultured for several days in suspension before being plated onto gelatinised tissue culture dishes for 2-3 weeks; the dishes are then searched for beating areas which are only present in 8-25% of EBs (Passier and Mummery, 2005a); this process is time-consuming. Yet there are other protocols which introduce bone morphogenic protein-2 (BMP-2) in day 30 EBs (Kim et al., 2008d) or BMP-4 to day 4 EBs (Takei et al., 2009). Mummery and colleagues have also developed cardiomyocytes through the co-culture of EBs with visceral-endoderm-like cells from mice (Mummery et al., 2003b). Better assays for hESC differentiation need to be developed that will be reproducible in different laboratories and produce a uniform outcome.

An *in vivo* assay where hESCs are injected into severe combined immunodeficient (SCID) mice and induce teratoma formation is a true test of pluripotency, which has been performed in many studies involving hESCs (Thomson et al., 1998a; Xu et al., 2001d; Reubinoff et al., 2001i; Zhou et al., 2004d; Li et al., 2010a). The resulting teratomas have been found to contain cells representing the three germ layers.

### 6.3.4 Expression of aquaporins on hESC membranes

Additional data that may be worth investigating in order to improve the optimisation process of a cryopreservation protocol is determining which aquaporins are embedded in the plasma membrane of cells. Aquaporins were first detected on the plasma membrane of human erythrocytes as proteins which aided water transport (Agre et al., 1993b). There are several aquaporins, among which is aquaporin 3 (AQP3) which has been found to transport both water and CPAs in xenopus oocyte and mouse morulae (Yamaji et al., 2006b;Edashige et al., 2007b). In mouse morulae, glycerol and ethylene glycol were found to be transported by AQP3 (Edashige et al., 2007c), while Yamaji and colleagues showed that AQP3 not only transports glycerol and ethylene glycol but also acetamide, PG and Me<sub>2</sub>SO in xenopus oocytes (Yamaji et al., 2006c). However, the transport of Me<sub>2</sub>SO was not as efficient in xenopus oocytes as for the other CPAs (Yamaji et al., 2006d). It is therefore possible that aquaporins may be involved in the movement of solutes across the membranes of hEC cells and hESCs. If this is true, then any damage to the aquaporins will affect the length of time it takes for the cells to equilibrate and may explain why some of the cells in the experiments described in Chapter 3 did not regain their original cell volume. Although  $L_p$  and  $P_s$  values provide information about cell membrane permeability, the mechanism by which water and solutes traverse the membrane is unknown. The presence of an additional protein for the transport of CPAs and water may also affect the type of CPA used in cryopreservation as every CPA will vary in molecular weight; larger molecules may require a carrier protein to traverse the plasma membrane.

## 6.4 Study conclusion

The *in vitro* propagation of RH1 and SHEF3 in this study involved the use of animal components such as MEF feeders and cryopreservation medium containing FCS, which restricts the hESC lines to research purposes alone. However, alternative use of xenogeneic-free cultures (Stojkovic et al., 2005b;Inzunza et al., 2005e;Mallon et al., 2006) and autogenic feeders (hESC-derived fibroblasts) (Stojkovic et al., 2005c;Chen et al., 2009b) will render these hESC lines more clinically applicable. Designed protocols for RH1 and SHEF3 developed in this study can therefore be used in cryopreserving potential hESC lines for therapeutic purposes.

The UK stem cell bank (UKSCB) which acts as a depository and a centre for standardising protocols pertaining to hESCs will also benefit from the design of an optimised cryopreservation protocol because it will not only improve current storage methods but will advance the use of uniform protocols between recipient laboratories. Each hESC line sent out from the UKSCB is accompanied with protocols for its

---

propagation and cryopreservation. As a result, a more optimal cryopreservation protocol will reduce the delay that can be caused by several unsuccessful attempts to resurrect hESCs after receipt of cells from the UKSCB.

In conclusion, it is clear that investigating the fundamental biophysical properties of cells is beneficial and essential for the design of an optimal cryopreservation protocol. All of the results indicate that the designed protocols allowed the effective storage of a single cell suspension of hESCs. The protocols also produced hESCs which maintained their expression of pluripotent markers and a lower percentage of necrotic and apoptotic cells than that of the unoptimised protocol currently used to freeze hESCs. A systematic approach to the design of a cryopreservation procedure, therefore, is crucial for the survival of hESCs. Further research into other cell membrane properties such as the composition of aquaporins, and the addition of caspase inhibitors to cryoprotective medium will enhance cell survival.

**Optimal cryopreservation protocol designed for SHEF3 and RH1****Freezing SHEF3 using 10% Me<sub>2</sub>SO as a cryoprotectant.**

1. Add cryoprotectant in increments of 2.5% allowing cells to equilibrate for 18 minutes.
2. Transfer cells into a cryovial.
3. Place cryovial into a rate-controlled freezer and set cooling rate to 1°C/min. Cool cells to -50°C and transfer into a liquid nitrogen dewar.

**Thawing SHEF3 frozen in 10% Me<sub>2</sub>SO**

1. Add medium containing 2% mannitol to dilute the concentration to 5% Me<sub>2</sub>SO. Then carry out subsequent dilutions until the concentration is 1.25% (each dilution step should reduce CPA concentration to half the initial concentration). Allow 35 minutes after for first step and 15 minutes for subsequent steps for cells to equilibrate.
2. Pellet the cells by centrifuging at 1200rpm for 5 minutes.
3. Resuspend cells in growth medium.

**Freezing RH1 using 10% Me<sub>2</sub>SO as a cryoprotectant.**

1. Add 10% Me<sub>2</sub>SO to the cells allowing an equilibration period of 4 minutes.
2. Transfer cells into a cryovial.
3. Place cryovial into a rate-controlled freezer and set cooling rate to 1°C/min. Cool cells to -50°C and transfer into a liquid nitrogen dewar.

**Thawing RH1 frozen in 10% Me<sub>2</sub>SO**

1. Add medium containing 2% mannitol to dilute the concentration to 5% Me<sub>2</sub>SO. Then carry out subsequent dilutions until the concentration is 2.5% (each dilution step should reduce CPA concentration to half the initial concentration). Allow 4 minutes for cells to equilibrate after each dilution step.
2. Pellet the cells by centrifuging at 1200rpm for 5 minutes.
3. Resuspend cells in growth medium.

---

**Abbreviations**

°C	degree Celsius
AQP	Aquaporin
bFGF	Basic fibroblast growth factor
BMP	Bone morphogenic protein
bp	base pair
BSA	Bovine serum albumin
CPA	Cryoprotectant
DAPI	4',6-diamidino-2-phenylindole
DIA	Differentiation inhibiting activity
DMEM	Dulbecco's Modified Eagle's medium
EB	Embryoid body
EC	Embryonal carcinoma
ECM	Extracellular matrix
FADD	Fas-associated death domain
FBS	Fetal bovine serum
FGF	Fibroblast growth factor
FTIR	Fourier transform infrared spectroscopy
HEPES	4-(2-hydroxyethyl)-1-piperazineethanesulfonic acid
hESC	Human embryonic stem cells
HPC	Haematopoietic progenitor cell
HSC	Haematopoietic stem cell
ICM	Inner cell mass
IIF	Intracellular ice formation

---

iPSC	Induced pluripotent stem cell
IVF	<i>In vitro</i> fertilisation
JAK	Janus family tyrosine kinases
LIF	Leukaemia inhibitory factor
$L_p$	Hydraulic conductivity
LPT	Lipid-phase transition
MDCK	Madin-Darby canine kidney
$Me_2SO$	Dimethyl sulfoxide
MEF	Mouse embryonic fibroblast
MTT	3-(4,5-dimethylthazol-2-yl)-2,5-diphenyl tetrazolium bromide
PBS	Phosphate buffered saline
PBS <sup>+</sup>	Phosphate buffered saline with bovine serum albumin
PG	Propylene glycol
$P_s$	Solute permeability
rpm	Rotations per minute
RT	Room temperature
S/V	Surface to volume ratio
SEM	Standard error of mean
T <sub>g</sub>	Glass transition temperature
UKSCB	UK Stem Cell Bank
$V_b$	Non-osmotic volume
$\Pi$	pi
$\chi^2$	Chi square

## References

1. Abrahamsen, J.F., A.M.Bakken, and O.Bruserud. 2002b. Cryopreserving human peripheral blood progenitor cells with 5-percent rather than 10-percent DMSO results in less apoptosis and necrosis in CD34+ cells. *Transfusion* 42:1573-1580.
2. Abrahamsen, J.F., A.M.Bakken, and O.Bruserud. 2002a. Cryopreserving human peripheral blood progenitor cells with 5-percent rather than 10-percent DMSO results in less apoptosis and necrosis in CD34+ cells. *Transfusion* 42:1573-1580.
3. Abrahamsen, J.F., L.Rusten, A.M.Bakken, and O.Bruserud. 2004. Better preservation of early hematopoietic progenitor cells when human peripheral blood progenitor cells are cryopreserved with 5 percent dimethylsulfoxide instead of 10 percent dimethylsulfoxide. *Transfusion* 44:785-789.
4. Acker, J.P., A.Larese, H.Yang, A.Petrenko, and L.E.McGann. 1999. Intracellular Ice Formation Is Affected by Cell Interactions. *Cryobiology* 38:363-371.
5. Acker, J.P. and L.E.McGann. 2000a. Cell-Cell Contact Affects Membrane Integrity after Intracellular Freezing. *Cryobiology* 40:54-63.
6. Acker, J.P. and L.E.McGann. 2000b. Cell-Cell Contact Affects Membrane Integrity after Intracellular Freezing. *Cryobiology* 40:54-63.
7. Acker, J.P. and L.E.McGann. 2000c. Cell-Cell Contact Affects Membrane Integrity after Intracellular Freezing. *Cryobiology* 40:54-63.
8. Adams, S.L., F.W.Kleinhans, P.V.Mladenov, and P.A.Hessian. 2003. Membrane permeability characteristics and osmotic tolerance limits of sea urchin (*Evechinus chloroticus*) eggs. *Cryobiology* 47:1-13.
9. Adewumi, O., B.Aflatoonian, L.Ahrlund-Richter, M.Amit, P.W.Andrews, G.Beighton, P.A.Bello, N.Benvenisty, L.S.Berry, S.Bevan, B.Blum, J.Brooking, K.G.Chen, A.B.Choo, G.A.Churchill, M.Corbel, I.Damjanov, J.S.Draper, P.Dvorak, K.Emanuelsson, R.A.Fleck, A.Ford, K.Gertow, M.Gertsenstein, P.J.Gokhale, R.S.Hamilton, A.Hampl, L.E.Healy, O.Hovatta, J.Hyllner, M.P.Imreh, J.Itskovitz-Eldor, J.Jackson, J.L.Johnson, M.Jones, K.Kee, B.L.King, B.B.Knowles, M.Lako, F.Lebrin, B.S.Mallon, D.Manning, Y.Mayshar, R.D.McKay, A.E.Michalska, M.Mikkola, M.Mileikovsky, S.L.Minger, H.D.Moore, C.L.Mummery, A.Nagy, N.Nakatsuji, C.M.O'Brien, S.K.Oh, C.Olsson, T.Otonkoski, K.Y.Park, R.Passier, H.Patel, M.Patel, R.Pedersen, M.F.Pera, M.S.Piekarczyk, R.A.Pera, B.E.Reubinoff, A.J.Robins, J.Rossant, P.Rugg-Gunn, T.C.Schulz, H.Semb, E.S.Sherrer, H.Siemen, G.N.Stacey, M.Stojkovic, H.Suemori, J.Szatkiwicz, T.Turetsky, T.Tuuri, B.S.van den, K.Vintersten, S.Vuoristo, D.Ward, T.A.Weaver, L.A.Young, and W.Zhang. 2007a.

Characterization of human embryonic stem cell lines by the International Stem Cell Initiative. *Nat Biotechnol.* 25:803-816.

10. Adewumi, O., B.Aflatoonian, L.Ahrlund-Richter, M.Amit, P.W.Andrews, G.Beighton, P.A.Bello, N.Benvenisty, L.S.Berry, S.Bevan, B.Blum, J.Brooking, K.G.Chen, A.B.Choo, G.A.Churchill, M.Corbel, I.Damjanov, J.S.Draper, P.Dvorak, K.Emanuelsson, R.A.Fleck, A.Ford, K.Gertow, M.Gertsenstein, P.J.Gokhale, R.S.Hamilton, A.Hampl, L.E.Healy, O.Hovatta, J.Hyllner, M.P.Imreh, J.Itskovitz-Eldor, J.Jackson, J.L.Johnson, M.Jones, K.Kee, B.L.King, B.B.Knowles, M.Lako, F.Lebrin, B.S.Mallon, D.Manning, Y.Mayshar, R.D.McKay, A.E.Michalska, M.Mikkola, M.Mileikovsky, S.L.Minger, H.D.Moore, C.L.Mummery, A.Nagy, N.Nakatsuji, C.M.O'Brien, S.K.Oh, C.Olsson, T.Otonkoski, K.Y.Park, R.Passier, H.Patel, M.Patel, R.Pedersen, M.F.Pera, M.S.Piekarczyk, R.A.Pera, B.E.Reubinoff, A.J.Robins, J.Rossant, P.Rugg-Gunn, T.C.Schulz, H.Semb, E.S.Sherrer, H.Siemen, G.N.Stacey, M.Stojkovic, H.Suemori, J.Szatkiewicz, T.Turetsky, T.Tuuri, B.S.van den, K.Vintersten, S.Vuoristo, D.Ward, T.A.Weaver, L.A.Young, and W.Zhang. 2007b. Characterization of human embryonic stem cell lines by the International Stem Cell Initiative. *Nat Biotechnol.* 25:803-816.
11. Adewumi, O., B.Aflatoonian, L.Ahrlund-Richter, M.Amit, P.W.Andrews, G.Beighton, P.A.Bello, N.Benvenisty, L.S.Berry, S.Bevan, B.Blum, J.Brooking, K.G.Chen, A.B.Choo, G.A.Churchill, M.Corbel, I.Damjanov, J.S.Draper, P.Dvorak, K.Emanuelsson, R.A.Fleck, A.Ford, K.Gertow, M.Gertsenstein, P.J.Gokhale, R.S.Hamilton, A.Hampl, L.E.Healy, O.Hovatta, J.Hyllner, M.P.Imreh, J.Itskovitz-Eldor, J.Jackson, J.L.Johnson, M.Jones, K.Kee, B.L.King, B.B.Knowles, M.Lako, F.Lebrin, B.S.Mallon, D.Manning, Y.Mayshar, R.D.McKay, A.E.Michalska, M.Mikkola, M.Mileikovsky, S.L.Minger, H.D.Moore, C.L.Mummery, A.Nagy, N.Nakatsuji, C.M.O'Brien, S.K.Oh, C.Olsson, T.Otonkoski, K.Y.Park, R.Passier, H.Patel, M.Patel, R.Pedersen, M.F.Pera, M.S.Piekarczyk, R.A.Pera, B.E.Reubinoff, A.J.Robins, J.Rossant, P.Rugg-Gunn, T.C.Schulz, H.Semb, E.S.Sherrer, H.Siemen, G.N.Stacey, M.Stojkovic, H.Suemori, J.Szatkiewicz, T.Turetsky, T.Tuuri, B.S.van den, K.Vintersten, S.Vuoristo, D.Ward, T.A.Weaver, L.A.Young, and W.Zhang. 2007c. Characterization of human embryonic stem cell lines by the International Stem Cell Initiative. *Nat Biotechnol.* 25:803-816.
12. Adewumi, O., B.Aflatoonian, L.Ahrlund-Richter, M.Amit, P.W.Andrews, G.Beighton, P.A.Bello, N.Benvenisty, L.S.Berry, S.Bevan, B.Blum, J.Brooking, K.G.Chen, A.B.Choo, G.A.Churchill, M.Corbel, I.Damjanov, J.S.Draper, P.Dvorak, K.Emanuelsson, R.A.Fleck, A.Ford, K.Gertow, M.Gertsenstein, P.J.Gokhale, R.S.Hamilton, A.Hampl, L.E.Healy, O.Hovatta, J.Hyllner, M.P.Imreh, J.Itskovitz-Eldor, J.Jackson, J.L.Johnson, M.Jones, K.Kee, B.L.King, B.B.Knowles, M.Lako, F.Lebrin, B.S.Mallon, D.Manning, Y.Mayshar, R.D.McKay, A.E.Michalska, M.Mikkola, M.Mileikovsky, S.L.Minger, H.D.Moore, C.L.Mummery, A.Nagy, N.Nakatsuji, C.M.O'Brien, S.K.Oh, C.Olsson, T.Otonkoski, K.Y.Park, R.Passier, H.Patel, M.Patel, R.Pedersen, M.F.Pera, M.S.Piekarczyk, R.A.Pera, B.E.Reubinoff, A.J.Robins, J.Rossant, P.Rugg-Gunn, T.C.Schulz, H.Semb, E.S.Sherrer, H.Siemen, G.N.Stacey, M.Stojkovic, H.Suemori, J.Szatkiewicz, T.Turetsky, T.Tuuri, B.S.van den, K.Vintersten, S.Vuoristo, D.Ward, T.A.Weaver, L.A.Young, and W.Zhang. 2007d. Characterization of human embryonic stem cell lines by the International Stem Cell Initiative. *Nat Biotechnol.* 25:803-816.

13. Adewumi, O., B.Aflatoonian, L.Ahrlund-Richter, M.Amit, P.W.Andrews, G.Beighton, P.A.Bello, N.Benvenisty, L.S.Berry, S.Bevan, B.Blum, J.Brooking, K.G.Chen, A.B.Choo, G.A.Churchill, M.Corbel, I.Damjanov, J.S.Draper, P.Dvorak, K.Emanuelsson, R.A.Fleck, A.Ford, K.Gertow, M.Gertsenstein, P.J.Gokhale, R.S.Hamilton, A.Hampl, L.E.Healy, O.Hovatta, J.Hyllner, M.P.Imreh, J.Itskovitz-Eldor, J.Jackson, J.L.Johnson, M.Jones, K.Kee, B.L.King, B.B.Knowles, M.Lako, F.Lebrin, B.S.Mallon, D.Manning, Y.Mayshar, R.D.McKay, A.E.Michalska, M.Mikkola, M.Mileikovsky, S.L.Minger, H.D.Moore, C.L.Mummery, A.Nagy, N.Nakatsuji, C.M.O'Brien, S.K.Oh, C.Olsson, T.Otonkoski, K.Y.Park, R.Passier, H.Patel, M.Patel, R.Pedersen, M.F.Pera, M.S.Piekarczyk, R.A.Pera, B.E.Reubinoff, A.J.Robins, J.Rossant, P.Rugg-Gunn, T.C.Schulz, H.Semb, E.S.Sherrer, H.Siemen, G.N.Stacey, M.Stojkovic, H.Suemori, J.Szatkiwicz, T.Turetsky, T.Tuuri, B.S.van den, K.Vintersten, S.Vuoristo, D.Ward, T.A.Weaver, L.A.Young, and W.Zhang. 2007e. Characterization of human embryonic stem cell lines by the International Stem Cell Initiative. *Nat Biotechnol.* 25:803-816.
14. Adewumi, O., B.Aflatoonian, L.Ahrlund-Richter, M.Amit, P.W.Andrews, G.Beighton, P.A.Bello, N.Benvenisty, L.S.Berry, S.Bevan, B.Blum, J.Brooking, K.G.Chen, A.B.Choo, G.A.Churchill, M.Corbel, I.Damjanov, J.S.Draper, P.Dvorak, K.Emanuelsson, R.A.Fleck, A.Ford, K.Gertow, M.Gertsenstein, P.J.Gokhale, R.S.Hamilton, A.Hampl, L.E.Healy, O.Hovatta, J.Hyllner, M.P.Imreh, J.Itskovitz-Eldor, J.Jackson, J.L.Johnson, M.Jones, K.Kee, B.L.King, B.B.Knowles, M.Lako, F.Lebrin, B.S.Mallon, D.Manning, Y.Mayshar, R.D.McKay, A.E.Michalska, M.Mikkola, M.Mileikovsky, S.L.Minger, H.D.Moore, C.L.Mummery, A.Nagy, N.Nakatsuji, C.M.O'Brien, S.K.Oh, C.Olsson, T.Otonkoski, K.Y.Park, R.Passier, H.Patel, M.Patel, R.Pedersen, M.F.Pera, M.S.Piekarczyk, R.A.Pera, B.E.Reubinoff, A.J.Robins, J.Rossant, P.Rugg-Gunn, T.C.Schulz, H.Semb, E.S.Sherrer, H.Siemen, G.N.Stacey, M.Stojkovic, H.Suemori, J.Szatkiwicz, T.Turetsky, T.Tuuri, B.S.van den, K.Vintersten, S.Vuoristo, D.Ward, T.A.Weaver, L.A.Young, and W.Zhang. 2007f. Characterization of human embryonic stem cell lines by the International Stem Cell Initiative. *Nat Biotechnol.* 25:803-816.
15. Adhikary, S. and M.Eilers. 2005. Transcriptional regulation and transformation by Myc proteins. *Nat. Rev. Mol. Cell Biol.* 6:635-645.
16. Agca, Y., J.Liu, J.J.McGrath, A.T.Peter, E.S.Critser, and J.K.Critser. 1998. Membrane Permeability Characteristics of Metaphase II Mouse Oocytes at Various Temperatures in the Presence of Me2SO. *Cryobiology* 36:287-300.
17. Agre, P., G.M.Preston, B.L.Smith, J.S.Jung, S.Raina, C.Moon, W.B.Guggino, and S.Nielsen. 1993a. Aquaporin CHIP: the archetypal molecular water channel. *Am. J Physiol* 265:F463-F476.
18. Agre, P., S.Sasaki, and M.J.Chrispeels. 1993b. Aquaporins: a family of water channel proteins. *Am. J Physiol* 265:F461.
19. Akashi, K., D.Traver, T.Miyamoto, and I.L.Weissman. 2000. A clonogenic common myeloid progenitor that gives rise to all myeloid lineages. *Nature* 404:193-197.
20. Ambrosetti, D.C., C.Basilico, and L.Dailey. 1997. Synergistic activation of the fibroblast growth factor 4 enhancer by Sox2 and Oct-3 depends on protein-

- protein interactions facilitated by a specific spatial arrangement of factor binding sites. *Mol. Cell Biol.* 17:6321-6329.
21. Ambrosetti, D.C., H.R.Scholer, L.Dailey, and C.Basilico. 2000. Modulation of the activity of multiple transcriptional activation domains by the DNA binding domains mediates the synergistic action of Sox2 and Oct-3 on the fibroblast growth factor-4 enhancer. *J Biol. Chem.* 275:23387-23397.
  22. Amit, M. and J.Itskovitz-Eldor. 2006. Feeder-Free Culture of Human Embryonic Stem Cells. *In Methods in Enzymology Stem Cell Tools and Other Experimental Protocols.* Irina Klimanskaya and Robert Lanza, editor. Academic Press, 37-49.
  23. Amps, K.J., M.Jones, D.Baker, and H.D.Moore. 2010. In situ cryopreservation of human embryonic stem cells in gas-permeable membrane culture cassettes for high post-thaw yield and good manufacturing practice. *Cryobiology* In Press, Uncorrected Proof.
  24. Ancho doguy, T.J., J.F.Carpenter, J.H.Crowe, and L.M.Crowe. 1992. Temperature-dependent perturbation of phospholipid bilayers by dimethylsulfoxide. *Biochim. Biophys. Acta* 1104:117-122.
  25. Ancho doguy, T.J., A.S.Rudolph, J.F.Carpenter, and J.H.Crowe. 1987c. Modes of interaction of cryoprotectants with membrane phospholipids during freezing. *Cryobiology* 24:324-331.
  26. Ancho doguy, T.J., A.S.Rudolph, J.F.Carpenter, and J.H.Crowe. 1987a. Modes of interaction of cryoprotectants with membrane phospholipids during freezing. *Cryobiology* 24:324-331.
  27. Ancho doguy, T.J., A.S.Rudolph, J.F.Carpenter, and J.H.Crowe. 1987b. Modes of interaction of cryoprotectants with membrane phospholipids during freezing. *Cryobiology* 24:324-331.
  28. Andrews, P.W. 2002a. From teratocarcinomas to embryonic stem cells. *Philos. Trans. R. Soc. Lond B Biol. Sci.* 357:405-417.
  29. Andrews, P.W. 2002b. From teratocarcinomas to embryonic stem cells. *Philos. Trans. R. Soc. Lond B Biol. Sci.* 357:405-417.
  30. Andrews, P.W., G.Banting, I.Damjanov, D.Arnaud, and P.Avner. 1984a. Three monoclonal antibodies defining distinct differentiation antigens associated with different high molecular weight polypeptides on the surface of human embryonal carcinoma cells. *Hybridoma* 3:347-361.
  31. Andrews, P.W., I.Damjanov, J.Berends, S.Kumpf, V.Zappavigna, F.Mavilio, and K.Sampath. 1994. Inhibition of proliferation and induction of differentiation of pluripotent human embryonal carcinoma cells by osteogenic protein-1 (or bone morphogenetic protein-7). *Lab Invest* 71:243-251.
  32. Andrews, P.W., I.Damjanov, D.Simon, G.S.Banting, C.Carlin, N.C.Dracopoli, and J.Fogh. 1984b. Pluripotent embryonal carcinoma clones derived from the

- human teratocarcinoma cell line Tera-2. Differentiation in vivo and in vitro. *Lab Invest* 50:147-162.
33. Andrews, P.W., P.N.Goodfellow, L.H.Shevinsky, D.L.Bronson, and B.B.Knowles. 1982b. Cell-surface antigens of a clonal human embryonal carcinoma cell line: morphological and antigenic differentiation in culture. *Int. J Cancer* 29:523-531.
  34. Andrews, P.W., P.N.Goodfellow, L.H.Shevinsky, D.L.Bronson, and B.B.Knowles. 1982a. Cell-surface antigens of a clonal human embryonal carcinoma cell line: morphological and antigenic differentiation in culture. *Int. J Cancer* 29:523-531.
  35. Arav, A., S.Yavin, Y.Zeron, D.Natan, I.Dekel, and H.Gacitua. 2002. New trends in gamete's cryopreservation. *Mol. Cell Endocrinol.* 187:77-81.
  36. Arav, A., Y.Zeron, S.B.Leslie, E.Behboodi, G.B.Anderson, and J.H.Crowe. 1996. Phase transition temperature and chilling sensitivity of bovine oocytes. *Cryobiology* 33:589-599.
  37. Armitage, W.J. and B.K.Juss. 2003a. Freezing monolayers of cells without gap junctions. *Cryobiology* 46:194-196.
  38. Armitage, W.J. and B.K.Juss. 2003b. Freezing monolayers of cells without gap junctions. *Cryobiology* 46:194-196.
  39. Ashwood-Smith, M.J. 1961. Preservation of mouse bone marrow at -79 degrees C. with dimethyl sulphoxide. *Nature* 190:1204-1205.
  40. Atienza-Samols, S.B. and M.I.Sherman. 1978. Outgrowth promoting factor for the inner cell mass of the mouse blastocyst. *Dev. Biol.* 66:220-231.
  41. Avner, P., D.Arnaud, C.Blaineau, and J.Le Pendu. 1985. Developmentally regulated cell surface structures on mouse and human embryonal carcinoma cell lines. *Cell Differentiation* 17:13-20.
  42. Badcock, G., C.Pigott, J.Goepel, and P.W.Andrews. 1999. The human embryonal carcinoma marker antigen TRA-1-60 is a sialylated keratan sulfate proteoglycan. *Cancer Res.* 59:4715-4719.
  43. Baharvand, H., G.H.Salekdeh, A.Taei, and S.Mollamohammadi. 2010. An efficient and easy-to-use cryopreservation protocol for human ES and iPS cells. *Nat. Protocols* 5:588-594.
  44. Baudot, A., L.Alger, and P.Boutron. 2000. Glass-forming tendency in the system water-dimethyl sulfoxide. *Cryobiology* 40:151-158.
  45. Baudot, A. and V.Odagescu. 2004. Thermal properties of ethylene glycol aqueous solutions. *Cryobiology* 48:283-294.

46. Baust, J.M. 2002a. Molecular Mechanisms of Cellular Demise Associated with Cryopreservation Failure. *Cell Preservation Technology* 1:17-30.
47. Baust, J.M. 2002b. Molecular Mechanisms of Cellular Demise Associated with Cryopreservation Failure. *Cell Preservation Technology* 1:17-30.
48. Baust, J.M., W.Corwin, N.Diaz-Mayoral, H.Cooley, W.Shao, R.Van Buskirk, J.G.Baust, and L.M.Cosentino. 2007b. Influence of storage parameters on the activation of apoptosis and necrosis during peripheral blood mononuclear cell cryopreservation. *Cryobiology* 55:331.
49. Baust, J.M., W.Corwin, N.Diaz-Mayoral, H.Cooley, W.Shao, R.Van Buskirk, J.G.Baust, and L.M.Cosentino. 2007a. Influence of storage parameters on the activation of apoptosis and necrosis during peripheral blood mononuclear cell cryopreservation. *Cryobiology* 55:331.
50. Baust, J.M., R.Van Buskirk, and J.G.Baust. 2002. Gene activation of the apoptotic caspase cascade following cryogenic storage. *Cell Preservation Technology* 1:63-80.
51. Bauwens, C.L., R.Peerani, S.Niebruegge, K.A.Woodhouse, E.Kumacheva, M.Husain, and P.W.Zandstra. 2008. Control of Human Embryonic Stem Cell Colony and Aggregate Size Heterogeneity Influences Differentiation Trajectories. *Stem Cells* 26:2300-2310.
52. Benga, G., O.Popescu, V.Borza, V.I.Pop, A.Muresan, I.Mocsy, A.Brain, and J.M.Wrigglesworth. 1986. Water permeability in human erythrocytes: identification of membrane proteins involved in water transport. *Eur. J Cell Biol.* 41:252-262.
53. Benham, F.J., P.W.Andrews, B.B.Knowles, D.L.Bronson, and H.Harris. 1981. Alkaline phosphatase isozymes as possible markers of differentiation in human testicular teratocarcinoma cell lines. *Dev. Biol.* 88:279-287.
54. Benson, C.T. and J.K.Critser. 1994. Variation of Water Permeability ( $L_p$ ) and Its Activation Energy ( $E_a$ ) among Unfertilized Golden Hamster and ICR Murine Oocytes. *Cryobiology* 31:215-223.
55. Berger, C.N. and K.S.Sturm. 1997. Self renewal of embryonic stem cells in the absence of feeder cells and exogenous leukaemia inhibitory factor. *Growth Factors* 14:145-159.
56. Berger, W.K. and B.Uhrik. 1996. Freeze-induced shrinkage of individual cells and cell-to-cell propagation of intracellular ice in cell chains from salivary glands. *Experientia* 52:843-850.
57. Bernard, A. and B.J.Fuller. 1996. Cryopreservation of human oocytes: a review of current problems and perspectives. *Hum. Reprod Update.* 2:193-207.
58. Bernstine, E.G., M.L.Hooper, S.Grandchamp, and B.Ephrussi. 1973. Alkaline Phosphatase Activity in Mouse Teratoma. *Proceedings of the National Academy of Sciences of the United States of America* 70:3899-3903.

59. Bevington, P.R. 1969. Data reduction and error analysis for the physical sciences. McGraw-Hill, New York.
60. Bhattacharya, B., J.Cai, Y.Luo, T.Miura, J.Mejido, S.N.Brimble, X.Zeng, T.C.Schulz, M.S.Rao, and R.K.Puri. 2005. Comparison of the gene expression profile of undifferentiated human embryonic stem cell lines and differentiating embryoid bodies. *BMC. Dev. Biol.* 5:22.
61. Bielby, R.C., A.R.Boccaccini, J.M.Polak, and L.D.Buttery. 2004b. In vitro differentiation and in vivo mineralization of osteogenic cells derived from human embryonic stem cells. *Tissue Eng* 10:1518-1525.
62. Bielby, R.C., A.R.Boccaccini, J.M.Polak, and L.D.Buttery. 2004c. In vitro differentiation and in vivo mineralization of osteogenic cells derived from human embryonic stem cells. *Tissue Eng* 10:1518-1525.
63. Bielby, R.C., A.R.Boccaccini, J.M.Polak, and L.D.Buttery. 2004a. In vitro differentiation and in vivo mineralization of osteogenic cells derived from human embryonic stem cells. *Tissue Eng* 10:1518-1525.
64. Bobo, C.M.G. 1967. Nonsolvent Water in Human Erythrocytes and Hemoglobin Solutions. *J. Gen. Physiol.* 50:2547-2564.
65. Bongso, A., C.Y.Fong, S.C.Ng, and S.Ratnam. 1994. Isolation and culture of inner cell mass cells from human blastocysts. *Hum. Reprod* 9:2110-2117.
66. Boutron, P. and F.Arnaud. 1984. Comparison of the cryoprotection of red blood cells by 1,2-propanediol and glycerol. *Cryobiology* 21:348-358.
67. Boyer, L.A., T.I.Lee, M.F.Cole, S.E.Johnstone, S.S.Levine, J.P.Zucker, M.G.Guenther, R.M.Kumar, H.L.Murray, R.G.Jenner, D.K.Gifford, D.A.Melton, R.Jaenisch, and R.A.Young. 2005b. Core transcriptional regulatory circuitry in human embryonic stem cells. *Cell* 122:947-956.
68. Boyer, L.A., T.I.Lee, M.F.Cole, S.E.Johnstone, S.S.Levine, J.P.Zucker, M.G.Guenther, R.M.Kumar, H.L.Murray, R.G.Jenner, D.K.Gifford, D.A.Melton, R.Jaenisch, and R.A.Young. 2005a. Core transcriptional regulatory circuitry in human embryonic stem cells. *Cell* 122:947-956.
69. Boyer, L.A., T.I.Lee, M.F.Cole, S.E.Johnstone, S.S.Levine, J.P.Zucker, M.G.Guenther, R.M.Kumar, H.L.Murray, R.G.Jenner, D.K.Gifford, D.A.Melton, R.Jaenisch, and R.A.Young. 2005c. Core transcriptional regulatory circuitry in human embryonic stem cells. *Cell* 122:947-956.
70. Brons, I.G., L.E.Smithers, M.W.B.Trotter, P.Rugg-Gunn, B.Sun, S.Chuva de Sousa Lopes, S.K.Howlett, A.Clarkson, L.hrlund-Richter, R.A.Pedersen, and L.Vallier. 2007. Derivation of pluripotent epiblast stem cells from mammalian embryos. *Nature* 448:191-195.
71. Broxmeyer, H.E., E.F.Srour, G.Hangoc, S.Cooper, S.A.Anderson, and D.M.Bodine. 2003. High-efficiency recovery of functional hematopoietic

- progenitor and stem cells from human cord blood cryopreserved for 15 years. *Proc. Natl. Acad. Sci. U. S. A* 100:645-650.
72. Buchanan, S.S., S.A.Gross, J.P.Acker, M.Toner, J.F.Carpenter, and D.W.Pyatt. 2004. Cryopreservation of stem cells using trehalose: evaluation of the method using a human hematopoietic cell line. *Stem Cells Dev.* 13:295-305.
  73. Cai, J., A.Cheng, Y.Luo, C.Lu, M.P.Mattson, M.S.Rao, and K.Furukawa. 2004. Membrane properties of rat embryonic multipotent neural stem cells. *J Neurochem.* 88:212-226.
  74. Cao, T., B.C.Heng, C.P.Ye, H.Liu, W.S.Toh, P.Robson, P.Li, Y.H.Hong, and L.W.Stanton. 2005d. Osteogenic differentiation within intact human embryoid bodies result in a marked increase in osteocalcin secretion after 12 days of in vitro culture, and formation of morphologically distinct nodule-like structures. *Tissue Cell* 37:325-334.
  75. Cao, T., B.C.Heng, C.P.Ye, H.Liu, W.S.Toh, P.Robson, P.Li, Y.H.Hong, and L.W.Stanton. 2005a. Osteogenic differentiation within intact human embryoid bodies result in a marked increase in osteocalcin secretion after 12 days of in vitro culture, and formation of morphologically distinct nodule-like structures. *Tissue Cell* 37:325-334.
  76. Cao, T., B.C.Heng, C.P.Ye, H.Liu, W.S.Toh, P.Robson, P.Li, Y.H.Hong, and L.W.Stanton. 2005b. Osteogenic differentiation within intact human embryoid bodies result in a marked increase in osteocalcin secretion after 12 days of in vitro culture, and formation of morphologically distinct nodule-like structures. *Tissue Cell* 37:325-334.
  77. Cao, T., B.C.Heng, C.P.Ye, H.Liu, W.S.Toh, P.Robson, P.Li, Y.H.Hong, and L.W.Stanton. 2005c. Osteogenic differentiation within intact human embryoid bodies result in a marked increase in osteocalcin secretion after 12 days of in vitro culture, and formation of morphologically distinct nodule-like structures. *Tissue Cell* 37:325-334.
  78. Carpenter, M.K., E.Rosler, and M.S.Rao. 2003. Characterization and differentiation of human embryonic stem cells. *Cloning Stem Cells* 5:79-88.
  79. Carpenter, M.K., E.S.Rosler, G.J.Fisk, R.Brandenberger, X.Ares, T.Miura, M.Lucero, and M.S.Rao. 2004. Properties of four human embryonic stem cell lines maintained in a feeder-free culture system. *Dev. Dyn.* 229:243-258.
  80. Chambers, I., D.Colby, M.Robertson, J.Nichols, S.Lee, S.Tweedie, and A.Smith. 2003. Functional Expression Cloning of Nanog, a Pluripotency Sustaining Factor in Embryonic Stem Cells. *Cell* 113:643-655.
  81. Chan, S.Y. and M.J.Evans. 1991a. In situ freezing of embryonic stem cells in multiwell plates. *Trends Genet.* 7:76.
  82. Chan, S.Y. and M.J.Evans. 1991c. In situ freezing of embryonic stem cells in multiwell plates. *Trends Genet.* 7:76.

83. Chan, S.Y. and M.J.Evans. 1991b. In situ freezing of embryonic stem cells in multiwell plates. *Trends Genet.* 7:76.
84. Chaveiro, A., J.Liu, S.Mullen, H.Woelders, and J.K.Critser. 2004. Determination of bull sperm membrane permeability to water and cryoprotectants using a concentration-dependent self-quenching fluorophore. *Cryobiology* 48:72-80.
85. Chen, H.F., C.Y.Chuang, Y.K.Shieh, H.W.Chang, H.N.Ho, and H.C.Kuo. 2009b. Novel autogenic feeders derived from human embryonic stem cells (hESCs) support an undifferentiated status of hESCs in xeno-free culture conditions. *Hum. Reprod.* 24:1114-1125.
86. Chen, H.F., C.Y.Chuang, Y.K.Shieh, H.W.Chang, H.N.Ho, and H.C.Kuo. 2009a. Novel autogenic feeders derived from human embryonic stem cells (hESCs) support an undifferentiated status of hESCs in xeno-free culture conditions. *Hum. Reprod.* 24:1114-1125.
87. Chiou, S.K., W.S.Moon, M.K.Jones, and A.S.Tarnawski. 2003. Survivin expression in the stomach: implications for mucosal integrity and protection. *Biochem. Biophys. Res. Commun.* 305:374-379.
88. Claassen, D.A., M.M.Desler, and A.Rizzino. 2009d. ROCK inhibition enhances the recovery and growth of cryopreserved human embryonic stem cells and human induced pluripotent stem cells. *Mol. Reprod Dev.* 76:722-732.
89. Claassen, D.A., M.M.Desler, and A.Rizzino. 2009a. ROCK inhibition enhances the recovery and growth of cryopreserved human embryonic stem cells and human induced pluripotent stem cells. *Mol. Reprod Dev.* 76:722-732.
90. Claassen, D.A., M.M.Desler, and A.Rizzino. 2009b. ROCK inhibition enhances the recovery and growth of cryopreserved human embryonic stem cells and human induced pluripotent stem cells. *Mol. Reprod Dev.* 76:722-732.
91. Claassen, D.A., M.M.Desler, and A.Rizzino. 2009c. ROCK inhibition enhances the recovery and growth of cryopreserved human embryonic stem cells and human induced pluripotent stem cells. *Mol. Reprod Dev.* 76:722-732.
92. Claassen, D.A., M.M.Desler, and A.Rizzino. 2009e. ROCK inhibition enhances the recovery and growth of cryopreserved human embryonic stem cells and human induced pluripotent stem cells. *Mol. Reprod Dev.* 76:722-732.
93. Conley, B.J., J.C.Young, A.O.Trounson, and R.Mollard. 2004a. Derivation, propagation and differentiation of human embryonic stem cells. *The International Journal of Biochemistry & Cell Biology* 36:555-567.
94. Conley, B.J., J.C.Young, A.O.Trounson, and R.Mollard. 2004b. Derivation, propagation and differentiation of human embryonic stem cells. *The International Journal of Biochemistry & Cell Biology* 36:555-567.
95. Conlon, F.L., K.M.Lyons, N.Takaesu, K.S.Barth, A.Kispert, B.Herrmann, and E.J.Robertson. 1994. A primary requirement for nodal in the formation and maintenance of the primitive streak in the mouse. *Development* 120:1919-1928.

96. Cook, J.S. 1967a. Nonsolvent water in human erythrocytes. *J. Gen. Physiol* 50:1311-1325.
97. Cook, J.S. 1967b. Nonsolvent water in human erythrocytes. *J. Gen. Physiol* 50:1311-1325.
98. Damjanov, I., Z.M.Zhu, P.W.Andrews, and B.A.Fenderson. 1994. Embryonal carcinoma cells differentiate into parietal endoderm via an intermediate stage corresponding to primitive endoderm. *In Vivo* 8:967-973.
99. Darr, H., Y.Mayshar, and N.Benvenisty. 2006. Overexpression of NANOG in human ES cells enables feeder-free growth while inducing primitive ectoderm features. *Development* 133:1193-1201.
100. Davila, J.C., G.G.Cezar, M.Thiede, S.Strom, T.Miki, and J.Trosko. 2004. Use and application of stem cells in toxicology. *Toxicol. Sci.* 79:214-223.
101. Dick, D.A.T. 1966. Cell Water. Butterworths, Oxford.
102. Dick, D.A.T. 1969. Osmotic behaviour of hemoglobin in vivo and in vitro. *J. Gen. Physiol.* 53:836-838.
103. Diller, K.R. 1979b. Intracellular freezing of glycerolized red cells. *Cryobiology* 16:125-131.
104. Diller, K.R. 1979a. Intracellular freezing of glycerolized red cells. *Cryobiology* 16:125-131.
105. Diller, K.R. 1979c. Intracellular freezing of glycerolized red cells. *Cryobiology* 16:125-131.
106. Dormeyer, W., H.D.van, S.R.Braam, A.J.Heck, C.L.Mummery, and J.Krijgsveld. 2008. Plasma membrane proteomics of human embryonic stem cells and human embryonal carcinoma cells. *J Proteome. Res.* 7:2936-2951.
107. Dowgert, M.F. and P.L.Steponkus. 1983. Effect of cold acclimation on intracellular ice formation in isolated protoplasts. *Plant Physiol* 72:978-988.
108. Draper, J.S. and P.W.Andrews. 2002. Embryonic stem cells: advances toward potential therapeutic use. *Curr. Opin. Obstet. Gynecol.* 14:309-315.
109. Draper, J.S., K.Smith, P.Gokhale, H.D.Moore, E.Maltby, J.Johnson, L.Meisner, T.P.Zwaka, J.A.Thomson, and P.W.Andrews. 2004. Recurrent gain of chromosomes 17q and 12 in cultured human embryonic stem cells. *Nat. Biotechnol.* 22:53-54.
110. Drobnis, E.Z., L.M.Crowe, T.Berger, T.J.Anchoroguy, J.W.Overstreet, and J.H.Crowe. 1993c. Cold shock damage is due to lipid phase transitions in cell membranes: a demonstration using sperm as a model. *J Exp. Zool.* 265:432-437.

111. Drobnis, E.Z., L.M.Crowe, T.Berger, T.J.Anchoroguy, J.W.Overstreet, and J.H.Crowe. 1993b. Cold shock damage is due to lipid phase transitions in cell membranes: a demonstration using sperm as a model. *J Exp. Zool.* 265:432-437.
112. Drobnis, E.Z., L.M.Crowe, T.Berger, T.J.Anchoroguy, J.W.Overstreet, and J.H.Crowe. 1993a. Cold shock damage is due to lipid phase transitions in cell membranes: a demonstration using sperm as a model. *J Exp. Zool.* 265:432-437.
113. Dumont, F., P.A.Marechal, and P.Gervais. 2004. Cell size and water permeability as determining factors for cell viability after freezing at different cooling rates. *Appl. Environ. Microbiol.* 70:268-272.
114. Edashige, K., S.Ohta, M.Tanaka, T.Kuwano, D.M.Valdez, Jr., T.Hara, B.Jin, S.Takahashi, S.Seki, C.Koshimoto, and M.Kasai. 2007c. The Role of Aquaporin 3 in the Movement of Water and Cryoprotectants in Mouse Morulae. *Biol Reprod* 77:365-375.
115. Edashige, K., S.Ohta, M.Tanaka, T.Kuwano, D.M.Valdez, Jr., T.Hara, B.Jin, S.Takahashi, S.Seki, C.Koshimoto, and M.Kasai. 2007b. The Role of Aquaporin 3 in the Movement of Water and Cryoprotectants in Mouse Morulae. *Biol Reprod* 77:365-375.
116. Edashige, K., S.Ohta, M.Tanaka, T.Kuwano, D.M.Valdez, Jr., T.Hara, B.Jin, S.Takahashi, S.Seki, C.Koshimoto, and M.Kasai. 2007a. The Role of Aquaporin 3 in the Movement of Water and Cryoprotectants in Mouse Morulae. *Biol Reprod* 77:365-375.
117. Edashige, K., M.Sakamoto, and M.Kasai. 2000b. Expression of mRNAs of the aquaporin family in mouse oocytes and embryos. *Cryobiology* 40:171-175.
118. Edashige, K., M.Sakamoto, and M.Kasai. 2000a. Expression of mRNAs of the aquaporin family in mouse oocytes and embryos. *Cryobiology* 40:171-175.
119. Edashige, K., M.Tanaka, N.Ichimar, S.Ota, K.Yazawa, Y.Higashino, M.Sakamoto, Y.Yamaji, T.Kuwano, D.M.Valdez, Jr., F.W.Kleinhans, and M.Kasai. 2006a. Channel-Dependent Permeation of Water and Glycerol in Mouse Morulae. *Biol Reprod* 74:625-632.
120. Edashige, K., M.Tanaka, N.Ichimar, S.Ota, K.Yazawa, Y.Higashino, M.Sakamoto, Y.Yamaji, T.Kuwano, D.M.Valdez, Jr., F.W.Kleinhans, and M.Kasai. 2006b. Channel-Dependent Permeation of Water and Glycerol in Mouse Morulae. *Biol Reprod* 74:625-632.
121. Egashira, K., K.Nishii, K.Nakamura, M.Kumai, S.Morimoto, and Y.Shibata. 2004. Conduction abnormality in gap junction protein connexin45-deficient embryonic stem cell-derived cardiac myocytes. *Anat. Rec. A Discov. Mol. Cell Evol. Biol.* 280:973-979.

122. Ellerstrom, C., R.Strehl, K.Moya, K.Andersson, C.Bergh, K.Lundin, J.Hyllner, and H.Semb. 2006b. Derivation of a xeno-free human embryonic stem cell line. *Stem Cells* 24:2170-2176.
123. Ellerstrom, C., R.Strehl, K.Moya, K.Andersson, C.Bergh, K.Lundin, J.Hyllner, and H.Semb. 2006a. Derivation of a xeno-free human embryonic stem cell line. *Stem Cells* 24:2170-2176.
124. Ellerstrom, C., R.Strehl, K.Noaksson, J.Hyllner, and H.Semb. 2007c. Facilitated Expansion of Human Embryonic Stem Cells by Single-Cell Enzymatic Dissociation. *Stem Cells* 25:1690-1696.
125. Ellerstrom, C., R.Strehl, K.Noaksson, J.Hyllner, and H.Semb. 2007d. Facilitated Expansion of Human Embryonic Stem Cells by Single-Cell Enzymatic Dissociation. *Stem Cells* 25:1690-1696.
126. Ellerstrom, C., R.Strehl, K.Noaksson, J.Hyllner, and H.Semb. 2007b. Facilitated Expansion of Human Embryonic Stem Cells by Single-Cell Enzymatic Dissociation. *Stem Cells* 25:1690-1696.
127. Ellerstrom, C., R.Strehl, K.Noaksson, J.Hyllner, and H.Semb. 2007a. Facilitated Expansion of Human Embryonic Stem Cells by Single-Cell Enzymatic Dissociation. *Stem Cells* 25:1690-1696.
128. Ellington, J.E., J.Samper, A.Jones, S.A.Oliver, K.Burnett, and R.W.Wright. 1999. Effects of bovine serum albumin on function of cryopreserved stallion spermatozoa during medium culture and uterine tube epithelial cell coculture. *Am. J Vet. Res.* 60:363-367.
129. Ema, H. and H.Nakauchi. 2003. Self-renewal and lineage restriction of hematopoietic stem cells. *Current Opinion in Genetics & Development* 13:508-512.
130. Evans, M.J. and M.H.Kaufman. 1981g. Establishment in culture of pluripotential cells from mouse embryos. *Nature* 292:154-156.
131. Evans, M.J. and M.H.Kaufman. 1981f. Establishment in culture of pluripotential cells from mouse embryos. *Nature* 292:154-156.
132. Evans, M.J. and M.H.Kaufman. 1981a. Establishment in culture of pluripotential cells from mouse embryos. *Nature* 292:154-156.
133. Evans, M.J. and M.H.Kaufman. 1981e. Establishment in culture of pluripotential cells from mouse embryos. *Nature* 292:154-156.
134. Evans, M.J. and M.H.Kaufman. 1981c. Establishment in culture of pluripotential cells from mouse embryos. *Nature* 292:154-156.
135. Evans, M.J. and M.H.Kaufman. 1981d. Establishment in culture of pluripotential cells from mouse embryos. *Nature* 292:154-156.

136. Evans, M.J. and M.H.Kaufman. 1981b. Establishment in culture of pluripotential cells from mouse embryos. *Nature* 292:154-156.
137. Fagundez, C.B., M.A.Loresi, Q.M.Ojea, S.M.Delcourt, R.Testa, S.J.Gogorza, and P.F.Argibay. 2009. A simple approach for mouse embryonic stem cells isolation and differentiation inducing embryoid body formation. *Cell Biology International* In Press, Accepted Manuscript.
138. Fahy, G.M., D.R.MacFarlane, C.A.Angell, and H.T.Meryman. 1984. Vitrification as an approach to cryopreservation. *Cryobiology* 21:407-426.
139. Fahy, G.M., B.Wowk, J.Wu, and S.Paynter. 2004. Improved vitrification solutions based on the predictability of vitrification solution toxicity. *Cryobiology* 48:22-35.
140. Fenderson, B.A., P.W.Andrews, E.Nudelman, H.Clausen, and S.Hakomori. 1987. Glycolipid core structure switching from globo- to lacto- and ganglio-series during retinoic acid-induced differentiation of TERA-2-derived human embryonal carcinoma cells. *Dev. Biol.* 122:21-34.
141. Feng, B., J.Jiang, P.Kraus, J.H.Ng, J.C.Heng, Y.S.Chan, L.P.Yaw, W.Zhang, Y.H.Loh, J.Han, V.B.Vega, V.Cacheux-Rataboul, B.Lim, T.Lufkin, and H.H.Ng. 2009. Reprogramming of fibroblasts into induced pluripotent stem cells with orphan nuclear receptor Esrrb. *Nat. Cell Biol.* 11:197-203.
142. Fernandez, P.C., S.R.Frank, L.Wang, M.Schroeder, S.Liu, J.Greene, A.Cocito, and B.Amati. 2003. Genomic targets of the human c-Myc protein. *Genes Dev.* 17:1115-1129.
143. Finch, B.W. and B.Ephrussi. 1967a. Retention of multiple developmental potentialities by cells of a mouse testicular teratocarcinoma during prolonged culture in vitro and their extinction upon hybridization with cells of permanent lines. *Proc. Natl. Acad. Sci. U. S. A* 57:615-621.
144. Finch, B.W. and B.Ephrussi. 1967b. Retention of multiple developmental potentialities by cells of a mouse testicular teratocarcinoma during prolonged culture in vitro and their extinction upon hybridization with cells of permanent lines. *Proc. Natl. Acad. Sci. U. S. A* 57:615-621.
145. Fleming, K.K. and A.Hubel. 2006a. Cryopreservation of hematopoietic and non-hematopoietic stem cells. *Transfusion and Apheresis Science* 34:309-315.
146. Fleming, K.K. and A.Hubel. 2006b. Cryopreservation of hematopoietic and non-hematopoietic stem cells. *Transfusion and Apheresis Science* 34:309-315.
147. Fogh, J. and G.Trempe. 1975. New human tumour cell lines. *In* Human tumour cells in vitro. J.Fogh, editor. New York: Plenum. 115-159.
148. Gao, D.Y., Q.Chang, C.Liu, K.Farris, K.Harvey, L.E.McGann, D.English, J.Jansen, and J.K.Critser. 1998. Fundamental cryobiology of human hematopoietic progenitor cells. I: Osmotic characteristics and volume distribution. *Cryobiology* 36:40-48.

149. Gendall, A.R., A.R.Dunn, and M.Ernst. 1997b. Isolation and characterization of a leukemia inhibitory factor-independent embryonic stem cell line. *Int. J Biochem. Cell Biol.* 29:829-840.
150. Gendall, A.R., A.R.Dunn, and M.Ernst. 1997a. Isolation and characterization of a leukemia inhibitory factor-independent embryonic stem cell line. *Int. J Biochem. Cell Biol.* 29:829-840.
151. Gerecht-Nir, S. and J.Itskovitz-Eldor. 2004. Human embryonic stem cells: a potential source for cellular therapy. *Am. J. Transplant.* 4 Suppl 6:51-57.
152. Gilmore, J.A., L.E.McGann, J.Liu, D.Y.Gao, A.T.Peter, F.W.Kleinhans, and J.K.Critser. 1995a. Effect of cryoprotectant solutes on water permeability of human spermatozoa. *Biol. Reprod.* 53:985-995.
153. Gilmore, J.A., L.E.McGann, J.Liu, D.Y.Gao, A.T.Peter, F.W.Kleinhans, and J.K.Critser. 1995c. Effect of cryoprotectant solutes on water permeability of human spermatozoa. *Biol. Reprod.* 53:985-995.
154. Gilmore, J.A., L.E.McGann, J.Liu, D.Y.Gao, A.T.Peter, F.W.Kleinhans, and J.K.Critser. 1995e. Effect of cryoprotectant solutes on water permeability of human spermatozoa. *Biol. Reprod.* 53:985-995.
155. Gilmore, J.A., L.E.McGann, J.Liu, D.Y.Gao, A.T.Peter, F.W.Kleinhans, and J.K.Critser. 1995b. Effect of cryoprotectant solutes on water permeability of human spermatozoa. *Biol. Reprod.* 53:985-995.
156. Gilmore, J.A., L.E.McGann, J.Liu, D.Y.Gao, A.T.Peter, F.W.Kleinhans, and J.K.Critser. 1995d. Effect of cryoprotectant solutes on water permeability of human spermatozoa. *Biol. Reprod.* 53:985-995.
157. Giorgetti, A., N.Montserrat, T.Aasen, F.Gonzalez, I.Rodr guez-Piz , R.Vassena, A.Raya, S.Bou , M.J.Barrero, B.a.A.Corbella, M.Torrabadella, A.Veiga, and J.C.I.Belmonte. 2009a. Generation of Induced Pluripotent Stem Cells from Human Cord Blood Using OCT4 and SOX2. *Cell Stem Cell* 5:353-357.
158. Giorgetti, A., N.Montserrat, T.Aasen, F.Gonzalez, I.Rodr guez-Piz , R.Vassena, A.Raya, S.Bou , M.J.Barrero, B.a.A.Corbella, M.Torrabadella, A.Veiga, and J.C.I.Belmonte. 2009b. Generation of Induced Pluripotent Stem Cells from Human Cord Blood Using OCT4 and SOX2. *Cell Stem Cell* 5:353-357.
159. Gluckman, E. 2001. Hematopoietic stem-cell transplants using umbilical-cord blood. *N. Engl. J Med.* 344:1860-1861.
160. Grilli, G., A.Porcellini, and G.Lucarelli. 1980a. Role of serum on cryopreservation and subsequent viability of mouse bone marrow hemopoietic stem cells. *Cryobiology* 17:516-520.

161. Grilli, G., A.Porcellini, and G.Lucarelli. 1980b. Role of serum on cryopreservation and subsequent viability of mouse bone marrow hemopoietic stem cells. *Cryobiology* 17:516-520.
162. Gu, Z., E.M.Reynolds, J.Song, H.Lei, A.Feijen, L.Yu, W.He, D.T.MacLaughlin, van den Eijnden-van Raaij, P.K.Donahoe, and E.Li. 1999. The type I serine/threonine kinase receptor ActRIA (ALK2) is required for gastrulation of the mouse embryo. *Development* 126:2551-2561.
163. Guan, M., D.M.Rawson, and T.Zhang. 2008. Cryopreservation of zebrafish (*Danio rerio*) oocytes using improved controlled slow cooling protocols. *Cryobiology* 56:204-208.
164. Gunsilius, E., G.Gastl, and A.L.Petzer. 2001a. Hematopoietic stem cells. *Biomedecine & Pharmacotherapy* 55:186-194.
165. Gunsilius, E., G.Gastl, and A.L.Petzer. 2001b. Hematopoietic stem cells. *Biomedecine & Pharmacotherapy* 55:186-194.
166. Gunsilius, E., G.Gastl, and A.L.Petzer. 2001c. Hematopoietic stem cells. *Biomedecine & Pharmacotherapy* 55:186-194.
167. Ha, S.Y., B.C.Jee, C.S.Suh, H.S.Kim, S.K.Oh, S.H.Kim, and S.Y.Moon. 2005a. Cryopreservation of human embryonic stem cells without the use of a programmable freezer. *Hum. Reprod.* 20:1779-1785.
168. Ha, S.Y., B.C.Jee, C.S.Suh, H.S.Kim, S.K.Oh, S.H.Kim, and S.Y.Moon. 2005b. Cryopreservation of human embryonic stem cells without the use of a programmable freezer. *Hum. Reprod.* 20:1779-1785.
169. Ha, S.Y., B.C.Jee, C.S.Suh, H.S.Kim, S.K.Oh, S.H.Kim, and S.Y.Moon. 2005d. Cryopreservation of human embryonic stem cells without the use of a programmable freezer. *Hum. Reprod.* 20:1779-1785.
170. Ha, S.Y., B.C.Jee, C.S.Suh, H.S.Kim, S.K.Oh, S.H.Kim, and S.Y.Moon. 2005c. Cryopreservation of human embryonic stem cells without the use of a programmable freezer. *Hum. Reprod.* 20:1779-1785.
171. Haase, A., R.Olmer, K.Schwanke, S.Wunderlich, S.Merkert, C.Hess, R.Zweigerdt, I.Gruh, J.Meyer, S.Wagner, L.S.Maier, D.W.Han, S.Glage, K.Miller, P.Fischer, H.R.Schäfer, and U.Martin. 2009b. Generation of Induced Pluripotent Stem Cells from Human Cord Blood. *Cell Stem Cell* 5:434-441.
172. Haase, A., R.Olmer, K.Schwanke, S.Wunderlich, S.Merkert, C.Hess, R.Zweigerdt, I.Gruh, J.Meyer, S.Wagner, L.S.Maier, D.W.Han, S.Glage, K.Miller, P.Fischer, H.R.Schäfer, and U.Martin. 2009a. Generation of Induced Pluripotent Stem Cells from Human Cord Blood. *Cell Stem Cell* 5:434-441.
173. Harris, C.L., M.Toner, A.Hubel, E.G.Cravalho, M.L.Yarmush, and R.G.Tompkins. 1991. Cryopreservation of isolated hepatocytes: intracellular ice formation under various chemical and physical conditions. *Cryobiology* 28:436-444.

174. Hasegawa, K., T.Fujioka, Y.Nakamura, N.Nakatsuji, and H.Suemori. 2006b. A Method for the Selection of Human Embryonic Stem Cell Sublines with High Replating Efficiency After Single-Cell Dissociation. *Stem Cells* 24:2649-2660.
175. Hasegawa, K., T.Fujioka, Y.Nakamura, N.Nakatsuji, and H.Suemori. 2006a. A Method for the Selection of Human Embryonic Stem Cell Sublines with High Replating Efficiency After Single-Cell Dissociation. *Stem Cells* 24:2649-2660.
176. Hasegawa, K., T.Fujioka, Y.Nakamura, N.Nakatsuji, and H.Suemori. 2006c. A Method for the Selection of Human Embryonic Stem Cell Sublines with High Replating Efficiency After Single-Cell Dissociation. *Stem Cells* 24:2649-2660.
177. Healy, L., C.Hunt, L.Young, and G.Stacey. 2005a. The UK Stem Cell Bank: its role as a public research resource centre providing access to well-characterised seed stocks of human stem cell lines. *Adv. Drug Deliv. Rev.* 57:1981-1988.
178. Healy, L., C.Hunt, L.Young, and G.Stacey. 2005b. The UK Stem Cell Bank: its role as a public research resource centre providing access to well-characterised seed stocks of human stem cell lines. *Adv. Drug Deliv. Rev.* 57:1981-1988.
179. Heng, B.C., S.M.Bested, S.H.Chan, and T.Cao. 2005b. A proposed design for the cryopreservation of intact and adherent human embryonic stem cell colonies. *In Vitro Cell Dev. Biol. Anim* 41:77-79.
180. Heng, B.C., S.M.Bested, S.H.Chan, and T.Cao. 2005a. A proposed design for the cryopreservation of intact and adherent human embryonic stem cell colonies. *In Vitro Cell Dev. Biol. Anim* 41:77-79.
181. Heng, B.C., M.V.Clement, and T.Cao. 2007. Caspase inhibitor Z-VAD-FMK enhances the freeze-thaw survival rate of human embryonic stem cells. *Biosci. Rep.* 27:257-264.
182. Heng, B.C., L.L.Kuleshova, S.M.Bested, H.Liu, and T.Cao. 2005c. The cryopreservation of human embryonic stem cells. *Biotechnol. Appl. Biochem.* 41:97-104.
183. Heng, B.C., C.P.Ye, H.Liu, W.S.Toh, A.J.Rufaihah, Z.Yang, B.H.Bay, Z.Ge, H.W.Ouyang, E.H.Lee, and T.Cao. 2006c. Loss of viability during freeze-thaw of intact and adherent human embryonic stem cells with conventional slow-cooling protocols is predominantly due to apoptosis rather than cellular necrosis. *J. Biomed. Sci.* 13:433-445.
184. Heng, B.C., C.P.Ye, H.Liu, W.S.Toh, A.J.Rufaihah, Z.Yang, B.H.Bay, Z.Ge, H.W.Ouyang, E.H.Lee, and T.Cao. 2006f. Loss of viability during freeze-thaw of intact and adherent human embryonic stem cells with conventional slow-cooling protocols is predominantly due to apoptosis rather than cellular necrosis. *J. Biomed. Sci.* 13:433-445.
185. Heng, B.C., C.P.Ye, H.Liu, W.S.Toh, A.J.Rufaihah, Z.Yang, B.H.Bay, Z.Ge, H.W.Ouyang, E.H.Lee, and T.Cao. 2006b. Loss of viability during freeze-thaw of intact and adherent human embryonic stem cells with conventional slow-

- cooling protocols is predominantly due to apoptosis rather than cellular necrosis. *J. Biomed. Sci.* 13:433-445.
186. Heng, B.C., C.P.Ye, H.Liu, W.S.Toth, A.J.Rufaihah, Z.Yang, B.H.Bay, Z.Ge, H.W.Ouyang, E.H.Lee, and T.Cao. 2006d. Loss of viability during freeze-thaw of intact and adherent human embryonic stem cells with conventional slow-cooling protocols is predominantly due to apoptosis rather than cellular necrosis. *J. Biomed. Sci.* 13:433-445.
187. Heng, B.C., C.P.Ye, H.Liu, W.S.Toth, A.J.Rufaihah, Z.Yang, B.H.Bay, Z.Ge, H.W.Ouyang, E.H.Lee, and T.Cao. 2006a. Loss of viability during freeze-thaw of intact and adherent human embryonic stem cells with conventional slow-cooling protocols is predominantly due to apoptosis rather than cellular necrosis. *J. Biomed. Sci.* 13:433-445.
188. Heng, B.C., C.P.Ye, H.Liu, W.S.Toth, A.J.Rufaihah, Z.Yang, B.H.Bay, Z.Ge, H.W.Ouyang, E.H.Lee, and T.Cao. 2006e. Loss of viability during freeze-thaw of intact and adherent human embryonic stem cells with conventional slow-cooling protocols is predominantly due to apoptosis rather than cellular necrosis. *J. Biomed. Sci.* 13:433-445.
189. Henry, M.A., E.E.Noiles, D.Gao, P.Mazur, and J.K.Critser. 1993. Cryopreservation of human spermatozoa. IV. The effects of cooling rate and warming rate on the maintenance of motility, plasma membrane integrity, and mitochondrial function. *Fertil. Steril.* 60:911-918.
190. Higgins, A.Z. 2010a. 30. Mathematical minimization of toxicity during addition and removal of cryoprotectants. *Cryobiology* 61:371.
191. Higgins, A.Z. 2010b. 30. Mathematical minimization of toxicity during addition and removal of cryoprotectants. *Cryobiology* 61:371.
192. Higgins, A.Z. and J.O.M.Karlsson. 2010. Curve fitting approach for measurement of cellular osmotic properties by the electrical sensing zone method. II. Membrane water permeability. *Cryobiology* 60:117-128.
193. Hochi, S., E.Semple, and S.P.Leibo. 1996b. Effect of cooling and warming rates during cryopreservation on survival of in vitro-produced bovine embryos. *Theriogenology* 46:837-847.
194. Hochi, S., E.Semple, and S.P.Leibo. 1996a. Effect of cooling and warming rates during cryopreservation on survival of in vitro-produced bovine embryos. *Theriogenology* 46:837-847.
195. Hubel, A. 1997. Parameters of cell freezing: Implications for the cryopreservation of stem cells. *Transfusion Medicine Reviews* 11:224-233.
196. Huettner, J.E., A.Lu, Y.Qu, Y.Wu, M.Kim, and J.W.McDonald. 2006. Gap junctions and connexon hemichannels in human embryonic stem cells. *Stem Cells* 24:1654-1667.

197. Hunt, C.J. 2007. The Banking and Cryopreservation of Human Embryonic Stem Cells. *Transfusion Medicine and Hemotherapy*.
198. Hunt, C.J., S.E.Armitage, and D.E.Pegg. 2003c. Cryopreservation of umbilical cord blood: 1. Osmotically inactive volume, hydraulic conductivity and permeability of CD34(+) cells to dimethyl sulphoxide. *Cryobiology* 46:61-75.
199. Hunt, C.J., S.E.Armitage, and D.E.Pegg. 2003h. Cryopreservation of umbilical cord blood: 1. Osmotically inactive volume, hydraulic conductivity and permeability of CD34(+) cells to dimethyl sulphoxide. *Cryobiology* 46:61-75.
200. Hunt, C.J., S.E.Armitage, and D.E.Pegg. 2003k. Cryopreservation of umbilical cord blood: 2. Tolerance of CD34(+) cells to multimolar dimethyl sulphoxide and the effect of cooling rate on recovery after freezing and thawing. *Cryobiology* 46:76-87.
201. Hunt, C.J., S.E.Armitage, and D.E.Pegg. 2003a. Cryopreservation of umbilical cord blood: 1. Osmotically inactive volume, hydraulic conductivity and permeability of CD34(+) cells to dimethyl sulphoxide. *Cryobiology* 46:61-75.
202. Hunt, C.J., S.E.Armitage, and D.E.Pegg. 2003b. Cryopreservation of umbilical cord blood: 2. Tolerance of CD34(+) cells to multimolar dimethyl sulphoxide and the effect of cooling rate on recovery after freezing and thawing. *Cryobiology* 46:76-87.
203. Hunt, C.J., S.E.Armitage, and D.E.Pegg. 2003e. Cryopreservation of umbilical cord blood: 1. Osmotically inactive volume, hydraulic conductivity and permeability of CD34(+) cells to dimethyl sulphoxide. *Cryobiology* 46:61-75.
204. Hunt, C.J., S.E.Armitage, and D.E.Pegg. 2003f. Cryopreservation of umbilical cord blood: 1. Osmotically inactive volume, hydraulic conductivity and permeability of CD34(+) cells to dimethyl sulphoxide. *Cryobiology* 46:61-75.
205. Hunt, C.J., S.E.Armitage, and D.E.Pegg. 2003g. Cryopreservation of umbilical cord blood: 1. Osmotically inactive volume, hydraulic conductivity and permeability of CD34(+) cells to dimethyl sulphoxide. *Cryobiology* 46:61-75.
206. Hunt, C.J., S.E.Armitage, and D.E.Pegg. 2003d. Cryopreservation of umbilical cord blood: 1. Osmotically inactive volume, hydraulic conductivity and permeability of CD34(+) cells to dimethyl sulphoxide. *Cryobiology* 46:61-75.
207. Hunt, C.J., S.E.Armitage, and D.E.Pegg. 2003i. Cryopreservation of umbilical cord blood: 1. Osmotically inactive volume, hydraulic conductivity and permeability of CD34(+) cells to dimethyl sulphoxide. *Cryobiology* 46:61-75.
208. Hunt, C.J., S.E.Armitage, and D.E.Pegg. 2003j. Cryopreservation of umbilical cord blood: 1. Osmotically inactive volume, hydraulic conductivity and permeability of CD34(+) cells to dimethyl sulphoxide. *Cryobiology* 46:61-75.
209. Hunt, C.J., D.E.Pegg, and S.E.Armitage. 2006. Optimising cryopreservation protocols for haematopoietic progenitor cells: a methodological approach for umbilical cord blood. *Cryo. Letters*. 27:73-86.

210. Hunt, C.J. and P.M.Timmons. 2007. Cryopreservation of Human Embryonic Stem Cell Lines. *In* Cryopreservation and Freeze-drying. J.Day and G.Stacey, editors. Humana Press.
211. Inzunza, J., K.Gertow, M.A.Stromberg, E.Matilainen, E.Blennow, H.Skottman, S.Wolbank, L.Ahrlund-Richter, and O.Hovatta. 2005c. Derivation of human embryonic stem cell lines in serum replacement medium using postnatal human fibroblasts as feeder cells. *Stem Cells* 23:544-549.
212. Inzunza, J., K.Gertow, M.A.Stromberg, E.Matilainen, E.Blennow, H.Skottman, S.Wolbank, L.Ahrlund-Richter, and O.Hovatta. 2005d. Derivation of human embryonic stem cell lines in serum replacement medium using postnatal human fibroblasts as feeder cells. *Stem Cells* 23:544-549.
213. Inzunza, J., K.Gertow, M.A.Stromberg, E.Matilainen, E.Blennow, H.Skottman, S.Wolbank, L.Ahrlund-Richter, and O.Hovatta. 2005b. Derivation of human embryonic stem cell lines in serum replacement medium using postnatal human fibroblasts as feeder cells. *Stem Cells* 23:544-549.
214. Inzunza, J., K.Gertow, M.A.Stromberg, E.Matilainen, E.Blennow, H.Skottman, S.Wolbank, L.Ahrlund-Richter, and O.Hovatta. 2005a. Derivation of human embryonic stem cell lines in serum replacement medium using postnatal human fibroblasts as feeder cells. *Stem Cells* 23:544-549.
215. Inzunza, J., K.Gertow, M.A.Stromberg, E.Matilainen, E.Blennow, H.Skottman, S.Wolbank, L.Ahrlund-Richter, and O.Hovatta. 2005e. Derivation of human embryonic stem cell lines in serum replacement medium using postnatal human fibroblasts as feeder cells. *Stem Cells* 23:544-549.
216. Ishibashi, K., M.Kuwahara, Y.Gu, Y.Kageyama, A.Tohsaka, F.Suzuki, F.Marumo, and S.Sasaki. 1997b. Cloning and functional expression of a new water channel abundantly expressed in the testis permeable to water, glycerol, and urea. *J Biol. Chem.* 272:20782-20786.
217. Ishibashi, K., M.Kuwahara, Y.Gu, Y.Kageyama, A.Tohsaka, F.Suzuki, F.Marumo, and S.Sasaki. 1997a. Cloning and functional expression of a new water channel abundantly expressed in the testis permeable to water, glycerol, and urea. *J Biol. Chem.* 272:20782-20786.
218. Ishibashi, K., M.Kuwahara, Y.Gu, Y.Kageyama, A.Tohsaka, F.Suzuki, F.Marumo, and S.Sasaki. 1997c. Cloning and functional expression of a new water channel abundantly expressed in the testis permeable to water, glycerol, and urea. *J Biol. Chem.* 272:20782-20786.
219. Ishibashi, K., S.Sasaki, K.Fushimi, S.Uchida, M.Kuwahara, H.Saito, T.Furukawa, K.Nakajima, Y.Yamaguchi, T.Gojobori, and . 1994c. Molecular cloning and expression of a member of the aquaporin family with permeability to glycerol and urea in addition to water expressed at the basolateral membrane of kidney collecting duct cells. *Proc. Natl. Acad. Sci. U. S. A* 91:6269-6273.
220. Ishibashi, K., S.Sasaki, K.Fushimi, S.Uchida, M.Kuwahara, H.Saito, T.Furukawa, K.Nakajima, Y.Yamaguchi, T.Gojobori, and . 1994d. Molecular cloning and expression of a member of the aquaporin family with permeability to

- glycerol and urea in addition to water expressed at the basolateral membrane of kidney collecting duct cells. *Proc. Natl. Acad. Sci. U. S. A* 91:6269-6273.
221. Ishibashi, K., S.Sasaki, K.Fushimi, S.Uchida, M.Kuwahara, H.Saito, T.Furukawa, K.Nakajima, Y.Yamaguchi, T.Gojobori, and . 1994a. Molecular cloning and expression of a member of the aquaporin family with permeability to glycerol and urea in addition to water expressed at the basolateral membrane of kidney collecting duct cells. *Proc. Natl. Acad. Sci. U. S. A* 91:6269-6273.
222. Ishibashi, K., S.Sasaki, K.Fushimi, S.Uchida, M.Kuwahara, H.Saito, T.Furukawa, K.Nakajima, Y.Yamaguchi, T.Gojobori, and . 1994b. Molecular cloning and expression of a member of the aquaporin family with permeability to glycerol and urea in addition to water expressed at the basolateral membrane of kidney collecting duct cells. *Proc. Natl. Acad. Sci. U. S. A* 91:6269-6273.
223. Ishimori, H., K.Saeki, M.Inai, Y.Nagao, J.Itasaka, Y.Miki, N.Seike, and H.Kainuma. 1993. Vitrification of bovine embryos in a mixture of ethylene glycol and dimethyl sulfoxide. *Theriogenology* 40:427-433.
224. Ishimori, H., Y.Takahashi, and H.Kanagawa. 1992. Factors affecting survival of mouse blastocysts vitrified by a mixture of ethylene glycol and dimethyl sulfoxide. *Theriogenology* 38:1175-1185.
225. Itskovitz-Eldor, J., M.Schuldiner, D.Karsenti, A.Eden, O.Yanuka, M.Amit, H.Soreq, and N.Benvenisty. 2000a. Differentiation of human embryonic stem cells into embryoid bodies compromising the three embryonic germ layers. *Mol. Med.* 6:88-95.
226. Itskovitz-Eldor, J., M.Schuldiner, D.Karsenti, A.Eden, O.Yanuka, M.Amit, H.Soreq, and N.Benvenisty. 2000d. Differentiation of human embryonic stem cells into embryoid bodies compromising the three embryonic germ layers. *Mol. Med.* 6:88-95.
227. Itskovitz-Eldor, J., M.Schuldiner, D.Karsenti, A.Eden, O.Yanuka, M.Amit, H.Soreq, and N.Benvenisty. 2000b. Differentiation of human embryonic stem cells into embryoid bodies compromising the three embryonic germ layers. *Mol. Med.* 6:88-95.
228. Itskovitz-Eldor, J., M.Schuldiner, D.Karsenti, A.Eden, O.Yanuka, M.Amit, H.Soreq, and N.Benvenisty. 2000c. Differentiation of human embryonic stem cells into embryoid bodies compromising the three embryonic germ layers. *Mol. Med.* 6:88-95.
229. Jackowski, S., S.P.Leibo, and P.Mazur. 1980. Glycerol permeabilities of fertilized and infertilized mouse ova. *J Exp. Zool.* 212:329-341.
230. Jacobs, M.H. 1933b. The simultaneous measurement of cell permeability to water and to dissolved substances. *Journal of Cellular and Comparative Physiology* 2:427-444.
231. Jacobs, M.H. 1962a. Early Osmotic History of the Plasma Membrane. *Circulation* 26:1013-1021.

- 
232. Jacobs, M.H. 1962b. Early Osmotic History of the Plasma Membrane. *Circulation* 26:1013-1021.
233. Jacobs, M.H. 1933c. The simultaneous measurement of cell permeability to water and to dissolved substances. *Journal of Cellular and Comparative Physiology* 2:427-444.
234. Jacobs, M.H. 1933a. The simultaneous measurement of cell permeability to water and to dissolved substances. *Journal of Cellular and Comparative Physiology* 2:427-444.
235. Jacobs, M.H. 1962c. Early Osmotic History of the Plasma Membrane. *Circulation* 26:1013-1021.
236. Jacobsen, I.A., D.E.Pegg, H.Starklint, J.Chemnitz, C.Hunt, P.Barfort, and M.P.Diaper. 1984. Effect of cooling and warming rate on glycerolized rabbit kidneys. *Cryobiology* 21:637-653.
237. James, D., A.J.Levine, D.Besser, and A.Hemmati-Brivanlou. 2005a. TGFbeta/activin/nodal signaling is necessary for the maintenance of pluripotency in human embryonic stem cells. *Development* 132:1273-1282.
238. James, D., A.J.Levine, D.Besser, and A.Hemmati-Brivanlou. 2005b. TGFbeta/activin/nodal signaling is necessary for the maintenance of pluripotency in human embryonic stem cells. *Development* 132:1273-1282.
239. Ji, L., J.J.de Pablo, and S.P.Palecek. 2004f. Cryopreservation of adherent human embryonic stem cells. *Biotechnol. Bioeng.* 88:299-312.
240. Ji, L., J.J.de Pablo, and S.P.Palecek. 2004d. Cryopreservation of adherent human embryonic stem cells. *Biotechnol. Bioeng.* 88:299-312.
241. Ji, L., J.J.de Pablo, and S.P.Palecek. 2004c. Cryopreservation of adherent human embryonic stem cells. *Biotechnol. Bioeng.* 88:299-312.
242. Ji, L., J.J.de Pablo, and S.P.Palecek. 2004b. Cryopreservation of adherent human embryonic stem cells. *Biotechnol. Bioeng.* 88:299-312.
243. Ji, L., J.J.de Pablo, and S.P.Palecek. 2004a. Cryopreservation of adherent human embryonic stem cells. *Biotechnol. Bioeng.* 88:299-312.
244. Ji, L., J.J.de Pablo, and S.P.Palecek. 2004e. Cryopreservation of adherent human embryonic stem cells. *Biotechnol. Bioeng.* 88:299-312.
245. Jones, R.J., M.I.Collector, J.P.Barber, M.S.Vala, M.J.Fackler, W.S.May, C.A.Griffin, A.L.Hawkins, B.A.Zehnbauser, J.Hilton, O.M.Colvin, and S.J.Sharkis. 1996. Characterization of mouse lymphohematopoietic stem cells lacking spleen colony-forming activity. *Blood* 88:487-491.
246. Josephson, R., C.J.Ording, Y.Liu, S.Shin, U.Lakshmiopathy, A.Toumadje, B.Love, J.D.Chesnut, P.W.Andrews, M.S.Rao, and J.M.Auerbach. 2007.

- Qualification of embryonal carcinoma 2102Ep as a reference for human embryonic stem cell research. *Stem Cells* 25:437-446.
247. Josephson, R., G.Sykes, Y.Liu, C.Ording, W.Xu, X.Zeng, S.Shin, J.Loring, A.Maitra, M.S.Rao, and J.M.Auerbach. 2006. A molecular scheme for improved characterization of human embryonic stem cell lines. *BMC. Biol.* 4:28.
248. Kannagi, R., N.A.Cochran, F.Ishigami, S.Hakomori, P.W.Andrews, B.B.Knowles, and D.Solter. 1983. Stage-specific embryonic antigens (SSEA-3 and -4) are epitopes of a unique globo-series ganglioside isolated from human teratocarcinoma cells. *EMBO J.* 2:2355-2361.
249. Kannagi, R., E.Nudelman, S.B.Leverly, and S.Hakomori. 1982. A series of human erythrocyte glycosphingolipids reacting to the monoclonal antibody directed to a developmentally regulated antigen SSEA-1. *J. Biol. Chem.* 257:14865-14874.
250. Kasai, M., J.H.Komi, A.Takakamo, H.Tsudera, T.Sakurai, and T.Machida. 1990. A simple method for mouse embryo cryopreservation in a low toxicity vitrification solution, without appreciable loss of viability. *J Reprod Fertil* 89:91-97.
251. Kashuba Benson, C.M., J.D.Benson, and J.K.Critser. 2008k. An improved cryopreservation method for a mouse embryonic stem cell line. *Cryobiology* 56:120-130.
252. Kashuba Benson, C.M., J.D.Benson, and J.K.Critser. 2008l. An improved cryopreservation method for a mouse embryonic stem cell line. *Cryobiology* 56:120-130.
253. Kashuba Benson, C.M., J.D.Benson, and J.K.Critser. 2008m. An improved cryopreservation method for a mouse embryonic stem cell line. *Cryobiology* 56:120-130.
254. Kashuba Benson, C.M., J.D.Benson, and J.K.Critser. 2008n. An improved cryopreservation method for a mouse embryonic stem cell line. *Cryobiology* 56:120-130.
255. Kashuba Benson, C.M., J.D.Benson, and J.K.Critser. 2008i. An improved cryopreservation method for a mouse embryonic stem cell line. *Cryobiology* 56:120-130.
256. Kashuba Benson, C.M., J.D.Benson, and J.K.Critser. 2008h. An improved cryopreservation method for a mouse embryonic stem cell line. *Cryobiology* 56:120-130.
257. Kashuba Benson, C.M., J.D.Benson, and J.K.Critser. 2008o. An improved cryopreservation method for a mouse embryonic stem cell line. *Cryobiology* 56:120-130.

258. Kashuba Benson, C.M., J.D.Benson, and J.K.Critser. 2008f. An improved cryopreservation method for a mouse embryonic stem cell line. *Cryobiology* 56:120-130.
259. Kashuba Benson, C.M., J.D.Benson, and J.K.Critser. 2008g. An improved cryopreservation method for a mouse embryonic stem cell line. *Cryobiology* 56:120-130.
260. Kashuba Benson, C.M., J.D.Benson, and J.K.Critser. 2008a. An improved cryopreservation method for a mouse embryonic stem cell line. *Cryobiology* 56:120-130.
261. Kashuba Benson, C.M., J.D.Benson, and J.K.Critser. 2008b. An improved cryopreservation method for a mouse embryonic stem cell line. *Cryobiology* 56:120-130.
262. Kashuba Benson, C.M., J.D.Benson, and J.K.Critser. 2008c. An improved cryopreservation method for a mouse embryonic stem cell line. *Cryobiology* 56:120-130.
263. Kashuba Benson, C.M., J.D.Benson, and J.K.Critser. 2008d. An improved cryopreservation method for a mouse embryonic stem cell line. *Cryobiology* 56:120-130.
264. Kashuba Benson, C.M., J.D.Benson, and J.K.Critser. 2008e. An improved cryopreservation method for a mouse embryonic stem cell line. *Cryobiology* 56:120-130.
265. Kashuba Benson, C.M., J.D.Benson, and J.K.Critser. 2008j. An improved cryopreservation method for a mouse embryonic stem cell line. *Cryobiology* 56:120-130.
266. Katkov, I.I., N.G.Kan, F.Cimadamore, B.Nelson, E.Y.Snyder, and A.V.Terskikh. 2011. DMSO-Free Programmed Cryopreservation of Fully Dissociated and Adherent Human Induced Pluripotent Stem Cells. *Stem Cells Int.* 2011:981606.
267. Katkov, I.I., M.S.Kim, R.Bajpai, Y.S.Altman, M.Mercola, J.F.Loring, A.V.Terskikh, E.Y.Snyder, and F.Levine. 2006d. Cryopreservation by slow cooling with DMSO diminished production of Oct-4 pluripotency marker in human embryonic stem cells. *Cryobiology* 53:194-205.
268. Katkov, I.I., M.S.Kim, R.Bajpai, Y.S.Altman, M.Mercola, J.F.Loring, A.V.Terskikh, E.Y.Snyder, and F.Levine. 2006b. Cryopreservation by slow cooling with DMSO diminished production of Oct-4 pluripotency marker in human embryonic stem cells. *Cryobiology* 53:194-205.
269. Katkov, I.I., M.S.Kim, R.Bajpai, Y.S.Altman, M.Mercola, J.F.Loring, A.V.Terskikh, E.Y.Snyder, and F.Levine. 2006a. Cryopreservation by slow cooling with DMSO diminished production of Oct-4 pluripotency marker in human embryonic stem cells. *Cryobiology* 53:194-205.

270. Katkov, I.I., M.S.Kim, R.Bajpai, Y.S.Altman, M.Mercola, J.F.Loring, A.V.Terskikh, E.Y.Snyder, and F.Levine. 2006e. Cryopreservation by slow cooling with DMSO diminished production of Oct-4 pluripotency marker in human embryonic stem cells. *Cryobiology* 53:194-205.
271. Katkov, I.I., M.S.Kim, R.Bajpai, Y.S.Altman, M.Mercola, J.F.Loring, A.V.Terskikh, E.Y.Snyder, and F.Levine. 2006f. Cryopreservation by slow cooling with DMSO diminished production of Oct-4 pluripotency marker in human embryonic stem cells. *Cryobiology* 53:194-205.
272. Katkov, I.I., M.S.Kim, R.Bajpai, Y.S.Altman, M.Mercola, J.F.Loring, A.V.Terskikh, E.Y.Snyder, and F.Levine. 2006g. Cryopreservation by slow cooling with DMSO diminished production of Oct-4 pluripotency marker in human embryonic stem cells. *Cryobiology* 53:194-205.
273. Katkov, I.I., M.S.Kim, R.Bajpai, Y.S.Altman, M.Mercola, J.F.Loring, A.V.Terskikh, E.Y.Snyder, and F.Levine. 2006c. Cryopreservation by slow cooling with DMSO diminished production of Oct-4 pluripotency marker in human embryonic stem cells. *Cryobiology* 53:194-205.
274. Kaufman, D.S., E.T.Hanson, R.L.Lewis, R.Auerbach, and J.A.Thomson. 2001a. Hematopoietic colony-forming cells derived from human embryonic stem cells. *Proc. Natl. Acad. Sci. U. S. A* 98:10716-10721.
275. Kaufman, D.S., E.T.Hanson, R.L.Lewis, R.Auerbach, and J.A.Thomson. 2001b. Hematopoietic colony-forming cells derived from human embryonic stem cells. *Proc. Natl. Acad. Sci. U. S. A* 98:10716-10721.
276. Kedem, O. and A.Katchalsky. 1958e. Thermodynamic analysis of the permeability of biological membranes to non-electrolytes. *Biochim. Biophys. Acta* 27:229-246.
277. Kedem, O. and A.Katchalsky. 1958d. Thermodynamic analysis of the permeability of biological membranes to non-electrolytes. *Biochim. Biophys. Acta* 27:229-246.
278. Kedem, O. and A.Katchalsky. 1958c. Thermodynamic analysis of the permeability of biological membranes to non-electrolytes. *Biochim. Biophys. Acta* 27:229-246.
279. Kedem, O. and A.Katchalsky. 1958b. Thermodynamic analysis of the permeability of biological membranes to non-electrolytes. *Biochim. Biophys. Acta* 27:229-246.
280. Kedem, O. and A.Katchalsky. 1958a. Thermodynamic analysis of the permeability of biological membranes to non-electrolytes. *Biochim. Biophys. Acta* 27:229-246.
281. Kim, J.B., H.Zaehres, G.Wu, L.Gentile, K.Ko, V.Sebastiano, M.J.Arauzo-Bravo, D.Ruau, D.W.Han, M.Zenke, and H.R.Scholer. 2008c. Pluripotent stem cells induced from adult neural stem cells by reprogramming with two factors. *Nature* 454:646-650.

282. Kim, J.B., H.Zaehres, G.Wu, L.Gentile, K.Ko, V.Sebastiano, M.J.Arauzo-Bravo, D.Ruau, D.W.Han, M.Zenke, and H.R.Scholer. 2008b. Pluripotent stem cells induced from adult neural stem cells by reprogramming with two factors. *Nature* 454:646-650.
283. Kim, J.B., H.Zaehres, G.Wu, L.Gentile, K.Ko, V.Sebastiano, M.J.Arauzo-Bravo, D.Ruau, D.W.Han, M.Zenke, and H.R.Scholer. 2008a. Pluripotent stem cells induced from adult neural stem cells by reprogramming with two factors. *Nature* 454:646-650.
284. Kim, S.J., S.H.Cheon, S.J.Yoo, J.Kwon, J.H.Park, C.G.Kim, K.Rhee, S.You, J.Y.Lee, S.I.Roh, and H.S.Yoon. 2005. Contribution of the PI3K/Akt/PKB signal pathway to maintenance of self-renewal in human embryonic stem cells. *FEBS Lett.* 579:534-540.
285. Kim, Y.Y., S.Y.Ku, J.Jang, S.K.Oh, H.S.Kim, S.H.Kim, Y.M.Choi, and S.Y.Moon. 2008d. Use of long-term cultured embryoid bodies may enhance cardiomyocyte differentiation by BMP2. *Yonsei Med. J* 49:819-827.
286. Kleinhans, F.W. 1998b. Membrane permeability modeling: Kedem-Katchalsky vs a two-parameter formalism. *Cryobiology* 37:271-289.
287. Kleinhans, F.W. 1998d. Membrane permeability modeling: Kedem-Katchalsky vs a two-parameter formalism. *Cryobiology* 37:271-289.
288. Kleinhans, F.W. 1998a. Membrane permeability modeling: Kedem-Katchalsky vs a two-parameter formalism. *Cryobiology* 37:271-289.
289. Kleinhans, F.W. 1998c. Membrane permeability modeling: Kedem-Katchalsky vs a two-parameter formalism. *Cryobiology* 37:271-289.
290. Koga, S., A.Echigo, and K.Nunomura. 1966. Physical properties of cell water in partially dried *Saccharomyces cerevisiae*. *Biophys. J* 6:665-674.
291. Kristensen, D.M., M.Kalisz, and J.H.Nielsen. 2005. Cytokine signalling in embryonic stem cells. *APMIS* 113:756-772.
292. Kuroda, T., M.Tada, H.Kubota, H.Kimura, S.Y.Hatano, H.Suemori, N.Nakatsuji, and T.Tada. 2005. Octamer and Sox elements are required for transcriptional cis regulation of Nanog gene expression. *Mol. Cell Biol.* 25:2475-2485.
293. Kuwayama, M. 2007. Highly efficient vitrification for cryopreservation of human oocytes and embryos: the Cryotop method. *Theriogenology* 67:73-80.
294. Larman, M.G., M.G.Katz-Jaffe, C.B.Sheehan, and D.K.Gardner. 2007a. 1,2-propanediol and the type of cryopreservation procedure adversely affect mouse oocyte physiology. *Hum. Reprod.* 22:250-259.
295. Larman, M.G., M.G.Katz-Jaffe, C.B.Sheehan, and D.K.Gardner. 2007b. 1,2-propanediol and the type of cryopreservation procedure adversely affect mouse oocyte physiology. *Hum. Reprod.* 22:250-259.

296. Larman, M.G., M.G.Katz-Jaffe, C.B.Sheehan, and D.K.Gardner. 2007c. 1,2-propanediol and the type of cryopreservation procedure adversely affect mouse oocyte physiology. *Hum. Reprod.* 22:250-259.
297. Laurence, A.D. and A.H.Goldstone. 1999. High-dose therapy with hematopoietic transplantation for Hodgkin's lymphoma. *Semin. Hematol.* 36:303-312.
298. Lee Jr, R.E., J.P.Costanzo, E.C.Davidson, and J.R.Layne Jr. 1992. Dynamics of body water during freezing and thawing in a freeze-tolerant frog (*Rana sylvatica*). *Journal of Thermal Biology* 17:263-266.
299. Leibo, S.P. 1986. Cryobiology: preservation of mammalian embryos. *Basic Life Sci.* 37:251-272.
300. Leibo, S.P., H.M.Kubisch, R.D.Schramm, R.M.Harrison, and C.A.Vandevoort. 2007. Male-to-male differences in post-thaw motility of rhesus spermatozoa after cryopreservation of replicate ejaculates. *J Med. Primatol.* 36:151-163.
301. Lewis, J.P., M.Passovoy, M.Freeman, and F.E.Trobaugh, Jr. 1968. The repopulating potential and differentiation capacity of hematopoietic stem cells from the blood and bone marrow of normal mice. *J. Cell Physiol* 71:121-132.
302. Lewis, J.P. and F.E.TROBAUGH, Jr. 1964b. The assay of the transplantation potential of fresh and stored bone marrow by two in-vivo system. *Ann. N. Y. Acad. Sci.* 114:677-685.
303. Lewis, J.P. and F.E.TROBAUGH, Jr. 1964c. The assay of the transplantation potential of fresh and stored bone marrow by two in-vivo system. *Ann. N. Y. Acad. Sci.* 114:677-685.
304. Lewis, J.P. and F.E.TROBAUGH, Jr. 1964a. The assay of the transplantation potential of fresh and stored bone marrow by two in-vivo system. *Ann. N. Y. Acad. Sci.* 114:677-685.
305. Li, T., Q.Mai, J.Gao, and C.Zhou. 2010c. Cryopreservation of Human Embryonic Stem Cells with a New Bulk Vitrification Method. *Biology of Reproduction* 82:848-853.
306. Li, T., Q.Mai, J.Gao, and C.Zhou. 2010a. Cryopreservation of Human Embryonic Stem Cells with a New Bulk Vitrification Method. *Biology of Reproduction* 82:848-853.
307. Li, T., Q.Mai, J.Gao, and C.Zhou. 2010b. Cryopreservation of Human Embryonic Stem Cells with a New Bulk Vitrification Method. *Biology of Reproduction* 82:848-853.
308. Li, X., R.Krawetz, S.Liu, G.Meng, and D.E.Rancourt. 2008e. ROCK inhibitor improves survival of cryopreserved serum/feeder-free single human embryonic stem cells. *Hum. Reprod.*den404.

309. Li, X., R.Krawetz, S.Liu, G.Meng, and D.E.Rancourt. 2008d. ROCK inhibitor improves survival of cryopreserved serum/feeder-free single human embryonic stem cells. *Hum. Reprod.*den404.
310. Li, X., R.Krawetz, S.Liu, G.Meng, and D.E.Rancourt. 2008c. ROCK inhibitor improves survival of cryopreserved serum/feeder-free single human embryonic stem cells. *Hum. Reprod.*den404.
311. Li, X., R.Krawetz, S.Liu, G.Meng, and D.E.Rancourt. 2008b. ROCK inhibitor improves survival of cryopreserved serum/feeder-free single human embryonic stem cells. *Hum. Reprod.*den404.
312. Li, X., R.Krawetz, S.Liu, G.Meng, and D.E.Rancourt. 2008a. ROCK inhibitor improves survival of cryopreserved serum/feeder-free single human embryonic stem cells. *Hum. Reprod.*den404.
313. Li, X., G.Meng, R.Krawetz, S.Liu, and D.E.Rancourt. 2008g. The ROCK Inhibitor Y-27632 Enhances the Survival Rate of Human Embryonic Stem Cells Following Cryopreservation. *Stem Cells and Development* 17:1079.
314. Li, X., G.Meng, R.Krawetz, S.Liu, and D.E.Rancourt. 2008f. The ROCK Inhibitor Y-27632 Enhances the Survival Rate of Human Embryonic Stem Cells Following Cryopreservation. *Stem Cells and Development* 17:1079.
315. Li, X., G.Meng, R.Krawetz, S.Liu, and D.E.Rancourt. 2008i. The ROCK Inhibitor Y-27632 Enhances the Survival Rate of Human Embryonic Stem Cells Following Cryopreservation. *Stem Cells and Development* 17:1079.
316. Li, X., G.Meng, R.Krawetz, S.Liu, and D.E.Rancourt. 2008h. The ROCK Inhibitor Y-27632 Enhances the Survival Rate of Human Embryonic Stem Cells Following Cryopreservation. *Stem Cells and Development* 17:1079.
317. Li, Y., J.c.Tan, and L.s.Li. 2008j. Comparison of three methods for cryopreservation of human embryonic stem cells. *Fertility and Sterility* In Press, Corrected Proof.
318. Lim, J.M., J.J.Ko, W.S.Hwang, H.M.Chung, and K.Niwa. 1999. Development of in vitro matured bovine oocytes after cryopreservation with different cryoprotectants. *Theriogenology* 51:1303-1310.
319. Lim, J.W. and A.Bodnar. 2002. Proteome analysis of conditioned medium from mouse embryonic fibroblast feeder layers which support the growth of human embryonic stem cells. *Proteomics*. 2:1187-1203.
320. Lin, T., C.Chao, S.Saito, S.J.Mazur, M.E.Murphy, E.Appella, and Y.Xu. 2005. p53 induces differentiation of mouse embryonic stem cells by suppressing Nanog expression. *Nat. Cell Biol.* 7:165-171.
321. Lin, T.M., H.W.Chang, K.H.Wang, A.P.Kao, C.C.Chang, C.H.Wen, C.S.Lai, and S.D.Lin. 2007. Isolation and identification of mesenchymal stem cells from human lipoma tissue. *Biochem. Biophys. Res. Commun.* 361:883-889.

322. Linch, D.C., L.J.Knott, K.G.Patterson, D.A.Cowan, and P.G.Harper. 1982. Bone marrow processing and cryopreservation. *J. Clin. Pathol.* 35:186-190.
323. Litvan, G.G. 1972. Mechanism of cryoinjury in biological systems. *Cryobiology* 9:182-191.
324. Liu, C., C.T.Benson, D.Gao, B.W.Haag, L.E.McGann, and J.K.Critser. 1995. Water Permeability and Its Activation Energy for Individual Hamster Pancreatic Islet Cells. *Cryobiology* 32:493-502.
325. Lovelock, J.E. 1954. Biophysical aspects of the freezing and thawing of living cells. *Proc. R. Soc. Med.* 47:60-62.
326. Lovelock, J.E. 1953f. The haemolysis of human red blood-cells by freezing and thawing. *Biochim. Biophys. Acta* 10:414-426.
327. Lovelock, J.E. 1953b. The haemolysis of human red blood-cells by freezing and thawing. *Biochim. Biophys. Acta* 10:414-426.
328. Lovelock, J.E. 1953a. The haemolysis of human red blood-cells by freezing and thawing. *Biochim. Biophys. Acta* 10:414-426.
329. Lovelock, J.E. 1953c. The haemolysis of human red blood-cells by freezing and thawing. *Biochim. Biophys. Acta* 10:414-426.
330. Lovelock, J.E. 1953e. The mechanism of the protective action of glycerol against haemolysis by freezing and thawing. *Biochim. Biophys. Acta* 11:28-36.
331. Lovelock, J.E. 1953d. The mechanism of the protective action of glycerol against haemolysis by freezing and thawing. *Biochim. Biophys. Acta* 11:28-36.
332. Lovelock, J.E. 1953g. The mechanism of the protective action of glycerol against haemolysis by freezing and thawing. *Biochim. Biophys. Acta* 11:28-36.
333. Lovelock, J.E. and M.W.BISHOP. 1959. Prevention of freezing damage to living cells by dimethyl sulphoxide. *Nature* 183:1394-1395.
334. Lowry, W.E., L.Richter, R.Yachechko, A.D.Pyle, J.Tchieu, R.Sridharan, A.T.Clark, and K.Plath. 2008. Generation of human induced pluripotent stem cells from dermal fibroblasts. *Proc. Natl. Acad. Sci. U. S. A* 105:2883-2888.
335. Mallon, B.S., K.Y.Park, K.G.Chen, R.S.Hamilton, and R.D.G.McKay. 2006. Toward xeno-free culture of human embryonic stem cells. *The International Journal of Biochemistry & Cell Biology* 38:1063-1075.
336. Martin, G.R. 1981b. Isolation of a pluripotent cell line from early mouse embryos cultured in medium conditioned by teratocarcinoma stem cells. *Proc. Natl. Acad. Sci. U. S. A* 78:7634-7638.

337. Martin, G.R. 1981a. Isolation of a pluripotent cell line from early mouse embryos cultured in medium conditioned by teratocarcinoma stem cells. *Proc. Natl. Acad. Sci. U. S. A* 78:7634-7638.
338. Martin-Ibanez, R., C.Unger, A.Stromberg, D.Baker, J.M.Canals, and O.Hovatta. 2008e. Novel cryopreservation method for dissociated human embryonic stem cells in the presence of a ROCK inhibitor. *Hum. Reprod.*den316.
339. Martin-Ibanez, R., C.Unger, A.Stromberg, D.Baker, J.M.Canals, and O.Hovatta. 2008f. Novel cryopreservation method for dissociated human embryonic stem cells in the presence of a ROCK inhibitor. *Hum. Reprod.*den316.
340. Martin-Ibanez, R., C.Unger, A.Stromberg, D.Baker, J.M.Canals, and O.Hovatta. 2008d. Novel cryopreservation method for dissociated human embryonic stem cells in the presence of a ROCK inhibitor. *Hum. Reprod.*den316.
341. Martin-Ibanez, R., C.Unger, A.Stromberg, D.Baker, J.M.Canals, and O.Hovatta. 2008c. Novel cryopreservation method for dissociated human embryonic stem cells in the presence of a ROCK inhibitor. *Hum. Reprod.*den316.
342. Martin-Ibanez, R., C.Unger, A.Stromberg, D.Baker, J.M.Canals, and O.Hovatta. 2008b. Novel cryopreservation method for dissociated human embryonic stem cells in the presence of a ROCK inhibitor. *Hum. Reprod.*den316.
343. Martin-Ibanez, R., C.Unger, A.Stromberg, D.Baker, J.M.Canals, and O.Hovatta. 2008a. Novel cryopreservation method for dissociated human embryonic stem cells in the presence of a ROCK inhibitor. *Hum. Reprod.*den316.
344. Masaki, H., T.Ishikawa, S.Takahashi, M.Okumura, N.Sakai, M.Haga, K.Kominami, H.Migita, F.McDonald, F.Shimada, and K.Sakurada. 2008. Heterogeneity of pluripotent marker gene expression in colonies generated in human iPS cell induction culture. *Stem Cell Research* 1:105-115.
345. Mazur, P. 1963b. Kinetics of water loss from cells at subzero temperatures and the likelihood of intracellular freezing. *J. Gen. Physiol* 47:347-369.
346. Mazur, P. 2007. Principles of cryobiology. *Life in the Frozen State*4-65.
347. Mazur, P. 1965a. The role of cell membranes in the freezing of yeast and other single cells. *Ann. N. Y. Acad. Sci.* 125:658-676.
348. Mazur, P. 1984c. Freezing of living cells: mechanisms and implications. *Am. J. Physiol* 247:C125-C142.
349. Mazur, P. 1963a. Kinetics of water loss from cells at subzero temperatures and the likelihood of intracellular freezing. *J. Gen. Physiol* 47:347-369.
350. Mazur, P. 1965c. The role of cell membranes in the freezing of yeast and other single cells. *Ann. N. Y. Acad. Sci.* 125:658-676.

351. Mazur, P. 1965b. The role of cell membranes in the freezing of yeast and other single cells. *Ann. N. Y. Acad. Sci.* 125:658-676.
352. Mazur, P. 1984b. Freezing of living cells: mechanisms and implications. *Am. J. Physiol* 247:C125-C142.
353. Mazur, P. 1984a. Freezing of living cells: mechanisms and implications. *Am. J. Physiol* 247:C125-C142.
354. Mazur, P., J.Farrant, S.P.Leibo, and E.H.Chu. 1969b. Survival of hamster tissue culture cells after freezing and thawing. Interactions between protective solutes and cooling and warming rates. *Cryobiology* 6:1-9.
355. Mazur, P., J.Farrant, S.P.Leibo, and E.H.Chu. 1969a. Survival of hamster tissue culture cells after freezing and thawing. Interactions between protective solutes and cooling and warming rates. *Cryobiology* 6:1-9.
356. Mazur, P., S.P.Leibo, and E.H.Chu. 1972. A two-factor hypothesis of freezing injury. Evidence from Chinese hamster tissue-culture cells. *Exp. Cell Res.* 71:345-355.
357. Mazur, P., S.P.Leibo, and R.H.Miller. 1974. Permeability of the bovine red cell to glycerol in hyperosmotic solutions at various temperatures. *J. Membr. Biol* 15:107-136.
358. Mazur, P., W.F.Rall, and N.Rigopoulos. 1981b. Relative contributions of the fraction of unfrozen water and of salt concentration to the survival of slowly frozen human erythrocytes. *Biophys. J.* 36:653-675.
359. Mazur, P., W.F.Rall, and N.Rigopoulos. 1981a. Relative contributions of the fraction of unfrozen water and of salt concentration to the survival of slowly frozen human erythrocytes. *Biophys. J.* 36:653-675.
360. Mazur, P., N.Rigopoulos, S.C.Jackowski, and S.P.Leibo. 1976. Preliminary estimates of the permeability of mouse ova and early embryos to glycerol. *Biophys. J* 16:232a.
361. Mazur, P. and U.Schneider. 1986. Osmotic responses of preimplantation mouse and bovine embryos and their cryobiological implications. *Cell Biophys.* 8:259-285.
362. Mazur, P., U.Schneider, and A.P.Mahowald. 1992. Characteristics and kinetics of subzero chilling injury in *Drosophila* embryos. *Cryobiology* 29:39-68.
363. McElwain, T.J., D.W.Hedley, M.Y.Gordon, M.Jarman, J.L.Millar, and J.Pritchard. 1979. High dose melphalan and non-cryopreserved autologous bone marrow treatment of malignant melanoma and neuroblastoma. *Exp. Hematol.* 7 Suppl 5:360-371.
364. McGann, L.E., L.Hogg, A.R.Turner, and J.M.Turc. 1984. Influence of dimethyl sulfoxide on water permeability. *Cryobiology* 21:689-690.

365. McGann, L.E., A.R.Turner, and J.M.Turc. 1982. Microcomputer interface for rapid measurements of average volume using an electronic particle counter. *Med. Biol. Eng Comput.* 20:117-120.
366. McLaughlin, E.A., W.C.Ford, and M.G.Hull. 1992. Motility characteristics and membrane integrity of cryopreserved human spermatozoa. *J Reprod Fertil* 95:527-534.
367. McWilliams, R.B., W.E.Gibbons, and S.P.Leibo. 1995. Osmotic and physiological responses of mouse zygotes and human oocytes to mono- and disaccharides. *Hum. Reprod* 10:1163-1171.
368. Meryman, H.T. 1968. Modified model for the mechanism of freezing injury in erythrocytes. *Nature* 218:333-336.
369. Meryman, H.T. 1971. Osmotic stress as a mechanism of freezing injury. *Cryobiology* 8:489-500.
370. Meryman, H.T. 1974. Freezing Injury and its Prevention in Living Cells. *Annual Review of Biophysics and Bioengineering* 3:341-363.
371. Moezzi, L., A.A.Pourfathollah, K.Alimoghaddam, M.Soleimani, and A.R.Ardjmand. 2005. The Effect of Cryopreservation on Clonogenic Capacity and In Vitro Expansion Potential of Umbilical Cord Blood Progenitor Cells. *Transplantation Proceedings* 37:4500-4503.
372. Mollamohammadi, S., A.Taei, M.Pakzad, M.Totonchi, A.Seifinejad, N.Masoudi, and H.Baharvand. 2009c. A simple and efficient cryopreservation method for feeder-free dissociated human induced pluripotent stem cells and human embryonic stem cells. *Hum. Reprod.dep244*.
373. Mollamohammadi, S., A.Taei, M.Pakzad, M.Totonchi, A.Seifinejad, N.Masoudi, and H.Baharvand. 2009d. A simple and efficient cryopreservation method for feeder-free dissociated human induced pluripotent stem cells and human embryonic stem cells. *Hum. Reprod.dep244*.
374. Mollamohammadi, S., A.Taei, M.Pakzad, M.Totonchi, A.Seifinejad, N.Masoudi, and H.Baharvand. 2009e. A simple and efficient cryopreservation method for feeder-free dissociated human induced pluripotent stem cells and human embryonic stem cells. *Hum. Reprod.dep244*.
375. Mollamohammadi, S., A.Taei, M.Pakzad, M.Totonchi, A.Seifinejad, N.Masoudi, and H.Baharvand. 2009f. A simple and efficient cryopreservation method for feeder-free dissociated human induced pluripotent stem cells and human embryonic stem cells. *Hum. Reprod.dep244*.
376. Mollamohammadi, S., A.Taei, M.Pakzad, M.Totonchi, A.Seifinejad, N.Masoudi, and H.Baharvand. 2009a. A simple and efficient cryopreservation method for feeder-free dissociated human induced pluripotent stem cells and human embryonic stem cells. *Hum. Reprod.dep244*.

377. Mollamohammadi, S., A.Taei, M.Pakzad, M.Totonchi, A.Seifinejad, N.Masoudi, and H.Baharvand. 2009b. A simple and efficient cryopreservation method for feeder-free dissociated human induced pluripotent stem cells and human embryonic stem cells. *Hum. Reprod.* 24:244.
378. Moon, C., G.M.Preston, C.A.Griffin, E.W.Jabs, and P.Agre. 1993. The human aquaporin-CHIP gene. Structure, organization, and chromosomal localization. *J Biol. Chem.* 268:15772-15778.
379. Moore, J.C., S.Sadowy, M.Alikani, A.J.Toro-Ramos, M.R.Swerdel, R.P.Hart, and R.I.Cohen. 2010. A high-resolution molecular-based panel of assays for identification and characterization of human embryonic stem cell lines. *Stem Cell Research* 4:92-106.
380. Morris, G.J. and A.Clark. 1987. Cells at low temperatures. In *The Effects of Low Temperatures on Biological Temperatures*. B.W.W.Grout and G.J.Morris, editors. Edward Arnold, London. 72-119.
381. Moss, E.G., R.C.Lee, and V.Ambros. 1997. The cold shock domain protein LIN-28 controls developmental timing in *C. elegans* and is regulated by the *lin-4* RNA. *Cell* 88:637-646.
382. Moss, E.G. and L.Tang. 2003a. Conservation of the heterochronic regulator Lin-28, its developmental expression and microRNA complementary sites. *Dev. Biol.* 258:432-442.
383. Moss, E.G. and L.Tang. 2003b. Conservation of the heterochronic regulator Lin-28, its developmental expression and microRNA complementary sites. *Dev. Biol.* 258:432-442.
384. Mostert, M.C., A.J.Verkerk, P.M.van de, J.Heighway, P.Marynen, C.Rosenberg, A.G.van Kessel, E.J.van, J.B.de, J.W.Oosterhuis, and L.H.Looijenga. 1998. Identification of the critical region of 12p over-representation in testicular germ cell tumors of adolescents and adults. *Oncogene* 16:2617-2627.
385. Muldrew, K. and L.E.McGann. 1990b. Mechanisms of intracellular ice formation. *Biophys. J.* 57:525-532.
386. Muldrew, K. and L.E.McGann. 1990a. Mechanisms of intracellular ice formation. *Biophys. J.* 57:525-532.
387. Muldrew, K. and L.E.McGann. 1994. The osmotic rupture hypothesis of intracellular freezing injury. *Biophys. J.* 66:532-541.
388. Mummery, C., O.D.Ward-van, P.Doevendans, R.Spijker, B.S.van den, R.Hassink, H.M.van der, T.Ophhof, M.Pera, A.B.de la Riviere, R.Passier, and L.Tertoolen. 2003a. Differentiation of human embryonic stem cells to cardiomyocytes: role of coculture with visceral endoderm-like cells. *Circulation* 107:2733-2740.
389. Mummery, C., O.D.Ward-van, P.Doevendans, R.Spijker, B.S.van den, R.Hassink, H.M.van der, T.Ophhof, M.Pera, A.B.de la Riviere, R.Passier, and

- L.Tertoolen. 2003b. Differentiation of human embryonic stem cells to cardiomyocytes: role of coculture with visceral endoderm-like cells. *Circulation* 107:2733-2740.
390. Nakagawa, M., M.Koyanagi, K.Tanabe, K.Takahashi, T.Ichisaka, T.Aoi, K.Okita, Y.Mochiduki, N.Takizawa, and S.Yamanaka. 2008. Generation of induced pluripotent stem cells without Myc from mouse and human fibroblasts. *Nat Biotechnol.* 26:101-106.
391. Narumiya, S., T.Ishizaki, and M.Uehata. 2000. Use and properties of ROCK-specific inhibitor Y-27632. *Methods Enzymol.* 325:273-284.
392. Ng, E.S., R.P.Davis, L.Azzola, E.G.Stanley, and A.G.Elefanty. 2005b. Forced aggregation of defined numbers of human embryonic stem cells into embryoid bodies fosters robust, reproducible hematopoietic differentiation. *Blood* 106:1601-1603.
393. Ng, E.S., R.P.Davis, L.Azzola, E.G.Stanley, and A.G.Elefanty. 2005a. Forced aggregation of defined numbers of human embryonic stem cells into embryoid bodies fosters robust, reproducible hematopoietic differentiation. *Blood* 106:1601-1603.
394. Nichols, J., E.P.Evans, and A.G.Smith. 1990b. Establishment of germ-line-competent embryonic stem (ES) cells using differentiation inhibiting activity. *Development* 110:1341-1348.
395. Nichols, J., E.P.Evans, and A.G.Smith. 1990a. Establishment of germ-line-competent embryonic stem (ES) cells using differentiation inhibiting activity. *Development* 110:1341-1348.
396. Nichols, J., E.P.Evans, and A.G.Smith. 1990c. Establishment of germ-line-competent embryonic stem (ES) cells using differentiation inhibiting activity. *Development* 110:1341-1348.
397. Nishigaki, T., Y.Teramura, H.Suemori, and H.Iwata. 2009. Cryopreservation of primate embryonic stem cells with chemically-defined solution without Me<sub>2</sub>SO. *Cryobiology* In Press, Corrected Proof.
398. Nishimoto, M., A.Fukushima, A.Okuda, and M.Muramatsu. 1999. The gene for the embryonic stem cell coactivator UTF1 carries a regulatory element which selectively interacts with a complex composed of Oct-3/4 and Sox-2. *Mol. Cell Biol.* 19:5453-5465.
399. Noiles, E.E., P.Mazur, P.F.Watson, F.W.Kleinhans, and J.K.Critser. 1993. Determination of water permeability coefficient for human spermatozoa and its activation energy. *Biol. Reprod.* 48:99-109.
400. Oh, S.P. and E.Li. 1997. The signaling pathway mediated by the type IIB activin receptor controls axial patterning and lateral asymmetry in the mouse. *Genes Dev.* 11:1812-1826.

401. Ohgushi, M., M.Matsumura, M.Eiraku, K.Murakami, T.Aramaki, A.Nishiyama, K.Muguruma, T.Nakano, H.Suga, M.Ueno, T.Ishizaki, H.Suemori, S.Narumiya, H.Niwa, and Y.Sasai. 2010c. Molecular pathway and cell state responsible for dissociation-induced apoptosis in human pluripotent stem cells. *Cell Stem Cell* 7:225-239.
402. Ohgushi, M., M.Matsumura, M.Eiraku, K.Murakami, T.Aramaki, A.Nishiyama, K.Muguruma, T.Nakano, H.Suga, M.Ueno, T.Ishizaki, H.Suemori, S.Narumiya, H.Niwa, and Y.Sasai. 2010b. Molecular pathway and cell state responsible for dissociation-induced apoptosis in human pluripotent stem cells. *Cell Stem Cell* 7:225-239.
403. Ohgushi, M., M.Matsumura, M.Eiraku, K.Murakami, T.Aramaki, A.Nishiyama, K.Muguruma, T.Nakano, H.Suga, M.Ueno, T.Ishizaki, H.Suemori, S.Narumiya, H.Niwa, and Y.Sasai. 2010a. Molecular pathway and cell state responsible for dissociation-induced apoptosis in human pluripotent stem cells. *Cell Stem Cell* 7:225-239.
404. Okita, K., M.Nakagawa, H.Hyengjong, T.Ichisaka, and S.Yamanaka. 2008a. Generation of mouse induced pluripotent stem cells without viral vectors. *Science* 322:949-953.
405. Okita, K., M.Nakagawa, H.Hyengjong, T.Ichisaka, and S.Yamanaka. 2008b. Generation of mouse induced pluripotent stem cells without viral vectors. *Science* 322:949-953.
406. Okuno, Y., H.Iwasaki, C.S.Huettner, H.S.Radomska, D.A.Gonzalez, D.G.Tenen, and K.Akashi. 2002. Differential regulation of the human and murine CD34 genes in hematopoietic stem cells. *Proc. Natl. Acad. Sci. U. S. A* 99:6246-6251.
407. Park, I.H., R.Zhao, J.A.West, A.Yabuuchi, H.Huo, T.A.Ince, P.H.Lerou, M.W.Lensch, and G.Q.Daley. 2008a. Reprogramming of human somatic cells to pluripotency with defined factors. *Nature* 451:141-146.
408. Park, I.H., R.Zhao, J.A.West, A.Yabuuchi, H.Huo, T.A.Ince, P.H.Lerou, M.W.Lensch, and G.Q.Daley. 2008b. Reprogramming of human somatic cells to pluripotency with defined factors. *Nature* 451:141-146.
409. Passier, R. and C.Mummery. 2005b. Cardiomyocyte differentiation from embryonic and adult stem cells. *Curr. Opin. Biotechnol.* 16:498-502.
410. Passier, R. and C.Mummery. 2005a. Cardiomyocyte differentiation from embryonic and adult stem cells. *Curr. Opin. Biotechnol.* 16:498-502.
411. Passier, R., D.W.Oostwaard, J.Snapper, J.Kloots, R.J.Hassink, E.Kuijk, B.Roelen, A.B.de la Riviere, and C.Mummery. 2005b. Increased cardiomyocyte differentiation from human embryonic stem cells in serum-free cultures. *Stem Cells* 23:772-780.
412. Passier, R., D.W.Oostwaard, J.Snapper, J.Kloots, R.J.Hassink, E.Kuijk, B.Roelen, A.B.de la Riviere, and C.Mummery. 2005a. Increased cardiomyocyte

- differentiation from human embryonic stem cells in serum-free cultures. *Stem Cells* 23:772-780.
413. Paynter, S.J., A.Borini, V.Bianchi, S.L.De, C.Flamigni, and G.Coticchio. 2005b. Volume changes of mature human oocytes on exposure to cryoprotectant solutions used in slow cooling procedures. *Hum. Reprod* 20:1194-1199.
414. Paynter, S.J., A.Borini, V.Bianchi, S.L.De, C.Flamigni, and G.Coticchio. 2005a. Volume changes of mature human oocytes on exposure to cryoprotectant solutions used in slow cooling procedures. *Hum. Reprod* 20:1194-1199.
415. Paynter, S.J., A.Borini, V.Bianchi, S.L.De, C.Flamigni, and G.Coticchio. 2005c. Volume changes of mature human oocytes on exposure to cryoprotectant solutions used in slow cooling procedures. *Hum. Reprod* 20:1194-1199.
416. Paynter, S.J., A.Cooper, L.Gregory, B.J.Fuller, and R.W.Shaw. 1999c. Permeability characteristics of human oocytes in the presence of the cryoprotectant dimethylsulphoxide. *Hum. Reprod.* 14:2338-2342.
417. Paynter, S.J., A.Cooper, L.Gregory, B.J.Fuller, and R.W.Shaw. 1999b. Permeability characteristics of human oocytes in the presence of the cryoprotectant dimethylsulphoxide. *Hum. Reprod.* 14:2338-2342.
418. Paynter, S.J., A.Cooper, L.Gregory, B.J.Fuller, and R.W.Shaw. 1999a. Permeability characteristics of human oocytes in the presence of the cryoprotectant dimethylsulphoxide. *Hum. Reprod.* 14:2338-2342.
419. Paynter, S.J., A.Cooper, L.Gregory, B.J.Fuller, and R.W.Shaw. 1999d. Permeability characteristics of human oocytes in the presence of the cryoprotectant dimethylsulphoxide. *Hum. Reprod.* 14:2338-2342.
420. Paynter, S.J., B.J.Fuller, and R.W.Shaw. 1999e. Temperature Dependence of Kedem-Katchalsky Membrane Transport Coefficients for Mature Mouse Oocytes in the Presence of Ethylene Glycol. *Cryobiology* 39:169-176.
421. Paynter, S.J., B.J.Fuller, and R.W.Shaw. 1999f. Temperature Dependence of Kedem-Katchalsky Membrane Transport Coefficients for Mature Mouse Oocytes in the Presence of Ethylene Glycol. *Cryobiology* 39:169-176.
422. Paynter, S.J., L.O'Neil, B.J.Fuller, and R.W.Shaw. 2001b. Membrane permeability of human oocytes in the presence of the cryoprotectant propane-1,2-diol. *Fertility and Sterility* 75:532-538.
423. Paynter, S.J., L.O'Neil, B.J.Fuller, and R.W.Shaw. 2001c. Membrane permeability of human oocytes in the presence of the cryoprotectant propane-1,2-diol. *Fertility and Sterility* 75:532-538.
424. Paynter, S.J., L.O'Neil, B.J.Fuller, and R.W.Shaw. 2001a. Membrane permeability of human oocytes in the presence of the cryoprotectant propane-1,2-diol. *Fertility and Sterility* 75:532-538.

425. Peerani, R., B.M.Rao, C.Bauwens, T.Yin, G.A.Wood, A.Nagy, E.Kumacheva, and P.W.Zandstra. 2007b. Niche-mediated control of human embryonic stem cell self-renewal and differentiation. *EMBO J* 26:4744-4755.
426. Peerani, R., B.M.Rao, C.Bauwens, T.Yin, G.A.Wood, A.Nagy, E.Kumacheva, and P.W.Zandstra. 2007a. Niche-mediated control of human embryonic stem cell self-renewal and differentiation. *EMBO J* 26:4744-4755.
427. Peerani, R., B.M.Rao, C.Bauwens, T.Yin, G.A.Wood, A.Nagy, E.Kumacheva, and P.W.Zandstra. 2007c. Niche-mediated control of human embryonic stem cell self-renewal and differentiation. *EMBO J* 26:4744-4755.
428. Pegg, D.E. 1994. Cryobiology: life in the deep freeze. *Biologist* 41:53-56.
429. Pegg, D.E. 2006. Principles of Cryopreservation. *Methods in Molecular Biology* 368:39-57.
430. Pegg, D.E. and P.Lancaster. 1998. A digital device and software for capturing and analysing cell volume data from a coulter counter. *Cryobiology* 37:441.
431. Pegg, D.E. 1987. Mechanisms of freezing damage. *Symp. Soc. Exp. Biol.* 41:363-378.
432. Pegg, D.E. 1989. Viability assays for preserved cells, tissues, and organs. *Cryobiology* 26:212-231.
433. Pegg, D.E. 1984. Red cell volume in glycerol/sodium chloride/water mixtures. *Cryobiology* 21:234-239.
434. Pegg, D.E. and M.P.Diaper. 1990. Freezing Versus Vitrification: Basic Principles. 55-69.
435. Pegg, D.E. and M.P.Diaper. 1988. On the mechanism of injury to slowly frozen erythrocytes. *Biophys. J* 54:471-488.
436. Pegg, D.E., M.P.Diaper, H.L.Skaer, and C.J.Hunt. 1984b. The effect of cooling rate and warming rate on the packing effect in human erythrocytes frozen and thawed in the presence of 2 M glycerol. *Cryobiology* 21:491-502.
437. Pegg, D.E., M.P.Diaper, H.L.Skaer, and C.J.Hunt. 1984a. The effect of cooling rate and warming rate on the packing effect in human erythrocytes frozen and thawed in the presence of 2 M glycerol. *Cryobiology* 21:491-502.
438. Pegg, D.E., M.C.Wusteman, and L.Wang. 2006. Cryopreservation of articular cartilage. Part 1: Conventional cryopreservation methods. *Cryobiology* 52:335-346.
439. Polge, C., A.U.SMITH, and A.S.Parkes. 1949a. Revival of Spermatozoa after Vitrification and Dehydration at Low Temperatures. *Nature* 164:666.

- 
440. Polge, C., A.U.SMITH, and A.S.Parkes. 1949b. Revival of Spermatozoa after Vitrification and Dehydration at Low Temperatures. *Nature* 164:666.
441. Privalov, P.L. 1968. Water and its role in biological systems. *Biofizika* 13:163-177.
442. Quinn, P.J. 1985. A lipid-phase separation model of low-temperature damage to biological membranes. *Cryobiology* 22:128-146.
443. Rambhatla, L., C.P.Chiu, P.Kundu, Y.Peng, and M.K.Carpenter. 2003. Generation of hepatocyte-like cells from human embryonic stem cells. *Cell Transplant.* 12:1-11.
444. Remenyi, A., H.R.Scholer, and M.Wilmanns. 2004. Combinatorial control of gene expression. *Nat. Struct. Mol. Biol.* 11:812-815.
445. Reubinoff, B.E., P.Itsykson, T.Turetsky, M.F.Pera, E.Reinhartz, A.Itzik, and T.Ben-Hur. 2001a. Neural progenitors from human embryonic stem cells. *Nat. Biotechnol.* 19:1134-1140.
446. Reubinoff, B.E., M.F.Pera, C.Y.Fong, A.Trounson, and A.Bongso. 2000h. Embryonic stem cell lines from human blastocysts: somatic differentiation in vitro. *Nat. Biotechnol.* 18:399-404.
447. Reubinoff, B.E., M.F.Pera, C.Y.Fong, A.Trounson, and A.Bongso. 2000g. Embryonic stem cell lines from human blastocysts: somatic differentiation in vitro. *Nat. Biotechnol.* 18:399-404.
448. Reubinoff, B.E., M.F.Pera, C.Y.Fong, A.Trounson, and A.Bongso. 2000d. Embryonic stem cell lines from human blastocysts: somatic differentiation in vitro. *Nat. Biotechnol.* 18:399-404.
449. Reubinoff, B.E., M.F.Pera, C.Y.Fong, A.Trounson, and A.Bongso. 2000b. Embryonic stem cell lines from human blastocysts: somatic differentiation in vitro. *Nat. Biotechnol.* 18:399-404.
450. Reubinoff, B.E., M.F.Pera, C.Y.Fong, A.Trounson, and A.Bongso. 2000a. Embryonic stem cell lines from human blastocysts: somatic differentiation in vitro. *Nat. Biotechnol.* 18:399-404.
451. Reubinoff, B.E., M.F.Pera, C.Y.Fong, A.Trounson, and A.Bongso. 2000f. Embryonic stem cell lines from human blastocysts: somatic differentiation in vitro. *Nat. Biotechnol.* 18:399-404.
452. Reubinoff, B.E., M.F.Pera, C.Y.Fong, A.Trounson, and A.Bongso. 2000e. Embryonic stem cell lines from human blastocysts: somatic differentiation in vitro. *Nat. Biotechnol.* 18:399-404.
453. Reubinoff, B.E., M.F.Pera, C.Y.Fong, A.Trounson, and A.Bongso. 2000c. Embryonic stem cell lines from human blastocysts: somatic differentiation in vitro. *Nat. Biotechnol.* 18:399-404.

454. Reubinoff, B.E., M.F.Pera, G.Vajta, and A.O.Trounson. 2001b. Effective cryopreservation of human embryonic stem cells by the open pulled straw vitrification method. *Hum. Reprod.* 16:2187-2194.
455. Reubinoff, B.E., M.F.Pera, G.Vajta, and A.O.Trounson. 2001i. Effective cryopreservation of human embryonic stem cells by the open pulled straw vitrification method. *Hum. Reprod.* 16:2187-2194.
456. Reubinoff, B.E., M.F.Pera, G.Vajta, and A.O.Trounson. 2001c. Effective cryopreservation of human embryonic stem cells by the open pulled straw vitrification method. *Hum. Reprod.* 16:2187-2194.
457. Reubinoff, B.E., M.F.Pera, G.Vajta, and A.O.Trounson. 2001d. Effective cryopreservation of human embryonic stem cells by the open pulled straw vitrification method. *Hum. Reprod.* 16:2187-2194.
458. Reubinoff, B.E., M.F.Pera, G.Vajta, and A.O.Trounson. 2001e. Effective cryopreservation of human embryonic stem cells by the open pulled straw vitrification method. *Hum. Reprod.* 16:2187-2194.
459. Reubinoff, B.E., M.F.Pera, G.Vajta, and A.O.Trounson. 2001g. Effective cryopreservation of human embryonic stem cells by the open pulled straw vitrification method. *Hum. Reprod.* 16:2187-2194.
460. Reubinoff, B.E., M.F.Pera, G.Vajta, and A.O.Trounson. 2001h. Effective cryopreservation of human embryonic stem cells by the open pulled straw vitrification method. *Hum. Reprod.* 16:2187-2194.
461. Reubinoff, B.E., M.F.Pera, G.Vajta, and A.O.Trounson. 2001f. Effective cryopreservation of human embryonic stem cells by the open pulled straw vitrification method. *Hum. Reprod.* 16:2187-2194.
462. Richards, M., C.Y.Fong, S.Tan, W.K.Chan, and A.Bongso. 2004a. An efficient and safe xeno-free cryopreservation method for the storage of human embryonic stem cells. *Stem Cells* 22:779-789.
463. Richards, M., S.P.Tan, J.H.Tan, W.K.Chan, and A.Bongso. 2004b. The transcriptome profile of human embryonic stem cells as defined by SAGE. *Stem Cells* 22:51-64.
464. Richman, C.M., R.S.Weiner, and R.A.Yankee. 1976. Increase in circulating stem cells following chemotherapy in man. *Blood* 47:1031-1039.
465. Riento, K. and A.J.Ridley. 2003. ROCKs: multifunctional kinases in cell behaviour. *Nat Rev Mol Cell Biol* 4:446-456.
466. Robertson, E.J., D.P.Norris, J.Brennan, and E.K.Bikoff. 2003. Control of early anterior-posterior patterning in the mouse embryo by TGF-beta signalling. *Philos. Trans. R. Soc. Lond B Biol. Sci.* 358:1351-1357.

467. Rodrigues, J.P., F.H.Paraguass-Braga, L.Carvalho, E.Abdelhay, L.F.Bouzas, and L.C.Porto. 2008. Evaluation of trehalose and sucrose as cryoprotectants for hematopoietic stem cells of umbilical cord blood. *Cryobiology* 56:144-151.
468. Rosler, E.S., G.J.Fisk, X.Ares, J.Irving, T.Miura, M.S.Rao, and M.K.Carpenter. 2004b. Long-term culture of human embryonic stem cells in feeder-free conditions. *Dev. Dyn.* 229:259-274.
469. Rosler, E.S., G.J.Fisk, X.Ares, J.Irving, T.Miura, M.S.Rao, and M.K.Carpenter. 2004a. Long-term culture of human embryonic stem cells in feeder-free conditions. *Dev. Dyn.* 229:259-274.
470. Rosler, E.S., G.J.Fisk, X.Ares, J.Irving, T.Miura, M.S.Rao, and M.K.Carpenter. 2004d. Long-term culture of human embryonic stem cells in feeder-free conditions. *Dev. Dyn.* 229:259-274.
471. Rosler, E.S., G.J.Fisk, X.Ares, J.Irving, T.Miura, M.S.Rao, and M.K.Carpenter. 2004c. Long-term culture of human embryonic stem cells in feeder-free conditions. *Dev. Dyn.* 229:259-274.
472. Rosner, M.H., M.A.Vigano, K.Ozato, P.M.Timmons, F.Poirier, P.W.Rigby, and L.M.Staudt. 1990. A POU-domain transcription factor in early stem cells and germ cells of the mammalian embryo. *Nature* 345:686-692.
473. Rossant, J. 2004. Lineage development and polar asymmetries in the peri-implantation mouse blastocyst. *Semin. Cell Dev. Biol.* 15:573-581.
474. Rowland, B.D., R.Bernards, and D.S.Peeper. 2005. The KLF4 tumour suppressor is a transcriptional repressor of p53 that acts as a context-dependent oncogene. *Nat. Cell Biol.* 7:1074-1082.
475. Rowley, S.D., W.I.Bensinger, T.A.Gooley, and C.D.Buckner. 1994a. Effect of cell concentration on bone marrow and peripheral blood stem cell cryopreservation. *Blood* 83:2731-2736.
476. Rowley, S.D., W.I.Bensinger, T.A.Gooley, and C.D.Buckner. 1994b. Effect of cell concentration on bone marrow and peripheral blood stem cell cryopreservation. *Blood* 83:2731-2736.
477. Rowley, S.D., W.I.Bensinger, T.A.Gooley, and C.D.Buckner. 1994c. Effect of cell concentration on bone marrow and peripheral blood stem cell cryopreservation. *Blood* 83:2731-2736.
478. Rowley, S.D., W.I.Bensinger, T.A.Gooley, and C.D.Buckner. 1994d. Effect of cell concentration on bone marrow and peripheral blood stem cell cryopreservation. *Blood* 83:2731-2736.
479. Rubinsky, B. and D.E.Pegg. 1988. A mathematical model for the freezing process in biological tissue. *Proc. R. Soc. Lond B Biol. Sci.* 234:343-358.

480. Ruffing, N.A., P.L.Steponkus, R.E.Pitt, and J.E.Parks. 1993. Osmometric behavior, hydraulic conductivity, and incidence of intracellular ice formation in bovine oocytes at different developmental stages. *Cryobiology* 30:562-580.
481. Salinas-Flores, L., S.L.Adams, and M.H.Lim. 2008. Determination of the membrane permeability characteristics of Pacific oyster, *Crassostrea gigas*, oocytes and development of optimized methods to add and remove ethylene glycol. *Cryobiology* 56:43-52.
482. Sanchez-Osorio, J., C.Cuello, M.A.Gil, I.Parrilla, C.Almiñana, I.Caballero, J.Roca, J.M.Vazquez, H.Rodriguez-Martinez, and E.A.Martinez. 2010. In vitro postwarming viability of vitrified porcine embryos: Effect of cryostorage length. *Theriogenology* 74:486-490.
483. Schopperle, W.M. and W.C.DeWolf. 2007c. The TRA-1-60 and TRA-1-81 human pluripotent stem cell markers are expressed on podocalyxin in embryonal carcinoma. *Stem Cells* 25:723-730.
484. Schopperle, W.M. and W.C.DeWolf. 2007b. The TRA-1-60 and TRA-1-81 human pluripotent stem cell markers are expressed on podocalyxin in embryonal carcinoma. *Stem Cells* 25:723-730.
485. Schopperle, W.M. and W.C.DeWolf. 2007a. The TRA-1-60 and TRA-1-81 human pluripotent stem cell markers are expressed on podocalyxin in embryonal carcinoma. *Stem Cells* 25:723-730.
486. Schreuders, P.D., E.D.Smith, K.W.Cole, M.D.Valencia, A.Laughinghouse, and P.Mazur. 1996. Characterization of intraembryonic freezing in *Anopheles gambiae* embryos. *Cryobiology* 33:487-501.
487. Seki, S., T.Kouya, J.Valdez, B.Jin, T.Hara, N.Saida, M.Kasai, and K.Edashige. 2007. The permeability to water and cryoprotectants of immature and mature oocytes in the zebrafish (*Danio rerio*). *Cryobiology* 54:121-124.
488. Seoane, J., H.V.Le, and J.Massague. 2002. Myc suppression of the p21(Cip1) Cdk inhibitor influences the outcome of the p53 response to DNA damage. *Nature* 419:729-734.
489. Shevinsky, L.H., B.B.Knowles, I.Damjanov, and D.Solter. 1982. Monoclonal antibody to murine embryos defines a stage-specific embryonic antigen expressed on mouse embryos and human teratocarcinoma cells. *Cell* 30:697-705.
490. Shi, Y., C.Desponts, J.T.Do, H.S.Hahm, H.R.Scholer, and S.Ding. 2008a. Induction of pluripotent stem cells from mouse embryonic fibroblasts by Oct4 and Klf4 with small-molecule compounds. *Cell Stem Cell* 3:568-574.
491. Shi, Y., J.Tae Do, C.Desponts, H.S.Hahm, H.R.Scholer, and S.Ding. 2008b. A Combined Chemical and Genetic Approach for the Generation of Induced Pluripotent Stem Cells. *Cell Stem Cell* 2:525-528.

492. Si, W., J.D.Benson, H.Men, and J.K.Critser. 2006. Osmotic tolerance limits and effects of cryoprotectants on the motility, plasma membrane integrity and acrosomal integrity of rat sperm. *Cryobiology* 53:336-348.
493. Silva, J., I.Chambers, S.Pollard, and A.Smith. 2006. Nanog promotes transfer of pluripotency after cell fusion. *Nature* 441:997-1001.
494. Singer, S.J. and G.L.Nicolson. 1972. The fluid mosaic model of the structure of cell membranes. *Science* 175:720-731.
495. Smith, C. 2003a. Hematopoietic stem cells and hematopoiesis. *Cancer Control* 10:9-16.
496. Smith, C. 2003b. Hematopoietic stem cells and hematopoiesis. *Cancer Control* 10:9-16.
497. Solter, D. and B.B.Knowles. 1975. Immunosurgery of mouse blastocyst. *Proc. Natl. Acad. Sci. U. S. A* 72:5099-5102.
498. Son, J.H., Y.J.Heo, M.Y.Park, H.H.Kim, and K.S.Lee. 2010. Optimization of cryopreservation condition for hematopoietic stem cells from umbilical cord blood. *Cryobiology* 60:287-292.
499. Song, J., S.P.Oh, H.Schrewe, M.Nomura, H.Lei, M.Okano, T.Gridley, and E.Li. 1999. The type II activin receptors are essential for egg cylinder growth, gastrulation, and rostral head development in mice. *Dev. Biol.* 213:157-169.
500. Stacey, G.N., F.Cobo, A.Nieto, P.Talavera, L.Healy, and A.Concha. 2006. The development of 'feeder' cells for the preparation of clinical grade hES cell lines: Challenges and solutions. *Journal of Biotechnology* 125:583-588.
501. Stevens, L.C. and D.S.Varnum. 1974. The development of teratomas from parthenogenetically activated ovarian mouse eggs. *Dev. Biol.* 37:369-380.
502. Stiff, P.J., M.F.DeRisi, A.Langleben, S.Gulati, A.Koester, V.Lanzotti, and B.D.Clarkson. 1983a. Autologous bone marrow transplantation using unfractionated cells without rate-controlled freezing in hydroxyethyl starch and dimethyl sulfoxide. *Ann. N. Y. Acad. Sci.* 411:378-380.
503. Stiff, P.J., A.J.Murgo, C.G.Zaroulis, M.F.DeRisi, and B.D.Clarkson. 1983b. Unfractionated human marrow cell cryopreservation using dimethylsulfoxide and hydroxyethyl starch. *Cryobiology* 20:17-24.
504. Stiff, P.J., A.J.Murgo, C.G.Zaroulis, M.F.DeRisi, and B.D.Clarkson. 1983c. Unfractionated human marrow cell cryopreservation using dimethylsulfoxide and hydroxyethyl starch. *Cryobiology* 20:17-24.
505. Stojkovic, M., M.Lako, P.Stojkovic, R.Stewart, S.Przyborski, L.Armstrong, J.Evans, M.Herbert, L.Hyslop, S.Ahmad, A.Murdoch, and T.Strachan. 2004a. Derivation of human embryonic stem cells from day-8 blastocysts recovered after three-step in vitro culture. *Stem Cells* 22:790-797.

- 
506. Stojkovic, M., M.Lako, T.Strachan, and A.Murdoch. 2004b. Derivation, growth and applications of human embryonic stem cells. *Reproduction* 128:259-267.
507. Stojkovic, P., M.Lako, S.Przyborski, R.Stewart, L.Armstrong, J.Evans, X.Zhang, and M.Stojkovic. 2005a. Human-serum matrix supports undifferentiated growth of human embryonic stem cells. *Stem Cells* 23:895-902.
508. Stojkovic, P., M.Lako, S.Przyborski, R.Stewart, L.Armstrong, J.Evans, X.Zhang, and M.Stojkovic. 2005b. Human-serum matrix supports undifferentiated growth of human embryonic stem cells. *Stem Cells* 23:895-902.
509. Stojkovic, P., M.Lako, R.Stewart, S.Przyborski, L.Armstrong, J.Evans, A.Murdoch, T.Strachan, and M.Stojkovic. 2005c. An autogeneic feeder cell system that efficiently supports growth of undifferentiated human embryonic stem cells. *Stem Cells* 23:306-314.
510. Strauss, G., P.Schurtenberger, and H.Hauser. 1986. The interaction of saccharides with lipid bilayer vesicles: stabilization during freeze-thawing and freeze-drying. *Biochimica et Biophysica Acta (BBA) - Biomembranes* 858:169-180.
511. Suemori, H., K.Yasuchika, K.Hasegawa, T.Fujioka, N.Tsuneyoshi, and N.Nakatsuji. 2006. Efficient establishment of human embryonic stem cell lines and long-term maintenance with stable karyotype by enzymatic bulk passage. *Biochem. Biophys. Res. Commun.* 345:926-932.
512. Sui, H., B.G.Han, J.K.Lee, P.Walian, and B.K.Jap. 2001. Structural basis of water-specific transport through the AQP1 water channel. *Nature* 414:872-878.
513. Sum, A.K. and J.J.de Pablo. 2003. Molecular simulation study on the influence of dimethylsulfoxide on the structure of phospholipid bilayers. *Biophys. J* 85:3636-3645.
514. Sun, W.Q. 1999. State and phase transition behaviors of quercus rubra seed axes and cotyledonary tissues: relevance to the desiccation sensitivity and cryopreservation of recalcitrant seeds. *Cryobiology* 38:372-385.
515. Sutton, R.R. 1991. Critical Cooling Rates to avoid Ice Crystallization in Solutions Cryoprotective Agents. *J. Chem. Soc. Faraday Trans.* 87:101-105.
516. Takahashi, K., K.Tanabe, M.Ohnuki, M.Narita, T.Ichisaka, K.Tomoda, and S.Yamanaka. 2007b. Induction of pluripotent stem cells from adult human fibroblasts by defined factors. *Cell* 131:861-872.
517. Takahashi, K., K.Tanabe, M.Ohnuki, M.Narita, T.Ichisaka, K.Tomoda, and S.Yamanaka. 2007a. Induction of pluripotent stem cells from adult human fibroblasts by defined factors. *Cell* 131:861-872.
518. Takahashi, K., K.Tanabe, M.Ohnuki, M.Narita, T.Ichisaka, K.Tomoda, and S.Yamanaka. 2007c. Induction of pluripotent stem cells from adult human fibroblasts by defined factors. *Cell* 131:861-872.

519. Takahashi, K. and S.Yamanaka. 2006. Induction of pluripotent stem cells from mouse embryonic and adult fibroblast cultures by defined factors. *Cell* 126:663-676.
520. Takei, S., H.Ichikawa, K.Johkura, A.Mogi, H.No, S.Yoshie, D.Tomotsune, and K.Sasaki. 2009. Bone morphogenetic protein-4 promotes induction of cardiomyocytes from human embryonic stem cells in serum-based embryoid body development. *American Journal of Physiology - Heart and Circulatory Physiology* 296:H1793-H1803.
521. Tamm, M., A.Gratwohl, A.Tichelli, A.P.Perruchoud, and A.Tyndall. 1996. Autologous haemopoietic stem cell transplantation in a patient with severe pulmonary hypertension complicating connective tissue disease. *Ann. Rheum. Dis.* 55:779-780.
522. Thomson, J.A., J.Itskovitz-Eldor, S.S.Shapiro, M.A.Waknitz, J.J.Swiergiel, V.S.Marshall, and J.M.Jones. 1998e. Embryonic stem cell lines derived from human blastocysts. *Science* 282:1145-1147.
523. Thomson, J.A., J.Itskovitz-Eldor, S.S.Shapiro, M.A.Waknitz, J.J.Swiergiel, V.S.Marshall, and J.M.Jones. 1998d. Embryonic stem cell lines derived from human blastocysts. *Science* 282:1145-1147.
524. Thomson, J.A., J.Itskovitz-Eldor, S.S.Shapiro, M.A.Waknitz, J.J.Swiergiel, V.S.Marshall, and J.M.Jones. 1998g. Embryonic stem cell lines derived from human blastocysts. *Science* 282:1145-1147.
525. Thomson, J.A., J.Itskovitz-Eldor, S.S.Shapiro, M.A.Waknitz, J.J.Swiergiel, V.S.Marshall, and J.M.Jones. 1998a. Embryonic stem cell lines derived from human blastocysts. *Science* 282:1145-1147.
526. Thomson, J.A., J.Itskovitz-Eldor, S.S.Shapiro, M.A.Waknitz, J.J.Swiergiel, V.S.Marshall, and J.M.Jones. 1998f. Embryonic stem cell lines derived from human blastocysts. *Science* 282:1145-1147.
527. Thomson, J.A., J.Itskovitz-Eldor, S.S.Shapiro, M.A.Waknitz, J.J.Swiergiel, V.S.Marshall, and J.M.Jones. 1998b. Embryonic stem cell lines derived from human blastocysts. *Science* 282:1145-1147.
528. Thomson, J.A., J.Itskovitz-Eldor, S.S.Shapiro, M.A.Waknitz, J.J.Swiergiel, V.S.Marshall, and J.M.Jones. 1998c. Embryonic stem cell lines derived from human blastocysts. *Science* 282:1145-1147.
529. Thornberry, N.A., T.A.Rano, E.P.Peterson, D.M.Rasper, T.Timkey, M.Garcia-Calvo, V.M.Houtzager, P.A.Nordstrom, S.Roy, J.P.Vaillancourt, K.T.Chapman, and D.W.Nicholson. 1997. A combinatorial approach defines specificities of members of the caspase family and granzyme B. Functional relationships established for key mediators of apoptosis. *J Biol. Chem.* 272:17907-17911.
530. Thurston, L.M., K.Siggins, A.J.Mileham, P.F.Watson, and W.V.Holt. 2002. Identification of amplified restriction fragment length polymorphism markers

- linked to genes controlling boar sperm viability following cryopreservation. *Biol. Reprod* 66:545-554.
531. Tijssen, M.R., H.Woelders, A.de Vries-van Rossen, C.E.van der Schoot, C.Voermans, and J.W.M.Lagerberg. 2000. Improved postthaw viability and in vitro functionality of peripheral blood hematopoietic progenitor cells after cryopreservation with a theoretically optimized freezing curve. *Transfusion* 0:1-9.
532. Todorova, M.G., B.Soria, and I.Quesada. 2008. Gap junctional intercellular communication is required to maintain embryonic stem cells in a non-differentiated and proliferative state. *J. Cell. Physiol.* 214:354-362.
533. Toner, M., E.G.Cravalho, and M.Karel. 1990b. Thermodynamics and kinetics of intracellular ice formation during freezing of biological cells. *Journal of Applied Physics* 67:1582-1593.
534. Toner, M., E.G.Cravalho, and M.Karel. 1990a. Thermodynamics and kinetics of intracellular ice formation during freezing of biological cells. *Journal of Applied Physics* 67:1582-1593.
535. Toner, M., E.G.Cravalho, M.Karel, and D.R.Armant. 1991. Cryomicroscopic analysis of intracellular ice formation during freezing of mouse oocytes without cryoadditives. *Cryobiology* 28:55-71.
536. Tsukaguchi, H., C.Shayakul, U.V.Berger, B.Mackenzie, S.Devidas, W.B.Guggino, A.N.van Hoek, and M.A.Hediger. 1998. Molecular Characterization of a Broad Selectivity Neutral Solute Channel. *Journal of Biological Chemistry* 273:24737-24743.
537. Tyndall, A. and A.Gratwohl. 1996. Haemopoietic stem and progenitor cells in the treatment of severe autoimmune diseases. *Ann. Rheum. Dis.* 55:149-151.
538. Udy, G.B. and M.J.Evans. 1994. Microplate DNA preparation, PCR screening and cell freezing for gene targeting in embryonic stem cells. *Biotechniques* 17:887-894.
539. Ure, J.M., S.Fiering, and A.G.Smith. 1992a. A rapid and efficient method for freezing and recovering clones of embryonic stem cells. *Trends Genet.* 8:6.
540. Ure, J.M., S.Fiering, and A.G.Smith. 1992b. A rapid and efficient method for freezing and recovering clones of embryonic stem cells. *Trends Genet.* 8:6.
541. Valiunas, V., S.Doronin, L.Valiuniene, I.Potapova, J.Zuckerman, B.Walcott, R.B.Robinson, M.R.Rosen, P.R.Brink, and I.S.Cohen. 2004. Human mesenchymal stem cells make cardiac connexins and form functional gap junctions. *J Physiol* 555:617-626.
542. Vallier, L., D.Reynolds, and R.A.Pedersen. 2004. Nodal inhibits differentiation of human embryonic stem cells along the neuroectodermal default pathway. *Dev. Biol.* 275:403-421.

543. Van den Abbeel, E., U.Schneider, J.Liu, Y.Agca, J.K.Critser, and A.Van Steirteghem. 2007. Osmotic responses and tolerance limits to changes in external osmolalities, and oolemma permeability characteristics, of human in vitro matured MII oocytes. *Hum. Reprod.* 22:1959-1972.
544. Van Hoof, D., S.R.Braam, W.Dormeyer, D.Ward-van Oostwaard, A.J.R.Heck, J.Krijgsveld, and C.L.Mummery. 2008b. Feeder-Free Monolayer Cultures of Human Embryonic Stem Cells Express an Epithelial Plasma Membrane Protein Profile. *Stem Cells* 26:2777-2781.
545. Van Hoof, D., S.R.Braam, W.Dormeyer, D.Ward-van Oostwaard, A.J.R.Heck, J.Krijgsveld, and C.L.Mummery. 2008a. Feeder-Free Monolayer Cultures of Human Embryonic Stem Cells Express an Epithelial Plasma Membrane Protein Profile. *Stem Cells* 26:2777-2781.
546. van't Hoff, J.H. 1887. The role of osmotic pressure in the analogy between solutions and gases. *Zeitschrift fur physikalische Chemie* 1:481-508.
547. Villalon, L., J.Odriozola, P.Ramos, M.L.Ramos, P.Herrera, and J.P.de Oteyza. 2002. Cryopreserving with increased cellular concentrations of peripheral blood progenitor cells: clinical results. *Haematologica* 87:ELT06.
548. Wagh, V., K.Meganathan, S.Jagtap, J.A.Gaspar, J.Winkler, D.Spitkovsky, J.Hescheler, and A.Sachinidis. 2011. Effects of cryopreservation on the transcriptome of human embryonic stem cells after thawing and culturing. *Stem Cell Rev.* 7:506-517.
549. Walcerz, D.B., M.J.Taylor, and A.L.Busza. 1995. Determination of the kinetics of permeation of dimethyl sulfoxide in isolated corneas. *Cell Biophys.* 26:79-102.
550. Ware, C.B., A.M.Nelson, and C.A.Blau. 2005b. Controlled-rate freezing of human ES cells. *Biotechniques* 38:879-3.
551. Ware, C.B., A.M.Nelson, and C.A.Blau. 2005e. Controlled-rate freezing of human ES cells. *Biotechniques* 38:879-3.
552. Ware, C.B., A.M.Nelson, and C.A.Blau. 2005f. Controlled-rate freezing of human ES cells. *Biotechniques* 38:879-3.
553. Ware, C.B., A.M.Nelson, and C.A.Blau. 2005d. Controlled-rate freezing of human ES cells. *Biotechniques* 38:879-3.
554. Ware, C.B., A.M.Nelson, and C.A.Blau. 2005c. Controlled-rate freezing of human ES cells. *Biotechniques* 38:879-3.
555. Ware, C.B., A.M.Nelson, and C.A.Blau. 2005a. Controlled-rate freezing of human ES cells. *Biotechniques* 38:879-3.
556. Watanabe, K., M.Ueno, D.Kamiya, A.Nishiyama, M.Matsumura, T.Wataya, J.B.Takahashi, S.Nishikawa, S.Nishikawa, K.Muguruma, and Y.Sasai. 2007b. A

- ROCK inhibitor permits survival of dissociated human embryonic stem cells. *Nat Biotech* 25:681-686.
557. Watanabe, K., M.Ueno, D.Kamiya, A.Nishiyama, M.Matsumura, T.Wataya, J.B.Takahashi, S.Nishikawa, S.Nishikawa, K.Muguruma, and Y.Sasai. 2007a. A ROCK inhibitor permits survival of dissociated human embryonic stem cells. *Nat Biotech* 25:681-686.
558. Watson, P.F. and G.J.Morris. 1987. Cold shock injury in animal cells. *Symp. Soc. Exp. Biol.* 41:311-340.
559. Wernig, M., A.Meissner, R.Foreman, T.Brambrink, M.Ku, K.Hochedlinger, B.E.Bernstein, and R.Jaenisch. 2007. In vitro reprogramming of fibroblasts into a pluripotent ES-cell-like state. *Nature* 448:318-324.
560. Whittingham, D.G., S.P.Leibo, and P.Mazur. 1972. Survival of mouse embryos frozen to -196 degrees and -269 degrees C. *Science* 178:411-414.
561. Wilson, A., E.Laurenti, G.Oser, R.C.van der Wath, W.Blanco-Bose, M.Jaworski, S.Offner, C.F.Dunant, L.Eshkind, E.Bockamp, P.Li, H.R.MacDonald, and A.Trumpp. 2008. Hematopoietic Stem Cells Reversibly Switch from Dormancy to Self-Renewal during Homeostasis and Repair. *Cell* 135:1118-1129.
562. Woelders, H. and A.Chaveiro. 2004. Theoretical prediction of 'optimal' freezing programmes. *Cryobiology* 49:258-271.
563. Wong, R.C., A.Pebay, L.T.Nguyen, K.L.Koh, and M.F.Pera. 2004. Presence of functional gap junctions in human embryonic stem cells. *Stem Cells* 22:883-889.
564. Wong, R.C.B., M.Dottori, K.L.L.Koh, L.T.V.Nguyen, M.F.Pera, and A.Pebay. 2006. Gap junctions modulate apoptosis and colony growth of human embryonic stem cells maintained in a serum-free system. *Biochemical and Biophysical Research Communications* 344:181-188.
565. Woods, E.J., J.Liu, C.W.Derrow, F.O.Smith, D.A.Williams, and J.K.Critser. 2000a. Osmometric and permeability characteristics of human placental/umbilical cord blood CD34+ cells and their application to cryopreservation. *J Hematother. Stem Cell Res.* 9:161-173.
566. Woods, E.J., J.Liu, C.W.Derrow, F.O.Smith, D.A.Williams, and J.K.Critser. 2000b. Osmometric and permeability characteristics of human placental/umbilical cord blood CD34+ cells and their application to cryopreservation. *J Hematother. Stem Cell Res.* 9:161-173.
567. Woods, E.J., J.Liu, J.A.Gilmore, T.J.Reid, D.Y.Gao, and J.K.Critser. 1999a. Determination of Human Platelet Membrane Permeability Coefficients Using the Kedem-Katchalsky Formalism: Estimates from Two- vs Three-Parameter Fits. *Cryobiology* 38:200-208.
568. Woods, E.J., J.Liu, J.A.Gilmore, T.J.Reid, D.Y.Gao, and J.K.Critser. 1999c. Determination of Human Platelet Membrane Permeability Coefficients Using the

- Kedem-Katchalsky Formalism: Estimates from Two- vs Three-Parameter Fits. *Cryobiology* 38:200-208.
569. Woods, E.J., J.Liu, J.A.Gilmore, T.J.Reid, D.Y.Gao, and J.K.Critser. 1999b. Determination of Human Platelet Membrane Permeability Coefficients Using the Kedem-Katchalsky Formalism: Estimates from Two- vs Three-Parameter Fits. *Cryobiology* 38:200-208.
570. Woods, E.J., J.Liu, K.Pollok, J.Hartwell, F.O.Smith, D.A.Williams, M.C.Yoder, and J.K.Critser. 2003a. A theoretically optimized method for cord blood stem cell cryopreservation. *J. Hematother. Stem Cell Res.* 12:341-350.
571. Woods, E.J., J.Liu, K.Pollok, J.Hartwell, F.O.Smith, D.A.Williams, M.C.Yoder, and J.K.Critser. 2003b. A theoretically optimized method for cord blood stem cell cryopreservation. *J. Hematother. Stem Cell Res.* 12:341-350.
572. Woods, E.J., D.Gao, K.Pollok, M.A.Byers, E.L.Calloway, M.C.Yoder, and J.K.Critser. 2006. An optimized system for cryopreservation and post-thaw recovery of cord blood stem cells. *Cryobiology* 53:387.
573. Woods, E.J., B.C.Perry, J.J.Hockema, L.Larson, D.Zhou, and W.S.Goebel. 2009. Optimized cryopreservation method for human dental pulp-derived stem cells and their tissues of origin for banking and clinical use. *Cryobiology* 59:150-157.
574. Wright, A.J. and P.W.Andrews. 2009. Surface marker antigens in the characterization of human embryonic stem cells. *Stem Cell Research* 3:3-11.
575. Wu, C.F., H.C.Tsung, W.J.Zhang, Y.Wang, J.H.Lu, Z.Y.Tang, Y.P.Kuang, W.Jin, L.Cui, W.Liu, and Y.L.Cao. 2005f. Improved cryopreservation of human embryonic stem cells with trehalose. *Reprod. Biomed. Online.* 11:733-739.
576. Wu, C.F., H.C.Tsung, W.J.Zhang, Y.Wang, J.H.Lu, Z.Y.Tang, Y.P.Kuang, W.Jin, L.Cui, W.Liu, and Y.L.Cao. 2005a. Improved cryopreservation of human embryonic stem cells with trehalose. *Reprod. Biomed. Online.* 11:733-739.
577. Wu, C.F., H.C.Tsung, W.J.Zhang, Y.Wang, J.H.Lu, Z.Y.Tang, Y.P.Kuang, W.Jin, L.Cui, W.Liu, and Y.L.Cao. 2005b. Improved cryopreservation of human embryonic stem cells with trehalose. *Reprod. Biomed. Online.* 11:733-739.
578. Wu, C.F., H.C.Tsung, W.J.Zhang, Y.Wang, J.H.Lu, Z.Y.Tang, Y.P.Kuang, W.Jin, L.Cui, W.Liu, and Y.L.Cao. 2005c. Improved cryopreservation of human embryonic stem cells with trehalose. *Reprod. Biomed. Online.* 11:733-739.
579. Wu, C.F., H.C.Tsung, W.J.Zhang, Y.Wang, J.H.Lu, Z.Y.Tang, Y.P.Kuang, W.Jin, L.Cui, W.Liu, and Y.L.Cao. 2005d. Improved cryopreservation of human embryonic stem cells with trehalose. *Reprod. Biomed. Online.* 11:733-739.
580. Wu, C.F., H.C.Tsung, W.J.Zhang, Y.Wang, J.H.Lu, Z.Y.Tang, Y.P.Kuang, W.Jin, L.Cui, W.Liu, and Y.L.Cao. 2005e. Improved cryopreservation of human embryonic stem cells with trehalose. *Reprod. Biomed. Online.* 11:733-739.

- 
581. Wu, W.T., S.R.Lyu, and W.H.Hsieh. 2005i. Cryopreservation and biophysical properties of articular cartilage chondrocytes. *Cryobiology* 51:330-338.
582. Wu, W.T., S.R.Lyu, and W.H.Hsieh. 2005g. Cryopreservation and biophysical properties of articular cartilage chondrocytes. *Cryobiology* 51:330-338.
583. Wu, W.T., S.R.Lyu, and W.H.Hsieh. 2005j. Cryopreservation and biophysical properties of articular cartilage chondrocytes. *Cryobiology* 51:330-338.
584. Wu, W.T., S.R.Lyu, and W.H.Hsieh. 2005h. Cryopreservation and biophysical properties of articular cartilage chondrocytes. *Cryobiology* 51:330-338.
585. Wusteman, M.C., D.E.Pegg, M.P.Robinson, L.H.Wang, and P.Fitch. 2002. Vitrification media: toxicity, permeability, and dielectric properties. *Cryobiology* 44:24-37.
586. Xu, C., M.S.Inokuma, J.Denham, K.Golds, P.Kundu, J.D.Gold, and M.K.Carpenter. 2001a. Feeder-free growth of undifferentiated human embryonic stem cells. *Nat. Biotechnol.* 19:971-974.
587. Xu, C., M.S.Inokuma, J.Denham, K.Golds, P.Kundu, J.D.Gold, and M.K.Carpenter. 2001b. Feeder-free growth of undifferentiated human embryonic stem cells. *Nat. Biotechnol.* 19:971-974.
588. Xu, C., M.S.Inokuma, J.Denham, K.Golds, P.Kundu, J.D.Gold, and M.K.Carpenter. 2001d. Feeder-free growth of undifferentiated human embryonic stem cells. *Nat. Biotechnol.* 19:971-974.
589. Xu, C., M.S.Inokuma, J.Denham, K.Golds, P.Kundu, J.D.Gold, and M.K.Carpenter. 2001c. Feeder-free growth of undifferentiated human embryonic stem cells. *Nat. Biotechnol.* 19:971-974.
590. Xu, X., Z.Cui, and J.P.G.Urban. 2003a. Measurement of the chondrocyte membrane permeability to Me<sub>2</sub>SO, glycerol and 1,2-propanediol. *Medical Engineering & Physics* 25:573-579.
591. Xu, X., Z.Cui, and J.P.G.Urban. 2003b. Measurement of the chondrocyte membrane permeability to Me<sub>2</sub>SO, glycerol and 1,2-propanediol. *Medical Engineering & Physics* 25:573-579.
592. Yamaji, Y., J.Valdez, S.Seki, K.Yazawa, C.Urakawa, B.Jin, M.Kasai, F.W.Kleinhans, and K.Edashige. 2006b. Cryoprotectant permeability of aquaporin-3 expressed in *Xenopus* oocytes. *Cryobiology* 53:258-267.
593. Yamaji, Y., J.Valdez, S.Seki, K.Yazawa, C.Urakawa, B.Jin, M.Kasai, F.W.Kleinhans, and K.Edashige. 2006c. Cryoprotectant permeability of aquaporin-3 expressed in *Xenopus* oocytes. *Cryobiology* 53:258-267.
594. Yamaji, Y., J.Valdez, S.Seki, K.Yazawa, C.Urakawa, B.Jin, M.Kasai, F.W.Kleinhans, and K.Edashige. 2006d. Cryoprotectant permeability of aquaporin-3 expressed in *Xenopus* oocytes. *Cryobiology* 53:258-267.

- 
595. Yamaji, Y., J.Valdez, S.Seki, K.Yazawa, C.Urakawa, B.Jin, M.Kasai, F.W.Kleinhans, and K.Edashige. 2006a. Cryoprotectant permeability of aquaporin-3 expressed in *Xenopus* oocytes. *Cryobiology* 53:258-267.
596. Yang, D.H. and E.G.Moss. 2003. Temporally regulated expression of Lin-28 in diverse tissues of the developing mouse. *Gene Expr. Patterns.* 3:719-726.
597. Yang, H., J.Acker, A.Chen, and L.McGann. 1998. In situ assessment of cell viability. *Cell Transplant.* 7:443-451.
598. Yannas, I. 1968. Vitrification temperature of water. *Science* 160:298-299.
599. Yavin, S. and A.Arav. 2007. Measurement of essential physical properties of vitrification solutions. *Theriogenology* 67:81-89.
600. Ying, Q.L., J.Nichols, I.Chambers, and A.Smith. 2003a. BMP induction of Id proteins suppresses differentiation and sustains embryonic stem cell self-renewal in collaboration with STAT3. *Cell* 115:281-292.
601. Ying, Q.L., J.Nichols, I.Chambers, and A.Smith. 2003b. BMP induction of Id proteins suppresses differentiation and sustains embryonic stem cell self-renewal in collaboration with STAT3. *Cell* 115:281-292.
602. Yoder, M.C. 2005. Creative stem cell assays. *Blood* 105:2622.
603. Yu, J., M.A.Vodyanik, K.Smuga-Otto, J.Antosiewicz-Bourget, J.L.Frane, S.Tian, J.Nie, G.A.Jonsdottir, V.Ruotti, R.Stewart, I.I.Slukvin, and J.A.Thomson. 2007b. Induced pluripotent stem cell lines derived from human somatic cells. *Science* 318:1917-1920.
604. Yu, J., M.A.Vodyanik, K.Smuga-Otto, J.Antosiewicz-Bourget, J.L.Frane, S.Tian, J.Nie, G.A.Jonsdottir, V.Ruotti, R.Stewart, I.I.Slukvin, and J.A.Thomson. 2007a. Induced pluripotent stem cell lines derived from human somatic cells. *Science* 318:1917-1920.
605. Yu, J., M.A.Vodyanik, K.Smuga-Otto, J.Antosiewicz-Bourget, J.L.Frane, S.Tian, J.Nie, G.A.Jonsdottir, V.Ruotti, R.Stewart, I.I.Slukvin, and J.A.Thomson. 2007c. Induced pluripotent stem cell lines derived from human somatic cells. *Science* 318:1917-1920.
606. Yu, J., M.A.Vodyanik, K.Smuga-Otto, J.Antosiewicz-Bourget, J.L.Frane, S.Tian, J.Nie, G.A.Jonsdottir, V.Ruotti, R.Stewart, I.I.Slukvin, and J.A.Thomson. 2007d. Induced pluripotent stem cell lines derived from human somatic cells. *Science* 318:1917-1920.
607. Yuan, H., N.Corbi, C.Basilico, and L.Dailey. 1995. Developmental-specific activity of the FGF-4 enhancer requires the synergistic action of Sox2 and Oct-3. *Genes Dev.* 9:2635-2645.

- 
608. Zeron, Y., M.Tomczak, J.Crowe, and A.Arav. 2002. The effect of liposomes on thermotropic membrane phase transitions of bovine spermatozoa and oocytes: implications for reducing chilling sensitivity. *Cryobiology* 45:143-152.
609. Zhang, W., D.E.Geiman, J.M.Shields, D.T.Dang, C.S.Mahatan, K.H.Kaestner, J.R.Biggs, A.S.Kraft, and V.W.Yang. 2000. The gut-enriched Kruppel-like factor (Kruppel-like factor 4) mediates the transactivating effect of p53 on the p21WAF1/Cip1 promoter. *J Biol. Chem.* 275:18391-18398.
610. Zhao, Y., X.Yin, H.Qin, F.Zhu, H.Liu, W.Yang, Q.Zhang, C.Xiang, P.Hou, Z.Song, Y.Liu, J.Yong, P.Zhang, J.Cai, M.Liu, H.Li, Y.Li, X.Qu, K.Cui, W.Zhang, T.Xiang, Y.Wu, Y.Zhao, C.Liu, C.Yu, K.Yuan, J.Lou, M.Ding, and H.Deng. 2008. Two Supporting Factors Greatly Improve the Efficiency of Human iPSC Generation. *Cell Stem Cell* 3:475-479.
611. Zhou, C.Q., Q.Y.Mai, T.Li, and G.L.Zhuang. 2004a. Cryopreservation of human embryonic stem cells by vitrification. *Chin Med. J. (Engl.)* 117:1050-1055.
612. Zhou, C.Q., Q.Y.Mai, T.Li, and G.L.Zhuang. 2004d. Cryopreservation of human embryonic stem cells by vitrification. *Chin Med. J. (Engl.)* 117:1050-1055.
613. Zhou, C.Q., Q.Y.Mai, T.Li, and G.L.Zhuang. 2004b. Cryopreservation of human embryonic stem cells by vitrification. *Chin Med. J. (Engl.)* 117:1050-1055.
614. Zhou, C.Q., Q.Y.Mai, T.Li, and G.L.Zhuang. 2004c. Cryopreservation of human embryonic stem cells by vitrification. *Chin Med. J. (Engl.)* 117:1050-1055.